Valorization of lignin by employing solution chemistry and mechanochemical conditions

Von der Fakultät für Mathematik, Informatik und Naturwissenschaften der RWTH Aachen University zur Erlangung des akademischen Grades einer Doktorin der Naturwissenschaften genehmigte Dissertation

von

Master of Science

Saumya Dabral

aus Delhi, Indien

Berichter: Prof. Dr. rer. nat. Carsten Bolm

Prof. Dr. rer. nat. Dieter Enders

Tag der mündlichen Prüfung: 9. Oktober 2017

The work presented in this dissertation was carried out from April 2014 until June 2017 at the Institute of Organic Chemistry, RWTH Aachen University, Aachen, Germany under the supervision of Professor Dr. Carsten Bolm. Parts of the experiments presented in chapters III.1 and III.2 were conducted from June until August 2015 and from September until October 2016 at the Department of Chemistry, University of St Andrews, Fife, United Kingdom under the supervision of Professor Dr. Paul C. J. Kamer.

I would like to thank Professor Dr. Carsten Bolm for giving me an opportunity to perfom my doctoral work in his group and for the help and guidance he has given me during the entire process. I am grateful to Professor Dr. Dieter Enders for being my second examiner.

Furthermore, I would like to thank Professor Dr. Paul C. J. Kamer for making my stay at St Andrews possible and being a mentor over the last three years.

I am grateful to the Subicat project and the European Commission (SuBiCat Initial Training Network, Call FP7-PEOPLE-2013-ITN, grant no. 607044) for my predoctoral stipends. I am also thankful for the immense support of my entirely family and friends back home and within the group.

Parts of this work have already been published as follows:

1) S. Dabral, J. Mottweiler, T. Rinesch, C. Bolm, *Green Chem*. **2015**, *17*, 4908−4917.

2) S. Dabral, J. G. Hernández, P. C. J. Kamer, C. Bolm, *ChemSusChem* **2017**, *10*, 1−8.

3) S. Dabral, M. Turberg, A. Wanninger, C. Bolm, J. G. Hernández, *Molecules* **2017**, *22,* 146.

For my family

Table of Contents

I. Motivation

The 21st century is facing energy related challenges which are affecting the economics and environment worldwide. Fossil reserves are being exploited as the major energy reservoir to meet the demands of the growing population and fast-paced urbanization of developing countries.[1,2] This unbridled utilization and depletion of oil, coal and natural gas reservoirs illustrates that the fossil based fuels cannot be relied on to meet the long term future energy demands.

According to the World Energy Outlook report published in 2016 by the International Energy Agency,[3] there will be a predictable growth of 30% in global energy demands by the year 2040. Increased oil use for transportation and petrochemicals is going to drive the demand even higher, from 90 million barrels per day (mb/d) in 2013 to 103 mb/d in 2040.[3,4] The difference between supply and demand thus created is likely to grow every year and have huge implications, especially for the energy supply to non-oil producing nations. Other than this, there have been worldwide debates, concerning the measurable global climate changes with crude oil contributing significantly to the global carbon emissions, second only to coal. The reports released by the Inter-governmental panel on Climatic Change (IPCC) in 2014 also highlighted the necessity of companies and governments to divest from fossil fuel investments in order to avoid the catastrophic climatic changes that are being caused by increasing greenhouse gas emissions.[5] Along these lines, the recent Paris climate change agreement aims to curtail the excessive emissions of greenhouse gases into the atmosphere and restrain the global temperature rise below 2 °C by the end of the century.[6]

Collectively, these impending crises have motivated the scientists worldwide to focus on sustainable energy alternatives that address the issues of energy security, price predictability and reduce the environmental impacts associated with the energy uses by reductions in the nation's carbon emission footprint.

Amongst the various fields of ongoing research on clean energy sources, the use of abundant renewable feedstock as an alternative source for chemicals and energy is an attractive possibility.[4,5] It has also been reported that in the 21st century, there shall be enough biomass waste produced globally to supply 20–30% of the total energy demands corresponding to approximately 10^{20} Joules per year. Keeping in mind the world population explosion and pressure on arable land, utilizing non-edible stocks of lignocellulosic biomass with their transformation into next generation biofuel or platform chemicals may thus be considered a promising alternative to depleting fossil resources while concomitantly managing the global carbon balance.[7]

One such target set by the European Union is "Vision 2030" with the goal to replace 25% of fossil fuels by biofuels until the year 2030.[8] Similarly, the US Department of Energy aims to replace 30% of liquid petroleum-based fuels by biofuels and produce 20% of its industrial organic chemicals from bio-derived chemicals by 2025.[7]

II. Introduction and research aim

1. Lignocellulosic biomass

Lignocellulose represents an abundant source of cheap and available renewable biomass that is mainly found in the plant cell wall (*e.g.* trees, switchgrass, bagasse), providing it with structural rigidity and protection.[9] The carbohydrates (cellulose and hemicellulose) and heterogeneous phenolic polymer lignin are the primary components of lignocellulosic biomass.[9] Despite its wide abundance in nature, this resource had not been extensively utilized until the recent awareness of depleting fossil reservoirs, rising environmental pollution and carbon levels. Current biorefineries, working towards the conversion of the carbohydrate part of lignocellulosic biomass to bio-ethanol (by fermentation), produce large amounts of lignin as bio-residue.[10] The advantage of producing such materials (bio-ethanol) from a biorefinery process is their carbon neutral nature since no additional carbon is added to the environment, beyond what was previously consumed during plant growth.[11] Nevertheless, to improve the overall economic viability of the biofuel production process from lignocellulosic biomass, it is necessary to add value to the lignin residue.[12] This is even more important keeping in mind the goals of Vision 2030, as a result of which huge amounts of additional lignin will be produced in addition to their current production in the paper and pulp industry. A way to tackle this situation is to develop techniques that shall further valorize the lignin residues to value added chemicals.

2. Lignin

Lignin represents nature's most abundant aromatic polymer accounting for 15% to 30% on weight basis and around 40% on energy basis of the total lignocellulosic biomass. It mainly consists of three phenyl propanoid units that originate from monolignols *p*-coumaryl, coniferyl and sinapyl alcohol (Figure II.1). These units are randomly interconnected to each other through a variety of three dimensional C–C (aryl-aryl, aryl-aliphatic, aliphatic-aliphatic) and C–O (ether and aryl-ether) cross-linkages.[9,12] Amongst them, the 5-5′ bonds represent the most stable C–C linkages. They have a bond dissociation enthalpy of about 117 kcal·mol^{-1} which is one of the highest to be found in nature.[13] Other than this, the β-O-4 linkages represent the most accessible (40% to 60% depending on the wood type) aryl-ether interconnecting bonds to be found in lignin. Compared to 5-5′ bonds, they are relatively easier cleavage

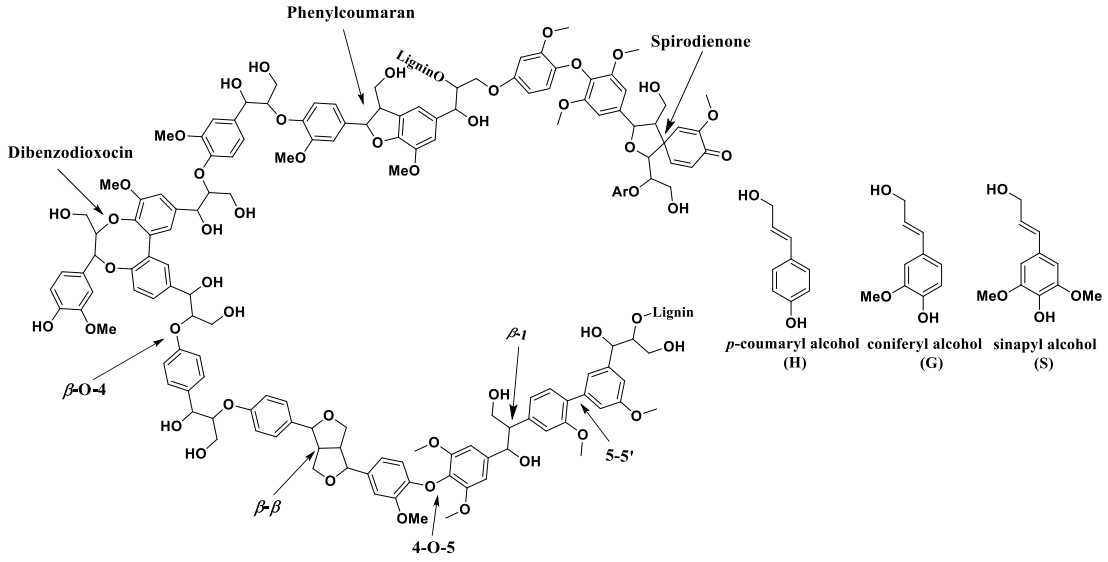

Figure II.1. Schematic representation of a segment of the lignin polymer and its three building blocks.

targets owing to their lower bond dissociation enthalpies, varying from 69.3 kcal·mol^{-1} to 72.9 kcal·mol^{-1}.[13] Other typical bonds found within lignin are the phenylcoumaran (β-5), resinol (β-β), β-1, 4-O-5, dibenzodioxocin and spirodienone structures.[9,12,13] This diverse range of interconnecting bonds makes lignin polymer highly recalcitrant in nature. Hence, its valorization and product separation pose major hindrance compared to the cellulosic and hemicelulosic counterparts. Nevertheless, due to its high calorific value, the majority of the lignin produced is burned as low-value fuel in an integrated biorefinery.[14]

However, realizing the importance of this biopolymer as an abundant source of readily available aromatics, there has been an immense rise in research interests diverted towards lignin pretreatment (upstream processes) and valorization (downstream processes) over the last few years.[12c] This is clearly reflected by the increasing number of publications and themed lignin issues in high impact journals. Most of these valorization studies have been focused on the cleavage of β-O-4 linkages because of their abundance in the biopolymer. For the same reason, they are also the prime focus of all the degradation studies conducted during the time frame of this dissertation.

3. Lignin pretreatment processes (upstream approach)

Different types of biomass upstream processing techniques are used to separate lignin from the cellulosic and hemicellulosic fractions. There are four common types of lignin denoted according to their pretreatment processes: 1) organosolv lignin; 2) kraft lignin; 3) soda lignin; 4) sulphite lignin. The process variations during lignin isolation have a significant impact on both the physical and chemical properties of the polymer including the identity and ratios of their chemical linkages. Since for this dissertation the lignin cleavage studies were developed on organosolv and kraft lignins, therefore only their corresponding pretreatment techniques will be briefly discussed in this chapter.

3.1. Organosolv pretreatment process

The organosolv process utilizes solvents like ethanol, methanol, acetone and ethylene glycol. Cyclic ethers like 1,4-dioxane or THF are also employed as solvents.[9, 12, 15] Lignin is extracted by treating the plant biomass with one or a mixture of these organic solvents in combination with water at elevated temperature and pressure. [9, 12, 15] One variation of the organosolv process involves the use of acid catalysts like HCl, H_2SO_4 or acetic acid. At a pH value between 2 to 4 and at temperatures ranging from 140 °C to 190 °C, the lignocellulosic fraction is delignified in a solvolytic reaction.[15] This process is mainly attributed to the β-ether bond cleavage following an acid ether hydrolysis step. A common organosolv pretreatment method is the Alcell process, which is either achieved by an ethanol:water (1:1) pulping (Lignol©-Canada)[16] or by pulping in mixtures of acetic acid with small amounts of either HCl or H_2SO_4 (Acetosolv).[17] Recently, an alternative process based on formic acid/acetic acid/water mixtures has been developed by CIMV Company (France).[18]

In conclusion, the organosolv process results in an effective lignin separation from cellulose and hemicellulose fractions of biomass. A big advantage of this process is that it effectively yields sulfur-free lignin that is soluble in organic solvents. This is particularly beneficial for further chemocatalytic processing. Furthermore, the organosolv lignins that are obtained without additional acid catalysts are likely to preserve a significant amount of the β-O-4 linkages and are thus often more susceptible to chemical downstream valorization procedures.[15]

3.2. Kraft pretreatment process

Kraft process in one of the most common lignin upstream processes invented by Carl F. Dahl in 1879 in Germany.[19] This process is used during the pulping of paper, where lignin is produced as a by-product of wood delignification.[20] First, the lignin and hemicellulose are separated as a black liquor from the cellulose fiber in a strongly alkaline aqueous solution of NaOH and Na_2S (white liquor) at temperatures between 150 °C to 180 °C.[20, 21] Under these harsh conditions, the β-O-4 rich native lignins are converted by cleavage of phenolic (and to some extent non-phenolic) β-ethers. The products are highly condensed and cross-linked kraft lignins featuring high amounts of C–C linkages with comparatively high dissociation energies.[22] Soluble lignin is then precipitated from the black liquor upon lowering the pH of the solution.[20, 21]

4. Lignin valorization

In recent years, lignin has been utilized for several value-added applications such as blenders with polyphenols, giving UV stabilization and protection, blending with poly(lactic acid) (PLA) to give 100% renewable resins or implementing uses of its antioxidant and antimicrobial properties.[23] For more extensive applications of lignin, research strategies are directed towards its efficient revalorization to discrete monomers or classes of lower molecular weight aromatics. These include compounds such as phenols, aromatic acids, esters, ethers, etc., which are currently obtained as petrochemical products. This is possible by developing controlled C–C or C–O bond cleavage in lignin by selective catalytic depolymerization technique. Besides this, there have been few articles focused on harnessing the multi-functionl nature of lignin/lignin derivatives as catalysts in organic synthesis. Both these topics of lignin as a substrate and as a catalyst have been researched upon in this dissertation and shall be elaborated with our findings in the upcoming chapters.

5. Catalytic lignin depolymerization (downstream approach)

Over the last few decades, there have been numerous strategies devoted towards the catalytic degradation of lignin β-O-4 model compounds and extracted lignin samples through reductive,[24] redox-neutral,[25] oxidative,[26-28] acid-[29] and base-[30-33] catalyzed cleavage pathways. Since the current scope of our findings is limited to base-catalyzed and oxidative cleavage pathways, only research interests pertinent to these two fields shall be discussed.

5.1. Homogeneous base-catalyzed lignin depolymerization

Homogeneous alkaline catalysis is one of the extensively studied lignin depolymerization pathways. Most of the reports on the base-catalyzed depolymerization approaches highlight the advantage of using cheap and readily available reagents (NaOH, KOH, $Ca(OH)_2$, LiOH, etc).[30] As mentioned before, some of the common industrial pretreatment processes (kraft and soda pulping) use sodium hydroxide (NaOH) as a catalyst (often in combination with anthraquinone)[20a] to remove lignin from biomass and retain the polysaccharides.[20, 30n] According to the previous reports and a recent computational study by Yu *et al.*, a base-initiated β-O-4 bond cleavage reaction, for both upstream and downstream processes, could follow a similar degradation pathway. This includes a nucleophilic attack of the deprotonated hydroxyl groups present at the α-position of the β-O-4 ether bond to the neighbouring aroxy substituent, thus eliminating a guaiacolate and forming an oxirane intermediate.[31, 32] Schemes II.1. and II.2. illustrate the cleavage reactions of β-O-4 bonds with phenolic and non-phenolic aryl substituents by nucleophilic reaction during an alkaline process.[30, 31]

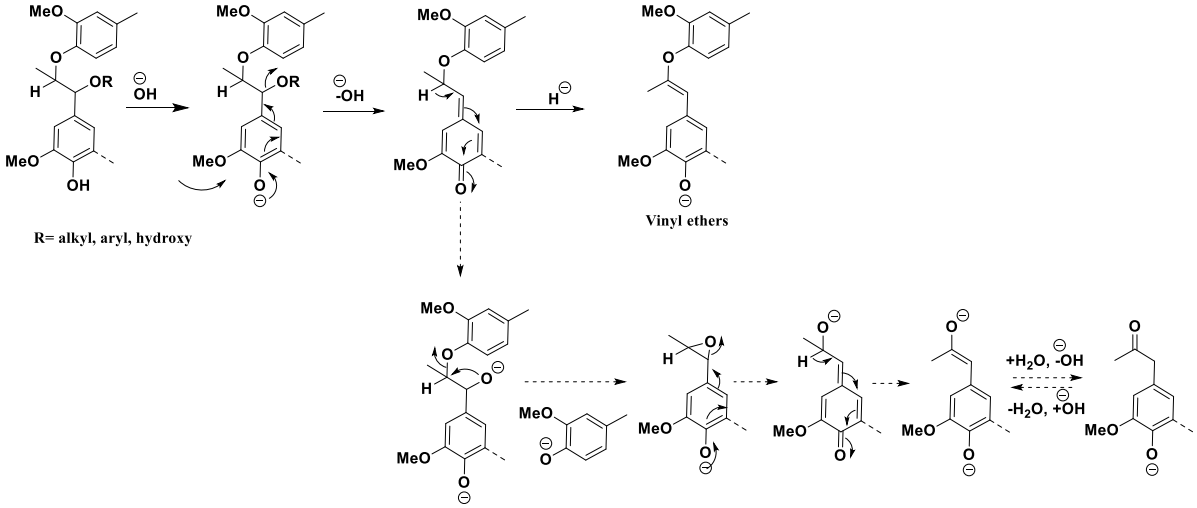

Scheme II.1. Reaction of phenolic β-O-4 linkages in an alkaline process.

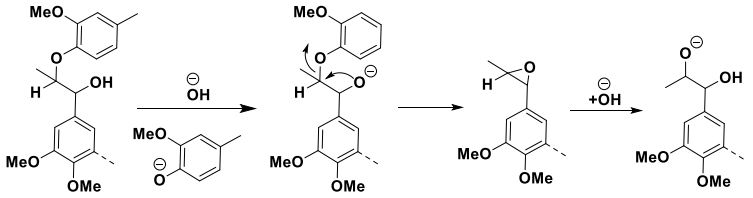

Scheme II.2. Reaction of non-phenolic β-O-4 linkages in an alkaline process.

One of the earliest downstream studies was conducted in 1994 by Thring using an Alcell lignin with NaOH. The main focus was to monitor the effect of time and temperature on the distribution of liquid products, which were obtained in about 30% yield.[30a] This was followed by a series of two-step lignin depolymerization strategies investigated by Shabtai, Chornet, Johnson and co-workers.[30c-h] These reactions were mainly conducted on pulping lignins with the first step being a base-mediated degradation (NaOH) process followed by an additional catalytic hydrodeoxygenation step to finally produce the gasoline-range aromatic fuels. Chornet also developed a fractionation procedure to obtain various lignin-derived aromatic monomers from base-promoted degradation processes involving a series of extraction, distillation, chromatography, and crystallization steps.[30h] During the same time, the research group of Miller also investigated the base-catalyzed lignin depolymerization using a mixture of solvents (alcohols

and water). The studies investigated the effect of base, temperature as well as the lignin to solvent ratio on the overall reaction outcome.[30i] With alcohols as solvent for the lignin model compound studies, it was observed that the depolymerization was first initiated by the solvolysis of the ether linkages (Scheme II.3.). It was also found that molar excess of a strong base gave better results. Similar efficiency could be obtained by combining lower quantity of a strong base with larger amounts of a weaker base. In another study carried out in water, they compared the reactivity of a number of alkali and alkaline-earth metal bases (LiOH, NaOH, Na_2CO_3. KOH, CsOH, $Ca(OH)_2$). Their studies reflected that stronger bases such as NaOH and KOH favoured more conversion and hence gave higher yields of low molecular weight species than LiOH (weak base).[30c,j]

Recently, Beckham and co-workers reported the base-initiated depolymerization of lignin-rich biomass obtained from the conventional and emerging biochemical conversion processes.[30s] The depolymerization studies included the effect of NaOH concentration as well as the variation in reaction temperatures (270 °C, 300 °C and 330 °C) on the depolymerization of the residue to low molecular weight, water soluble species. The authors further highlighted that the yield of water soluble fraction depended on the biomass pretreatment methods used prior to the base-catalyzed depolymerization (BCD) and therefore an acid pretreatment resulted in the lowering of aqueous yields. They were also able to tune the product selectivity with respect to the reaction temperatures, thus affording the methoxyphenols at a lower temperature and benzenediols, with a greater extent of alkylation on the aromatic rings, at a higher reaction temperature. Cumulatively, these results indicated that a significant fraction (45−78%) of the starting lignin-rich material could be depolymerized to low molecular weight, water soluble species.

Most of the above-mentioned BCD reactions were carried out at elevated temperatures between 200 °C to 340 °C and were generally accompanied by high pressures. Although these conditions were optimized to give high conversions and oil yields (organic solvent soluble products with lower molecular weight relative to parent lignin), the quantity of mono-aromatic products obtained from lignin was low with decreased product selectivities. One reason for this was contemplated to be the secondary side reactions taking place between the reactive phenolate and aldehyde/ketone intermediates formed after the β-O-4 bond cleavage reactions.

Similar observations were reported by Lercher and co-workers where the proposed BCD pathway involved the formation of a sodium cation-lignin adduct, leading to the polarization of the ether bonds followed by a heterolytic cleavage reaction (Scheme II.3.).[30m]

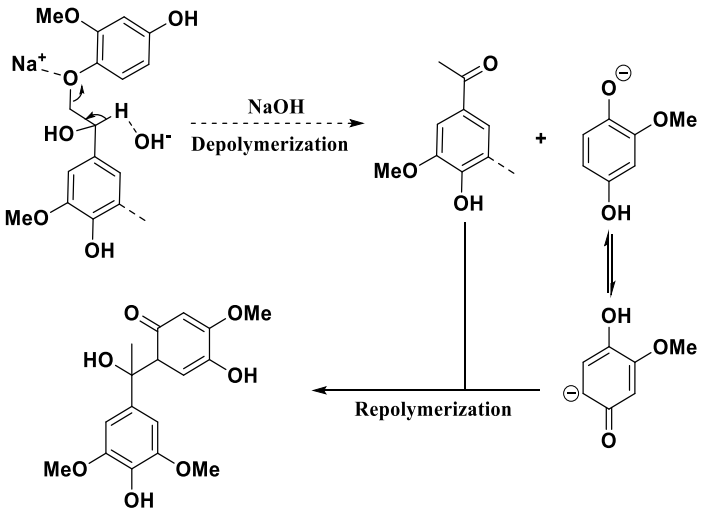

Scheme II.3. Repolymerization reaction initiated between a phenolate and acetophenone.

The degradation products included a phenolate and an intermediate carbenium ion, which was neutralized by a hydroxide ion and rearranged to give an acetophenone derivative. The phenolate was further speculated to readjust its charge and form a carbanion that could further initiate the repolymerization reactions by aldol addition as shown in Scheme II.3. To circumvent this issue and obtain higher yields for the monomer rich oil fractions, the use of boric acid as capping agents was proposed. This was forseen as a way to protect the phenolic OH- groups and prevent further product repolymerization.[30m] Thus under the optimized reaction conditions capped phenolic esters were formed which resulted in increased oil yield from an average of 25 wt% to 52 wt% (w(oil)/w(starting lignin)).

The research group of Labidi also reported their findings on BCD of organosolv lignin from olive prunings. Their first investigations, without any capping reagent, resulted in oil yields between 5% and 20%. These were reported after the acidification of the reaction mixtures to pH 1−2 and the subsequent extraction of the acidified liquid phase with ethyl acetate.[30o] They further observed that the addition of phenols, as capping agents, to the BCD reaction was able to drastically improve the oil yield, provided the phenol to lignin ratio was optimized. The main monomeric products observed after the phenolic capping included cresols, catechols and ferulic acid.[30p]

It is worth noting that although attributed as a base-catalyzed approach, most of the aforementioned studies have been conducted using stoichiometric amounts of bases in relation to the monomer units present in lignin.[30b-f, m-o,s] The catalyst loadings have often been reported in wt% relative to the weight of the solvent and not lignin.[30b-q,s] For example, one commonly employed reaction condition using NaOH as base requires 10% (w(lignin)/w(solvent)) lignin loading and 2% to 4% (w(base)/w(solvent)) base loading.[10d,l-n,s] The catalyst base loadings relative to lignin are therefore actually between 20 wt% and 40 wt%.

5.2. Heterogeneous base-catalyzed lignin depolymerization

The successful outcomes from base-promoted lignin degradation studies in a homogeneous system subsequently encouraged investigations into the heterogeneous base-catalyzed lignin degradation pathways. The driving force being the developement of a more economical process that enhances the chances of catalyst separation and recycling. For this purpose, layered double hydroxides (LDH) such as hydrotalcite $Mg_6Al_2(OH)_{16}(CO_3)\cdot 4H_2O$ (HT) have often been employed in combination with other metal catalysts.[33] The positively charged brucite-type layer with interstitial anions offer a range of tunable sites as both the metals in the brucite layers and the anions in the interstitial layers are easily exchangeable. Hence the LDHs can either be used directly or as an active support for metal ions to initiate catalysis.

The nickel supported on hydrotalcite (Ni/HT) is one such example of HT supported metal ions that were applied to cleave the β-O-4 ether bond in the lignin model compound, 2-phenoxy-1-phenethanol (**PE**). At 270 °C with 5 wt% Ni/HT catalyst, a conversion of >90% was achieved with phenol and acetophenone being the major cleavage products (Scheme II.4.).[33e] Here, it is hypothesized that Ni/HT could depolymerise lignin by a base-catalyzed mechanism mediated by the hydroxide anions in the brucite-

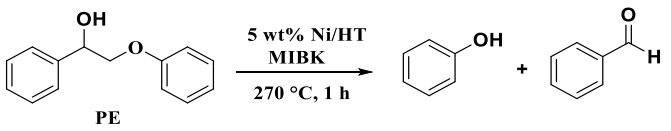

Scheme II.4. Ni/HT catalyzed cleavage of β-O-4 bond in lignin model compound **PE**.

layers of the hydrotalcite. The nickel metal was speculated to play an important role by forming a strong interaction with the ether oxygen which weakened the C–O bond and hence promoted cleavage. The same catalyst was also effective in the depolymerization of organosolv and ballmilled lignin, resulting in a mixture of alkyl-aromatic products.[33e]

Furthermore, Ford and co-workers extensively studied the conversion of organosolv lignin over a hydrotalcite-derived Cu-doped porous metal oxide (PMO) catalyst at 300 °C in supercritical methanol.[33c] A similar reaction system was also employed on cellulose and crude lignocellulosic biomass.[33d] Due to the highly reductive and deoxygenative environment, the main products observed were cyclohexanol derivatives. To tune the product selectivity of the Cu-PMO system towards the generation of aromatic compounds, Barta *et al.,* carried out the depolymerization of organosolv lignin in supercritical methanol under relatively milder reaction conditions.[33f]

Another report, directed towards the use of a solid base catayst for lignin depolymerization, highlighted MgO as a suitable catalyst that led to the depolymerization of pine lignin in THF at 250 °C, yielding around 13% of phenolic monomers.[33g] The major drawback for this method was the formation of higher molecular weight recondensed solid residue post the lignin degradation reaction.

Beckham and co-workers also developed a nitrate-intercalated hydrotalcite catalyst to cleave the *β*-O-4 linkages in monolignol 2-phenoxyl-1-phenethanol (**PE**) resulting in phenol, acetophenone and 1-phenethanol as the major cleavage products (Scheme II.5.).[33h] The system was further extended to evaluate the depolymerization of lignin-enriched substrates at 275 °C, thus producing 8% yield for monomers. The use of high temperature, difficulties in effective recycling of catalyst and low yields with lignin substrates were the shortcomings of this study.

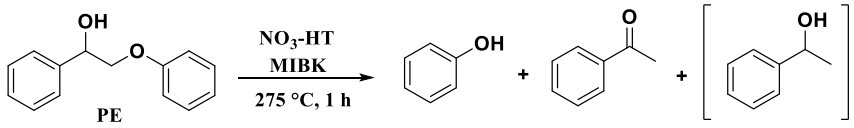

Scheme II.5. NO_3-HT catalyzed cleavage of *β*-O-4 bond in lignin model compound **PE**.

A recent report by Chaudhary *et al.,* explored the depolymerization efficiency of alkaline lignin using a solid base catalysts including zeolites (NaX, NaY, NaP, KLTL), anionic clay (Hydrotalcite), single metal oxides (MgO, CaO) and hydroxyapatite (HAP).[33i] The reactions were performed at 250 °C and the resulting oil yields varied between 10–51% with the maximum yield (51%) corresponding to the NaX catalyst. The oil included a range of mono-aromatic products such as substituted phenols, vanilin and eugenol. It is however noteworthy, that the base was employed in stoichiometric amounts with a lignin to catalyst mass ratio being maintained at 1:1 and significantly decreased yields for low molecular weight products (monomers to trimers) was observed (51% to 34%) in the first catalyst recycle run.[11g]

Having learnt the above-mentioned conditions, one of the primary aims of this dissertation has been to develop an actual base-catalyzed lignin depolymerization approach. Considering the previously mentioned limitations related to product re-condensation and catalyst loadings, the base amounts were restricted to 10 wt% (w(base)/w(lignin)) and dimethyl carbonate (DMC) was applied both as a solvent and as a capping agent.[30r] This system has been further elaborated upon in the results and discussion section of the thesis.

5.3. Oxidative lignin cleavage

Lignin cleavage reactions proceeding through oxidative pathways form another extensively investigated area of research in the field of biomass valorization. Several research articles displaying homogeneous[26] and heterogeneous[27] metal-catalyzed oxidative depolymerization routes for lignin model compounds and lignin have been published over the years, thus highlighting the vast potential of this approach. Along the same line of research, Bolm and co-workers also studied the oxidative lignin depolymerization reactions using homogeneous iron, copper, and vanadium catalysts and heterogeneous transition-metal containing hydrotalcites (HT-Cu-V) systems.[26 w.x] Though successful, several of these reactions employ harsh reaction conditions that not only promote oxidation of the polymer but also lead to C–C/C–O bond cleavage reactions. Such multiple reactions taking place in parallel makes it difficult to control the overall product yields and selectivities owing to the highly complex nature of the system.

5.3.1. Cleavage of lignin by two-step depolymerization strategy

Realizing the need to develop the selective depolymerization approaches for oxidative cleavage of the biopolymer, several research groups in the recent past have focused on the selective oxidation of alcohol units present in the abundantly found β-O-4 linkages within the lignin structure.[28] This approach is further supported by the DFT calculations indicating that the C–O bonds of the β-O-4 linkage are significantly weakened (~14 kcal·mol^{-1}) upon the oxidation of the α- or γ-carbons.[34] These C–O bonds in the oxidized lignin, therefore become relatively easier targets to cleave and give higher product selectivities after the two-step degradation strategy.

Although energetically favourable, up until now these two-step oxidative depolymerization pathways described in literature mostly exemplify the degradation reactions following a secondary (benzylic) alcohol oxidation route (Scheme II.6.; Top). Described below are the recent examples highlighting such chemoselective oxidation reactions in lignin model compounds and lignin.

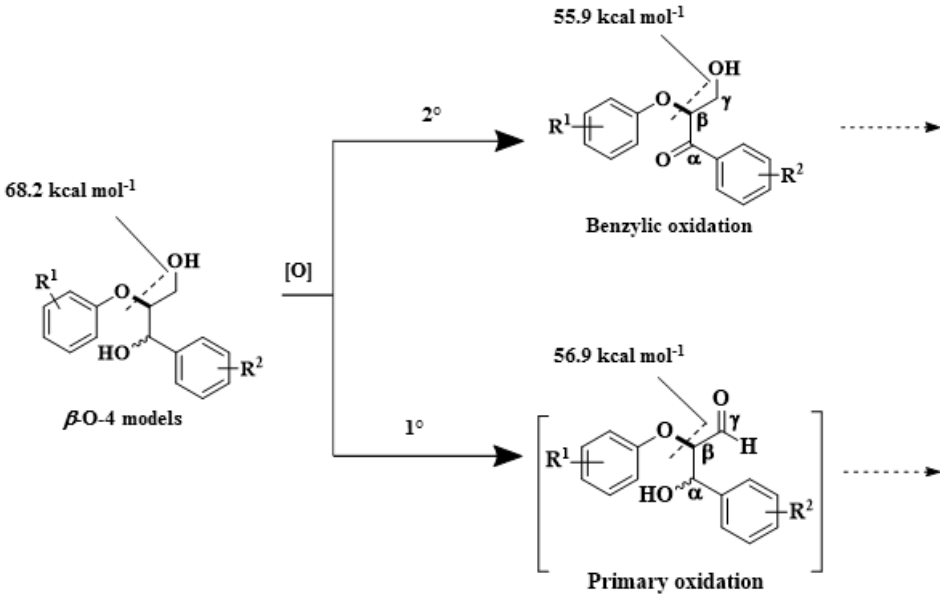

Scheme II.6. Bond dissociation enthalpies indicating the weakened β-O-4 linkages after alcohol oxidation.

5.3.1.1. Cleavage reactions proceeding through benzylic alcohol oxidation

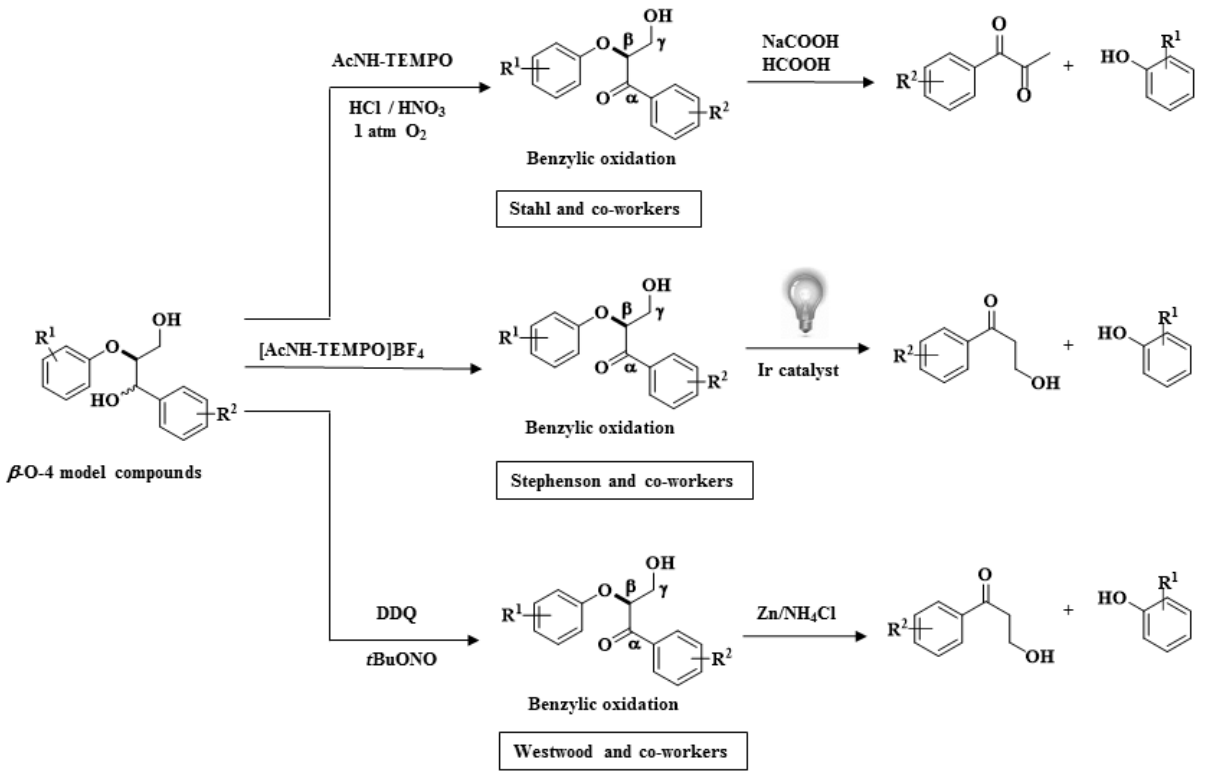

Scheme II.7. Chemoselective benzylic alcohol oxidation in 1,3-dilignols followed by C–O/C–C bond cleavage.

One of the first reports, primarily aimed at the chemoselective benzylic oxidation of advanced lignin *β*-O-4 model compounds (1,3-dilignols), was published in 2013 by Stahl and co-workers.[28b] The authors carried out an extensive screening of conventional reagents for alcohol oxidation, that eventually concluded with TEMPO-based reagents to be the best catalytic system in combination with inorganic nitrogen oxide as a co-catalyst. Thus, 5 mol% AcNH-TEMPO in combination with 10 mol% HNO_3 and 10 mol% HCl as co-catalysts in CH_3CN:H_2O (19:1) as the solvent under 1 atm O_2 at 45 °C for 24 h gave excellent yields of benzylic oxidation for a wide range of dilignols (Scheme II.7, top). A follow up publication by the same authors focused on the subsequent formic-acid-induced degradation of oxidized lignin model compounds that resulted in mono-aromatics formed primarily after the C–O bond cleavage reactions.[28c] This system was further applied for the depolymerization of an aspen lignin sample following a similar two-step approach. Here, the system again proved to be effective in first selectively oxidizing the lignin sample and then cleaving the bonds using a formic acid/sodium formate initiated C–O bond cleavage. The yields for the identified aromatics were obtained in as high as 52 wt% of the original lignin sample.

Stephenson and co-workers also established a two-step redox-neutral method for the oxidative cleavage of a similar set of dilignol model compounds (Scheme II.7, middle).[25h] The oxidation step was carried out using stoichiometric amounts of Bobbit's salt [4-AcNH-TEMPO]BF_4, followed by the C–O bond cleavage reactions using an iridium based photocatalyst in combination with the visible-light. The reactions were further shown to be effective using batch-flow reactors, where the oxidative step was performed in batch and the consecutive C–O reductive cleavage reactions were carried out in a flow set-up. However, bearing in mind the potential problems of irradiating dark colored lignin samples, both the steps were shown to be effective in a flow reactor system even in the presence of a lignosulfonate additive. It is however important to note that the applicability of this system still needs to be tested on real lignin samples.

Following the similar approach towards chemoselective benzylic oxidation and successive cleavage studies, Westwood and co-workers studied the oxidation of 1,3-dilignol model compounds using catalytic amounts of 2,3-dichlor-5,6-dicyano-1,4-benzochinon (DDQ) in combination with *tert*-butyl nitrite (*t*BuONO) and oxygen as a secondary oxidant.[28e] The DDQ/*t*BuONO/O_2 catalytic system with 2-methoxyethanol as solvent gave excellent selectivity and reactivity towards the oxidation of the benzylic alcohols for a range of model compounds. This was followed by reductive C–O bond cleavage using zinc/ammonium chloride (Zn/NH_4Cl) system. The two-step approach was also shown to be effective for the one-pot depolymerization of organosolv birch wood lignin. The mono-aromatic products were further reported to be isolated in 6 wt% with respect to the lignin starting material (Scheme II.7, bottom).

Another selective benzylic alcohol dehydrogenation of the lignin *β*-O-4 model compounds to the corresponding ketones was introduced by Dawange *et al*.[28f] They employed the use of a heterogeneous Pd/C catalyst in combination with additives in an EtOAc/H_2O solvent system giving corresponding ketones without C–O or C–C cleavage or *γ*- alcohol dehydrogenation (Scheme II.8.). The best additive found for this oxidation system employed the use of 0.4 equivalent of glucose, whose role was sought to prevent the aggregation of palladium and stabilize it on the support. However, once again the system was not explored on real lignin samples.

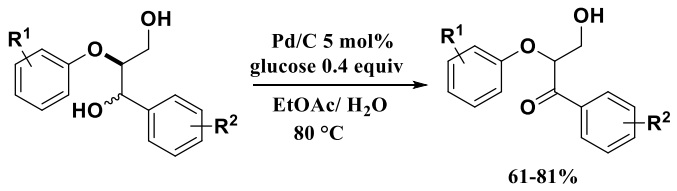

Scheme II.8. Pd/C catalyzed oxidation of 1,3-dilignols.[28f]

An article by Wang and co-workers elaborated upon the two-step catalytic C–C bond cleavage of lignin *β*-O-4 models to aromatic acids and phenols.[28h] The benzylic oxidation was catalyzed by a $VOSO_4$/TEMPO [(2,2,6,6-tetramethylpiperidin-1-yl)oxyl)] catalyst in the presence of oxygen. In the second step, the C–C bond of the oxidized model compound was selectively cleaved to acids and phenols by oxidation over a Cu/1,10-phenanthroline catalyst. The computational investigations suggested a copper-oxo-bridged dimer as the catalytically active site for hydrogen-abstraction from C_β–H bond, which was the rate-determining step for the C–C bond cleavage (Scheme II.9, top). The same group recently published another article on the depolymerization of lignin in a two-step reaction sequence following a O_2/$NaNO_2$/DDQ/NHPI system catalyzed benzylic alcohol oxidation route (Scheme II.9, bottom). The subsequent C–C bond cleavage step involved the hydrogenation of the oxidized intermediate by a NiMo sulfide catalyst.[28i]

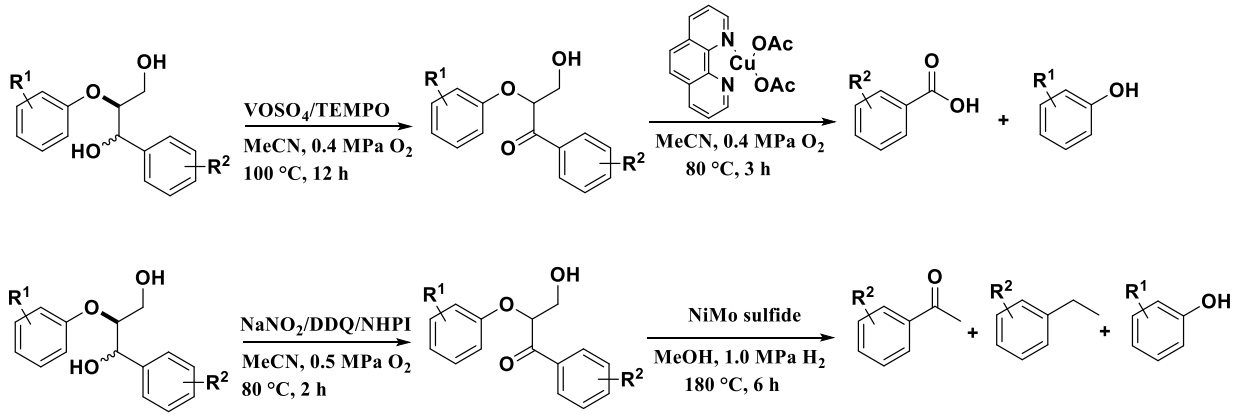

Scheme II.9. Two-step depolymerization reactions proceeding through benzylic alcohol oxidation.[28h,i]

6. Lignin as a catalyst for organic transformations

Besides depolymerization of lignin, the biopolymer and its derivatives have also been employed as catalysts in chemical reactions. Being readily available, this natural biopolymer represents a cost-effective and biodegradable catalyst system.

In this context, lignin-derived carbonaceous catalysts (LCC) have already been reported as efficient solid-acid catalysts, obtained after sulfonating the polymer with concentrated sulfuric acid (Scheme II.10). For example, Zhou and co-workers demonstrated an efficient process for the production of 5-hydroxymethylfurfural (5-HMF), formed after the solid acid-catalyzed dehydration of glucose and fructose monomers.[35] Using LCC, Guo *et al.,* also reported an esterification reaction for the synthesis of biodiesel from acidified soybean soapstock containing 56% fatty acids.[36] The catalyst was not only found to be more efficient than the corresponding sulfuric acid but was also recycled for upto three times. Dai and co-workers further modified the lignin residue to form a magnetic-LCC catalyst containing Fe_3O_4 component in addition to -SO_3H, - COOH and phenolic -OH groups of the lignin polymer.[37] This catalyst was also shown to be effective for the conversion of fructose to 5-HMF. The same transformation was studied by Xie *et al*., using ionic liquids as solvent and solid lignosulfonic acid (LSA) as catalyst.[38] A yield as high as 93% could be achieved for the formation of 5-HMF in only 10 min under mild conditions. The catalyst once again proved to be reusable while retaining its catalytic efficiency. In addition to the above, Sun and co-workers, for the first time, demonstrated an extensive application of lignosulfonic acids (LSA) as recyclable heterogeneous catalysts for some one-pot multicomponent reactions.[39] These include reactions such as benzoxanthene and amidoalkyl naphthols synthesis, Hantzsch reaction, and Strecker reactions.

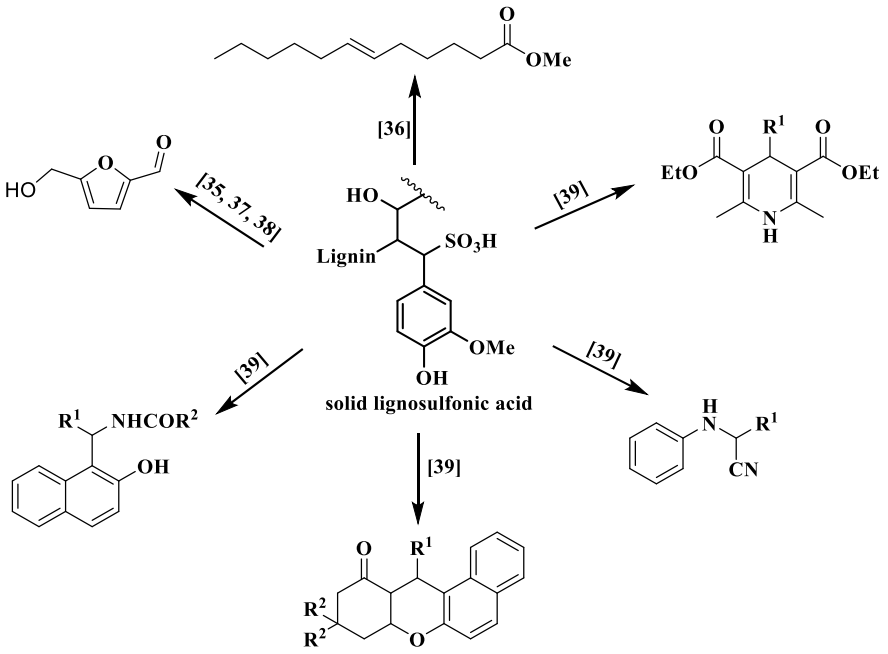

Scheme II.10. Solid lignosulfonic acid-catalyzed chemical transformations.[35-39]

Besides using sulfonated lignin as catalysts, Liu and co-workers also reported the direct use of lignin as a green catalyst by harnessing the inhernet functionalities of the polymer, without further structural modifications (Scheme II.11).[40] The lignin obtained after enzymatic hydrolytic treatment of corn stover (EHL) in combination with potassium iodide (KI) was shown to catalyze the chemical fixation of carbon dioxide with epoxides to form cyclic carbonates. Motivated by the above-mentioned works of directly applying lignin as cheap, reusable, and efficient catalysts, this thesis also includes our attempts made

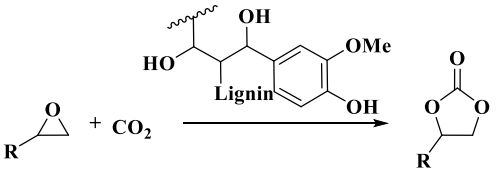

Scheme II.11. Lignin-catalyzed synthesis of cyclic carbonates from epoxides and CO_2.[40]

towards the lignocellulosic-catalyzed organic reactions. The approach further highlights an important alternative way of utilizing the biopolymer, besides focusing on its depolymerization route, to achieve the goals of residual lignin valorization.

7. Mechanochemistry and its application in lignocellulosic biomass

7.1. Mechanochemistry

Mechanochemically activated transformations date back to earlier times when mechanical force was applied manually (mortar and pestle) for crushing, grinding and mixing of both edible and non-edible substances.[41] Nowadays, mechanochemical techniques find similar application in large scale industrial milling processes where the energy comes from a typical ball mill, and is exploited mainly for crushing large chunks of ores and minerals to reduce their particle size and allow effective mixing.[41] Over the decades, mechanochemistry has also found applications in chemical and pharmaceutical laboratories for the activation of various chemical reactions.[42] These include fields pertinent to organic,[43] inorganic,[44] organometallic,[45] polymer,[46] enzyme,[47] supramolecular,[48] coordination,[49] medicinal chemistry,[50] and many more. The mechanochemically induced reactions are believed to take place by the direct absorption of mechanochemical energy,[51] contrary to chemical reactions initiated by thermal energy inputs such as heating, absorption of photons (photochemistry) or electrochemical energy.

Besides enabling the reduction of solvents during solvent-free grinding or liquid assisted grinding (LAG), a typical milling reaction often includes other advantages over solution chemistry such as shorter reaction times along with high throughput screening.[51] It also provides a platform to use reagents having poor or no solubility and hence low performance in organic solvents.[43d] This, in turn, helps surpass the need to employ biphasic solvent systems to achieve high reactivity. Along with these benefits, mechanochemical energy has also been reported to induce reactivity differing from those in the solution counterparts.[52] This further elaborates the potential of mechanochemistry to help in exploring different or unexpected reaction pathways.[53]

7.2. Types of milling media

A typical laboratory scale mechanochemical reaction relies on the energy input supplied by grinding (either manually or in ball mills), shearing and stretching.[54] Although there are several examples reported by manual grinding using the conventional mortar-pestle, the biggest drawback of this technique is its poor reproducibility and difficulty while scaling up a process.[42] Hence, automated milling medias including ball mills (**BM**), disc mills (**DM**) and mortar-pestle mills (**MPM**), are superior alternatives to carry out milligram to kilograms scale transformations under defined and consistent milling conditions.[43b]

A general automated milling setup includes milling jars in combination with milling balls in the case of a ball mill or milling vessels with either a disc (disc mill) or a connected pestle (mortar and pestle mill).

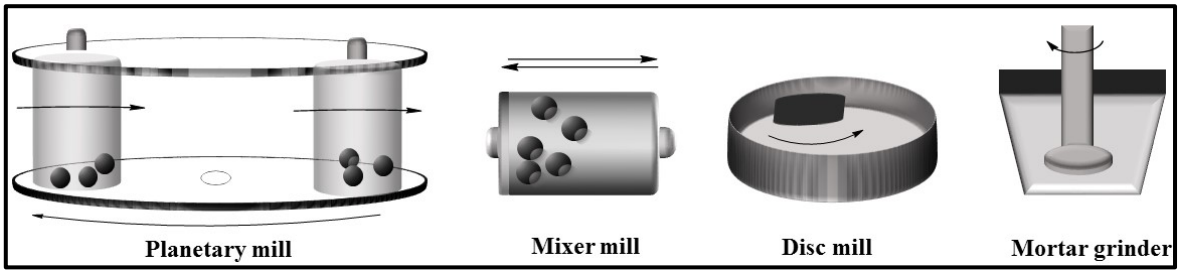

Figure II.2. Schematic representation of the commonly used milling equipments.

The reactants are transferred into the above-mentioned milling medias and subjected to one or several milling cycles under desired milling parameters (time, rotation speed, no. of balls). The types of ball mills included in our study are planetary and mixer mills. While in the planetary mill (**PM**) the rotation of the milling jars/balls is opposite to that of the bottom disc resulting in centrifugal trajectories, the mixer mill (**MM**) generates energy by oscillating the milling jars at variable frequencies on a horizontal plane. This causes the collosions to occur with the top and the bottom ends of the beaker (Figure II.2). Furthermore, depending on the required energy input to carry out reactions, the milling vessel and milling balls can also be varied from lighter (low energy input) material such as agate (2.7 $g \cdot cm^{-3}$), zirconium dioxide (ZrO_2, 5.7 $g \cdot cm^{-3}$) to relatively heavier (high energy input) materials like stainless steel (SS, 7.8 $g \cdot cm^{-3}$) and tungsten carbide (WC, 15.6 $g \cdot cm^{-3}$).

7.3. Application of mechanochemical energy on lignocellulosic transformations

Mechanochemistry finds a special application in the particle size reduction of lignocellulosic biomass. The mechanical refining (shearing, grinding and milling) of woodchips is mostly done using ball mills, extruders or disk mills.[55] Furthermore, ball mills have also been utilized to reduce the particle size of cellulose[56], chitosan[57] and lignin[58].

Besides their ability to decrease the particle size, mechanochemical activations are now being recognized as a valuable tool to initiate specific chemical bond cleavage reactions. This is contrary to their general application to catalyze bond formation, specially in the case of biomass valorization. The important aspect of utilizing these solvent free milling techniques is that they help bypass the solubility concerns faced when working with lignocellulosic materials, reagents, and catalysts of different solubility profiles.

In line with this approach, Hick *et al.,* published an article on the mechanocatalytic depolymerization of cellulose to glucose achieved by milling the biopolymer in the presence of heterogeneous catalysts such as clays.[59] They showed that milling the water insoluble cellulose with a cheap layered heterogeneous catalyst such as kaolinite resulted in high conversions and good yields of glucose monomer along with the detection of some dehydration products such as levoglucosan, levoglucosenone and 5-hydroxymethyfurfural. The method was further mentioned to be efficient for the conversion of cellulose even in the presence of lignin and other traces of hemicellulose, thus allowing any cellulosic biomass source to be utilized.[59] Following a similar pathway, Rinaldi and Schüth also reported on a mechanocatalytic, solid-state depolymerization of cellulose impregnated with catalytic quantities of H_2SO_4 to monomeric glucose. This step, when combined with Ru/C catalyzed hydrogenolysis in water, resulted in the formation of hexitol in 94% yield.[60]

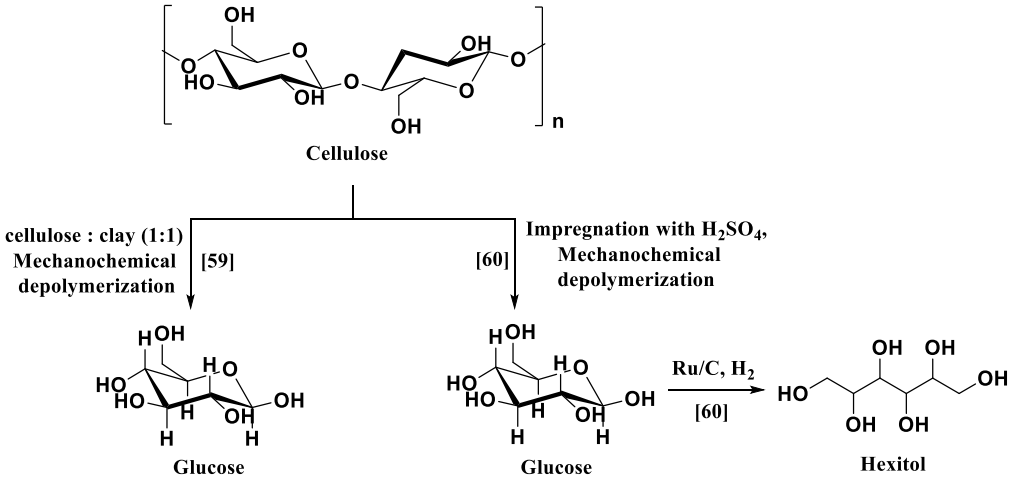

Scheme II.12. Depolymerization of cellulose to glucose under milling conditions using acid/base catalysts.[59,60]

Additionally, Rinaldi and co-workers published a series of reports highlighting the effect of mechanical grinding on Brønsted acid (H_2SO_4 or HCl) pre-impregnated lignocelullosic fibres.[61-63] The mechanical energy here was believed to force the dormant state, generated by impregnating the lignocellulosic fibers with a Brønsted acid catalyst into action, hence resulting in a mixture of water soluble products which comprised of oligosaccharides and lignin fragments.[61] Although, heating the above acidic aqueous solution at 145 °C resulted in the full saccarification (> 80−90% yield for glucose and xylose), lignin was obtained as a precipitate without any depolymerization.[62] Furthermore, these water-soluble oligosaccharides were also applied as a useful feedstock for the high yield production of 5-hydroxymethylfurfural (HMF) and furfural in biphasic reactors.[63]

With the aim to utilize the mechanical energy for the depolymerization of lignin, Bolm and co-workers developed a base-catalyzed depolymerization (BCD) approach on lignin β-O-4 model compounds and lignin using readily available solid bases in planetary ball mills (Scheme II.13).[64]

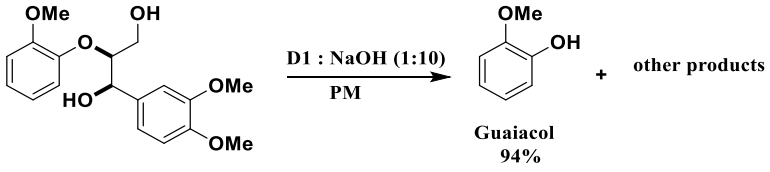

Scheme II.13. Mechanochemically initiated BCD of lignin β-O-4 model compounds.[64]

A recent article by Chen *et al.,* also highlighted a more efficient solvent-free milling of chitin to lower molecular weight chitosan in the presence of catalytic amounts of base (Scheme II.14).[65]

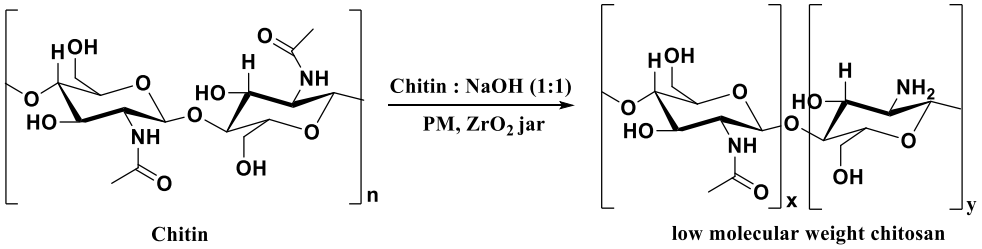

Scheme II.14. Mechanochemically initiated BCD of chitin to chitosan.[65]

8. Aim of this work

This work has been directed towards the valorization of lignin. The aim can be achieved either by conducting selective lignin depolymerization reactions to lower molecular weight products of commercial viability or by the direct utilization of the biopolymer itself. Keeping in mind both these approaches, this thesis has been further subdivided, based on the different reactions pathways employed (base-catalyzed or oxidative degradation) and degradation techniques used (solution or solvent-free reaction).

The first three projects of this dissertation deal with the selective cleavage of lignin using base-catalyzed and oxidative cleavage pathways while the last part lays emphasis on the application of lignin as a catalyst in the Strecker reaction under mechanochemical conditions. To understand the activity and selectivity of the reaction systems, as well as to elaborate upon the mechanistic aspects, lignin model compounds have been utilized initially for all the mentioned cleavage studies. Different organosolv lignins and kraft lignin were subsequently utilized for studies with the natural polymer. Detailed comparative studies on the biopolymers were done using 2D-NMR, ^{31}P NMR, GPC, GC-MS, IR and TGA analysis.

III. Results and Discussions

1. Base-catalyzed cleavage of lignin β-O-4 model compounds and lignin initiated by alkali metal bases in dimethyl carbonate

Research Background

One of the goals of this work has been to develop a suitable base-mediated catalytic system that promotes the efficient cleavage of lignin interconnecting bonds and simultaneously curtails the probability of re-polymerization of the formed phenolic monomers. Along these lines, considering the low cost of the commercially available alkali metal bases and the prevalence of β-O-4 linkages in lignin,[9,12.13] the optimization studies initially focused on the base-catalyzed depolymerization (BCD) of lignin β-O-4 model compounds. These model compounds were synthesized following published procedures.[64,66] The identification of cleavage products from these preliminary studies was forseen as an opportunity to develop a better understanding of the involved reaction pathways. This was important before performing catalytic reactions on the actual lignin macromolecule, where the complexity of the polymer would eventually pose a major hurdle while investigating the intricate reactivity details.

A literature survey led us to an article by Hartwig and co-workers which elaborated on the cleavage of a β-O-4 model compound such as **D1** using stoichiometric amounts of a strong base (NaO*t*-Bu) at 100 °C in *m*-xylene, thus yielding guaiacol in 89% along with numerous other products after a 2 h reaction (Scheme III.1).[24b] These findings were in relation to previous base-promoted degradation approaches where the monomer yields dropped due to the reactive nature of the formed phenolic/ aldehyde products under basic conditions. Capping these products was thus speculated to be one way of increasing the yields of mono-aromatics obtained post lignin degradation.[29m,p] While developing such a strategy, we came accross the reagent dimethyl carbonate (DMC), which had been used previously for the methylation of kraft lignin.[67]

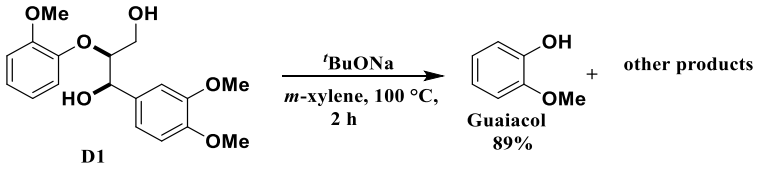

Scheme III.1. Base-promoted cleavage of β-O-4 model compound **D1** by Hartwig and co-workers.[24b]

DMC is a versatile compound applied in organic synthesis as a non-toxic and biodegradable carboxymethylating and methylating reagent (Scheme III.2).[67,68] At temperatures >90 °C DMC is known to generate methoxylates in the presence of catalytic amounts of base. Recognizing the potential of this chemical nature of DMC, we anticipated to get methoxy-capped cleavage products, from our studies, that would be less prone to secondary reactions.

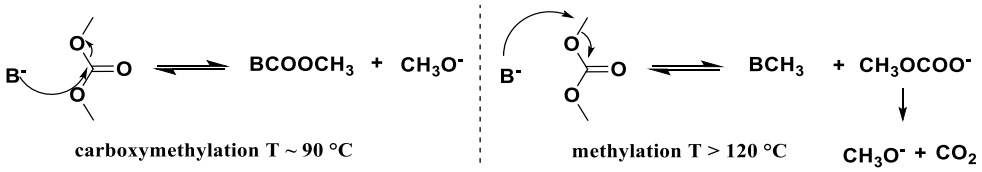

Scheme III.2. Temperature dependent carboxymethylation and methylation reactions of dimethyl carbonate in the presence of catalytic amounts of base (B^-).

1.1. Cleavage studies of lignin β-O-4 model compounds in dimethyl carbonate

The screening for the base-catalyzed degradation (BCD) reactions of dimeric lignin model compounds were performed with *erythro* dilignol **D1** on a 0.25 mmol scale. Sodium hydroxide (NaOH) was chosen as a standard inorganic base catalyst in the presence of dimethyl carbonate (DMC). The carbonate derivative in our system served both as a capping reagent and a solvent.

Initial reactions focused on the effect of reaction temperature and time on the conversion of **D1**. Base loading for these reactions was 0.5 equivalents in 1.3 mL DMC. The progress of the reactions was monitored by thin layer chromatography (TLC) analysis. Monocarboxylated (**MC**) and dicarboxylated (**DC**) products were first purified and characterized by ^{1}H NMR, ^{13}C NMR and HRMS measurements. After evaluating their corresponding signals, the conversion of **D1** and yields for **MC** and **DC** products were determined by quantitative ^{1}H NMR analysis of the crude reaction mixture with respect to 1,4-dinitrobenzene as an internal standard.

Table III.1: Effect of temperature on the conversion of dilignol **D1**.[a]

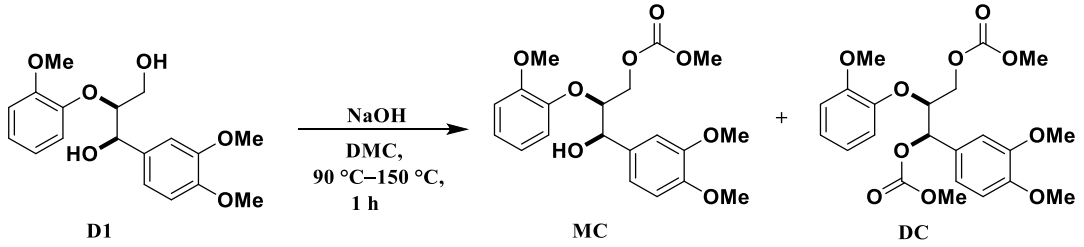

Entry	Temp [°C]	Conversion [%][b]	Product yields [%][b]	
			MC	**DC**
1	90	20	19	-
2	110	59	44	13
3	135	>99	65	35
4	150	>99	-	99
5	180	>99	-	99

[a] Reaction conditions: **D1** (83.6 mg, 1.0 equiv), sodium hydroxide (5.0 mg, 0.5 equiv), DMC (1.3 mL), 1 h. [b] Converisons and yields determined by ^{1}H NMR with respect to 1,4-dinitrobenzene as internal standard.

Table III.1 illustrates the effect of temperature on the conversion of dilignol **D1** in the temperature range from 90 °C to 180 °C. After 1 h of reaction time at 90 °C, a conversion of 20% was observed leading to the formation of γ-capped monocarboxylated product **MC** in 19% yield. An elevation of 20 °C resulted in increased reaction rates with the conversion of **D1** reaching 59%. This was accompanied by the formation of 44% **MC** along with the formation of dicarboxylated product **DC** in 13% yield. A further increase in the reaction temperatures between 135 °C to 180 °C resulted in full conversions for **D1** with the product ratio of **DC**:**MC** varying from 35:65 to 99:0.

Though a complete conversion of **D1** was achieved by varying the reaction temperature from 90 °C to 180 °C, there were no cleavage products observed in the initial 1 h of the reaction with the product scope being limited to dicarboxylated dilignol (**DC**) for temperatures of 150 °C and 180 °C. Subsequent reactions were thus carried out for a maximum of 24 h to monitor any cleavage in **D1**. The reactions were carried out at 0.5 and 0.1 equivalent base (NaOH) loadings (Table III.2).

Table III.2: Effect of time on the product distribution.[a]

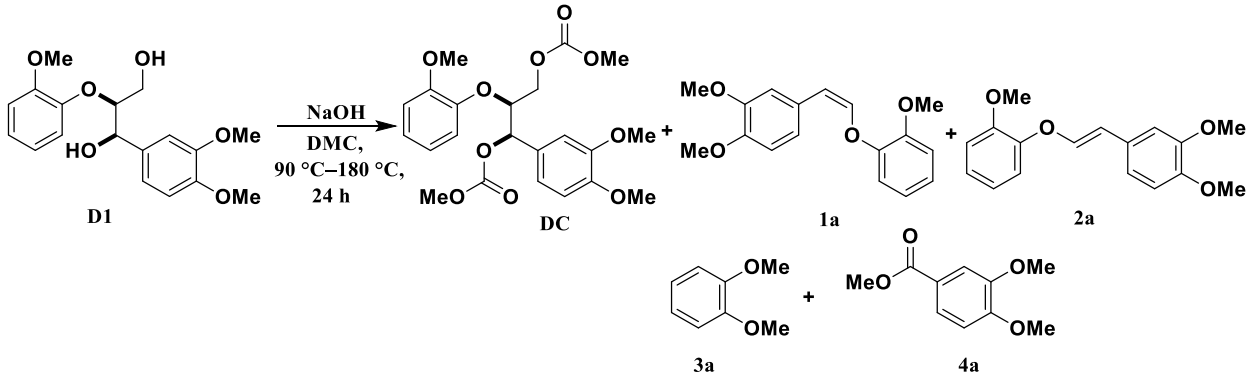

Entry	Temp [°C]	Conversion [%][c]	Product yields [%][c]				
			DC	**1a**	**2a**	**3a**	**4a**
1	90	90	78	-	-	-	-
2[b]	90	70	45	-	-	-	-
3	135	>99	58	12	-	19	-
4[b]	135	>99	77	7	-	9	-
5	150	>99	30	20	-	27	3
6[b]	150	>99	34	20	-	24	4
7	180	>99	-	37	3	40	3
8[b]	180	>99	-	39	-	40	3

[a] Reaction conditions: **D1** (83.6 mg, 1.0 equiv), NaOH (5.0 mg, 0.5 equiv), DMC (1.3 mL), 24 h. [b] Use of 0.1 equivalent NaOH. [c] Converisons and yields determined by HPLC with respect to 3,4-dimethoxybenzyl alcohol.

Although the reactions at 90 °C for 24 h resulted in higher yields of dicarboxylated product (**DC**) for both 0.5 and 0.1 equivalents of NaOH, no cleavage products were observed (entries 1 and 2). To our delight for the reaction at 135 °C after 24 h, we saw the formation of *cis*-alkene **1a** and cleavage product veratrole (**3a**) in 12% and 19% yield respectively along with **DC** in 58% yield (entry 3). The same reaction, when carried out with reduced amounts of NaOH (0.1 equiv), decreased the rate of the cleavage reaction, affording **DC** in 77% yield along with products **1a** (7%) and **3a** (9%) in minor quantities (entry 4). This effect of base concentration on the overall product ratio decreased at higher reaction temperatures and at 150 °C, reactions conducted with both 0.5 and 0.1 equivalents of NaOH led to analogous product distributions (entries 5 and 6). Furthermore, the BCD reactions at 180 °C favoured the complete consumption of **DC** for both base loadings affording alkene **1a** and veratrole (**3a**) in a 1:1 product ratio (entries 7 and 8).

Having finally optimized the reaction parameters towards the complete consumption of the dicarboxylated dilignol **DC** at 180 °C along with the formation of products **1a** (39%), **3a** (40%) and **4a** (3%) using 0.1 equivalent of NaOH, we next screened a number of readily available alkali metal based bases, with the purpose of observing an enhanced effect on the overall product selectivities (Table III.3).

It is worth noting that all the preliminary tests monitored above and here after were based on the conversions and yields obtained after quantitative HPLC analysis done with respect to individual standard lines made for the reactants, intermediates and products.

Table III.3: Effect of alkali metal bases on the product distribution.[a]

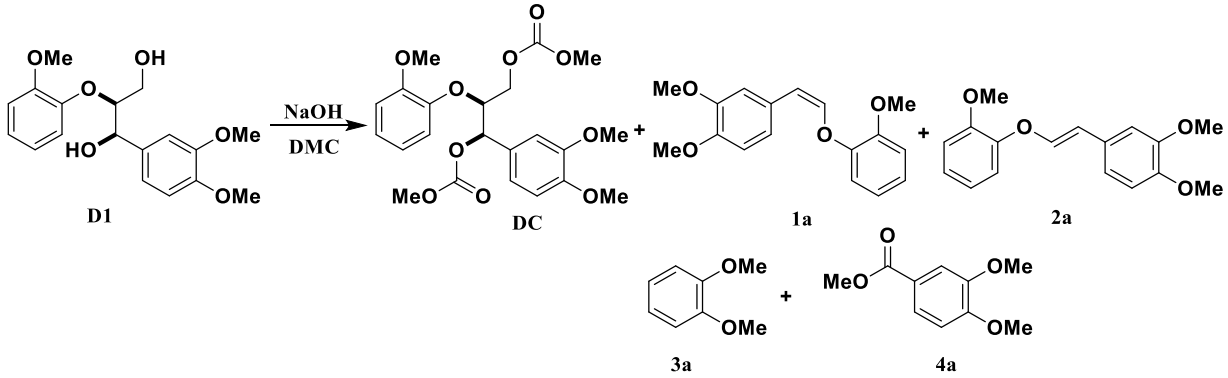

Entry	Base (equiv)	Time [h]	Product yields [%][b]				
			DC	**1a**	**2a**	**3a**	**4a**
1	LiOH (0.1)	24	25	34	2	-	-
2	LiO*t*-Bu (0.1)	24	-	70	11	-	-
3	LiO*t*-Bu (0.1)	12	-	75	9	-	-
4	LiO*t*-Bu (0.05)	12	-	75	9	-	-
5	LiO*t*-Bu (0.05)	1	93	-	-	-	-
6	Na_2CO_3 (0.1)	24	10	27	trace	33	10
7	$NaHCO_3$ (0.1)	24	17	22	trace	19	8
8	NaO*t*-Bu (0.1)	24	-	33	-	45	7
9	KOH (0.1)	24	Trace	-	-	60	18
10	KOH (0.05)	24	Trace	-	-	55	15
11	KOH (0.05)	12	2	-	-	36	7
12	KO*t*-Bu (0.05)	12	3	-	-	43	10
13	K_2CO_3 (0.05)	12	2	-	-	32	5
14	Cs_2CO_3 (0.1)	24	-	-	-	57	15
15	Cs_2CO_3 (0.1)	8	-	-	-	60	14
16	Cs_2CO_3 (0.05)	8	-	-	-	60	14
17	Cs_2CO_3 (0.05)	0.3	92	-	-	-	-

[a] Reaction conditions: **D1** (83.6 mg, 1.0 equiv), DMC (1.3 mL), 180 °C. [b] Yields determined by HPLC with respect to 3,4-dimethoxybenzyl alcohol as an internal standard.

Interestingly, a clear trend was observed for the change in product selectivity from *cis*-alkenes **1a** towards veratrole (**3a**) with the increase in cation radius from lithium to cesium. Both LiOH- and LiO*t*-Bu- catalyzed reactions afforded the *cis*-alkene **1a** as the major product (entries 1–4). Employing 0.1 equivalent of LiO*t*-Bu for a 24 h reaction gave **1a** in 70% yield along with the formation of **2a** in 11% yield (entry 2). The reaction time could be shortened and the catalyst loading reduced (12 h and 0.05 equiv), furnishing **1a** in 75% and **2a** in 9% yield (entries 3 and 4). When the cation-radius of the employed base was increased, the selectivity shifted towards the cleavage products veratrole (**3a**) and 3,4-dimethoxybenzoate (**4a**) (entries 6–14). Cs_2CO_3 gave the highest yield for veratrole with 57%, and concomitantly benzoate (**4a**) was formed in 15% (entry 14). A shorter reaction time of 8 h improved the yield of veratrole to 60% (entry 15). The catalyst loading could further be decreased to 0.05 equivalent without loss in the yields of veratrole and benzoate (entry 16).

Interestingly, despite the fact that reactions catalyzed by Cs_2CO_3 and LiO*t*-Bu ended with distinct product selectivities, both these reaction systems initially involved the formation of the intermediate dicarboxylated product **DC** (entries 5 and 17).

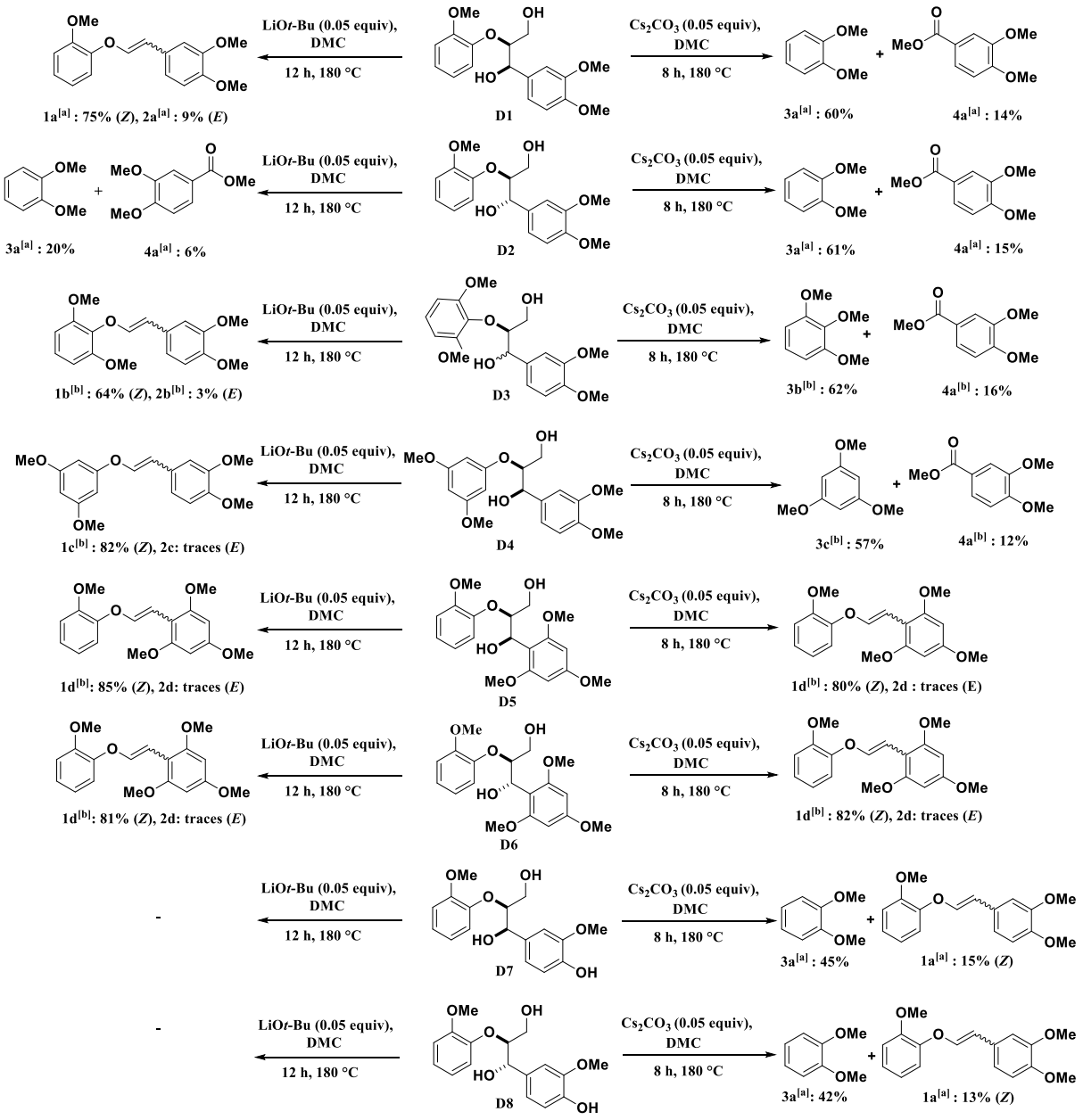

[a] Yields determined by HPLC with respect to 3,4-dimethoxybenzyl alcohol and diphenyl ether as te internal standards.
[b] Yields determined by column chromatography.

Scheme III.3. LiO*t*-Bu- and Cs_2CO_3- catalyzed reactions of lignin *β*-O-4 model compounds **D**.

The divergence in product selectivities seen for lithium- and cesium- catalyzed reactions on model **D1**, made it important to study the scope of the system on more challenging model substrates, prior to their application on real lignin samples. For this purpose, further investigations involved a variety of *β*-O-4 model substrates including those exhibiting different stereochemistry, greater steric hindrance and also containing a phenolic hydroxyl group. Using Cs_2CO_3 as the catalyst (Scheme III.3.), the corresponding *threo* diastereomer **D2** of dilignol **D1** afforded veratrole (**3a**) in 61% along with 15% benzoate product (**4a**). Surprisingly, the presence of LiO*t*-Bu as a base did not induce the formation of alkene **1a** from **D2**, but afforded veratrole (**3a**) in 20% as the main cleavage product (Scheme III.3.). Delightfully increased steric hindrance on either the *ortho*- or *meta*- position of the ring adjacent to the primary hydroxy group also resulted in a similar cleavage for Cs_2CO_3-catalyzed reactions, forming 1,2,3-trimethoxybenzene (**3b**) and 1,3,5-trimethoxybenzene (**3c**) as the main products in 62% and 57% yield, respectively, for the cleavage of **D3** and **D4**. However, the product selectivity for these model compounds reverted back

to those observed with model **D1** for the LiO*t*-Bu-catalyzed BCD reactions, thereby producing *cis*-alkenes **1b** and **1c** in 64% and 82% yields respectively for **D3** and **D4.** The trend was again discontinued when the steric hindrance was increased on the arene adjacent to the benzylic hydroxyl group for the *erythro* and *threo* diastereomer **D5** and **D6**. Both the bases (Cs_2CO_3 and LiO*t*-Bu) here resulted in the formation of *cis*-alkene **1d** as the major product in the range of 80–85% yield. This variation in selectivity specially needs to be considered when employing hardwood lignin sources that have a high content of sinapyl alcohol (**S**) derived building blocks.

Moving forward with the substrate capacity for the current system, more complex model compounds such as *erythro* dilignol **D7** which contained a reactive phenolic hydroxyl group was also investigated. As anticipated, for a cesium-catalyzed reaction, **D7** gave veratrole (**3a**) in a slightly lower yield (45%). Likewise, *threo* dilignol **D8** furnished **3a** in a similar yield of 42% as the corresponding *erythro* diastereomer under similar reaction conditions. Furthermore, it was noted that the reaction conditions with LiO*t*-Bu were unsuitable for model compounds **D7** and **D8**. Instead of the formation of alkene **1a** or veratrole (**3a**), a sticky polymeric material that was insoluble in any standard organic solvents, was formed at the bottom of the reaction vessel.

The results obtained after evaluating model compounds **D1**–**D6**, make it unequivocal to conclude that lithium with a smaller cation size favours the formation of 2-aryloxyvinyl benzene derivatives (**1a**–**d** and **2a**–**d**) in very good yields whereas cesium with a bigger cation size leads to the formation of methoxy-capped cleavage products (**3a**–**c** and **4a**) in dimethyl carbonate. To further understand this difference in the reaction pathway for both the bases, reactions with substituted lignin β-O-4 bonds were sought to be investigated.

1.2. Cleavage studies of substituted lignin β-O-4 model compounds in dimethyl carbonate

To gain a better understanding of the above established base-promoted degradation system in DMC, more substituted lignin β-O-4 model compounds were studied with some of their critical sites such as the α- proton, γ- proton, or either one or both the aliphatic hydroxyls being replaced by methyl or methoxy groups (Scheme III.4.). In comparison to **D1**, model compound **D9** which had both its γ- protons replaced by methyl groups, afforded veratrole (**3a**) and 3,4-dimethoxybenzoate (**4a**) in higher yields of 88% and 16% respectively for the Cs_2CO_3-catalyzed reaction. On the contrary, substituting the α- proton with a methyl group as done in model **D10** led to the formation of a complex mixture of products with the overall yields for **3a** decreasing by half (30%). This decrease in yield reflects on the possible involvement of the α- proton in the cleavage reactions including model **D1**. Following the trend of changed reactivities, reactions of both **D9** and **D10** with LiO*t*-Bu also resulted in decreased yields for the corresponding *cis*-alkenes **1a** and **1e**. This was probably because of the formation of an additional cyclic product such as **5**. Additionally, methoxy substitution of either one of the primary or benzylic hydroxyls such as in model **D12** and **D13** limited the reactions for both the bases at the monocarboxylated products **6** and **7**, hence recommending the necessity of free hydroxy groups at both the positions to initiate a successful cleavage and elimination reaction. This was further confirmed by reactions conducted on model **D13** that remained unreactive for both the base catalysts. Interestingly, a reaction with monolignol **M2** that lacked the primary hydroxyl group also resulted in a stark decrease in yield of **3a** to 18%. This result again ascertains the requirement of both the primary and benzylic hydroxy groups to successfully cleave the β-O-4 bonds. The decrease in yield for monolignol **M2** should not be regarded as a limitation for any applications on the biopolymer because this structural motif without an aliphatic hydroxyl is absent in native lignin.

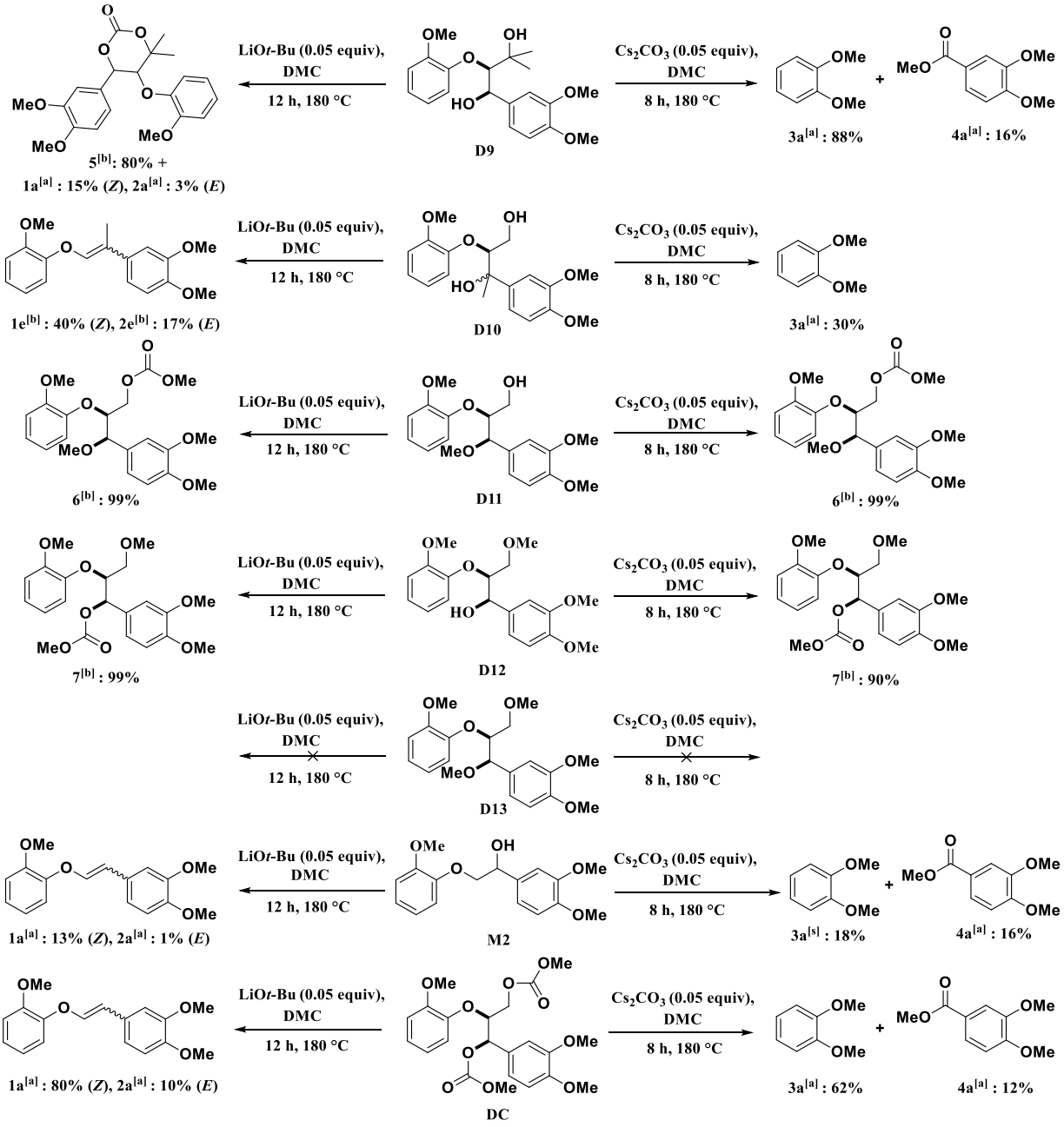

[a] Yields determined by HPLC with respect to 3,4-dimethoxybenzyl alcohol and diphenyl ether as te internal standards.
[b] Yields determined by column chromatography.

Scheme III.4. LiO*t*-Bu- and Cs_2CO_3- catalyzed reactions of substituted lignin *β*-O-4 model compounds **D**.

Based on our observations on the above model compound studies, dicarboxylated dilignol **DC** was obtained in sufficient quantities to conduct individual reactions with both Cs_2CO_3 and LiO*t*-Bu. The reactions resulted in product selectivities which were comparable to those obtained from model compound **D1** but with slightly increased yields. These experiments yet again ascertained **DC** to be a common intermediate for the pathway involving both the bases.

1.3. Reaction profile and rate constant calculation

Further studies focused on the reaction progress kinetic analysis (RPKA) for the cleavage of model compound **D1** under the Cs_2CO_3- and LiO*t*-Bu- catalyzed conditions (Figure III.1). The consumption of **D1** and formation of stable intermediates (**MC**, **DC**) and products (**1a**, **2a**, **3a** and **4a**) were monitored by HPLC analysis. The detailed description for these HPLC analysis are included in the experimental section of the thesis.

The change in the concentration of reactant **D1** and products (**MC**, **DC**, **1a**, **2a**, **3a**, **4a**) obtained after carrying out experimental analysis are represented by dots in Figure III.1. These results were used to elucidate the reaction pathways for both the base-catalyzed systems (Scheme III.4 and III.5). Based on these proposed pathways, the reaction progress curves were then modelled using the DynaFit software and overlaid with the experimental values (Figure III.1, plotted lines).

Having obtained a significant match between the experimental and modelled reaction profiles, the rate constants (k) for individual steps proposed for the cleavage reactions were calculated based on the modelled curves using the same software.

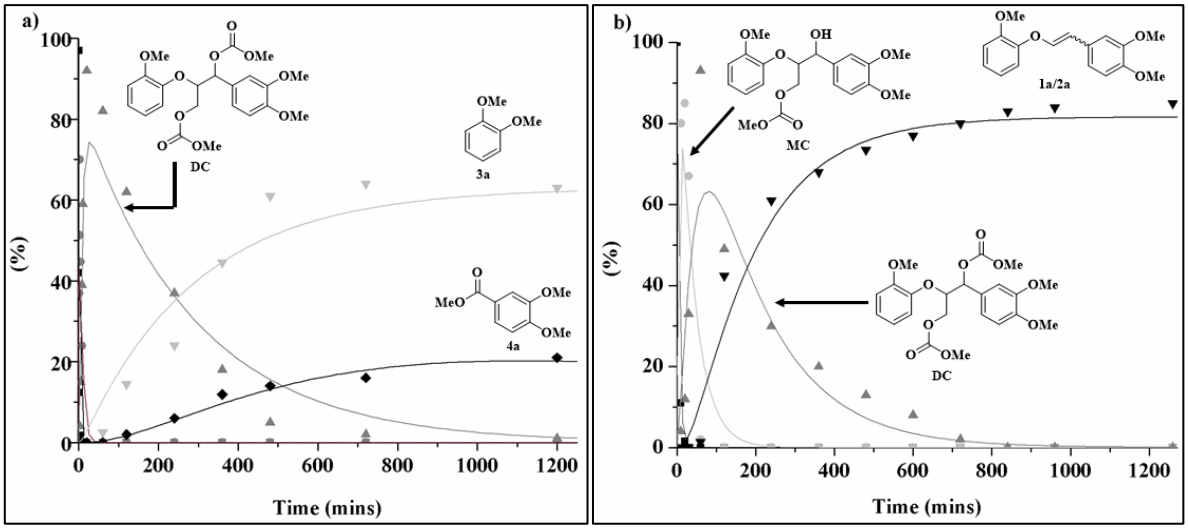

Figure III.1. Reaction profiles [a] Cs_2CO_3 180 °C in dimethyl carbonate with (*β*-O-4) model compound **D1**; [b] LiO*t*-Bu 180 °C in dimethyl carbonate with (*β*-O-4) model compound **D1**. Dots show experimental data points, whereas the line represents the modeled reaction.

Both Cs_2CO_3- and LiO*t*-Bu-catalyzed reactions were found to proceed through similar reaction intermediates during the initial stages of the reaction. The first intermediate step involved the carboxylation of the *γ*-hydroxy group (reaction rates for the formation of **MC** = 0.69 min^{-1} for Cs_2CO_3 and 0.20 min^{-1} for LiO*t*-Bu) followed by the carboxylation of the *α*-hydroxy group resulting in a second common intermediate **DC** (reaction rates for the formation of **DC** = 0.15 min^{-1} for Cs_2CO_3 and 0.025 min^{-1} for LiO*t*-Bu). Subsequently the reaction pathways diverged. The reaction with Cs_2CO_3 resulted in the cleavage of the C–O bond leading to the formation of veratrole (**3a**). The production of **3a** however does not correlate directly with the accruement of 3,4-dimethoxybenzoate (**4a**). A probable intermediate **I** is speculated to form prior to a subsequent reaction resulting in **4a**.

After the formation of **DC** in the reaction catalyzed by LiO*t*-Bu, the alkenes **1a** and **2a** were produced without any observable intermediates (rate of formation of **1a**/**2a** = 0.005 min^{-1}).

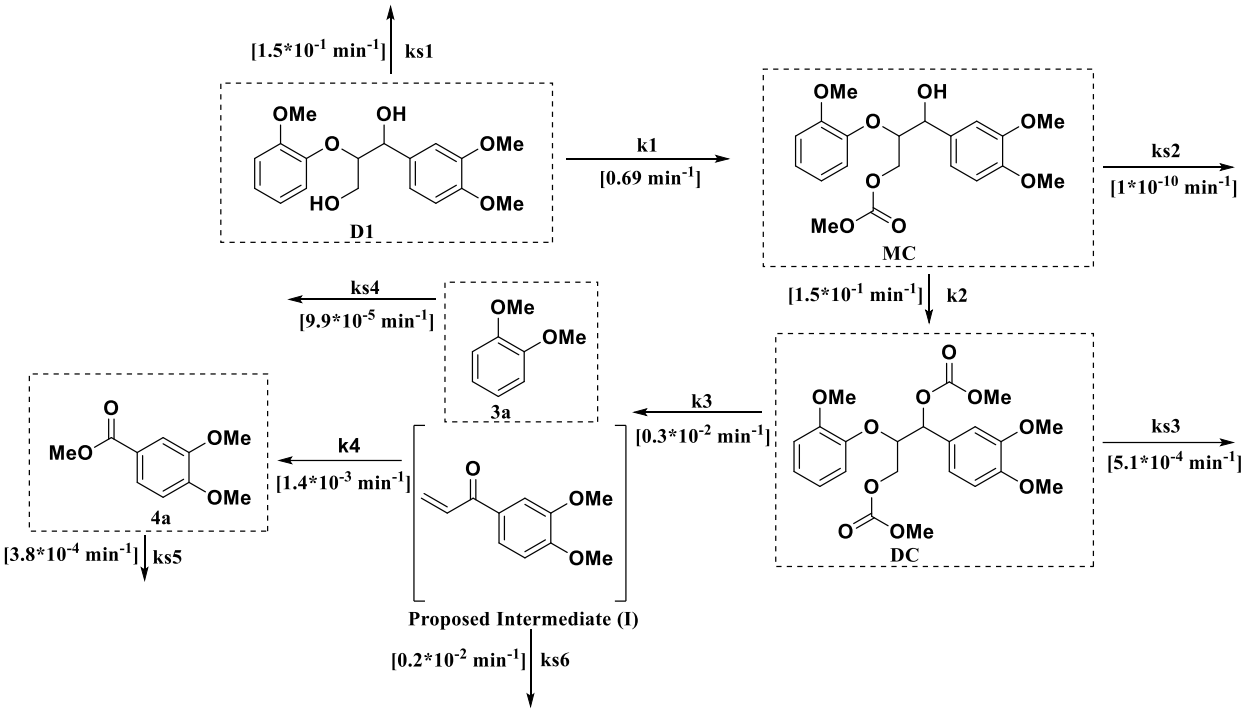

Scheme III.4. Reaction pathways considered in the reaction modelling parameters for the stepwise catalytic degradation of β-O-4 model compound **D1** using Cs_2CO_3. End products are veratrole **(3a)** and 3,4-dimethoxybenzoate **(4a)**.

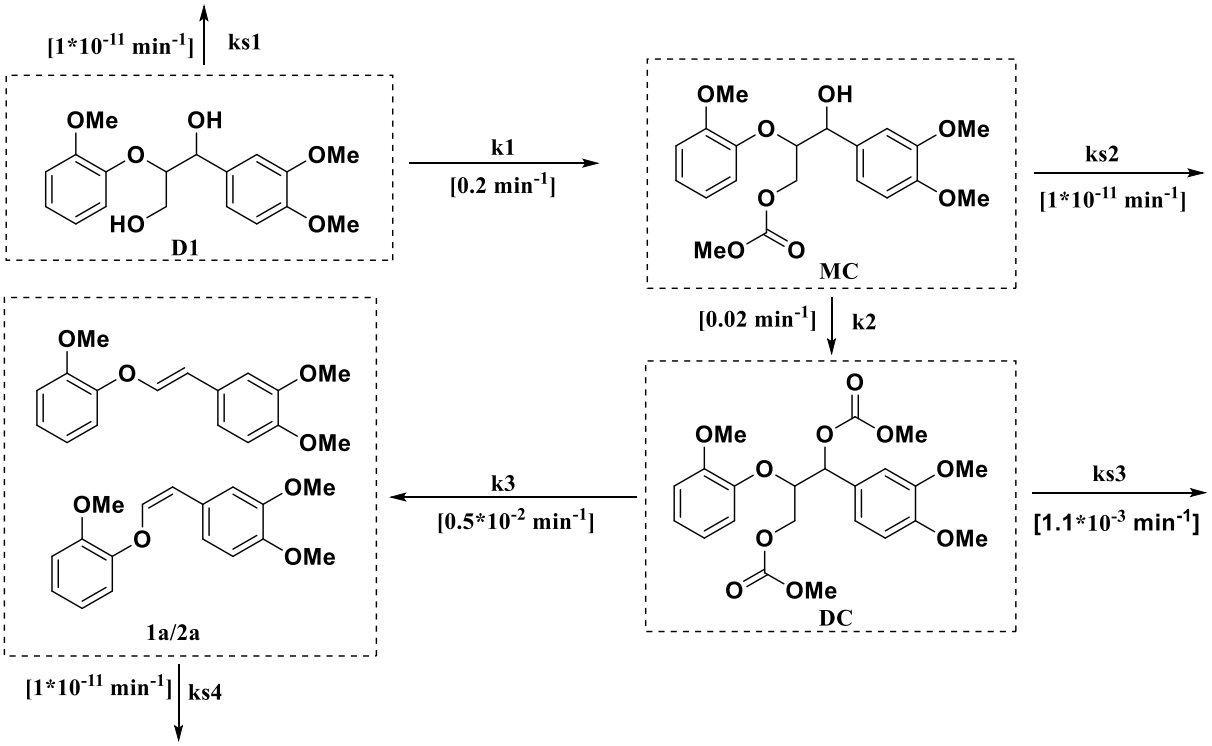

Scheme III.5. Reaction pathways considered in the reaction modelling parameters for the stepwise catalytic degradation of β-O-4 model compound **D1** using LiO*t*-Bu. End products are vinylethers (**1a** and **2a**).

1.4. Computational studies

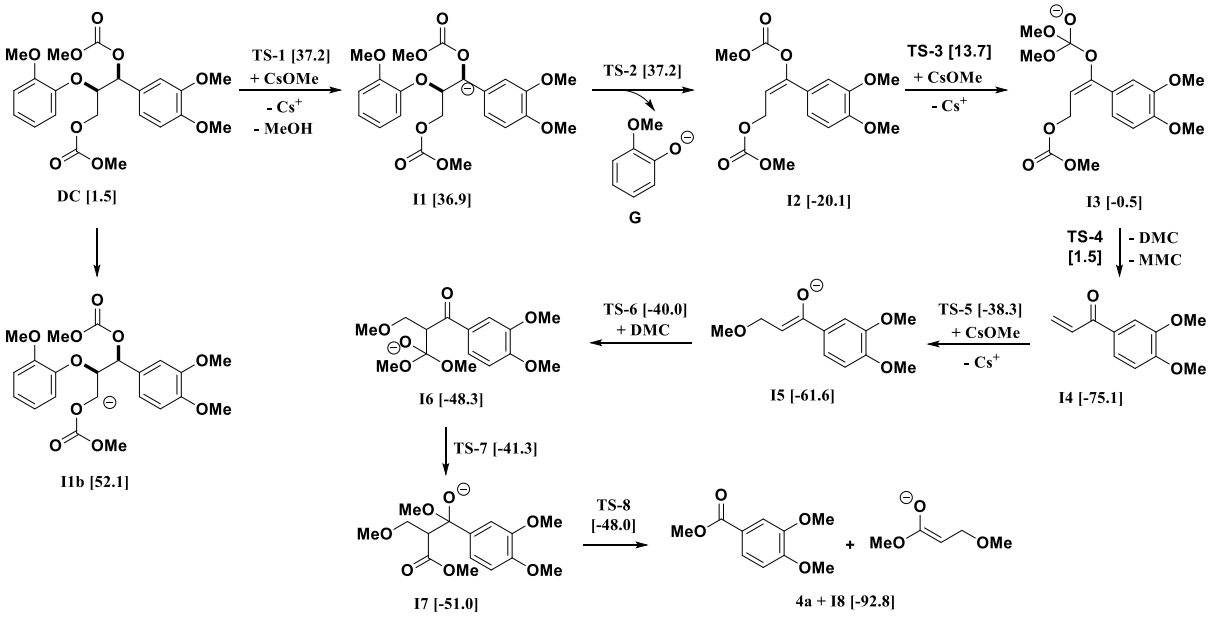

Scheme III.6. Reaction pathway from dicarboxylated dilignol **DC** to 3,4-dimethoxybenzoate (**4a**); **MMC**: monomethoxy carbonate; [Gibbs energies are relative to **D1** in kcal·mol^{-1}].

Next, to propose a rational mechanism for the selectivity difference observed while employing catalytic amounts of Cs_2CO_3 and LiO*t*-Bu, further quantum chemical calculations were carried out in collaboration with Dr. Julien Engel on dilignol **D1** and cesium methanolate (CsOMe) as a model base.[70] Cesium methanolate was hypothesized as the active base species in the reaction when considering the depletion of Cs_2CO_3 (0.05 equiv) over the course of the reaction, resulting in methanolate as a by-product in the presence of DMC. Furthermore, the investigated reaction pathways studied were also restricted to only intermediates and transition states without explicit coordination of the alkali metal ions (Cs or Li). This was because of the number of different structures and oligomers which would have to be taken into consideration for each step if actual coordination was considered. Besides this, the inaccuracy of the polarizable continuum (PCM) solvation model for the description of the solvated species in this system, also prevented reliability on comparing structures differently coordinated to the metal cations. Moreover, based on Pearson's HSAB principle, since lithium ions are prone to coordinate more firmly to the deprotonated oxygen atoms of the substrate than the softer cesium ions, it was decided that the uncoordinated intermediates and transition states would provide a better correlation with a cesium base than with a lithium base. This trend could also be justified by the increased energy for anionic intermediates observed, when the cation was changed to lithium, yet again confirming that a reaction pathway under coordination of the counterion was rather likely prone to proceed for lithium than for a cesium ion.

Scheme III.6 depicts the pathways considered for the computational calculations aimed towards the formation of veratrole (**3a**) and 3,4-dimethoxybenzoate (**4a**). As potrayed, the studies suggested the involvement of both the α- and γ- protons in the formation of these products. The reduction in the yield of **3a** starting from **D1** specifically indicated that these reaction products were formed after a deprotonation at the α-position. This deprotonation reaction, however, was thought to occur at the dicarboxylated dilignol **DC** since, in contrast to **D1**, it had no free hydroxy groups, which were more acidic than the aliphatic hydrogen atoms. Additionally, the experimental results had also indicated **DC** to be an intermediate in the formation of **3a** and **4a** (Scheme III.4; reaction of **DC** with Cs_2CO_3 and Figure III.1-a). The deprotonation at the α-carbon of **DC** led to the formation of intermediate **I1**

(Scheme III.6). The formation of this intermediate was favoured with a Gibbs energy difference of 15.2 kcal·mol^{-1} over **I1b**, which was formed owing to the deprotonation at the γ-carbon. The energy of **I1** was thus calculated to be 36.9 kcal·mol^{-1} relative to **D1**. The transition state of the deprotonation step (**TS-1**) also had a Gibbs energy of 37.2 kcal·mol^{-1} relative to **D1**. Moreover, the elimination of guaiacolate (**G**) from **I1** took place without a significant barrier and resulted in the enol-ether **I2**. Interestingly, the formation of veratrole from **D10** (Scheme III.4) could also be related to a deprotonation reaction at the γ-position. However, the lower acidity of the hydrogen at the γ-position compared to the one in α-position was possibly the reason for observing lower veratrole yields (**3a**). Furthermore, the absence of **4a** in the product spectrum of **D10** could be speculated because of a different intermediate being formed after the elimination process. Additionally, a similar product inhibition in the formation of veratrole (**3a**) by *o*-methoxy groups in models **D5** and **D6** was observed in Scheme III.3. The overall change of the selectivity thus indicates that the steric hindrance at the α-carbon might have been the reason for preventing the deprotonation.

The last step involved in the formation of **3a** included the methylation of **G** by dimethyl carbonate (DMC). The relative Gibbs energy of this transition state of the methylation under Walden inversion at the methyl group was calculated to be 24.5 kcal·mol^{-1} relative to **G**. Furthermore, **4a** was sought to be produced as a result of the decomposition of intermediate **I2**. The addition of a methanolate to the methoxy carbonate group was found to be endergonic. The resulting intermediate **I3** had a Gibbs energy of 19.6 kcal·mol^{-1} relative to **I2**. The transition state corresponding to this step had an energy of 33.8 kcal·mol^{-1} compared to **I2**. Elimination of dimethyl carbonate from **I3** resulted in a simultaneous elimination of monomethoxy carbonate (**MMC**). The transition state **TS-4** of this step was only 2.0 kcal·mol^{-1} higher in energy than **I3**. Moreover, the reaction was highly exergonic since the Gibbs energy of the vinyl ketone **I4** was −74.6 kcal·mol^{-1} lower than **I3** and the energy was 55.0 kcal·mol^{-1} lower than **I2**. The vinyl ketone **I4** was further proposed to react with methanolate to give the enolate **I5**. This addition reaction was calculated to be endergonic with an energy difference of 13.9 kcal·mol^{-1} and the corresponding transition state **TS-5** having an energy of 37.2 kcal·mol^{-1}. Addition of dimethyl carbonate to the α-carbon of **I5** in a Claisen condensation-type reaction (**TS-6**) resulted in intermediate **I6**. Instead of an elimination of a methanolate, a transfer of a methoxy group of the dimethyl carbonate group to the carbonyl group was likely to take place. The resulting intermediate **I7** resembled the intermediate of a Claisen condensation between 3,4-dimethoxybenzoate and the enolate **I8**. Hence, a retro-Claisen condensation-type step (**TS-8**) thus resulted in the formation of **4a**. The formation of **4a** and **I8** were seen to be highly exergonic having an energy difference of 92.8 kcal·mol^{-1} relative to **1a** (vinyl ether) and 17.7 kcal·mol^{-1} relative to **I4**. **TS-5** was the transition state with the highest Gibbs energy (35.1 kcal·mol^{-1} relative to **I4**) between **I4** and **4a**.

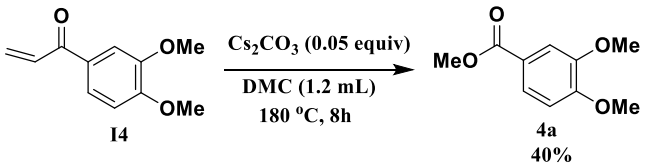

Scheme III.7. Reaction of **I4** with Cs_2CO_3 in dimethyl carbonate (DMC).

To support the proposed reaction pathway, intermediate vinyl ketone **I4** was also investigated. **I4** was synthesized (see experimental section for details) and used as a starting material in a reaction with the same conditions as shown for **D1** in Scheme III.3. The formation of **4a** in 40% yield when employing **I4** as the starting material indeed confirmed the possible reaction pathway between **I4** and **4a** (Scheme III.7). This is also in accordance with the proposed formation of an intermediate **I** while studying the reaction profile for the decomposition of **D1** with cesium carbonate to **4a** (Scheme III.4: **I** = **I4**).

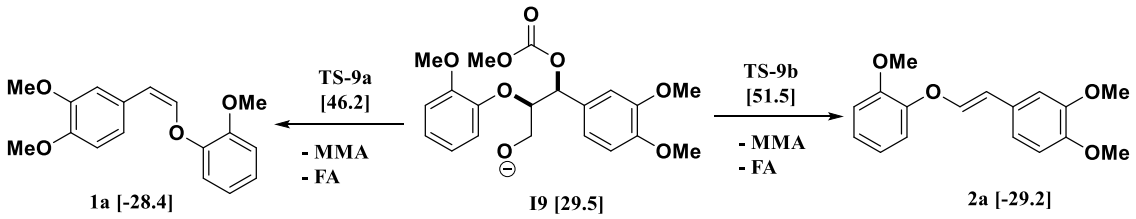

Scheme III.8. Reaction pathway of the formation of **1a** and **2a**; **FA**: formaldehyde [relative Gibbs energies in kcal·mol^{-1}]

Next, the formation of the alkenes **1a** and **2a** was investigated. During this reaction, the C–C bond between the β- and γ-carbon was cleaved. Previous reports also suggested an elimination of formaldehyde in this process.[69] This elimination could not have occured directly from the proposed intermediate **DC** due to the carboxylated primary hydroxy group. Instead, the monocarboxylated intermediate **MC** had to be formed first from either **D1** or **DC**. Depending on the conformation during the elimination reaction, **1a** or **2a** were proposed to be formed.

The calculations also showed that the elimination of methylcarbonate and formaldehyde on opposite sides (**TS-9a**) was 5.3 kcal·mol^{-1} lower in energy than the elimination on the same side (**TS-9b**). This energy difference reflected correctly the experimentally observed preference for the thermodynamically less stable (*Z*)-alkene **1a** with LiO*t*-Bu. Moreover, due to the high relative energy of the intermediate **I9** and especially the transition states **TS-9a** and **TS-9b**, this reaction pathway could not be compared with the one to **3a** and **4a** (Scheme III.7). The predicted preferred formation of **3a** and **4a** were thus found to be in agreement with the experimental results for the reaction of **D1** with Cs_2CO_3, but not with those of the reactions with the lithium base. This further indicates that the above investigated uncoordinated transition states were a suitable approximation for the reactions with Cs_2CO_3 but not for those with LiO*t*-Bu. Instead, it can be assumed that the lithium ions played a key role during the transition states, which resulted in a shift of the selectivity to the alkene products. However, the investigation of these transition states clearly exceedes the scope of the current study.

1.5. Base-catalyzed depolymerization on lignin samples in dimethyl carbonate

Subsequent research initiatives were aimed towards investigating the translation of the lignin model based BCD strategies on actual lignin samples. Different sources of organosolv lignin from beechwood, oak and cherry trees along with a source of Aldrich kraft lignin **#370959** was utilized. The organosolv beechwood lignin (**OS-BWL1**) was extracted from beechwood chips at the MPI für Kohlenforschung, Mülheim a.d.R., Germany, using an organosolv process with EtOH:H_2O = 50:50 without the addition of an acid catalyst. The oak and cherry lignins (**OS-OL** and **OS-CL**) were obtained from their respective sawdust using an organosolv process with 1,4-dioxane followed by the addition of 2N HCl solution.[28e] These lignins were supplied by Prof. Dr. Nicholas. J. Westwood from the University of St Andrews, Fife, United Kingdom.

1.5.1. Characterization of the lignin samples prior to BCD

Different isolation processes often influence the physical and chemical properties of lignin polymers, including the identity and ratio of their chemical linkages. Therefore, detailed characterization of the lignin samples was carried out by GPC, 2D-HSQC and ^{31}P NMR measurements, prior to their use for BCD studies. These methods helped determine the weight average distribution, abundance of *β*-O-4, *β*-5 and *β*-*β* linkages as well as the amount of hydroxyl groups present in individual samples. The molecular weight distribution for the lignin samples were determined following the gel permeation chromatography (GPC) measurements. The results discussed for this section are based on the RI-detector response (Figure III.2, Table III. 4). The GPC elugrams were recorded with HPLC grade DMF/0.2 M LiCl as eluent. External calibrations for the mass distributions were performed with polystyrene sulfonate standards. These calibrations are often proven to have a certain degree of mass deviation because even the most branched polystyrene sulfonate standards cannot provide an exact mass for the very heterogeneous lignin polymers.

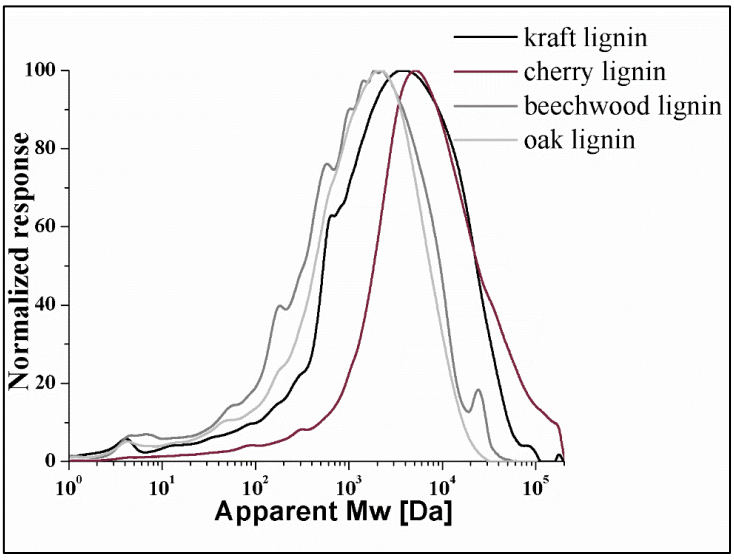

Figure III.2. Mass distribution of kraft, cherry, beechwood and oak lignin samples as determined by GPC.

Table III.4: The number average molar mass (Mn) and weight average molar mass (Mw) determined by GPC (DMF/0.2 M LiCl) using polystyrene standards.

Entry	Lignin	Mn (g·mol^{-1})	Mw (g·mol^{-1})
1	kraft	137	7106
2	Cherry	441	15220
3	beechwood	113	3103
4	oak	117	2610

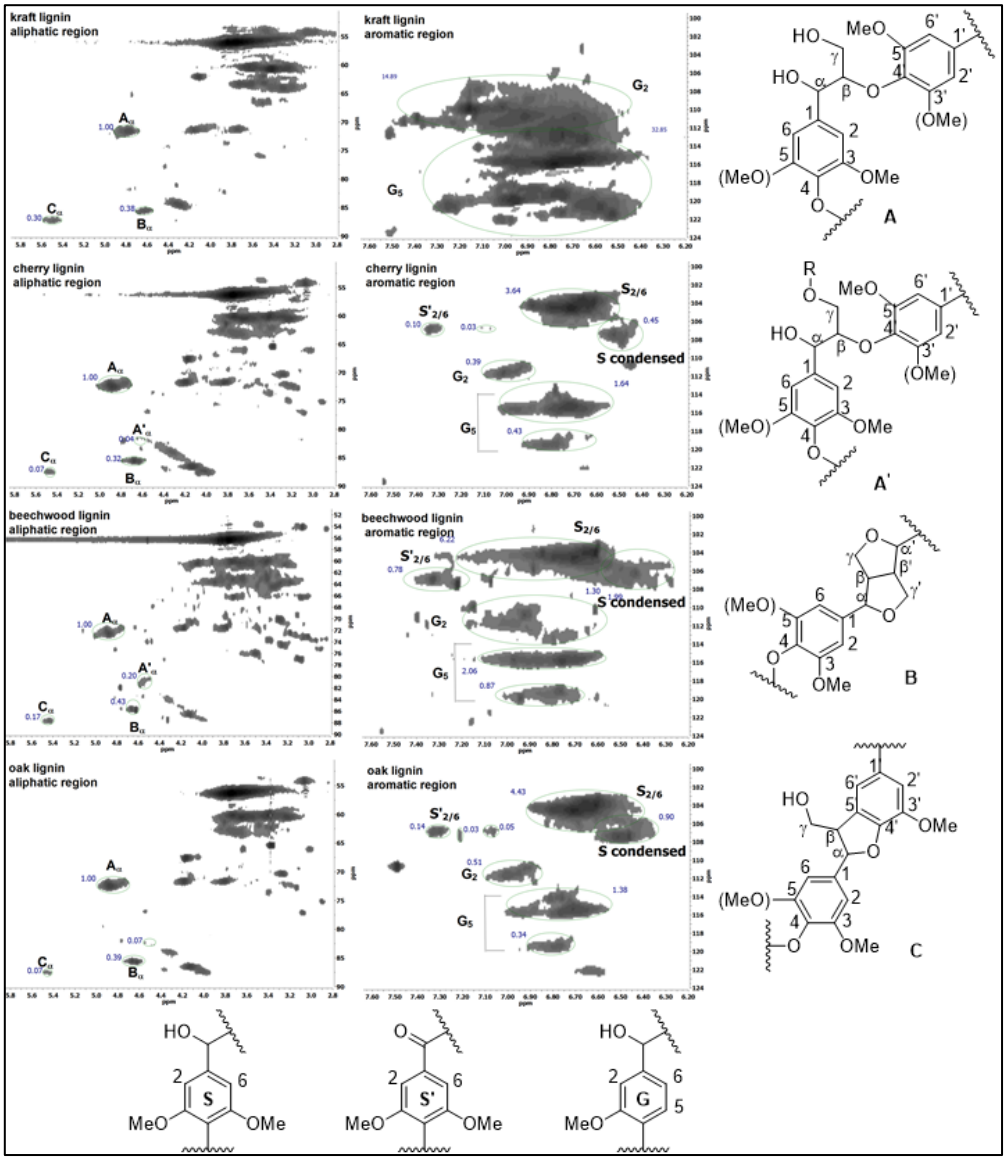

Figure III.3. 2D-HSQC NMR of lignins. Aliphatic regions are from 2.5–6.0, 90–50 ppm. Aromatic regions are from 7.2–7.6, 124–100 ppm. **A**: β-O-4' aryl ether linkages with a free-OH at the α-carbon; **A'**: β-O-4' aryl ether linkages with acetylated and/or *p*-hydroxybenzoated -OH at α-carbon; **B**: resinol substructures formed by β–β'-, α-O-γ'-, and γ-O-α'-linkages; **C**: phenyl coumaran substructures formed by β-5'- and α-O-4'-linkages; **S**: syringyl units; **S'**: syringyl unit with oxidized benzylic position; **G**: guaiacyl units.

Based on 2D-HSQC NMR of the four lignin samples, the signals for the major lignin linkages were assigned following an article by Sun.[71] Their respective areas were used to determine the relative quantities of the major linkages. This was done by taking integrals corresponding to the α-proton in different linkages (**A**: β-O-4, **B**: β-β, **C**: β-5) relative to their aromatic signals while maintaining the same contour level (Table III.5).

Table III.5: Characterization of lignins by 2D-HSQC NMR.

Lignin Source	S, G, H (%)[a]	Linkages (per 100 C9 units)[a]			
		β-O-4-OH[b]	β-O-4-OR[c]	β-5	β-β
OS-OL	85, 14, trace	27	6	3	5
OS-BWL1	73, 27, 0	20	4	3.2	4.1
OS-CL	86, 14, trace	37	1.4	2	6
Aldrich-Kraft	trace, 100, 0	5	0	1	1

[a] Determined by 2D-HSQC NMR by comparing the aliphatic and aromatic signal intensities. [b] Amounts of β-O-4 linkages with free α-OH. [c] Amounts of β-O-4 linkages with capped α-OH units.

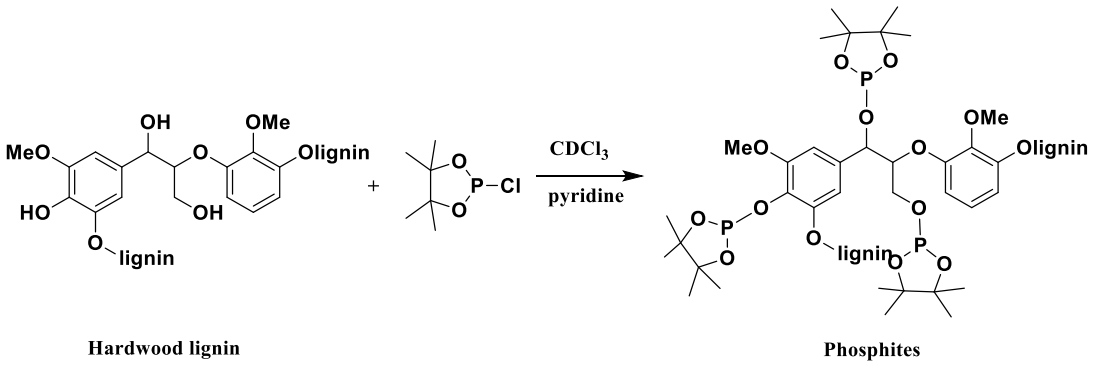

Scheme III.9. A typical reaction of hardwood lignin with TMDP.

Another quantification experiment involved the derivatization of the various hydroxy and phenoxy groups in lignin samples with the phosphorylating agent 2–chloro–4,4,5,5–tetramethyl–1,3,2–dioxaphospholane (TMDP) as portrayed in Scheme III.9. The resulting phosphites, were then resolved by ^{31}P NMR into separate regions arising from aliphatic hydroxyl, phenolic, and carboxylic acids groups (Figure III.4).[72] A detailed quantification of these regions done with respect to a known amount of cyclohexanol as an internal standard is included in Table III.6. Further details regarding the phosphorylation procedures can be found in the experimental section of this thesis.

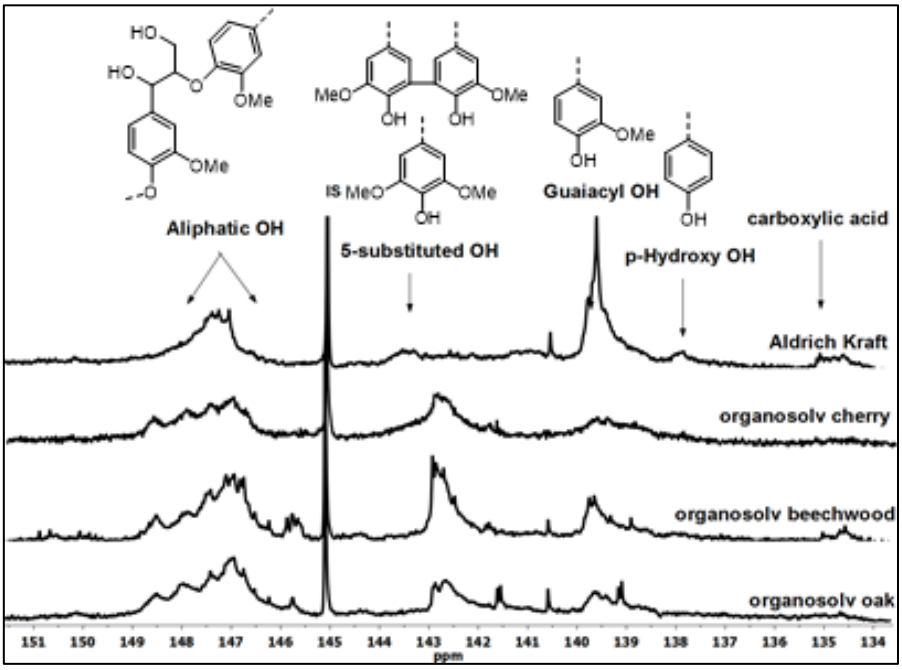

Figure III.4. Quantitative ^{31}P NMR spectra of lignin samples.

Table III.6: Lignin hydroxyl groups quantified by ^{31}P NMR using cyclohexanol as internal standard.

Lignins	OH (mmol·g^{-1})[a]				
	Aliphatic OH	5-Substituted + Syringyl OH	Guaiacyl OH (G)	*p*-Hydroxyphenyl OH (H)	Carboxyl OH
Kraft	1.79	0.90	1.77	0.17	0.20
Cherry	1.90	1.70	0.88	0.03	0.07
beechwood	2.38	1.24	0.69	0.01	0.01
Oak	2.37	1.06	0.56	0.05	0.12

[a] Amounts displayed with respect to a known amount of cyclohexanol.

1.5.2. Lignin cleavage studies after Cs_2CO_3- and LiO*t*-Bu- catalyzed BCD.

The characterized lignin samples were subjected to the base-catalyzed depolymerization (BCD) reactions in dimethyl carbonate (DMC). For this 100 mg of the corresponding lignin source was taken in a 25 mL pressure glass tube along with 10 wt% (w(base)/w(lignin)) of either Cs_2CO_3 or LiO*t*-Bu base in 5.0 mL DMC. The reactions were performed at 180 °C for either 8 h in case of Cs_2CO_3 or 12 h for LiO*t*-Bu- catalyzed reactions.

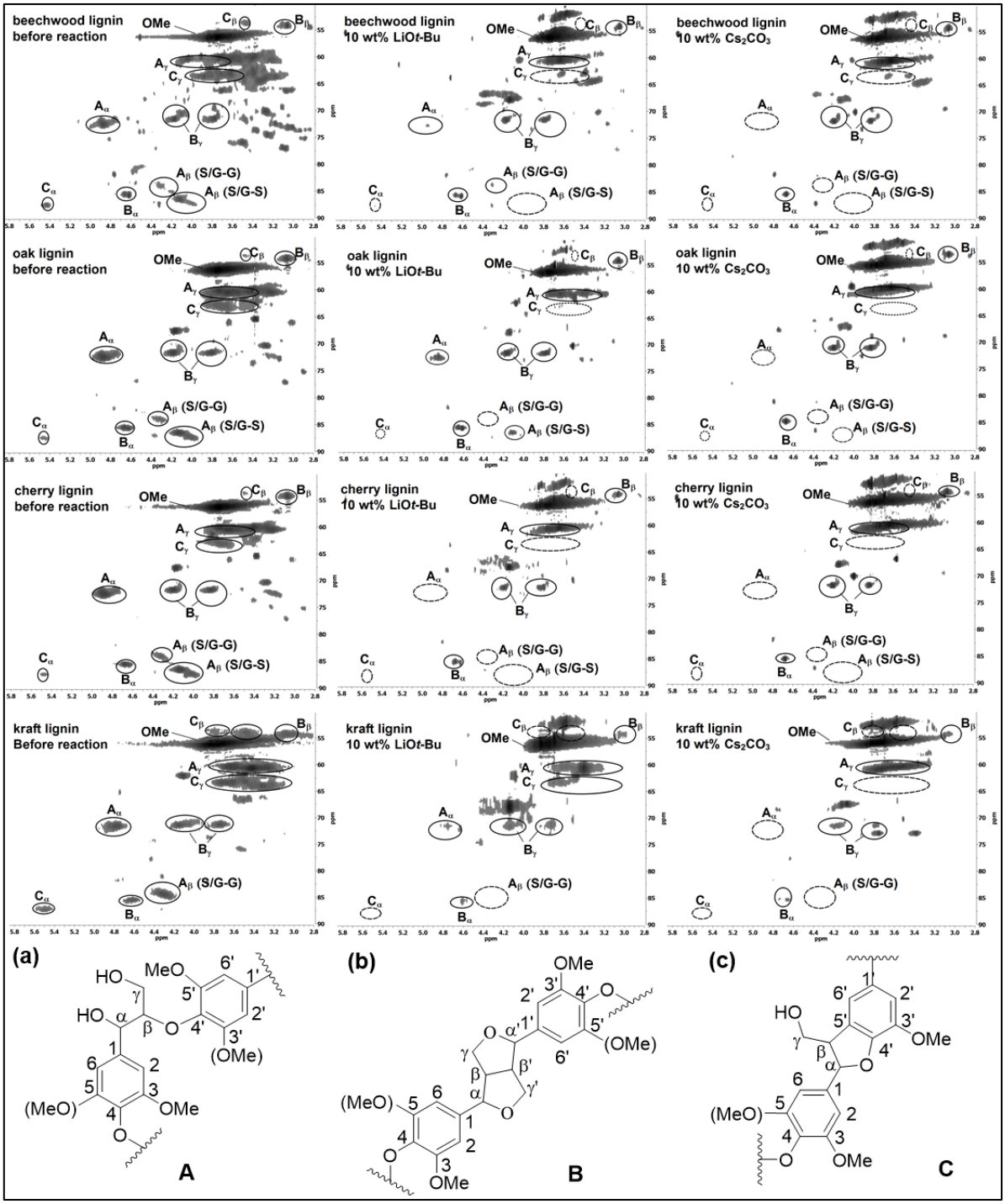

Figure III.5. 2D-HSQC NMR spectra (in DMSO-d_6) of organosolv beechwood, oak, cherry and Aldrich-kraft lignin; before the reaction; after the reaction with LiO*t*-Bu; after the reaction with Cs_2CO_3. (a) *β*-O-4' aryl ether linkages. (b) resinol substructures formed by *β*–*β*′, *α*-O-*γ*', and *γ*-O-*α*' linkages; (c) phenylcoumaran substructures formed by *β*-5' and *α*-O-4' linkages.

The reactions were first subjected to 2D-HSQC NMR analysis in order to determine the extent of cleavage for the characteristic bonds present in lignin after the BCD reactions catalyzed by both the bases (Figure III.5). Particularly, the two-dimensional $^{1}H–^{13}C$ (HSQC) correlation of the aliphatic oxygenated side chain regions ($\delta_C/\ \delta_H$ 50–90/2.5–5.8) of the spectra showed a major decrease in the contours corresponding to the *β*-aryl-ether (*β*-O-4) and phenylcoumaran (*β*-5) bonds. The resinol (*β*-*β*) linkages however remained unchanged for both the Cs_2CO_3-and LiO*t*-Bu-catalyzed BCD processes in all four lignin samples. This observation is not surprising considering the absence of aliphatic hydroxyls in the lignin *β*-*β* structures, whose presence during the mechanistic studies was concluded to be important to initiate the current degradation in DMC. This was further confirmed by performing corresponding experiments on sesamin (model representing *β*-*β* linkages) which was extracted from sesamin oil following a literature procedure.[29h] Indeed, as expected none of the two bases showed any reactivity for the cleavage of the sesamin moiety (Scheme III.10.).

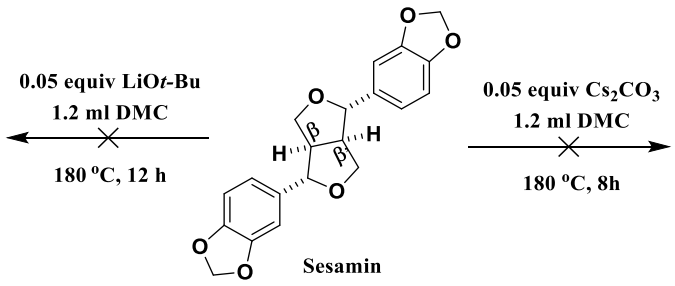

Scheme III.10. Reactivity of *β*-*β* model compound, sesamin in the BCD reactions.

Next GPC measurements were performed on all four reacted lignin samples, to see if the degradation of bonds portrayed by the HSQC results, also reflected any depolymerizationin of the polymer.

Figures III.6–III.9 represent the mass distribution chromatograms and the elugrams for the four lignin samples both before and after the BCD with 10 wt% (w(base)/w(lignin)) of Cs_2CO_3 and LiO*t*-Bu under the given reaction conditions. For better comparison of these results, individual values corresponding to the weight average molecular mass (Mw) for the reacted lignin samples were determined and are tabulated below (Table III.7).

Delightfully, the outcome of these analysis was in aggrement with the observations made while comparing the reactivity of LiO*t*-Bu and Cs_2CO_3 bases for the model compounds as well as during the mechanistic studies. Figures III.6–III.9 illustrate the sharp decrease observed in the Mw values for all the samples treated with Cs_2CO_3 (10 wt%, dark grey lines), in comparison to the corresponding LiO*t*-Bu-catalyzed reactions (10 wt%, light grey lines).

Table III.7: Average molecular weight change before and after the reactions.

Lignins	Mw (Da)		
	before reaction	10 wt% Cs_2CO_3	10 wt% LiO*t*-Bu
Organosolv-beechwood	3103	383	1898
Organosolv-oak	2610	212	2506
Organosolv-cherry	15220	253	3235
Aldrich-kraft	7106	1696	5790

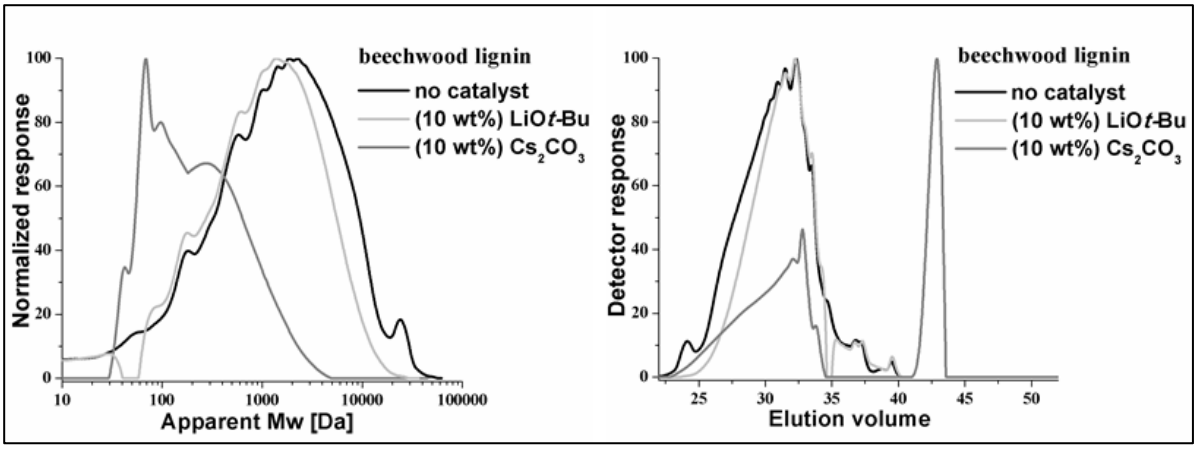

Figure III.6. GPC measurements for beechwood lignin (**OS-BWL1**): before reaction (no catalyst); after reaction with LiO*t*-Bu (10 wt%, 0.12 mmol), 12 h, 180 °C; after reaction with Cs_2CO_3 (10 wt%, 0.03 mmol), 8 h, 180 °C. **Left**:mass distribution with respect to sulfonated polystyrene standards calibration; **right:** elugram.

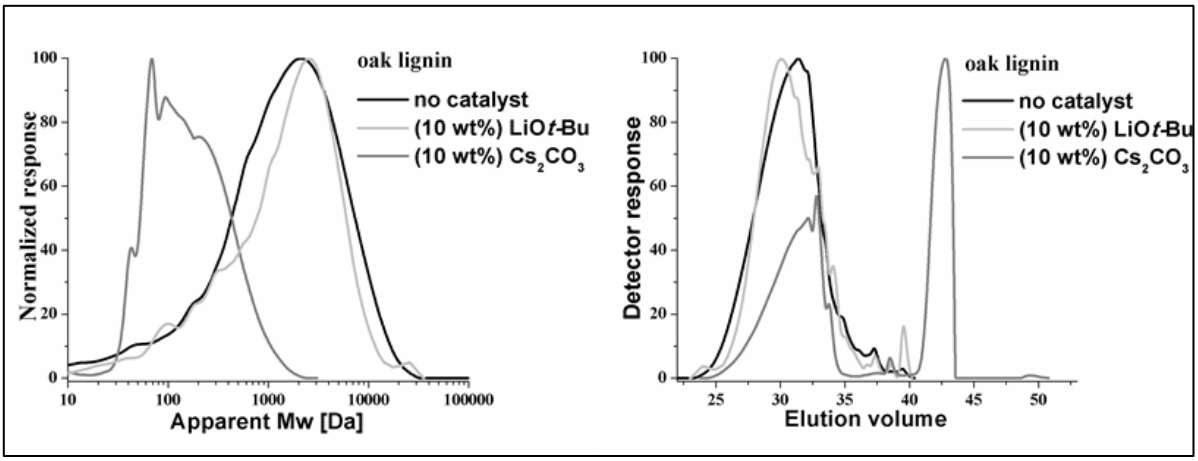

Figure III.7: GPC measurements for oak lignin (**OS-OL**): before reaction (no catalyst); after reaction with LiO*t*-Bu (10 wt%, 0.12 mmol), 12 h, 180 °C; after reaction with Cs_2CO_3 (10 wt%, 0.03 mmol), 8 h, 180 °C. **Left**: mass distribution with respect to sulfonated polystyrene standards calibration; **right:** elugram.

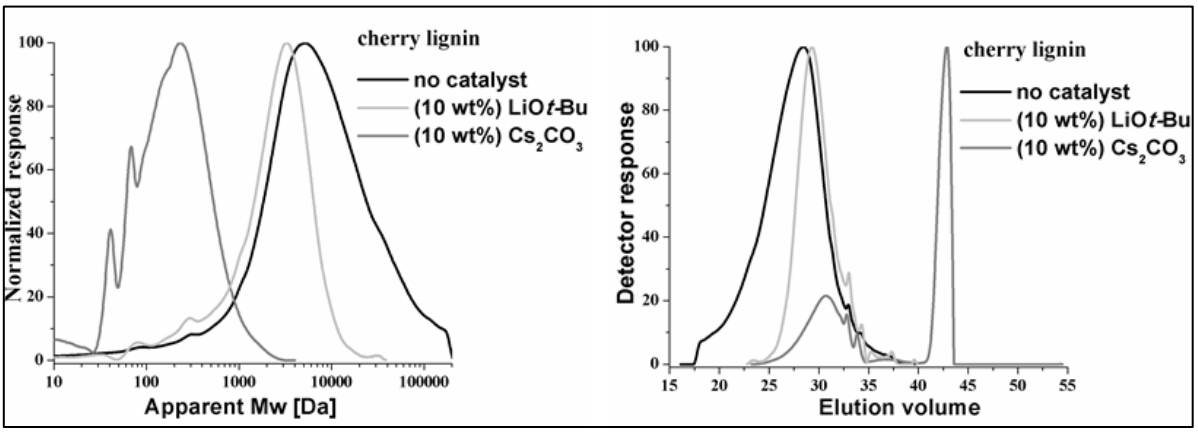

Figure III.8: GPC measurements for cherry lignin (**OS-CL**): before reaction (no catalyst); after reaction with LiO*t*-Bu (10 wt%, 0.12 mmol), 12 h, 180 °C; after reaction with Cs_2CO_3 (10 wt%, 0.03 mmol), 8 h, 180 °C. **Left**: mass distribution with respect to sulfonated polystyrene standards calibration; **right:** elugram.

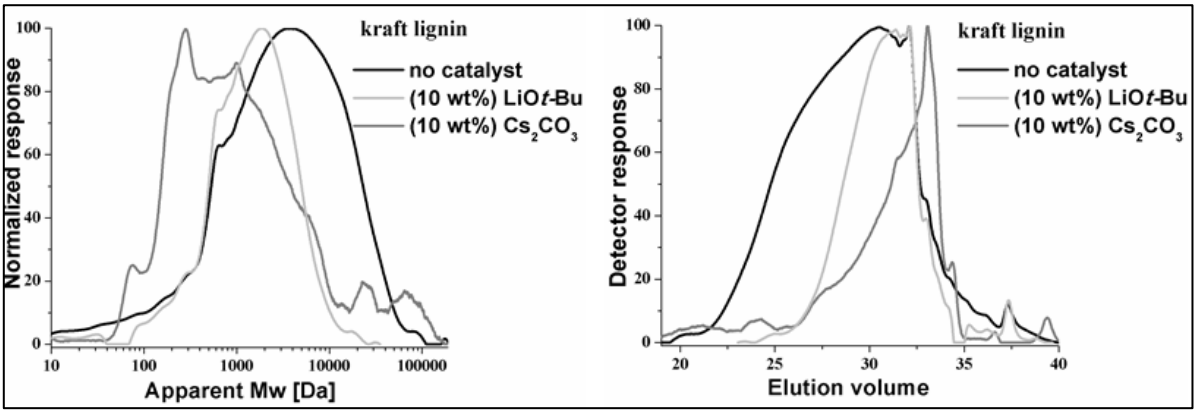

Figure III.9: GPC measurements for Aldrich kraft lignin: before reaction (no catalyst); after reaction with LiO*t*-Bu (10 wt%, 0.12 mmol), 12 h, 180 °C; after reaction with Cs_2CO_3 (10 wt%, 0.03 mmol), 8 h, 180 °C. **Left:** mass distribution with respect to sulfonated polystyrene standards calibration; **right:** elugram.

Although the organosolv lignins (beechwood, oak, cherry) depicted a significant decrease in their respective average mass values (as analyzed by GPC), the kraft lignin on the other hand resulted in an overall reduced mass value shift, compared to the untreated sample, even after the cesium-catalyzed reaction. This can be attributed to the rather condensed structure of the kraft lignin, due to highly invasive pretreatment conditions, which ultimately result in lesser amounts of labile alkyl-aryl ether linkages. Furthermore, absence of peaks at higher mass values compared to the initial samples also ruled out any repolymerization under the basic reaction environment. The observation is interesting as it proves the role of DMC as a capping reagent to prevent such side reactions in lignin samples. This was also the reason for using DMC in the current BCD studies while keeping in mind the drawbacks of previous base-catalyzed lignin depolymerization reactions.[29m,p]

To further investigate any changes induced in the prime functionalities (alcoholic, phenolic) of the reacted lignin samples, quantitative ^{31}P NMR studies were conducted in the presence of known amounts of cyclohexanol. Figure III.10 concludes that for both the bases an overall reduction in the amounts of aliphatic, phenolic and carboxylic -OHs was observed for all four lignin samples. However, the quantification studies revealed this decrease to be higher for the Cs_2CO_3-catalyzed reactions since the samples underwent complete transformation for all their corresponding -OH functional groups (Table III.8). The reason for the reduction of the aliphatic -OH groups could be a result of their transesterification reaction with DMC catalyzed by both the bases. This reactivity was also observed for dilignol **D1** (Scheme III.4). Previous reports further suggested that the various phenolic -OH groups easily underwent base promoted methylation reactions and this could be one reason for their stark reduction in the current ^{31}P NMR studies.[24h] Additionally, cleavage of various interconnecting bonds would also result in these decreased peak intensities for the defined regions of the ^{31}P NMR spectra thereby further corroborating with the above-mentioned GPC results.

Table III.8: Reduction in hydroxyl groups of lignins quantified by ^{31}P NMR using cyclohexanol.

	% Reduction in -OH			
	Lignin	Aliphatic-OH	5-Substituted OH	Guaiacyl OH
LiO*t*-Bu	OS-BWL1	89	68	74
	OS-OL	84	48	73
	OS-CL	92	64	74
	Kraft	96	93	93
Cs_2CO_3	OS-BWL1	99	97	98
	OS-OL	98	98	97
	OS-CL	97	98	97
	Kraft	99	99	94

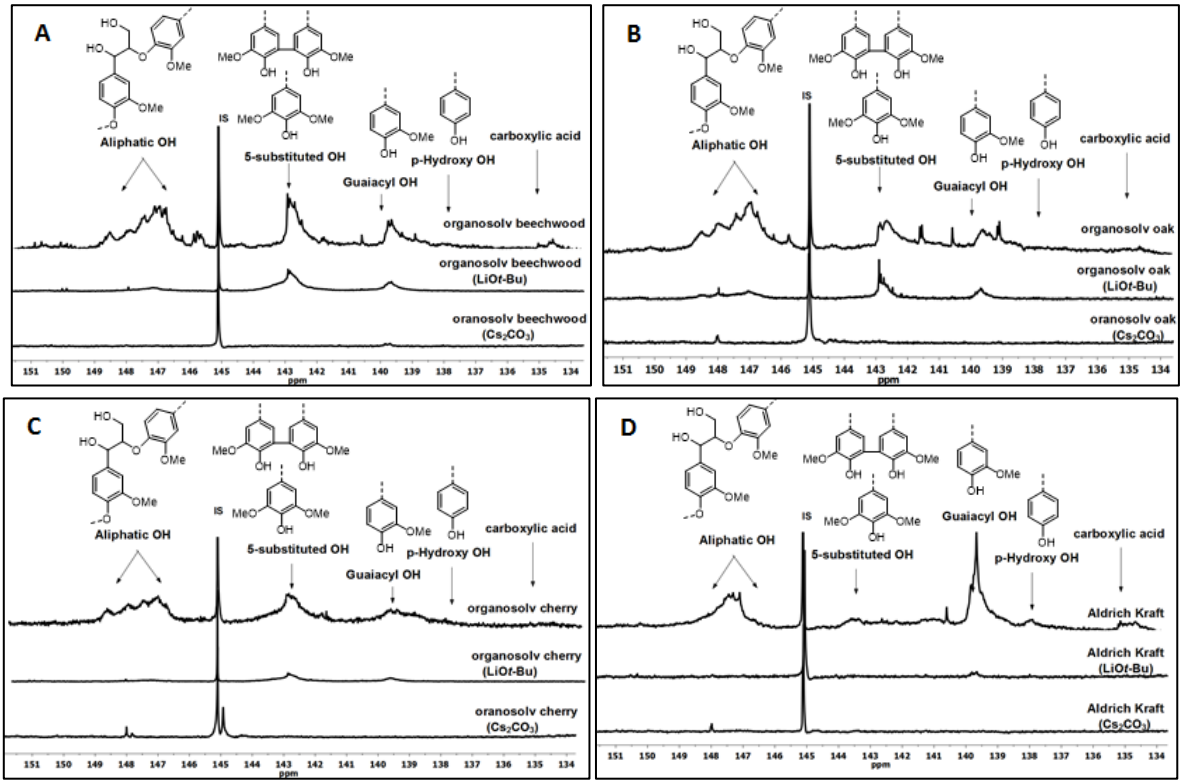

Figure III.10. ^{31}P NMR spectra of lignins before reaction, after reaction with 10 wt% Cs_2CO_3 and after reaction with 10 wt% LiO*t*-Bu. **A:** beechwood lignin; **B:** oak lignin; **C:** cherry lignin; **D:** Aldrich kraft lignin.

Finally based on the results obtained from various analytical techniques such as 2D-HSQC, GPC and ^{31}P NMR analaysis, it was concluded that the reactions catalyzed by 10 wt% Cs_2CO_3 displayed the highest reduction in the lignin molecular weights. Moreover, since the corresponding GPC analysis determined the Mw values in the range of aromatic monomers and oligomers (200–1900 Da) for all four lignin samples (Table III.7), the proceeding efforts were thus put into the separation and quantification of the major aromatic fragments from the solid residue of the post reaction lignin mixtures.

These low-molecular weight oil fractions were further separated from the solid reaction residues by consecutively extracting them into EtOAc (Figure III.11). The resulting oils that ranged between 52–67% (w(oil)/w(initial lignin)) were then subjected to GC-MS analysis after the addition of a known quantity of *n*-octadecane as an internal standard.

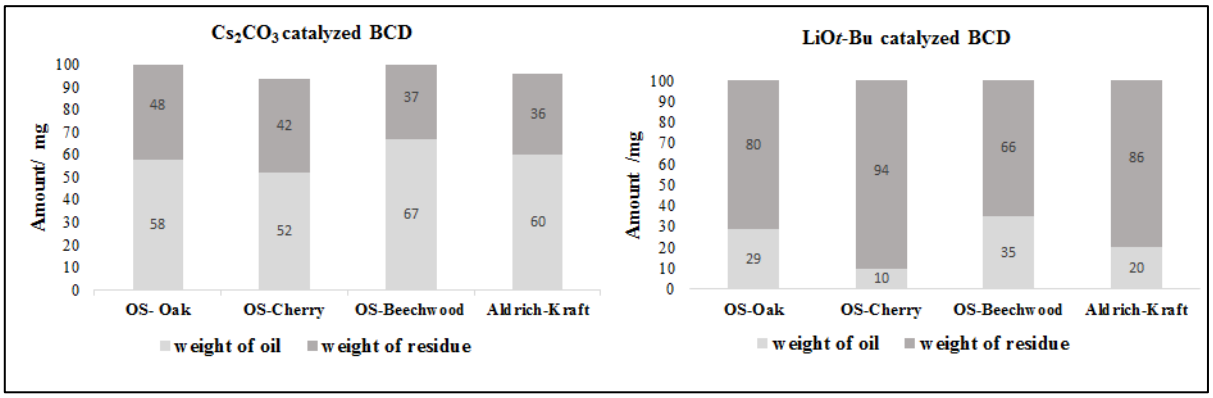

Figure III.11. Distribution of oil and solid residue obtained from Cs_2CO_3-catalyzed reaction in lignin samples.

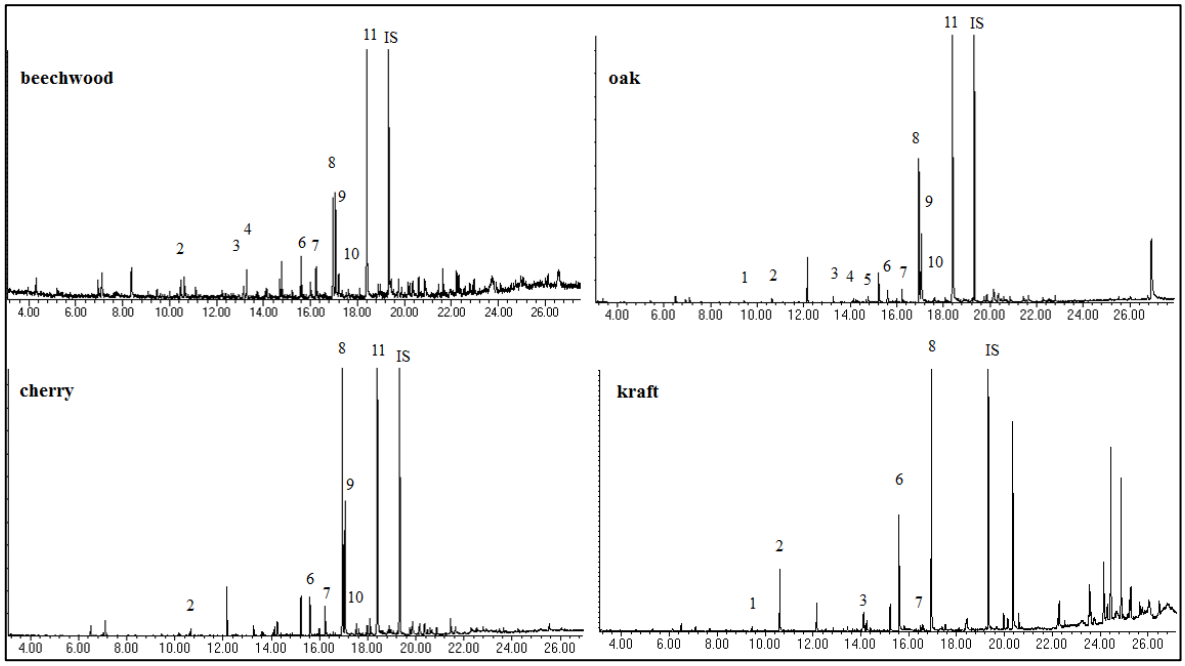

Figure III.12. Corresponding GC-FID traces for the oil fractions extracted from the residual solid lignins.

Delightfully, the GC-FID traces showed the presence of a range of low molecular weight products (Figure III.12). A careful analysis of the individual peaks validated the presence of methoxy-capped aromatics as the major cleavage products. Table III.9 summarizes the quantification results of the major mono-aromatic products present in the oil mixture (Figure III.12). A closer look at these products indeed affirmed the efficient derivatization of the aldehydes and phenols by DMC as expected to be seen with alliance to the extensive model based studies.

Furthermore, a good correlation was seen in the yields of the oil fractions and the general solubility of the lignin sample in the solvent DMC. Organosolv cherry lignin that had the lowest solubility in DMC afforded the lowest low-molecular weight oil fraction (52 wt%). As expected the product mixtures from the hardwood derived lignin (oak, cherry and beechwood) contained the capped syringaldehyde ester in major quantities while the capped guaiacyl ester yields remained within the ratio, corresponding well to the amount of **S** and **G** units in the lignin starting material (comparing Table III.6 and Table III.9). Because the kraft lignin from Sigma Aldrich (**#370959**) almost exclusively contains **G** units, the **S** unit containing products were only observed in trace quantities (Table III.9).

1.5.3. Cs_2CO_3-catalyzed BCD of beechwood chips.

Having successfully accomplished the Cs_2CO_3-initated degradation of four extracted lignin samples, one final application of the developed BCD system was further sought to be tested directly on beechwood chips (lignocellulosic raw material). The reaction was thus performed with a sample of pre-milled beechwood chips (100 mg) and Cs_2CO_3 (10 wt%) at 180 °C in dimethyl carbonate. Pleasingly an oil fraction of 40 wt% was recovered from the dark brown solid residue which accounted to around 60 wt% of the initail wood chip used. The oil fraction was yet again subjected to GC-MS analysis and gratifyingly the methoxy-capped monoaromatic products, similar to those detected for the extracted lignin samples, were again observed (Table III.9). A control reaction carried out in the absence of base however did not afford any cleavage products thereby ruling out the influence of pre-milling conditions on the product formation and distribution. The GC-FID traces for both these reactions are included in the experimental section of the thesis.

Table III.9: Methoxy-capped monomeric products obtained from BCD of lignins and beechwood chips.[a]

Peak No.	Monomers	OS-BWL1	OS-OL	OS-CL	KL	BW-chips
		wt% of starting material				
1	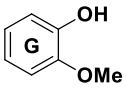	-	0.01	-	0.03	-
2	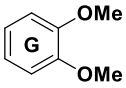	0.05	0.03	0.02	0.3	0.2
3	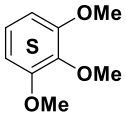	0.1	0.2	-	0.05	0.05
4	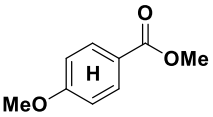	0.03	0.01	-	-	0.02
5	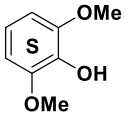	-	0.02	-		-
6	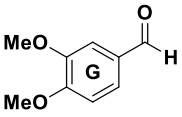	0.1	0.1	0.1	0.1	0.1
7	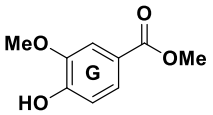	0.2	0.1	-	0.01	-
8	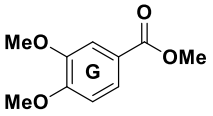	1.1	0.6	0.9	1.8	0.8
9	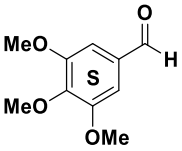	0.2	0.3	0.4	-	0.2
10	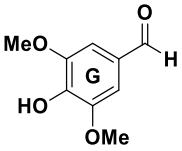	0.05	0.02	0.05	-	-
11	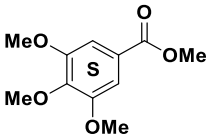	3.2	3.4	4.0	-	1.2
	Total	5.0	4.9	5.5	2.3	2.6

1.5.4. NaOH and KOH-catalyzed BCD of Aldrich Kraft lignin.

In the end, Kraft lignin (softwood) from Aldrich was also employed for a base-catalyzed depolymerization reaction in the presence of two relatively cheaper bases *viz* NaOH and KOH. Previous studies on lignin model compound **D1** for both these bases, had confirmed cleavage after comparatively longer reaction times (24 h) than when carried out with Cs_2CO_3 (Table III.2, entry 8 and Table III.3, entry 10). The depolymerization attempts with Kraft lignin were therefore carried out overnight with 10 wt% of either of the two base at 180 °C.

Pleasingly, both the reactions resulted in the formation of capped cleavage products but the yields obtained for KOH catalyzed reactions were higher and comparable to those obtained by Cs_2CO_3 catalyzed reaction. (Table III.10)

Table III.10: Methoxy-capped monomeric products obtained from BCD of Aldrich Kraft Lignin.[a]

Entry	Monomers	NaOH	KOH
		wt% of starting material	
1	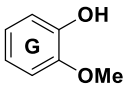	-	0.02
2	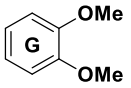	0.1	0.2
3	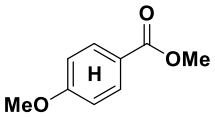	0.01	0.02
4	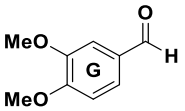	0.1	0.3
5	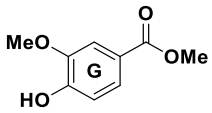	-	0.01
6	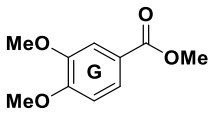	1.1	1.5
	Total	1.3	2.1

[a] Amounts are based on the individual calibrations done with respect to *n*-octadecane as an internal standard.

2. Chemoselective oxidation of primary alcohol followed by retro-aldol promoted cleavage of the C–C bond in lignin β-O-4 model compounds and lignin.

Research Background

In the introduction, it was elaborated that despite the presence of both 1° and 2° alcoholic groups in lignin, up until now the two-step chemoselective oxidative cleavage pathways have only been shown to proceed through benzylic alcohol (2°) oxidation (Scheme III.11)**.**[28] Although reports by both Stahl and co-workers and by Hanson and Baker include observations of cleavage products possibly formed through a primary alcohol oxidation route in β-O-4 and β-1 lignin model compounds using TEMPO/copper catalysts[28b] and vanadium catalysts[26n] independently, none of them pursued further investigations in this field. Driven by this less explored route, the current chapter is directed towards an organocatalytic one-pot two-step reaction pathway involving the chemoselective oxidation of the γ-alcohols followed by a retro-aldol reaction in lignin β-O-4 model compounds and lignin itself.

A literature survey on catalytic systems favouring such chemoselective alcohol oxidation reactions led us to a TEMPO/hypervalent iodine catalyzed oxidation pathway.[73-75] Iodine is a realtively cheap and environmentally benign element which is gaining popularity to catalyze a variety of chemical transformations. About 16% of the iodine produced annually is currently been used for various industrial catalytic processes.[74] Amongst other iodine based reagents, trivalent iodine reagents like iodosobenzene [PhIO], (diacetoxy)iodobenzene [$PhI(OAc)_2$, DAIB] and (phenyliodine bis(trifluoroacetate) [$PhI(OCOCF_3)_2$, PIFA] are commercially available, versatile and environmental safe iodine reagents, often used as mild and selective oxidants.[74] In fact, DAIB in combination with TEMPO has been found to selectively catalyze the oxidation of primary hydroxyl groups in the presence of secondary ones.[75] Applying this system to lignin was thus anticipated to open new synthetic opportunities in the field of lignin depolymerization recations.

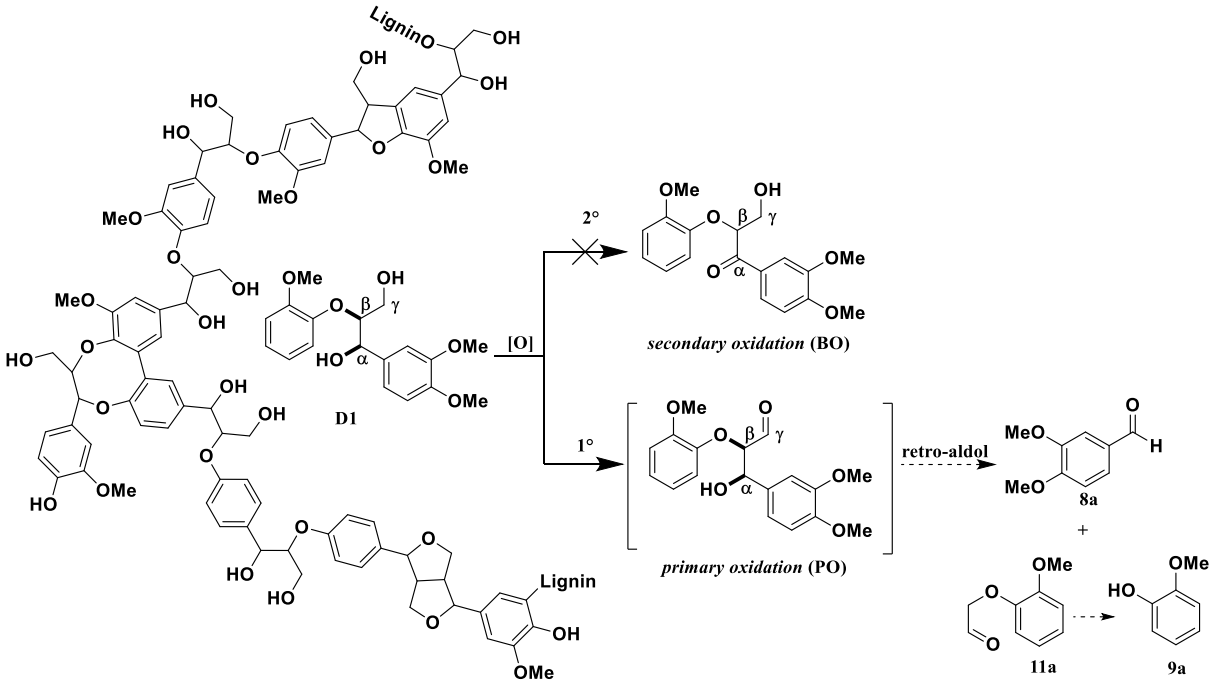

Scheme III.11. Chemoselective oxidation routes for lignin β-O-4 bonds.

2.1. Chemoselective oxidation of lignin β-O-4 model compounds

Table III.11: Chemoselective oxidation of γ-alcohol in lignin β-O-4 model compound **D1**[a]

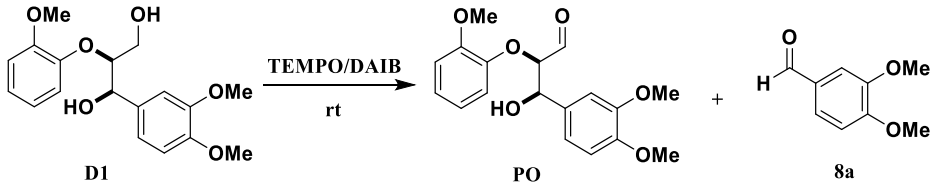

D1 PO 8a

Entry	TEMPO [equiv]	DAIB [equiv]	Solvent	Time [h]	Conv.[b] [%]	Yield [%][b]	
						PO	**8a**
1	1.00	-	CD_3CN	24	-	-	-
2	-	1.30	CD_3CN	24	10	-	-
3	0.30	1.30	CD_3CN	3	56	43	9
4	0.30	1.30	CD_3CN	7	>99	75	14
5	0.15	1.30	CD_3CN	7	>99	75	16
6[c]	0.15	1.30	CD_3CN	7	90	50	5
7	0.10	1.30	CD_3CN	7	>99	78	14
8	0.05	1.30	CD_3CN	7	70	45	5
9	0.15	1.00	CD_3CN	7	84	55	12
10	0.15	1.30	$CDCl_3$	7	>99	44	10
11	0.15	1.30	$(CD_3)_2CO$	7	>99	65	8
12	0.15	1.30	$(CD_3)_2SO$	7	50	10	5
13	0.15	1.30	$C_6D_5CD_3$	7	70	30	10
14	0.15	1.30	C_3H_7NO	7	65	34	4
15	0.15	1.30	DMC	7	20	15	4

[a] Reaction conditions: **D1** (83.60 mg, 0.25 mmol), TEMPO and DAIB were stirred in solvent (2.0 mL) at rt for the specified time. [b] The conversion of **D1** as well as the yields of **PO** and **8a** were determined by quantitative ^{1}H NMR with 1,4-dinitrobenzene as the internal standard. [c] Solvent (1.0 mL).

The *erythro* dilignol **D1** was again chosen as a standard β-O-4 model substrate. The optimization reactions were performed in deuterated solvents, in order to monitor the reaction progress by quantitative ^{1}H NMR with respect to 1,4-dinitrobenzene. The initial control reactions of **D1** in CD_3CN either with TEMPO (1.00 equiv) or DAIB (1.30 equiv) separately, did not result in considerable conversion even after 24 h of stirring at rt (Table III.11, entries 1–2). However, the combination of TEMPO (0.30 equiv) with DAIB (1.30 equiv) in CD_3CN led to a 56% conversion of **D1** in just 3 h at rt (emtry 3). The quantitative ^{1}H NMR of this reaction also showed the formation of a dimeric aldehyde product with shifted α- and β- protons relative to the substrate **D1**, hence suggesting the formation of a γ-oxidized primary oxidation product **PO** in 43% yield (Figure III.13, top)**.** Delightfully, the benzylic alcohol oxidation product was not observed thereby ascertaining the high selectivity of the process. Additional traces of veratraldehyde (**8a**) were also detected in the reaction mixture because of the retro-aldol reaction of **PO**, catalyzed by the *in-situ* generated AcOH (entry 3). A further increase in the reaction time from 3 h to 7 h resulted in the complete conversion of dilignol **D1**, affording **PO** and **8a** in higher yields of 75% and 14% respectively (entry 4; Figure III.13, bottom). At this stage, reducing the crude reaction mixture with $NaBD_4$ (2.00 equiv) in MeOH (1.0 mL) gave back the starting model **D1** with a deuterated γ-proton (**D1-*d***) as depicted by the 2D-HSQC experiment in Figure III.14. This experiment further ascertained **PO** to be the γ-oxidized product. Furthermore, reducing the amount of TEMPO from 0.30 equivlent to 0.10 equivalent, while keeping the amount of DAIB constant did not affect the outcome of the oxidation (entries 4–7). A further reduction of TEMPO to 0.05 equivalent, however, reduced the conversion of **D1** to 70% (entry 8). Finally, a decrease in the amount of DAIB to 1.00 equivalent with 0.15 equivalent TEMPO also gave lower yields of **PO** (55%) and **8** (12%) (entry 9). Additional solvent screenings resulted in relatively lower product yields and conversions (entries 10–15).

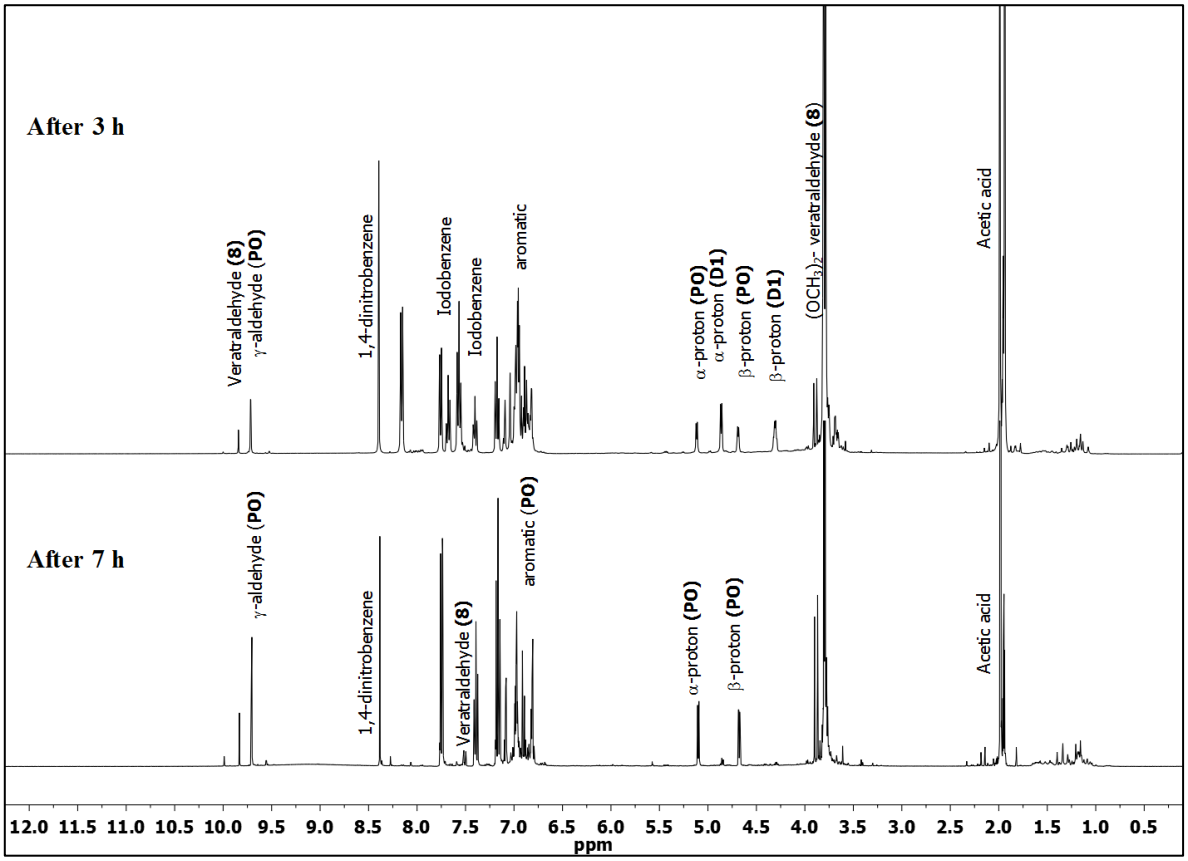

Figure III.13. Reaction mixtures stirred at rt consisting of **D1** (83.6 mg, 1.0 equiv), TEMPO (0.3 equiv), DAIB (1.30 equiv) and internal standard 1,4-dinitrobenzene (7.20 mg). **Top:** reaction mixture after 3 h; **Bottom:** reaction mixture after 7 h.

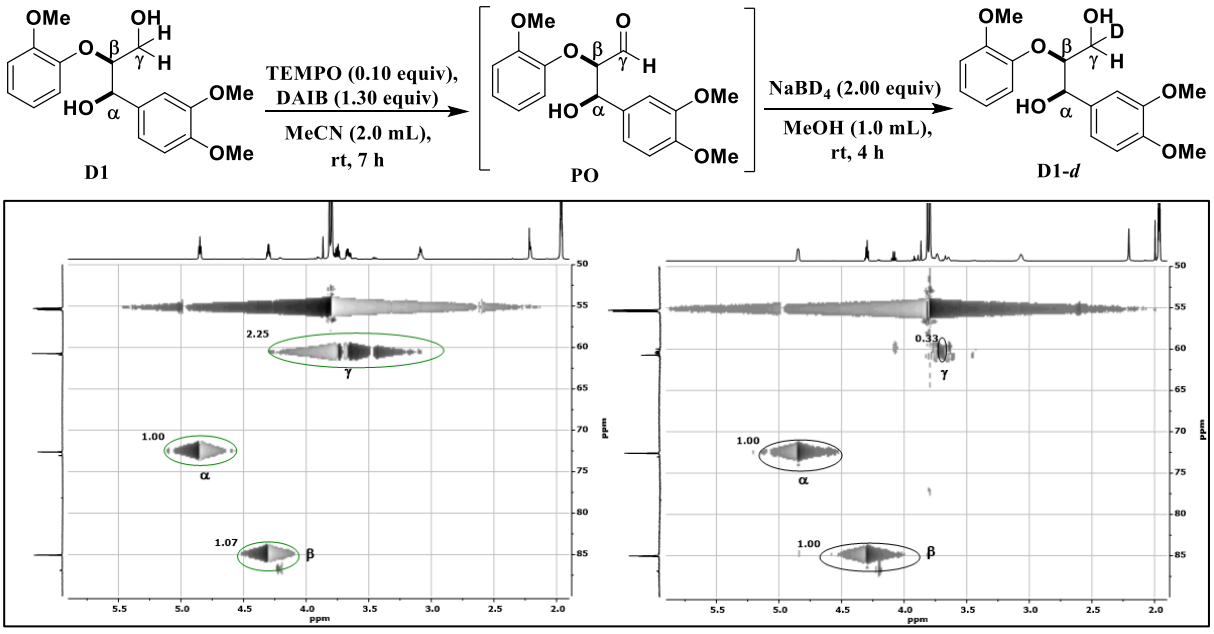

Figure III.14. 2D-HSQC NMR spectra (zoom of the region 5.4-2.0 ppm recorded in CD_3CN); (a) α,β,γ proton region in **D1** before the reaction (left). (b) α,β,γ proton region in **D1-*d*** after the $NaBD_4$ reduction of the γ-carbonyl in **PO** (right).

Table III.12: Screening various nitroxide radical species and terminal oxidants for the γ-alcohol oxidation in **D1**.[a]

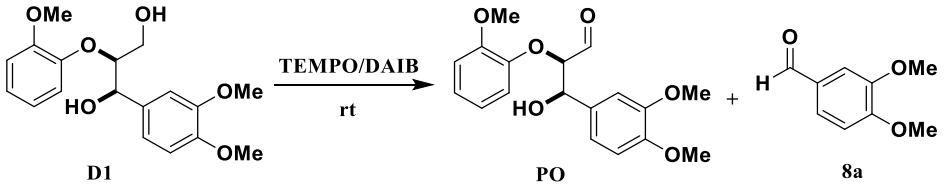

Entry	*N*-nitroxyl radical (equiv)	Terminal oxidant (equiv)	Conv. [%][b]	Yield [%][b]	
				PO	**8a**
1	TEMPO (0.15)	$PhIO_2$ (1.30)	30	-	-
2	TEMPO (0.15)	PhIO (1.30)	50	10	-
3	TEMPO (0.15)	PIFA (1.30)	60	-	15
4	TEMPO (0.15)	HTIB (1.30)	95	-	35
5	TEMPO (0.10)	DAIB(1.30)	>99	78	14
6	AcNH-TEMPO (0.15)	DAIB(1.30)	>99	60	14
7	OH-TEMPO (0.15)	DAIB(1.30)	60	45	8
8	NHPI (0.15)	DAIB(1.30)	17	7	-

[a] Reaction conditions: **D1** (0.25 mmol, 1.00 equiv), CD_3CN (2.0 mL), rt, 7 h. [b] Conversion of **D1** as well as the yields of **PO** and **8a** were determined by ^1H NMR spectroscopy with 1,4-dinitrobenzene as the internal standard. AcNH-TEMPO = 4-acetamido-TEMPO, OH-TEMPO = 4-hydroxy-TEMPO, NHPI = *N*-hydroxypthalimide.

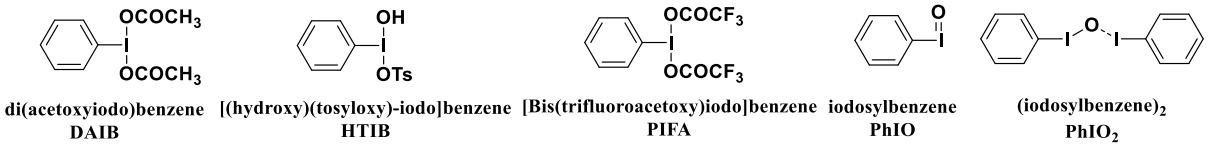

Figure III.15. Trivalent iodobenzene derivatives

With regards to optimizing the reaction conditions for the TEMPO/DAIB catalyzed chemoselective oxidation of γ-OH in model compounds **D1**, several other combinations of *N*-nitroxyl radicals and hypervalent iodobenzene reagents were screened as listed in Table III.12. These include the combination of catalytic amounts of TEMPO (0.15) with stoichiometric amounts of commercially available trivalent iodobenzenes DAIB, $PhIO_2$, PhIO, PIFA and HTIB (entries 1–5). Though moderate to high conversion of **D1** (30–95%) was obtained for the respective terminal oxidants (entires 1–4), the product spectra were not selective for the primary oxidation product **PO**. However, veratraldehyde (**8a**) was identified in 15 and 35 % respectively for PIFA and HTIB oxidized reaction mixtures (entries 3 and 4). On the other hand, replacing the TEMPO with its *para*- substituted derivatives such as 4-Acetamido-TEMPO (AcNH-TEMPO) and 4-Hydroxy-TEMPO (OH-TEMPO) resulted in a better product spectrum. Both AcNH-TEMPO and OH-TEMPO afforded a moderate to high conversion of **D1** yielding **PO** in 60% and 45% yield respectively (entries 6 and 7). Nonetheless, substitution with NHPI again resulted in a stark drop in the conversion of **D1** (entry 8).

Hence it could be concluded that amongst all the above combinations, the TEMPO/DAIB catalytic system indeed supported the oxidation of the γ-OH group with high chemoselectivity (entry 5).

Table III.13: One-pot chemoselective oxidation of **D1** followed by amine catalyzed retro-aldol of **PO**[a]

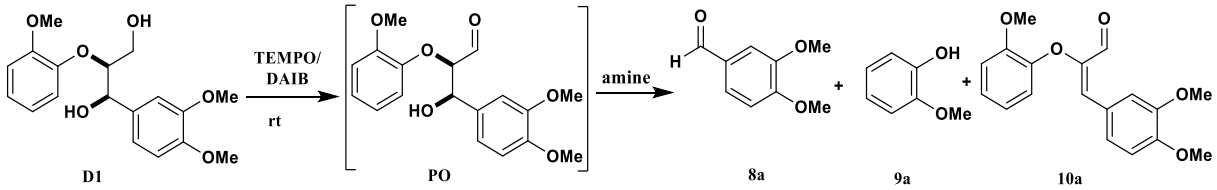

Entry	Catalyst	Amount (equiv)	Conv. [%][c]	Yield [%]			
				[PO]	**8a**	**9a**	**10a**
1[b,c]	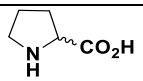	0.10	7	5	2	n.d.	-
2[c]	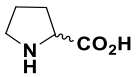	0.10	>99	25	52	n.d.	-
3[d]	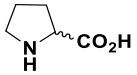	0.20	>99	-	70	26	5
4[c]	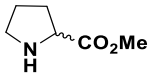	0.20	>99	40	23	n.d.	14
5[c]	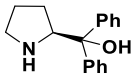	0.20	>99	50	26	n.d.	4
6[d]		0.20	>99	-	25	10	58
7[d]	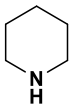	0.20	>99	-	25	12	55
8[d]	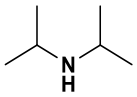	0.20	>99	-	25	4	37

[a] Reaction conditions: **D1** (0.25 mmol, 1.00 equiv), TEMPO (0.10 equiv), DAIB (1.30 equiv) were stirred in MeCN (2.0 mL) at rt for 7 h. Then the amine was added, and the stirring continued for 5 h at rt. [b] Proline was added from the start of the reaction. [c] Determined by ^{1}H NMR spectroscopy with respect to 1,4-dinitrobenzene. [d] Yields after column chromatography.

Subsequent efforts were directed towards the cleavage of C–C bond in **PO** initiated by retro-aldol. For this purpose, readily available amine-based organocatalysts were included into a one-pot reaction sequence starting with the above-developed chemoselective oxidation of the γ-OH in β-O-4 model compound **D1**. The first attempt was made with DL-proline, an organocatalyst known to initiate the aldol/retro-aldol reactions.[76] The additon of 0.10 equivalent of DL-proline from the onset of the oxidation reaction, resulted in the quenching of the system with the conversion falling to as low as 7% (Table III.13, entry 1). However, to our delight the organocatalyst proved to be compatible with the two-step sequential reaction conditions and with 0.20 equivalent DL-proline, the system afforded veratraldehyde (**8a**) along with guaiacol (**9a**) in 70% and 26% yields respectively (entries 2 and 3). The importance of the bifunctionality present in proline was demonstrated by testing its methyl ester and diphenylprolinol, which slowed down the retro-aldol reaction and also led to the formation of the elimination product **10a** (entries 4 and 5). Furthermore, α,β-unsaturated aldehyde **10a** was obtained preferentially when the more basic amines pyrrolidine and piperidine were used as a catalyst instead of DL-proline (entries 6 and 7). Using the noncyclic diisopropylamine, however, afforded both the cleavage product **8a** and elimination product **10a** in nearly equal proportions (entry 8).

Next, the one-pot two-step cleavage reaction for the model compound **D1** catalyzed by DL-proline was repeated with the aim to determine the full product profile apart from those obtained after column chromatography. This was done by subjecting the crude reaction mixture for quantitative GC-MS analysis with respect to an internal standard *n*-octadecane (Table III.14). Indeed, the GC-MS chromatogram helped in the determination of another retro-aldol product 2-(2-methoxyphenoxy) acetaldehyde (**11a**). This product was speculated to be unstable the under chromatographic conditions and was thus synthesized separately for GC peak matching and calibration purposes. The details for its synthesis have been included in the experimental section of the thesis. Additionally, stirring a solution of (**11a**) and DL-proline in MeCN at room temperature resulted in the formation of guaiacol (**9a**) in 62% GC yield after just 1 h. This observation further features the low stability of aldehyde (**11a**) and the pathway involved in the production of guaiacol in the reaction (Scheme III.12).

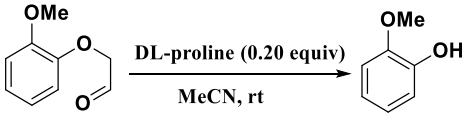

Time / h	Conv. [%] 11a	Yield [%] 9a
1	72	69

Scheme III.12. *In-situ* conversion of **11a** to **9a** under the reaction conditions.

Besides the above-mentioned product, minor oxidative by-products from veratraldehyde (**8a**) and guaiacol (**9a**) [77] were also observed as listed below.

Table III.14: GC-FID peak analysis for the crude mixture after the two-step oxidative degradation of dilignol (**D1**).[a]

Entry	r.t. (min)	*m/z*	Structure	Yield[%]	Database match (%)
1	9.5	124	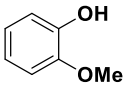	40	87 Sample injected
2	13.7	166	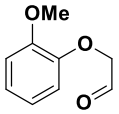	20	Sample injected
3	14.5	140	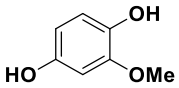	5	97 Sample injected
4	15.4	140	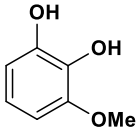	3	83 Sample injected
5	15.6	166	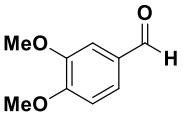	78	98 Sample injected
6	17.8	180	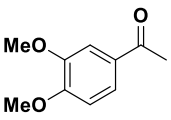	6	90 Sample injected
7	26.2	314	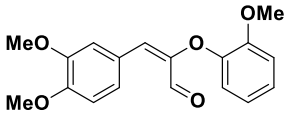	8	Sample injected

[a] Yields are based on the individual calibrations done with respect to *n*-octadecane as an internal standard.

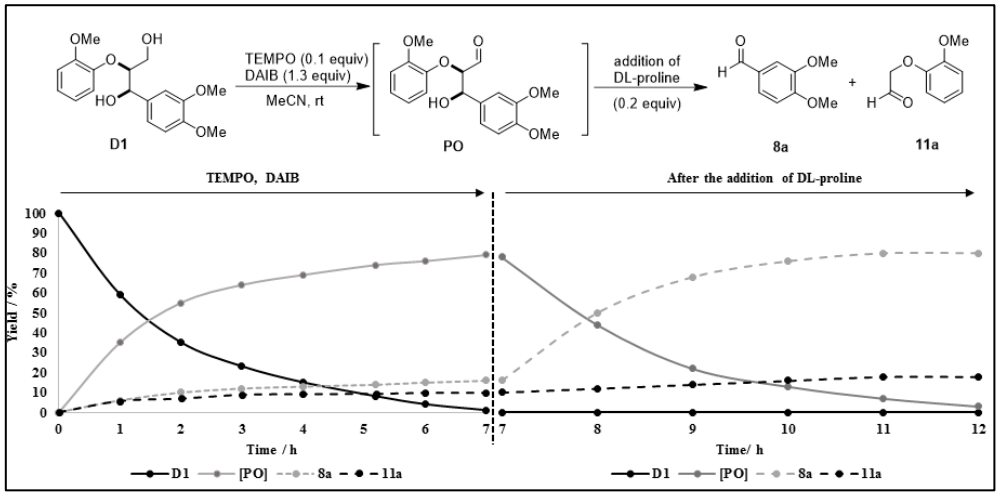

Figure III.16. Reaction profile for the one-pot two-step chemoselective γ-OH oxidation and cleavage of model compound **D1.**

To understand the reactivity and selectivity of both the steps, the reaction-time profile for **D1** was monitored by quantitative ^{1}H NMR analysis with respect to 1,4-dinitrobenzene (δ = 8.4 ppm) under the optimized reaction conditions (Figure III.16). GC was avoided for this purpose due to the decomposition of **PO** during chromatographic analysis. Furthermore, the consumption of **D1** and **PO** along with the formation of **8a** and **11a** was quantified relative to their α- proton peaks (**D1**: δ = 4.8 ppm, **PO**: δ = 5.1 ppm) and aldehyde peaks (**8a**: δ = 9.8 ppm, **11a**: δ = 10.0 ppm). The formation of guaiacol (**9a**) could not be traced effectively using ^{1}H NMR spectra owing to the overlapped aromatic and methoxy regions and was thus excluded from the reaction profile.

The cumulative plots displayed a good correlation between the consumption of **D1** (black line) and the formation of **PO** (grey line). A full conversion for **D1** was obtained after 7 h, affording **PO** in 79% and veratraldehyde (**8a**) (grey dash) in 16% yield respectively. Thereafter the addition of DL-proline initiated a spontaneous retro-aldol cleavage of **PO**. The yield of (**8a**) increased to 50% after the first hour of addition and plateaued out at 80% within the next 5 h. The retro-aldol product 2-(2-methoxyphenoxy) acetaldehyde (**11a**) (black dash) also followed a similar reaction pattern as **8a,** yielding 10% after 7 h. Finally based on the above observations, a reaction pathway could be proposed for the one-pot two-step chemoselective oxidation and subsequent the cleavage of C–C bonds in **D1 (**Scheme III.13).

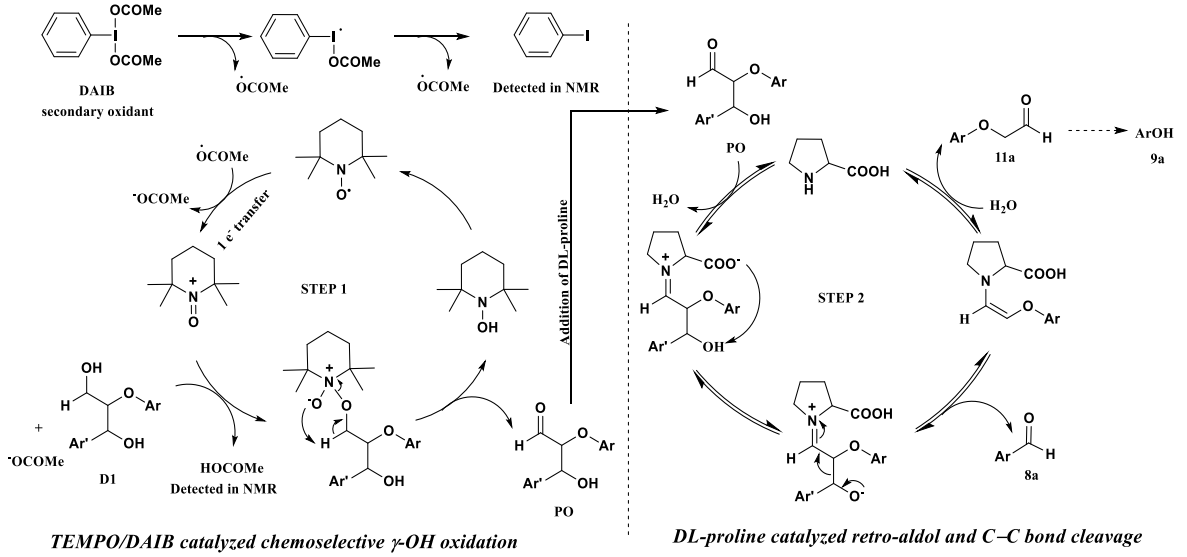

Scheme III.13. Proposed pathways for the one-pot two-step γ-OH oxidation and subsequent cleavage in **D1.**

Table III.15: One-pot two-step degradation of *β*-O-4 lignin model compounds.[16]

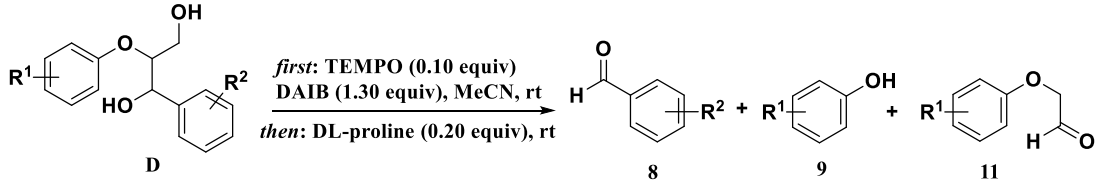

Entry	Substrate	1st + 2nd [h]	Cleavage products [Yield][a]		
1	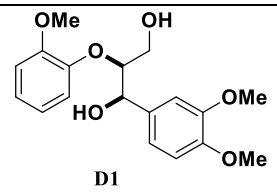 D1	7 + 5	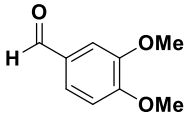 8a 76% (70%)	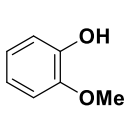 9a 40% (26%)	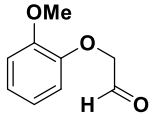 11a 20%
2	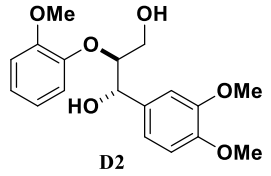 D2	7 + 5	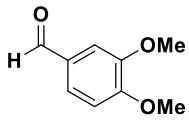 8a 74% (67%)	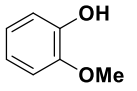 9a 42% (20%)	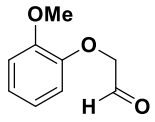 11a 19%
3	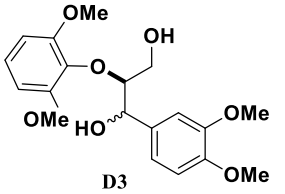 D3	10 + 7	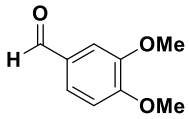 8a 73% (60%)	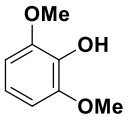 9b 29% (16%)	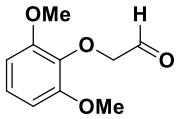 11b 32%
4	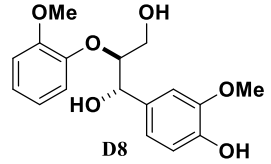 D8	7 + 5	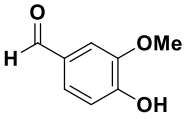 8b 24% (15%)	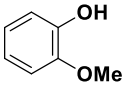 9a 17% (5%)	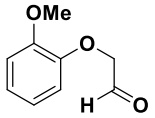 11a 6%
5	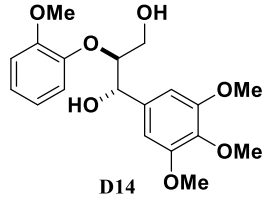 D14	7 + 5	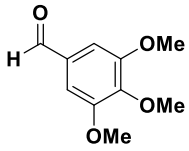 8c 79% (68%)	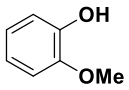 9a 46% (28%)	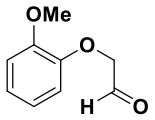 11a 18%
6	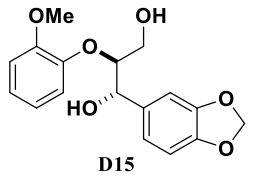 D15	7 + 5	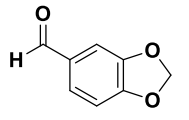 8d 70% (59%)	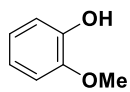 9a 35% (12%)	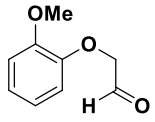 11a 14%

[a] Quantifications done by gas chromatography with respect to *n*-octadecane as an internal standard. Values within the parenthesis are obtained after column chromatography and are based on an average of two runs.

In a quest to further examine a wider applicability of this organocatalytic primary hydroxyl oxidation/retro-aldol approach, the analogous cleavage studies were performed on a series of *β*-O-4 lignin model compounds. These include compounds bearing both the benzylic and primary hydroxyl groups but differing in the proportions of guaiacyl (**G**) and syringyl (**S**) aromatic nuclei and their *erythro* and *threo* stereostructures (Table III.15, **D1**–**D3** and **D8**–**D14**, **D15**).[78] The TEMPO/DAIB system once again showed excellent selectivity towards the oxidation of the *γ*-OH group in models **D1**–**D3**, **D14** and **D15**. Furthermore, the following addition of DL-proline also effectively catalyzed the retro-aldol cleavage in the consecutive experiments. Table III.15 lists the GC yields for the corresponding major monoaromatic products **8**, **9** and **11** obtained after the two-step reaction.

In general, all the model compounds resulted in full conversion (>98%) after the organocatalytic two-step reaction. The *threo* diastereomer **D2** exhibited a similar reactivity as the *erythro* dilignol **D1**, affording veratraldehyde (**8a**) in 74% and guaiacol (**9a**) in 42% GC yields, along with the detection of 2-(2-methoxyphenoxy) acetaldehyde (**11a**) in 19% yield (entries 1 and 2). The model compound **D3** bearing an extra *ortho*- methoxy group at the phenoxy ring (**S**), however, required a slightly longer reaction time (Figure III.17). Despite this, the corresponding monoaromatics **8a**, **9b** and **11b** were obtained in good yields of 73%, 29% and 32% respectively after the two-step cleavage process (entry 3). Next, the **G** type model compound **D4** with a free phenolic OH- group was tested. Although the substrate was entirely consumed witin the first few hours of the reaction, vanillin (**8b**) was obtained in just 24% yield along with guaiacol **(9a)** in 17% and 2-(2-methoxyphenoxy) acetaldehyde (**11a)** in 6% yields, respectively. This can be attributed to the active phenolic OH-group that could get involved in other side reactions under an oxidative environment thereby resulting in decreased product selectivities. Furthermore, model compounds exhibiting different substitution pattern and steric variations at the arenes adjacent to the benzylic group were tested. Unlike substrate **D3**, model compound **D14** bearing an **S**-type methoxy substituted nuclei followed a similar reaction time profile as **D1**. The maximum *γ*-OH oxidized product was formed within 7 h of the start of the reaction and the highest yields for 3,4,5-trimethoxybenzaldehyde **8c** (79%) was obtained in the next 5 h after the addition of DL-proline (Figure III.18). Dilignol **D15**, bearing (methylenedioxy)phenyl capped arene moiety, also afforded **8d** in 59% after column chromatography (entry 6).

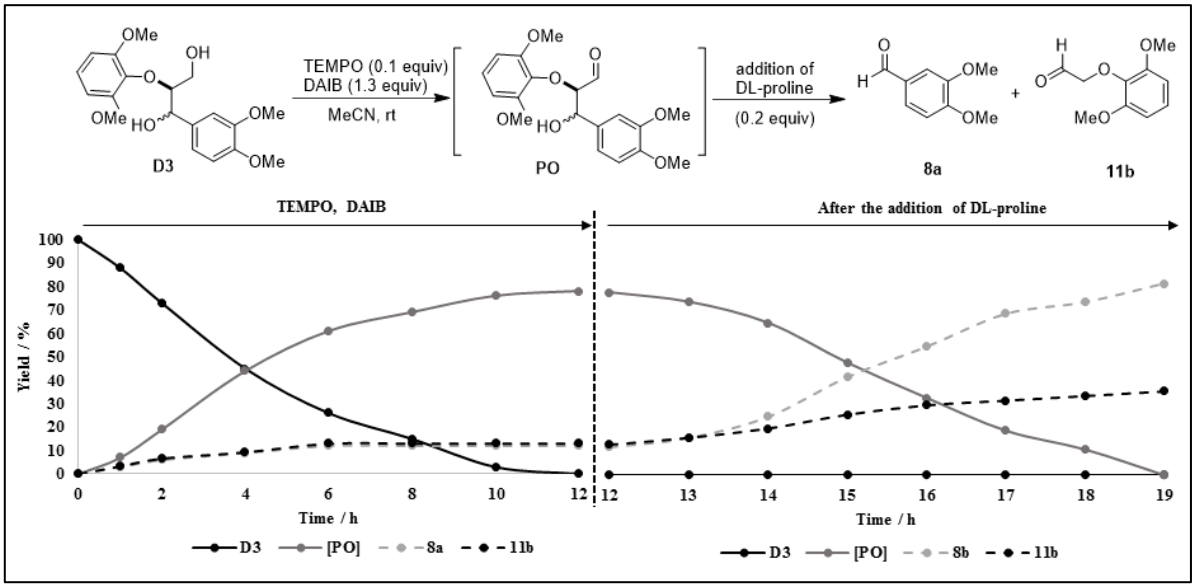

Figure III.17. Reaction profile for the one-pot two-step chemoselective *γ*-OH oxidation and cleavage of model compound **D3**.

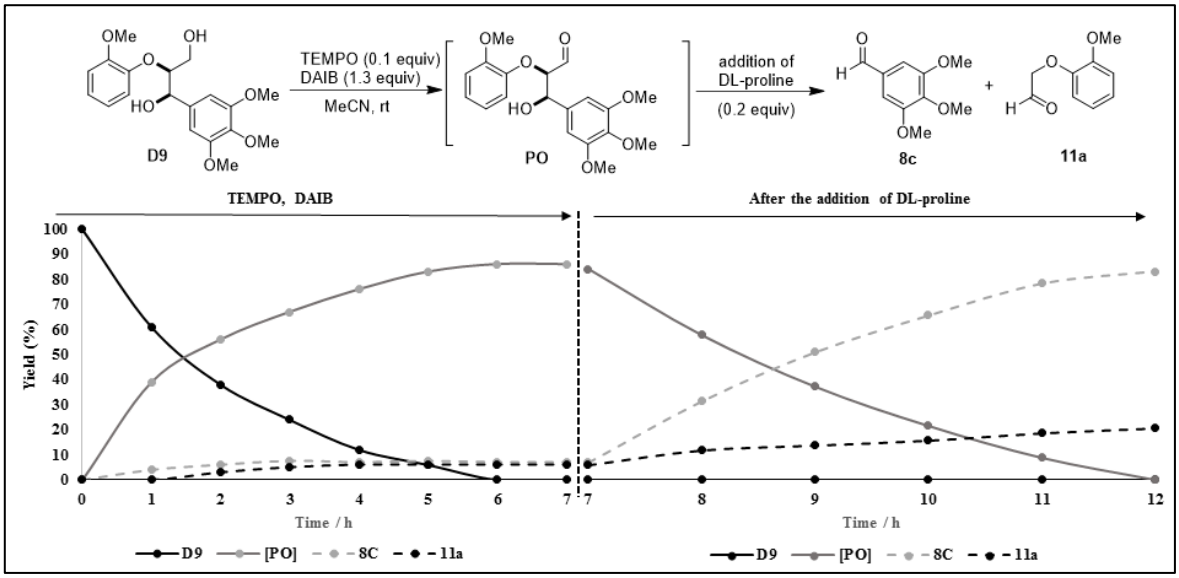

Figure III.18. Reaction profile for the one-pot two-step chemoselective *γ*-OH oxidation and cleavage of model compound **D9**.

After confirming the activity of the TEMPO/DAIB catalytic system for the chemoselective oxidation of a wide range of lignin models, the next aspect was to ponder upon the use of immobilized stoichiometric hypervalent oxidants in order to make the overall process more economical. Thus, replacing DAIB by an immobilized variant such as poly[4-(diacetoxyiodo)-styrene] [75 e,f]] was forseen as a propitious opportunity to achieve similar reactivity and product selectivity.

Indeed, a two-step room temperature degradation of **D1** using TEMPO/immobilized DAIB catalytic system after 28 h resulted in a mixture of products **8a** and **9a** in 80% and 48% yields, respectively (Scheme III.14). Pleasingly, using this recycled iodine reagent in a second reaction run again afforded the products with same selectivity and in similar yields as the first round (**8a**: 76%, **9a**: 50%).

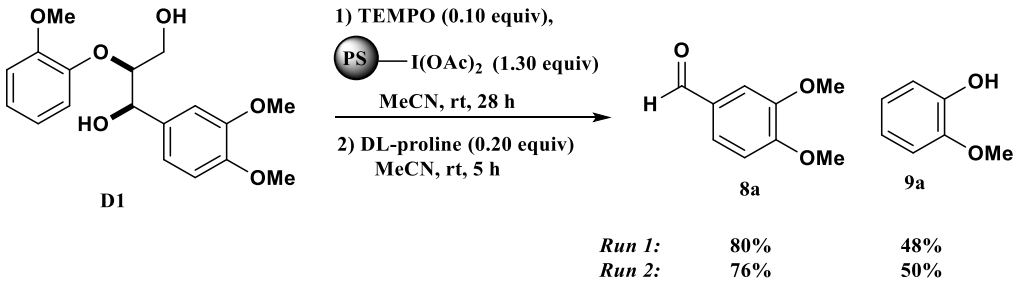

Scheme III.14. Use of immobilized DAIB catalyst as a terminal oxidant for the two-step oxidative degradation of **D1**.

2.2. Chemoselective oxidation of real lignin samples

The success of the sequential organocatalytic oxidative degradation strategy on lignin model compounds further encouraged us to test its applicability on the cleavage of two organosolv lignin samples from beechwood (**OS-BWL1**) and oak (**OS-OL**) following the one-pot procedure. Figure III.19 depicts the 2D-HSQC NMR spectra before and after the two-step degradation reactions of lignin samples **OS-BWL1** and **OS-OL**.[79] As revealed by the disappearance of their characteristic signals in the HSQC spectra, several interconnecting bonds including the β-O-4 linkages contained in substructures **A**, the phenylcoumaran substructure **C** and even the the resinol units **B** were completely cleaved following this degradation strategy.

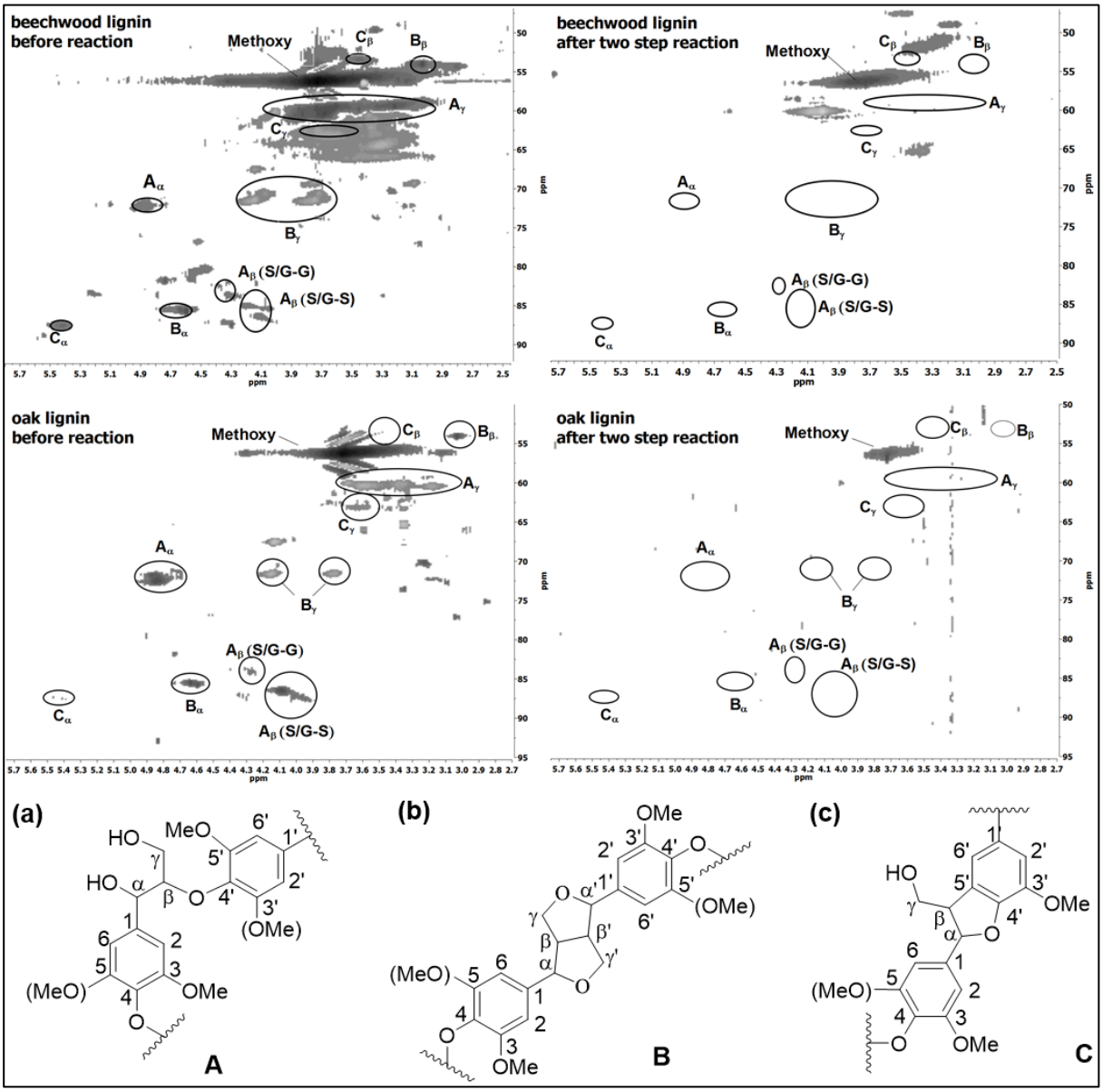

Figure III.19. 2D-HSQC NMR spectra (in DMSO-d_6). **Top**: beechwood lignin (**OS-BWL1**) before and after the two-step degradation reaction. **Bottom**: Oak lignin (**OS-OL**) before and after the two-step degradation reaction. (a) β-O-4' aryl ether linkages. (b) Resinol substructures formed by β–β'-, α-O-γ'-, and γ-O-α'-linkages; (c) phenylcoumaran substructures formed by β-5'- and α-O-4'-linkages.

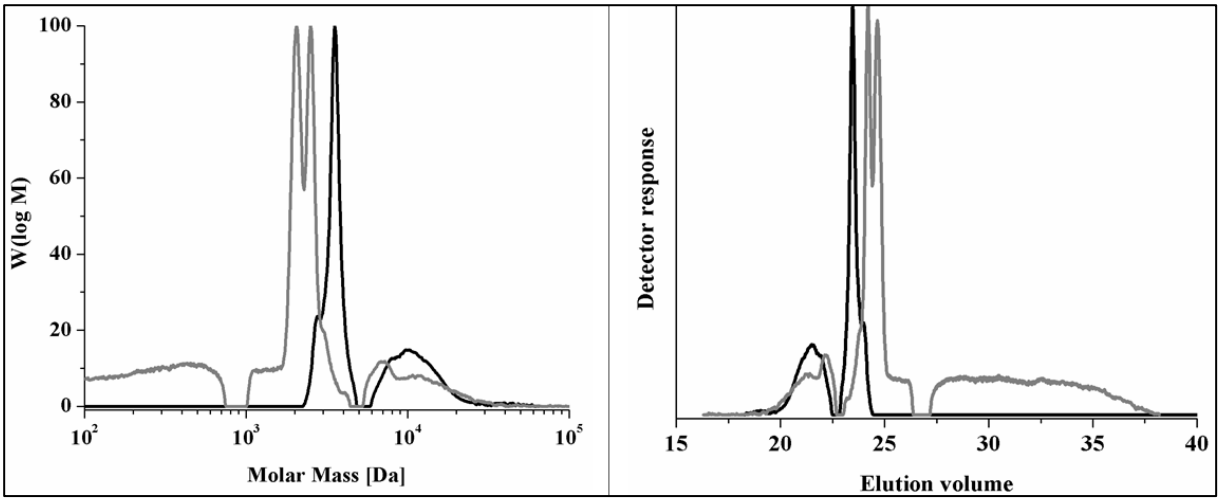

Figure III.20. GPC measurements for beechwood lignin (**OS-BWL1**): before reaction (black line); after the one-pot two-step degradation (grey). **Left:** mass distribution with respect to sulfonated polystyrene standard calibration; **right:** elugram.

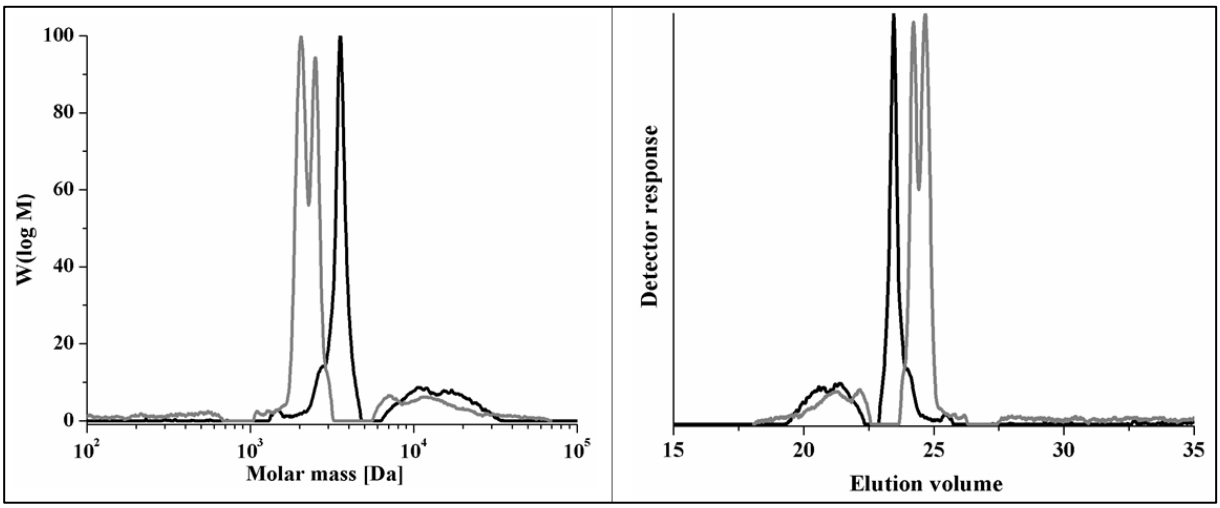

Figure III.21. GPC measurements for oak lignin (**OS-OL**): before reaction (black line); after the one-pot two-step degradation (grey). **Left:** mass distribution with respect to sulfonated polystyrene standard calibration; **right:** elugram.

Although the changes in HSQC spectra hinted towards the structural modifications after the two-step cleavage reactions, the reaction mixtures for samples **OS-BWL1** and **OS-OL** were analyzed by gel permeation chromatography (GPC) to determine the post degradation changes in their molecular weights. Figures III.20 and Figure III.21 depict the respective mass distribution chromatogram and the corresponding elugram for the organosolv lignins. For both these treated lignins, a double shift in the mass maximum was observed towards the lower molecular weights (grey line). In the case of **OS-BWL1**, the original mass maxima at 3537 Dalton (black line) was significantly reduced by 29% and 41% (grey lines). Additionally, a broad peak having initially a maximum mass value at approximately 10206 Dalton showed a decrease of 32% after the cleavage. Similarly, the maximum mass value in the original **OS-OL** sample at 3570 Dalton (Figure III.21, black line) was significantly reduced by 30% and 43% along with the broad peak at approximately 12375 Dalton showing a decrease of 27% after the cleavage.

To our delight, the absence of peaks at higher molecular weights with respect to the original mass values of **OS-BWL1** and **OS-OL** after the reactions, precluded the possibility of lignin re-polymerization under the described cleavage reaction conditions.

Furthermore, the organic fractions which accounted to 15 wt% of the starting lignin **OS-BWL1** and 20 wt% of the starting lignin **OS-OL**, were also analyzed by GC measurements. These confirmed the presence of low-molecular monomeric aromatics that are typical products found in the cleavage reactions of hardwood lignin (Table III.16).

Table III.16: Monomeric products obtained after the one-pot, two-step oxidative depolymerization of lignin.

Entry	Retention time [min]	Monomers	OS-BWL1	OS-OL
			[wt% of starting sample][a]	
1	9.5	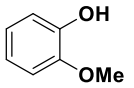	0.3 Sample injected	0.4 Sample injected
2	14.5	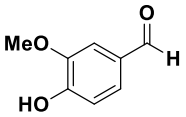	1.5 Sample injected	2.6 Sample injected
3	15.3	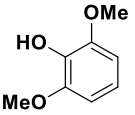	0.1 Sample injected	0.3 Sample injected
4	15.5	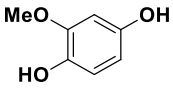	0.05 Sample injected	0.1 Sample injected
5	16.6	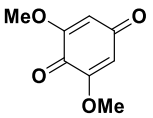	0.1 Sample injected	0.05 Sample injected
6	17.8	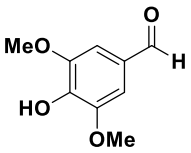	2.5 Sample injected	3.9 Sample injected
7	18.3	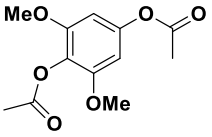	GC match: 95%	GC match: 95%
Total amount of mono-aromatics quantified			4.6	7.4

[a] Amounts are based on the individual calibrations done with respect to *n*-octadecane as an internal standard.

3. Mechanochemically induced oxidative depolymerization of lignin β-O-4 model-compounds and lignin

Research Background

Our group's previous achievement on lignin depolymerization in ball mills using inorganic bases,[64] prompted the further parallel investigations for the degradation studies by mechanochemical activation. The above established one-pot, two-step TEMPO/DAIB catalyzed C–C bond cleavage route for the lignin β-O-4 model compounds and lignin samples in acetonitrile (MeCN), was thus tested under solvent free conditions. This was also forseen as an opportunity to establish new oxidative degradation pathways for the biomacromolecule under milling conditions and enhance the degree of lignin depolymerization along with individual monomer yields by mechanochemical induction.

The chemoselective γ-OH oxidation step for the lignin model compound **D1** was re-addressed using a combination of TEMPO (0.1 equiv) and DAIB (1.3 equiv) catalytic system in a **RETSCH MM 400** mixer mill (**MM**) at 25 Hz using a 10 mL ZrO_2 milling jar with one ZrO_2 ball of 10 mm in diameter (Scheme III.15). After only 90 minutes of milling, a conversion of 73% was obtained for the dilignol **D1**, resulting in the formation of both primary oxidation (**PO**, 25%) and secondary (benzylic) oxidation (**BO** (**12d)**, 37%) products in the ratio of 1:1.5. This result was found to be at variance with the observations made in solution (Table III.11) and hence highlighted a major shift in product selectivity towards an additional benzylic oxidation product (**12d**) under the milling environment. Since no literature precedence was found addressing such chemoselective oxidation of lignin under mechanochemical conditons, this opportunity was envisaged to improve the observed reactivity for a more favourable benzylic alcohol oxidation product (**12d**) with a possible extension to lignin.

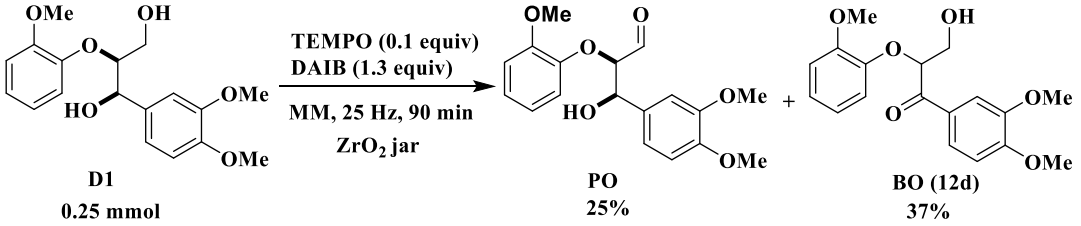

Scheme III.15. TEMPO/DAIB catalyzed oxidation of **D1** in a mixer mill (**MM**).

Owing to the absence of regular gas inlets (O_2 inlets) in the commercially available milling vessels, the oxidation reactions were first sought to be screened on a realtively simple lignin β-O-4 monolignol model **M1** by employing commercially available stoichiometric oxidants. Metal-free oxidation approach using Dess-Martin Periodinane (DMP), *o*-iodoxybenzoic acid (IBX) and catalytic amounts of TEMPO [(2,2,6,6-tetramethylpiperidin-1-yl)oxidanyl] in combination with the commercially available solid stoichiometric oxidants such as trichloroisocyanuric acid (TCCA), *N*-chlorosuccinimide (NCS), bleach (NaOCl) and Oxone® ($2KHSO_5{\cdot}KHSO_4{\cdot}K_2SO_4$) were employed as standard alcohol oxidation systems. The results from these studies and further reaction optimizations have been elaborated upon in the upcoming sections.

3.1 Oxidative transformations of lignin β-O-4 model compounds under milling conditions.

Table III.17: Catalyst screening for the oxidation of **M1**.[a]

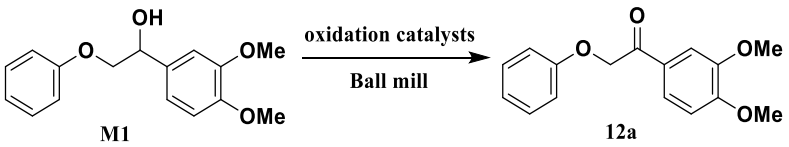

M1 12a

Entry	Catalytic systems [equiv]	Conv. [%][b]	**12a** [%][b]
1	-	-	-
2	IBX [1.5]	15	13
3	DMP [1.5]	9	6
4	Oxone [1.5]	10	10
5	TEMPO [1.0 equiv]	-	-
6	TCCA [1.5 equiv]	6	-
7	NCS [1.5 equiv]	-	-
8	Bleach [1.5 equiv]	7	3
9	TEMPO [0.2] / Oxone [1.5]	24	22
10	TEMPO [0.2] /*n*Bu_4NBr [0.2] / Oxone [1.5]	30	20
11	TEMPO [0.2] / KBr [0.2] / Oxone [1.5]	50	45
12	KBr [0.2] / Oxone [1.5]	-	-
13	TEMPO [0.2] / KBr [0.2] / TCCA [1.5]	20	7
14	TEMPO [0.2] / KBr [0.2] / NCS [1.5]	39	5
15	TEMPO [0.2] / KBr [0.2] / bleach [1.5]	45	38

[a] Reaction conditions: **M1** (0.250 mmol, 1 equiv), mixer mill (**MM**), ZrO_2 jars, 25 Hz, 180 min. [b] Conversion of **M1** as well as the yield of **12** were determined by ^{1}H NMR spectroscopy with 1,4-dinitrobenzene as the internal standard.

Prior to screening the various oxidation catalysts, a blank test was performed on monolignol **M1** in a mixer mill for 180 min at 25 Hz in the absence of additional oxidizing agents, other than the atmospheric oxygen present in the vessel (Table III.17, entry 1). No observable changes in the structure of **M1**, as analyzed by ^{1}H NMR of the milled substrate, ruled out the involvement of mechanochemical forces to induce direct reactivity in the substrate. The proceeding reactions were then performed in the presence of stoichiometric oxidants such as IBX, DMP and Oxone as they were previously seen to retain their activity under ball milling conditions.[80] Although the reagents did trigger oxidation of **M1**, the yields for the oxidized product **12a** were lower than anticipated (Table III.17, entries 2-4). Next, TEMPO in combination with different secondary oxidants such as Oxone, TCCA, NCS and bleach was tested to promote the oxidation in **M1**. Again, performing the milling reaction on **M1** with 1.0 equivalent of TEMPO alone did not give any reactivity (Table III.17, entry 5). A similar trend was observed for the other stoichiometric oxidants TCCA, NCS and bleach that led to almost negligible conversions (Tabl III.17, entries 6–8). Combining TEMPO with Oxone however afforded **12a** in 22% yield after 24% conversion of **M1**. To enhance the catalytic reactivity, a brominium ion source such as tetrabutylammonium bromide (*n*Bu_4NBr) or KBr were introduced into the system as these, in the presence of co-oxidants such as Oxone, are reported to form hypobromous acid (HOBr) which subsequently oxidise the TEMPO to an active *N*-oxoammonium bromide species[81] and hence accelerates the oxidation (Table III.17, entries 10 and 11). Of the two additives, 0.2 equivalent of KBr in combination with 0.2 equivalent of TEMPO and 1.5 equivalent of Oxone afforded the desired oxidation product **12a** in high selectivity (90%, Table III.17, entry 11). To rule out the direct effect of brominium ion (from KBr oxidation) in the catalysis reaction, a combination of KBr/Oxone (0.2/1.5) was employed on **M1** which gave negligible conversion (entry 12).

Table III.18: Oxidation in **M1** using TEMPO derivatives.[a]

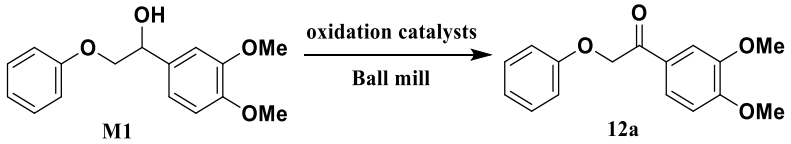

Entry	Catalytic systems [equiv]	Milling media	Milling conditions	Conv [%][b]	**12a** [%][b]
1	TEMPO [0.2] /KBr [0.2] /Oxone [1.5]	ZrO_2	25 Hz, 180 min	50	45
2	AcNH-TEMPO [0.2] /KBr [0.2] /Oxone [1.5]	ZrO_2	25 Hz, 180 min	33	26
3	OH-TEMPO [0.2] /KBr [0.2] /Oxone [1.5]	ZrO_2	25 Hz, 180 min	49	49
4	OH-TEMPO [0.2] /KBr [0.2] /Oxone [1.5]	ZrO_2	30 Hz, 180 min	90	86
5	OH-TEMPO [0.2] /KBr [0.2] /Oxone [1.0]	ZrO_2	30 Hz, 180 min	79	79
6	OH-TEMPO [0.2] /KBr [0.2] /Oxone [1.5]	SS	30 Hz, 180 min	95	90
7	OH-TEMPO [0.2] /KBr [0.2] /Oxone [1.5]	WC	30 Hz, 180 min	99	96
8	OH-TEMPO [0.2] /KBr [0.2] /Oxone [1.5]	WC	30 Hz, 90 min	99	97
9	OH-TEMPO [0.2] /KBr [0.2] /Oxone [1.5]	WC	30 Hz, 60 min	85	82

[a] Reaction conditions: **M1** (0.250 mmol, 1 equiv), mixer mill (**MM**). [b] Conversion of **M1** as well as the yield of **12a** were determined by ^{1}H NMR spectroscopy with 1,4-dinitrobenzene as the internal standard; AcNH-TEMPO = 4-acetamido-TEMPO, OH-TEMPO = 4-hydroxy-TEMPO.

Having obtained promising results with KBr as additive (0.2 equiv), the co-oxidants TCCA, NCS and bleach were again tested for the TEMPO/KBr catalytic system which resulted in relatively lower conversions and product selectivity in comparison to the TEMPO/KBr/Oxone system (Table III.17, entries 13–15).

Next, two TEMPO derivatives AcNH-TEMPO and OH-TEMPO were tested as TEMPO substitutes for the above reaction, as depicted in Table III.18. Both derivatives were chosen by keeping in mind their low production cost, beneficial during process upscaling. Though the substitution of acetamide at the fourth position of TEMPO resulted in decreased conversion of **M1** and **12a** yield (Table III.18, entry 2), the 4-OH-TEMPO derivative proved to be more selective towards the desired product **12a**, compared to TEMPO, while maintaining similar rate of conversion for a 180 minutes reaction time at 25 Hz in ZrO_2 jars (Table III.18, entry 3). Delightfully, an increase in the milling frequency from 25 Hz to 30 Hz for the OH-TEMPO/KBr/Oxone (0.2/0.2/1.5) catalytic system increased the yield of **12a** to 86% for the same reaction time (Table III.18, entry 4). This reaction, when conducted with a lower amount of Oxone (1 equiv) led to a 12% dip in the overall **M1** conversion. To further improve the conversion and decrease the reaction time, various milling media having higher density than ZrO_2 were employed. Pleasingly, stainless steel (SS) and tungsten carbide (WC) milling media had an impact on the reaction (Table III.18, entries 6–9). In particular, the reaction time was reduced by half (90 min) using tungsten carbide (WC) jars at 30 Hz while giving even higher product selectivity of 97% for a OH-TEMPO/KBr/Oxone (0.2/0.2/1.5) catalyzed oxidation reaction of **M1** (entry 8).

3.1.1 Scope of the oxidation reaction using lignin β-O-4 model compounds

To investigate a wider applicability of the oxidative system, aromatic ring substituted monolignol models **M2** and **M3** were subjected to the above established reaction conditions (Table III.19 entries 2 and 3). These model compounds gave the corresponding ketones **12b** and **12c** in 93% and 87% yield, respectively after column chromatography. The high yields for the ketones (**12a**–**c**) highlight the functional group tolerance of the current system (entries 1–3).

Table III.19: TEMPO/KBr/Oxone catalyzed oxidation of *β*-O-4 lignin model compounds.

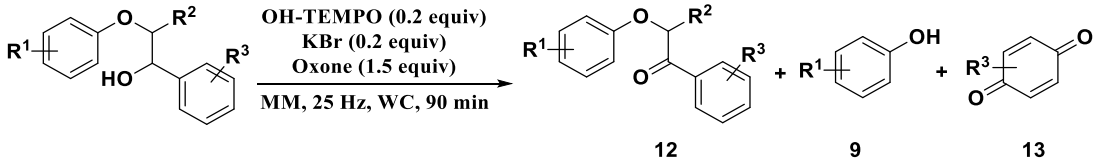

Entry	Substrate	Conv. [%][a]	Cleavage products [Yield %]		
1	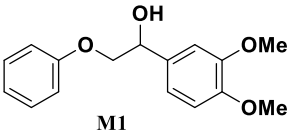 M1	>99	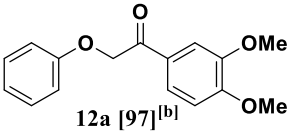 12a [97][b]		
2	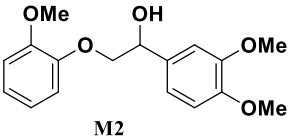 M2	>99	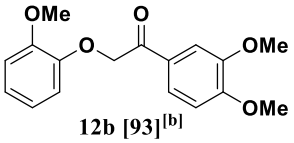 12b [93][b]		
3	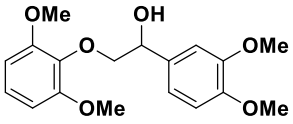 M3	>99	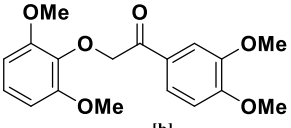 12c [87][b]		
4	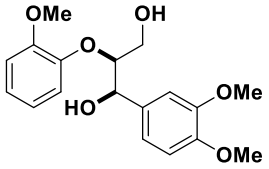 D1	>99	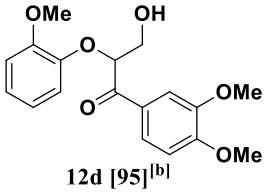 12d [95][b]		
5	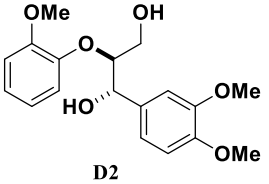 D2	>99	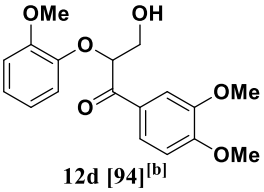 12d [94][b]		
6	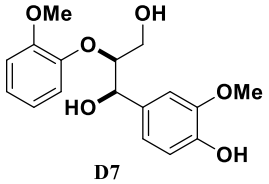 D7	>99		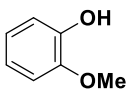 9a [76][c]	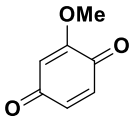 13a [82][c]
7	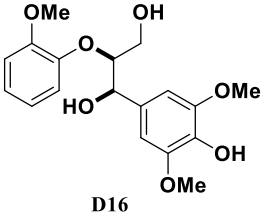 D16	>99		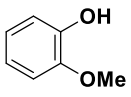 9a [82][c]	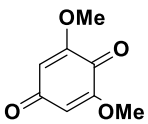 13b [91][c]

[a] Reaction progress monitored by TLC. [b] Yield after column chromatography. [c] Yield determined by GC calibrations with respect to *n*-octadecane as an internal standard.

After the successful oxidation of monolignols **M1**–**3**, the scope of the reaction system was extended to the more challenging non-phenolic and phenolic dimeric lignin model compounds **D1**, **D2**, **D7** and **D16** bearing both the secondary (benzylic) and primary alcoholic groups (Table III.19 entries 4–7). The substrates were tested under optimized reaction conditions (Table III.18). Pleasingly, both the non-phenolic dilignols *erythro* **D1** and *threo* **D2** resulted in the selective benzylic oxidation to ketone **12d** in 95% and 94% respectively (Table III.19, entries 4 and 5). However, interestingly, employing phenolic **G**-type dilignol **D7** led to the direct formation of cleavage products 2-methoxybenzoquinone (**13a**) in 82% yield and guaiacol (**9a**) in 76% yield. The yields for the cleavage products increased for the **S**-type phenolic model compound **D16**, forming 2,6-dimethoxybenzoquinone (**13b**) and guaiacol (**9a**) in 91% and 82% yield, respectively. This alternate behaviour exhibited by model compounds **D7** and **D16** could be attributed to the presence of reactive terminal phenolic groups. Also, the formation of quinone was found to be in line with the previously reported Oxone mediated mechanochemical transformations of methoxy/hydroxy benzenes to their corresponding quinones with higher selectivity as compared to the conventional solution based oxidation reactions.[82]

3.2. Oxidative transformation on beechwood lignin by mechanochemical activation

The optimized conditions on β-O-4 lignin model compounds in a mixer mill (**MM**) were further tested on an ethanosolv beechwood lignin (**OS-BWL2**) obtained as described in the experimental section. Initial progress of the oxidative transformations on beechwood lignin samples was monitored by comparing their individual 2D-HSQC NMR spectra (Figure III.22) and IR spectra (Figure III.23) with those of the untreated lignin sample (before reaction). To begin with, a control experiment was also conducted on 100 mg of **OS-BWL2** by milling it for 90 min in a WC jar in the absence of any catalytic system. The 2D-HSQC NMR spectrum of the resulting lignin residue (MM-WC-90 min-no catalyst) was compared with the lignin before the reaction, which showed negligible changes in the aliphatic (δ_C/ δ_H 50–90/2.5–5.8) as well as the aromatic (δ_C/ δ_H 100–124/7.2–7.6) regions (Figure III.22). This result was supported by the corresponding IR spectra of lignins before and after the milling reactions (Figure III.23). The stability of the individual β-O-4' aryl ether linkages **A** as well as the resinol **B** and the phenylcoumaran **C** substructures in the polymer were thus confirmed under mechanical stress in the ball mill.

Further reactions on the lignin sample (100 mg) were performed in the presence of catalytic amounts of OH-TEMPO (0.2 equiv) and KBr (0.2 equiv) with Oxone (1.5 equiv) as the stoichiometric oxidant. After milling the reagents together with **OS-BWL2** for 90 min in a WC jar, the lignin was again subjected to 2D-HSQC NMR and IR studies (MM-WC-90 min). Pleasingly, major changes in the aliphatic regions of the spectra were observed with diminished integrals corresponding to β-O-4' aryl ether and phenylcoumaran substructures. The corresponding aromatic region of the spectra also accounted for 40% benzylic oxidation in the polymer, with increased integrals for the cross peaks corresponding to oxidized syringyl S' and guaiacyl G' units (Figure III.22 and Table III.20, entry 3). The corresponding IR spectrum of the oxidized lignin (MM-WC-90 min) also showed the appearance of a new carbonyl band (C=O) at 1721 cm^{-1}. To further the oxidation reaction, milling was continued for another 90 min (MM-WC-180 min), which to our delight increased the degree of oxidation to 84% (Table III.20, entry 4). Moreover, this change was again highlighted in the IR spectra (Figure III.23) which showed the appearence of an even stronger carbonyl band at 1718 cm^{-1} with a relative decrease in the hydroxyl groups (3439 cm^{-1}) of the spectra.

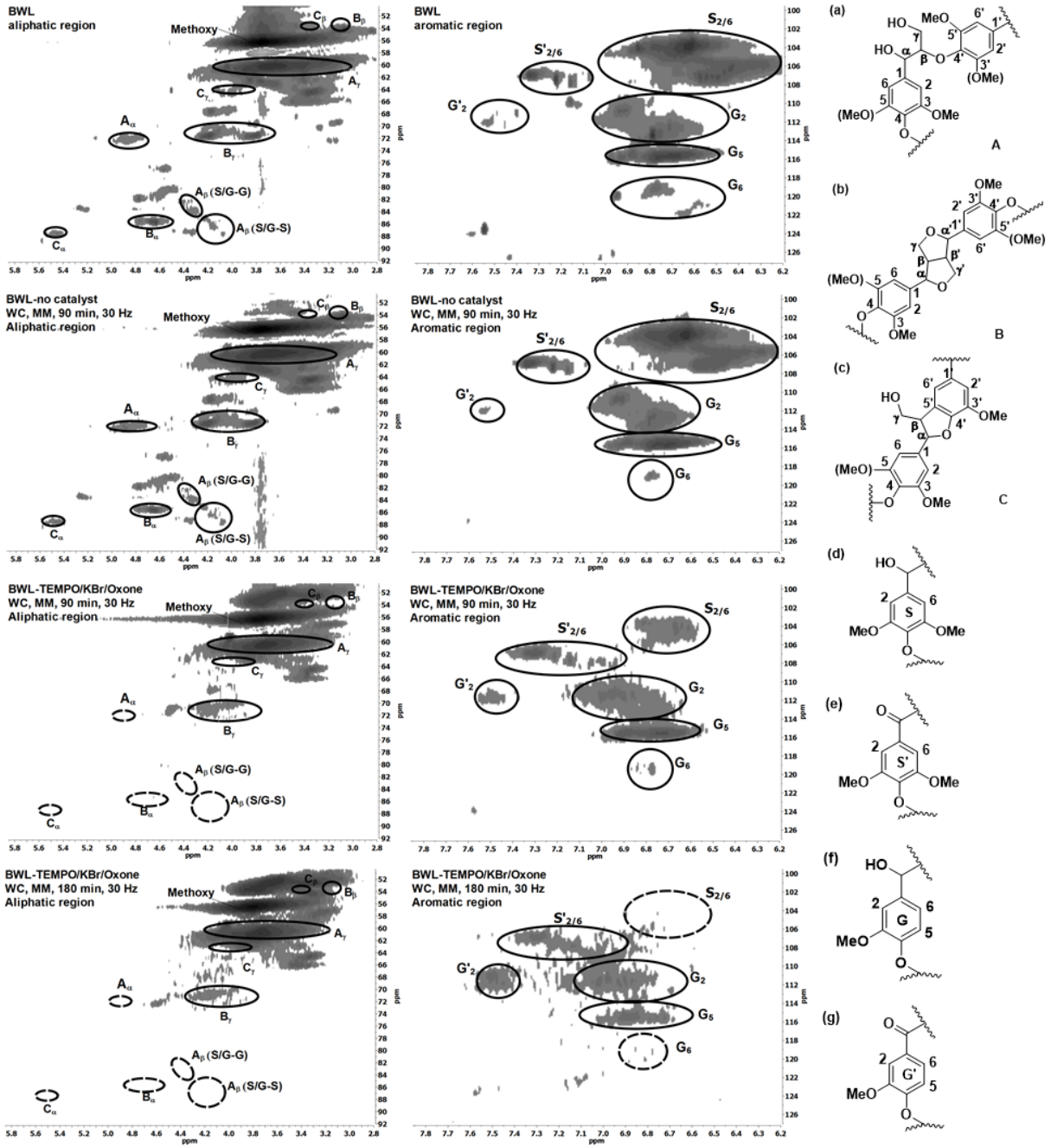

Figure III.22. Tracking the OH-TEMPO/KBr/Oxone (0.2/0.2/1.3) catalyzed oxidation reaction in beechwood lignin (**OS-BWL2**) by 2D-HSQC NMR spectra (in DMSO-d_6). **A:** β-O-4' aryl ether linkages with a free-OH at the α-carbon; A': β-O-4' aryl ether linkages with acetylated and/or *p*-hydroxybenzoated -OH at α-carbon; **B:** resinol substructures formed by β–β'-, α-O-γ'-, and γ-O-α'-linkages; **C:** phenyl coumaran substructures formed by β-5'- and α-O-4'-linkages; **S**: syringyl units; **S':** syringyl unit with oxidized benzylic position; **G:** guaiacyl units.

Table III.20: Selective oxidation of beechwood lignin.

Entry	beechwood Lignin [BWL2]	Ratio of areas integrated [oxidized/unoxidized][a]	Degree of Oxidation [%]
1	before reaction	0.06	6
2	MM-WC-90 min-no catalyst	0.09	8
3	MM-WC-90 min	0.66	40
4	MM-WC-180 min	5.47	84

[a] Ratios determined by comparing the integrals of the aromatic cross-peak that are characteristic of oxidized and unoxidized structures in the 2D-HSQC NMR.

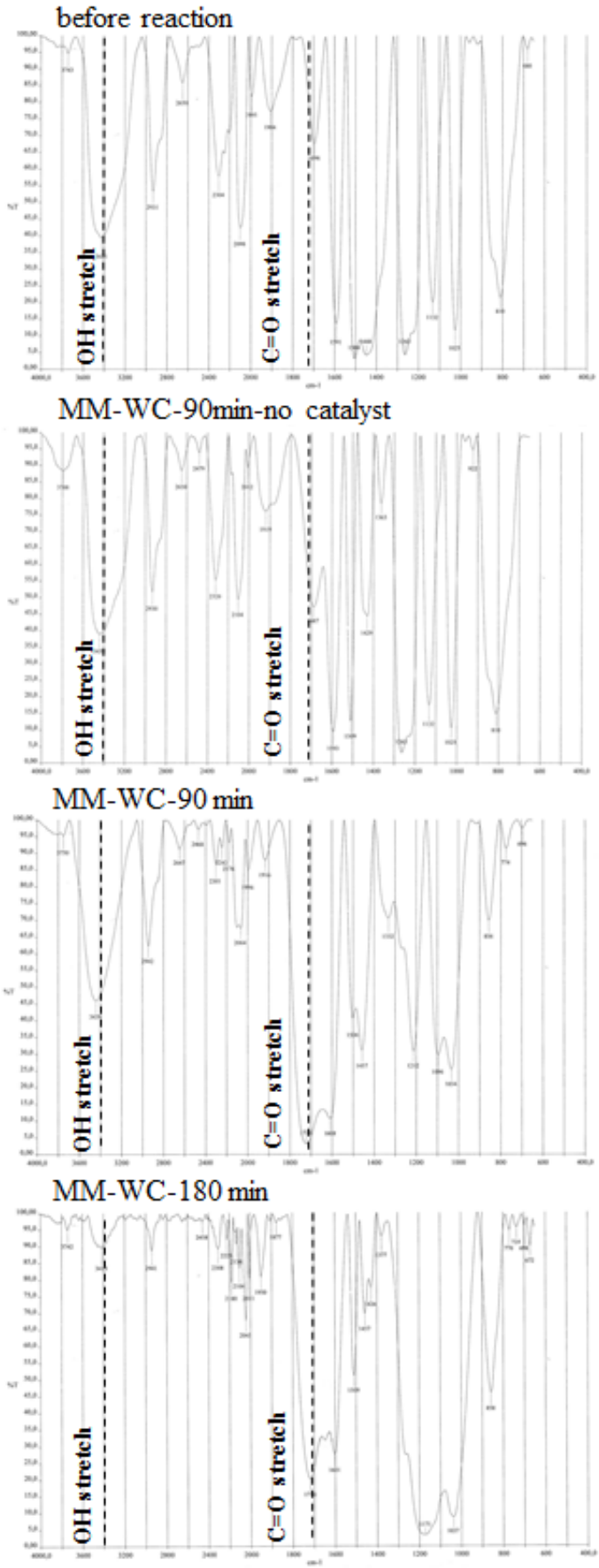

Figure III.23. Monitoring the oxidation reaction in beechwood lignin by comparing the -OH (hydroxy) and -C=O (carbonyl) stretching frequency in respective IR spectra (cm^{-1}).

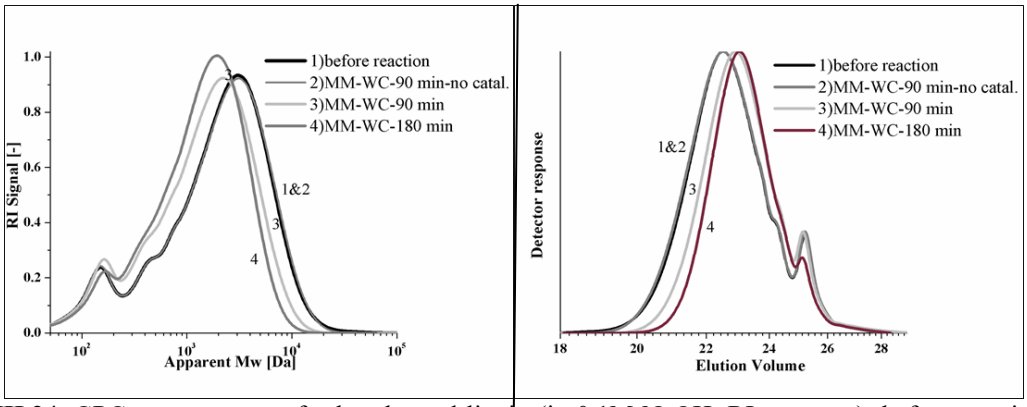

Figure III.24. GPC measurements for beechwood lignin (in 0.1M NaOH, RI response): before reaction (black line, 1); lignin milled without catalyst in **MM** at 30 Hz (dark grey, 2), lignin milled with catalyst for 90 min in **MM** at 30 Hz (grey, 3), lignin milled with catalyst for 180 min in a **MM** at 30 Hz (grey, 4). **Left**: mass distribution with respect to sulfonated polystyrene standards calibration; **right**: elugram.

Table III.21: Change in average lignin molecular weight (Mw) before and after the milling reactions.

Lignin	Mw (Da)			
	before reaction	MM-WC-90 min-blank	MM-WC-90 min	MM-WC-180 min
BWL2	$3.131 \cdot 10^3$	$3.126 \cdot 10^3$	$2.164 \cdot 10^3$	$1.855 \cdot 10^3$

Next, the raw beechwood lignin along with the lignin milled in a mixer mill (**MM**) at 30 Hz for 90 min without catalyst and lignins milled for 90 min and 180 min in the presence of OH-TEMPO/KBr/Oxone catalytic system, were analyzed by GPC to determine their respective average molecular weights. In corroboration with the previous observations, there was no significant change in the Mw values corresponding to the raw lignin (before reaction) and the lignin milled without any catalyst (MM-WC-90 min-blank), which again confirmed the stability of the polymer under the studied milling environment (Figure III.24 and Table III.21). However, a shift in the Mw values was observed for the two oxidized lignin samples with the 90 min oxidative milling resulting in 30% decrease while the 180 min milling resulting in 40% decrease in the Mw values. Intrigued by this shift in molecular weight values (Mw), the ether fraction of the lignin sample oxidized for 180 min was subjected to GC-MS analysis with a known amount of *n*-octadecane as an internal standard (Figure III.25). The analysis confirmed the formation of 3,5-dimethoxyquinone (2.5 wt% w.r.t the starting raw material) as the major monomer, formed possibly due to the oxidation of terminal phenolic groups present in the lignin. This observation can also be related to the model compound studies carried out on phenolic models **D7** and **D16.**

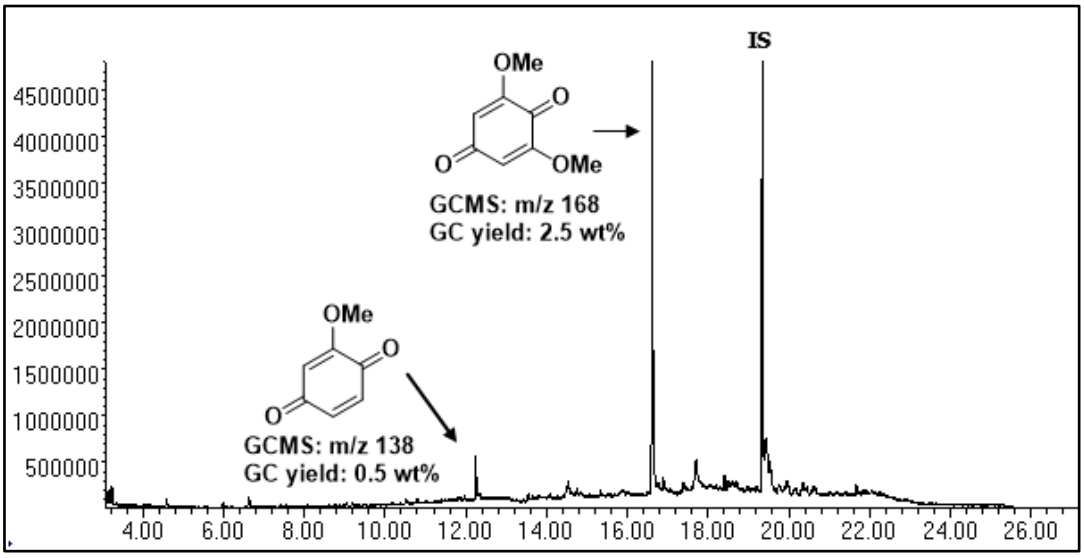

Figure III.25. GC-FID trace for ether soluble mono-aromatics obtained from lignin (MM-WC-180 min).

3.2.1 Reaction scale up

Prompted by the positive results obtained above, the following investigations focused on the scale-up process of the developed oxidation route using OH-TEMPO (0.2 equiv), KBr (0.2 equiv) and Oxone (1.5 equiv). As an initial scalability approach, the reactions were performed on 10 g of beechwood lignin (**OS-BWL2**) in two different mills, also made of tungsten carbide (WC). First one being a 250 ml SIEBTECHNIK disk swing mill-TS (**DM**) with a disc weighing 1.2 kg and the other being a 250 ml LAARMANN LMM6-100 mortar and pestle mill (**MPM**). Considering the larger energy impact of the milling media, compared to the laboratory scale mixer mill, the reaction time for both the mills was restricted to 30 minutes at a frequency of 20 Hz for **MPM** and 50 Hz for **DM**. Post reactions, the oxidized lignin samples were collected and 100 mg of the mixture was weighed out from the homogeneous mixture, to be subjected to a workup procedure described in Scheme III.16.

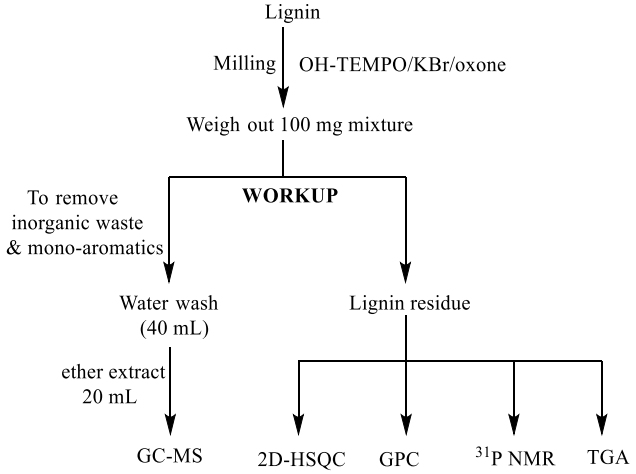

Scheme III.16. Workup procedure used for the oxidized lignin samples prior to analytical studies.

Once again, the 2D-NMR analysis was done on the beechwood lignin residues obtained after the oxidation reactions performed in the mortar and pestle mill (**MPM**) and the disc mill (**DM**). Surprisingly, the lignin milled in the mortar and pestle mill along with the OH-TEMPO/KBr/Oxone catalytic system (MPM-WC-30min) showed no change in the corresponding aliphatic and aromatic regions of the spectra, when compared with the raw lignin sample (table III.26 and Table III.22, entries 1 and 2). The GPC analysis for this sample also showed a negligible change in the Mw value correlated to the raw lignin data (Figure III.27 and Table III.23).

However, the 2D-NMR spectrum for the lignin oxidized in a disc mill (DM-WC-30 min) displayed a drastic change in its aliphatic (δ_C/δ_H 50–90/2.5–5.8) region, with the disappearance of integrals corresponding to β-O-4' aryl ether and phenylcoumaran substructures (Figure III.26). Furthermore, the comparative analysis of the integrals in the aromatic region (δ_C/δ_H 100–124/7.2–7.6) of the spectra pointed to 24% oxidation of the lignin obtained after the reaction. This low value could be rationalized by taking into account that the decrease in the integrals corresponding to the S and G units of the un-oxidized lignin could only be directly correlated to the S' and G' values of a selectively oxidized sample which did not undergo any depolymerization reactions. Moreover, as the GPC analysis of the **DM** oxidized lignin showed a greater drop of 48% in its Mw value compared to the lignin oxidized for 180 minutes in a mixer mill (WC-DM-180 min), the ether extracted sample from the aqueous wash was further subjected to GC-MS analysis. Pleasingly, the GC-FID chromatogram of the ether extract displayed the formation of a range of mono-aromatics and confirmed the depolymerization (Figure III.28) which helped in explaining the reduced oxidation values in the 2D-NMR as well as the shifted Mw values observed in the GPC.

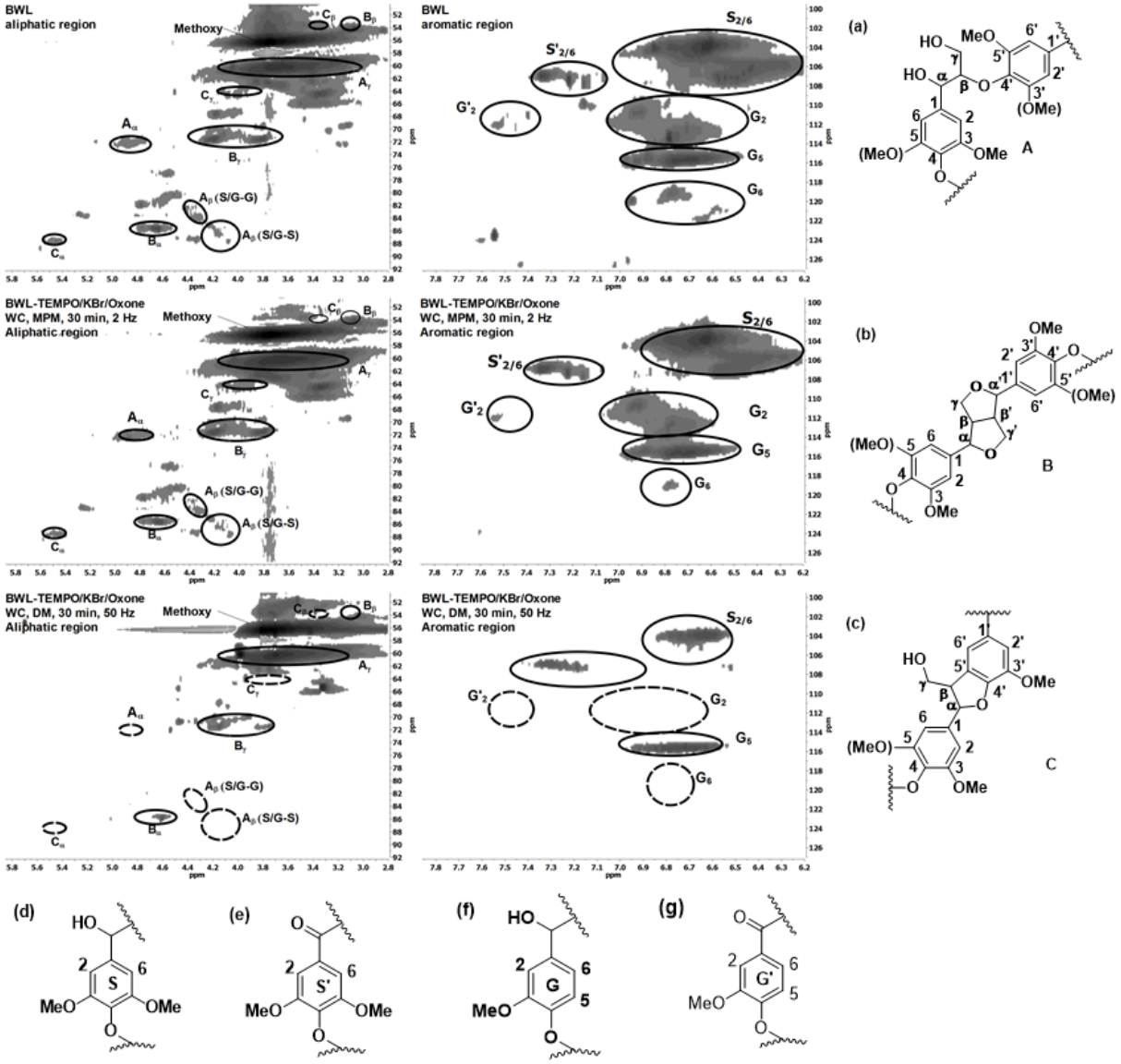

Figure III.26. Analyzing the OH-TEMPO/KBr/Oxone (0.2/0.2/1.3) catalyzed oxidation reaction in beechwood lignin (**OS-BWL2**) by 2D-HSQC NMR spectra (in DMSO-d_6). **A:** β-O-4' aryl ether linkages with a free-OH at the α-carbon; A': β-O-4' aryl ether linkages with acetylated and/or *p*-hydroxybenzoated -OH at α-carbon; **B:** resinol substructures formed by β–β'-, α-O-γ'-, and γ-O-α'-linkages; **C:** phenyl coumaran substructures formed by β-5'- and α-O-4'-linkages; **S:** syringyl units; **S':** syringyl unit with oxidized benzylic position; **G:** guaiacyl units.

Table III.22: Selective oxidation of beechwood lignin.

Entry	beechwood Lignin [BWL2]	Ratio of areas integrated [Oxidized / Unoxidized][a]	Degree of Oxidation [%]
1	before reaction	0.06	6
2	MPM-WC-30 min	0.09	9
3	DM-WC-30 min	0.32	24

[a] Ratios determined by comparing the integrals of the aromatic cross-peak that are characteristic of oxidized and unoxidized structures in the 2D-HSQC NMR. **MPM**: mortar and pestle mill; **DM**: disc mill.

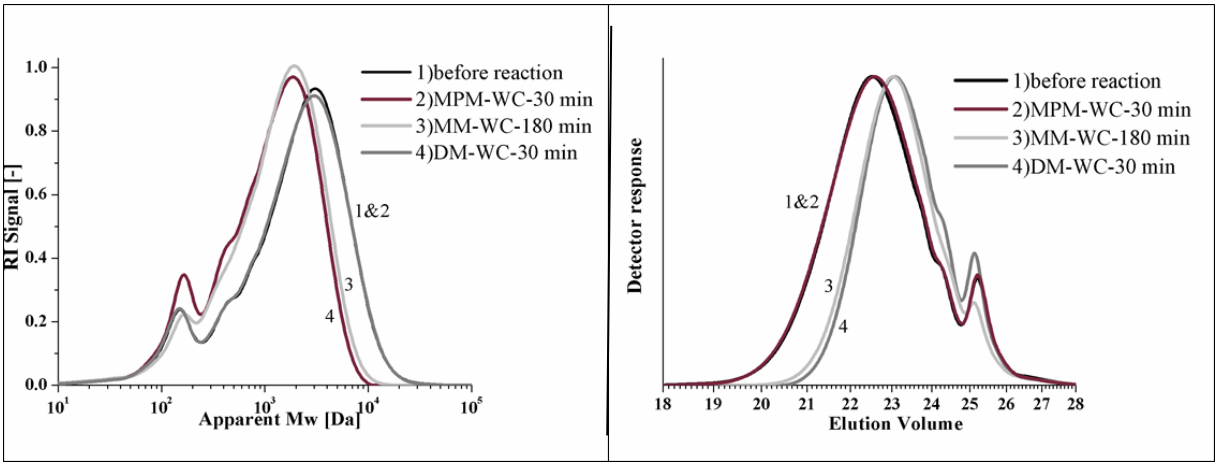

Figure III.27. GPC measurements for beechwood lignin (in 0.1M NaOH, RI response): before reaction (black line, 1); milling with OH-TEMPO/KBr/Oxone for 30 min in a mortar and pestle mill (**MPM**) (dark grey, 2), milling with OH-TEMPO/KBr/Oxone for 180 min in a mixer mill (**MM**) (light grey, 3); milling with OH-TEMPO/KBr/Oxone for 30 min in a disc mill (**DM**) (grey, 4). **Left**: mass distribution with respect to sulfonated polystyrene standards calibration; **right**: elugram.

Table III.23: Change in average lignin molecular weight before and after the milling reactions.

	Mw (Da)			
BWL2	before reaction	MPM-WC-30 min	MM-WC-180 min	DM-WC-30 min
	$3.131 \cdot 10^3$	$3.043 \cdot 10^3$	$1.855 \cdot 10^3$	$1.625 \cdot 10^3$

MPM: Mortar and Pestle mill; **MM**: Mixer mill; **DM**: Disc mill.

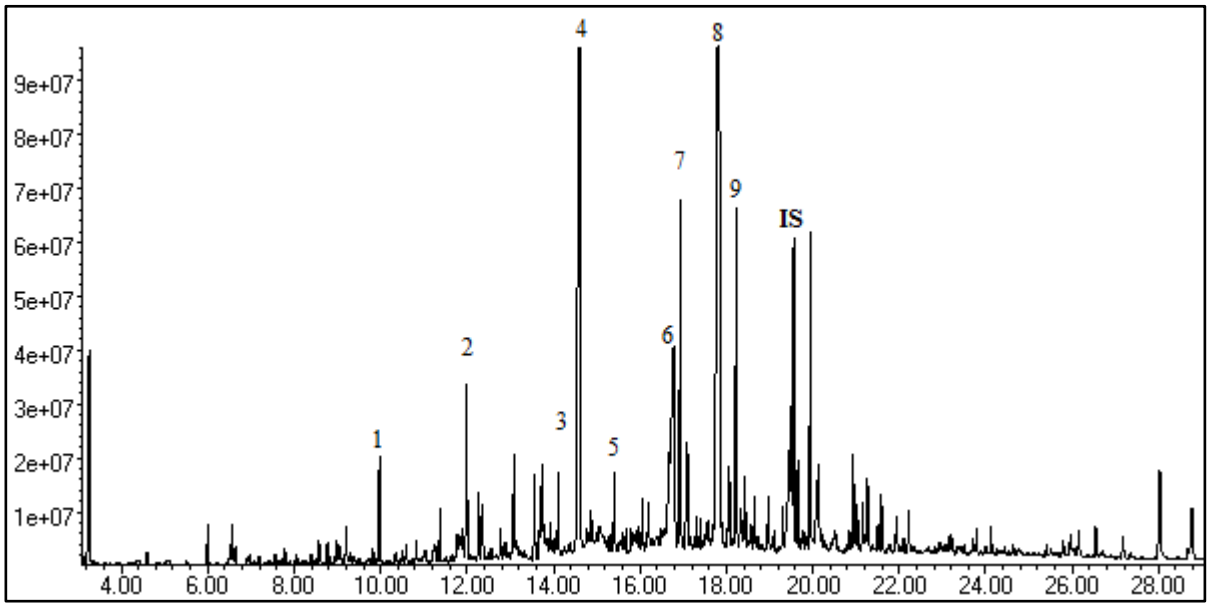

Figure III.28. GC-FID trace for ether soluble mono-aromatics obtained from beechwood lignin (**BWL2**) oxidized in disc mill (DM-WC-30 min). Detailed list of the mono-aromatics identified by GC-MS have been listed in Table III.24.

Table III.24: Monomeric products obtained after milling 10 g of beechwood lignin in a disc mill (**DM**).

Peak No.	Retention time [min]	Monomers	Yield[a] [wt% of starting sample]
1	9.5	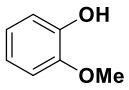	0.3 Sample injected
2	12.2	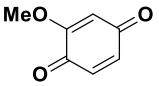	0.9 Sample injected
3	14.5	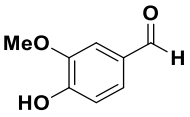	3.2 Sample injected
4	15.5	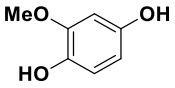	GC match: 87%
5	14.6	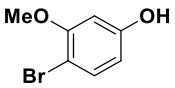	GC match: 92%
6	16.6	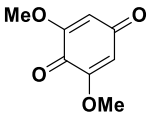	2.6 Sample injected
7	16.8	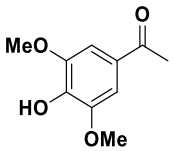	2.9 Sample injected
8	17.8	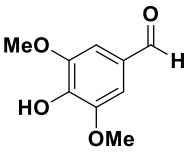	6.5 Sample injected
9	18.2	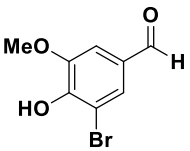	GC match: 95%
	Total mono-aromatics quantified		16.4

[a] Amounts are based on the individual calibrations done with respect to *n*-octadecane as an internal standard.

The quantitative analysis of the ether-soluble extract from **DM** resulted in the identification of several mono-aromatics affording the major products in a total yield of 17 wt% with respect to the 100 mg mixture of the oxidized lignin sample.

3.2.1.1. Characterization of the solid residue by ^{31}P NMR and TGA analysis

The subsequent changes in the aliphatic and phenolic hydroxyl groups of the biopolymer, incurred by oxidative transformations, were also confirmed by ^{31}P NMR studies which resulted in the quantification of these functionalities by forming stable phosphite bonds (Scheme III.9). A sequence of analysis was carried out on raw beechwood lignin (before reaction) followed by lignin oxidized for 90 and 180 min in the mixer mill (**MM**) and finally the oxidized lignin from the disc mill (Figure III.29 and Table III.25). For both the oxidized lignins (**MM** and **DM**), the total amount of -OH groups in the specified region, were found to be very low as reflected by the calculated values for a 180 minutes reaction. This was indeed the result of structural changes induced in the polymer by lignin oxidation and depolymerization reactions.

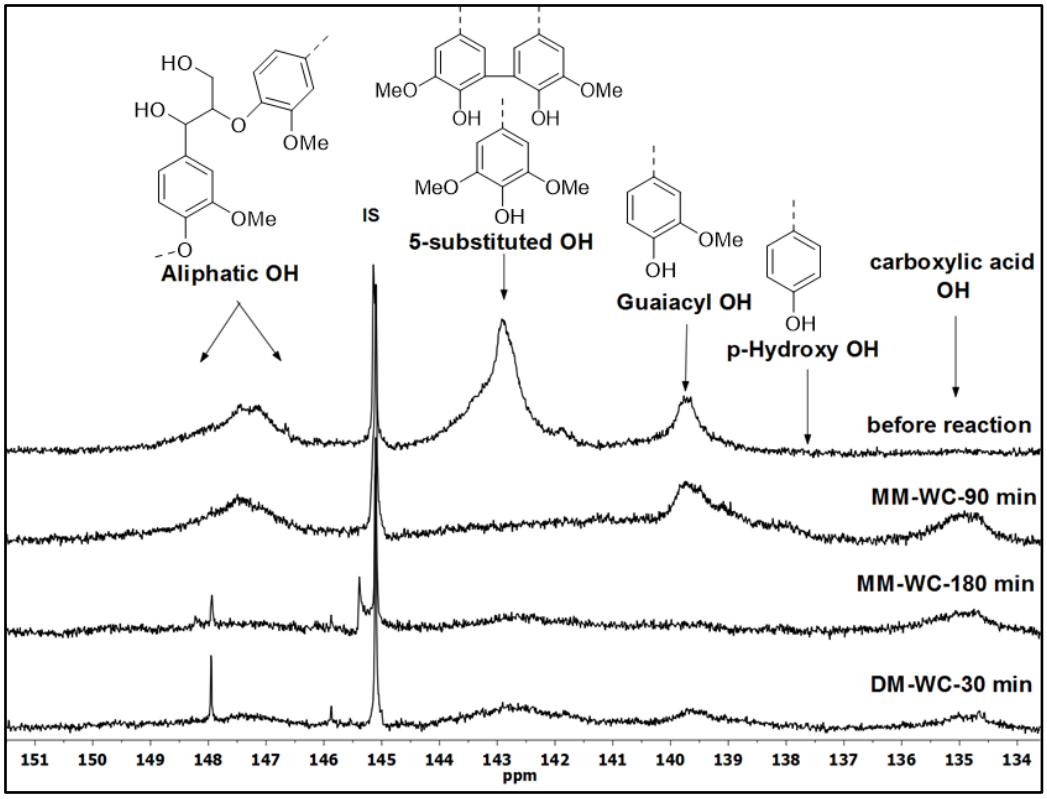

Figure III.29. Quantitative ^{31}P NMR spectra of beechwood lignin samples.

Table III. 25: Beechwood lignin hydroxyl groups quantified by ^{31}P NMR using cyclohexanol as internal standard.

beechwood Lignin	OH (mmol·g^{-1})[a]				
	Aliphatic OH	5-Substituted+Syringyl OH	Guaiacyl OH (G)	*p*-Hydroxyphenyl OH (H)	Carboxyl OH
before reaction	1.36	2.47	0.86	0.17	-
MM-WC-90 min	0.97	0.86	0.72	-	0.56
MM-WC-180 min	0.24	0.55	0.03	-	0.47
DM-WC-30 min	0.16	0.24	0.01	-	0.39

[a] Amounts displayed with respect to a known amount of cyclohexanol.

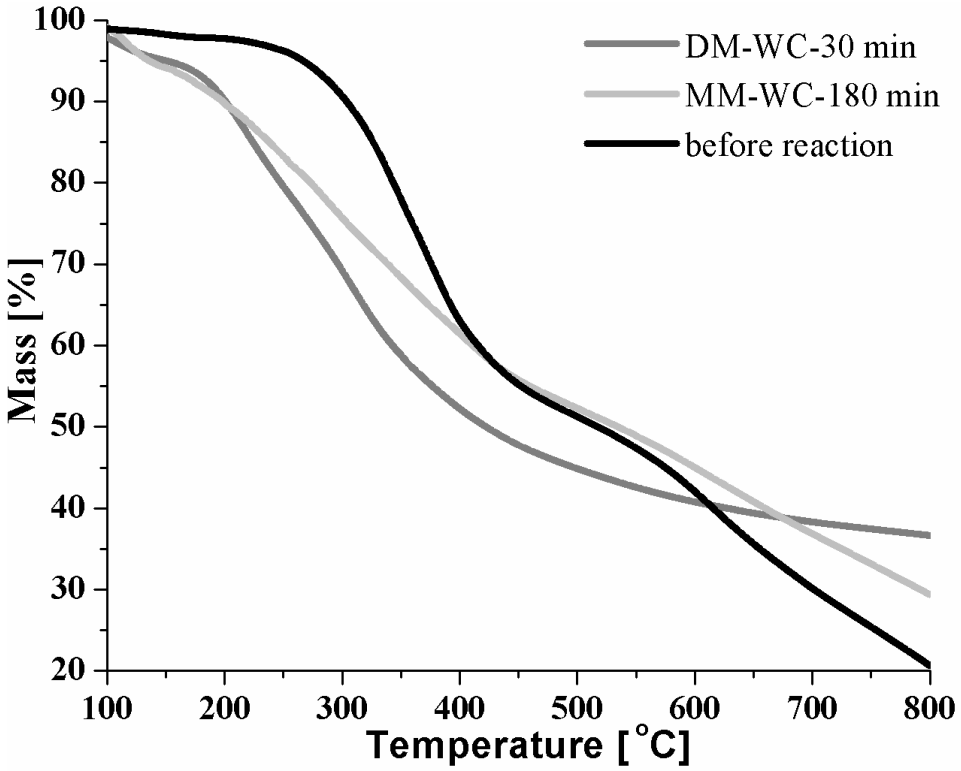

Figure III.30. Thermogravimetric analysis for untreated beechwood lignin (before reaction), lignin oxidized in a mixer mill (MM-WC-180 min) and in a disc mill (DM-WC-30 min).

Table III.26: Degradation temperature at 20 and 50% fiber degradation, obtained by TGA of untreated lignin and lignin oxidized by milling in the mixer mill and disc mill.

beechwood lignin	$T_{20\%}$	$T_{50\%}$	Residue at 800 °C [%]
before reaction	343.5	517.5	20.66
WC-MM-180 min	273.16	534.66	29.40
WC-DM-30 min	247.83	422.83	36.66

*T*p% represents the onset decomposition temperature of 20 and 50% weight loss.

The difference in the nature of the oxidized lignin residues obtained after aqueous washing from the disc mill (DM-WC-30 min) and the mixer mill (MM-WC-180 min) were sought to be compared to the raw lignin sample (before reaction) by conducting a TG analysis of the oven dried samples. It was particularly important to determine the thermal stability of the oxidized lignin residues as a higher degradation temperature directly correlated to a more condensed polymer, with respect to a raw lignin sample. As depicted in the Figure III.30, although the lignins followed a similar thermal degradation tendency, the thermal weight loss for both the oxidized lignin samples started at lower temperature (110 °C) than the raw lignin sample (165 °C). Furthermore the 20% weight loss ($T_{20\%}$) for the oxidized lignins occurred at much lower temperatures of 273 °C and 247 °C, compared to the raw lignin at 343 °C. The result could be justified by the fact that the lignin when subjected to oxidation reactions under mechanochemical stress underwent a degradation process that released monomers from the terminal phenolic groups in the case of a mixer mill as well as initiated the inter-unit cleavage in the more energetic disc mill, resulting in lowering of thermal stability of the polymer. Furthemore, the **DM** oxidized lignin underwent pyrolysis much more rapidly than the **MM** oxidized lignin between 300 to 400 °C. The char content at 800 °C was found to be 36% and 20% for **DM** oxidized and raw lignin, respectively, which demonstrated some degree of condensation in the oxidized lignin sample during the pyrolysis process.

4. Application of lignin as a Strecker reaction promoter under milling conditions

Research Background

The Strecker reaction is one of the oldest known pathways employed for the synthesis of α-aminonitriles.[83] A multicomponent reaction between an acetaldehyde, ammonia and hydrocyanic acid followed by hydrolysis affording racemic (DL)-alanine (Scheme III.17), was first investigated by Adolph Strecker in 1850.[84] Following its first discovery, this reaction has been studied extensively, particularly aiming towards the establishment of routes leading to optically pure α-aminoacids. These asymmetric Strecker reactions involve chiral auxiliaries[85] (carbohydrate, amine, ketimine) or chiral catalysts[86] (guanidine, chiral schiff bases, chiral phosphoric acids, squaramide**,** BINOL based-catalysts).

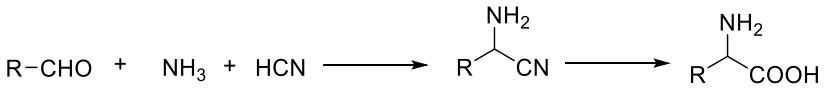

Scheme III.17. General representation of the Strecker reaction.

The advantages of following the above synthetic route for the synthesis of α-aminoacids (important building blocks for proteins, peptides, and pharmaceuticals)[83-86] is attributed to its effectiveness and simplicity along with the use of readily available and inexpensive starting materials. Furthermore, in several cases the cyanide source has also been varied overtime, involving reactions with HCN[86a-c,87] or metalcyanides (Na, K, Cu, etc.)[86b], TMSCN[86e,f], AcCN[86d]. Besides this, the presence of both the amino and nitrile functionalities in α-aminonitriles also makes them interesting intermediates for the construction of various heterocyclic scaffolds in organic synthesis.[88]

A classical Strecker reaction is proposed to involve three main steps represented by the nucleophilic addition of either a primary or a secondary amine to the carbonyl components affording a hemiaminal after intra- or intermolecular proton transfer of the tetrahedral intermediate. Protonation of the hemiaminal and subsequent elimination of water, giving rise to an imine (Schiff bases). Finally, the nucleophilic addition of the cyanide ion furnishing the desired α-aminonitrile (Scheme III.18).[89, 90]

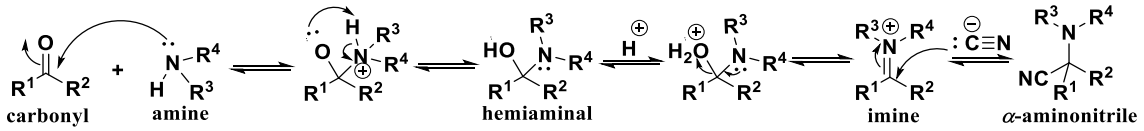

Scheme III.18. Proposed mechanism for the Strecker reaction.

To achieve higher reaction efficiency, the Strecker reactions are also accelerated following the activation of the intermediate imine by either Brønsted acid[91] catalyzed LUMO lowering hydrogen bonding interactions or by a Lewis acid[92] mediated LUMO lowering electrostatic interactions. Both these pathways result in a more polarized carbon atom which is prone to nucleophilic attack by the HOMO of the cyanide ion. Further activation of nucleophilic cyanide ion can also be carried out by HOMO raising hydrogen bonding interactions, specially in the case of Brønsted acid catalysis (Figure III.31).

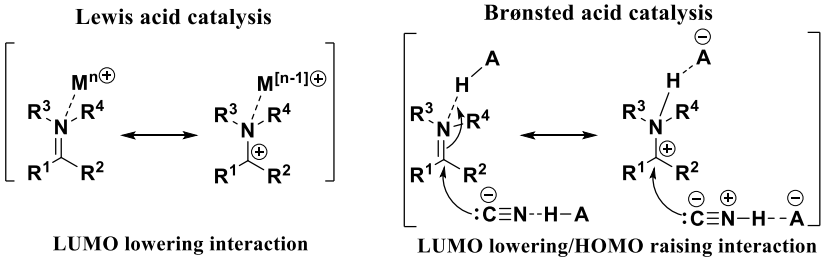

Figure III.31. Schematic representation of the activation mode in Lewis and Brønsted acid catalyzed reaction.

Recently, several reports have been published exemplifying the application of mechanochemical activation to perform reactions such as Gewald[93], Biginelli[94], Ugi and Passerini[95]. These examples successfully feature the extension of mechanochemistry for the initiation of complex multicomponent reactions. Additional advantages over conventional methodologies included significant reduction of the reaction time, improved product yields and reduction or elimination of solvents. Inspired by these above examples, Bolm and co-workers recently studied the development of the Strecker reaction in a mixer mill.[96] The milling was shown to be highly efficient for the synthesis of the corresponding α-aminonitriles promoted by the presence of readily available silica gel (SiO_2). These observations with silica could be attributed to the weak Brønsted acidity of its surface silanol groups that were found to be enough to create hydrogen bonding interactions with the substrates and the imine intermediate, thus promoting the Strecker reaction.

Searching for cheaper alternative materials other than SiO_2 as a stimulant in the Strecker synthesis under ball milling conditions, we thought of employing the abundantely available lignocellulosic biomass along with two of its major constituents cellulose (homopolymer of glucose consisting of β (1-4) bonds) or lignin as potential activators. This idea was perceived keeping in mind the variety of hydroxy groups present in the core structures of both cellulose and lignin along with the tested functional group stability of these polymers under milling conditions, which for the current study were envisioned to work as Brønsted acid functionalities.

4.1. Lignocellulosic materials as activators for the mechanochemical Strecker reaction

Initial attempts evaluating the effect of raw sources of lignocellulosic biopolymers on the outcome of a Strecker reaction were monitored on a reaction between 0.5 mmol benzaldehyde (**14a**), 0.5 mmol benzylamine (**15a**) and 0.55 mmol potassium cyanide (KCN) (Table III.27). Under mechanochemical conditions, using a mixer mill (**MM**) with 10 mL stainless steel milling vessel and one stainless steel milling ball of 10 mm in diameter at 30 Hz, the progress of all these reactions were monitored by ^{1}H NMR spectroscopy.

Milling the above-mentioned reactants, in the absence of additives, also resulted in the complete consumption of **14a** and **15a** in just 2 h. ^{1}H NMR analysis of the crude reaction mixture confirmed the formation of aldimine intermediate **16a** as the major product (85%) while the desired α-aminonitrile **17a** was observed in only minor quantities (15%), after the entire milling process (entry 1). This result was compared to a parallel solution-based reaction conducted for 2 h at 500 rpm in acetonitrile (MeCN, 3 mL), which also mainly afforded **16a** (97%) along with trace amounts of **17a** (entry 2). The observation is of interest as it highlights the improved efficiency of the reaction towards the desired product by mechnochemical activation.

Next, this multicomponent reaction between **14a**, **15a** and KCN was repeated with 200 mg of peanuts shell powder (**PSP**) as an additive for 2 h at 30 Hz in a **MM** and this resulted in a significant increase in the amount of α-aminonitrile **17a** (59%, entry 3) compared to the reaction without any additives (15%, entry 1). Having identified this increased reactivity of the Strecker reaction after the addition of a lignocellulosic raw material, the successive reactions were then individually studied in the presence of two main components *viz* cellulose and lignin. This was done to identify the main fraction (either cellulose or lignin) of the lignocellulosic biomass responsible to promote the Strecker reaction. For this purpose, crystalline cellulose and lignin samples from beechwood (**BWL1**, **BWL2**), oak (**OL**) cherry (**CL**) and kraft (**KL**) were tested under mechanochemical conditions for 2 h at 30 Hz (entries 4–10).

Table III.27: Mechanochemical Strecker reaction between **14a**, **15a** and KCN using biomass-based additives.[a]

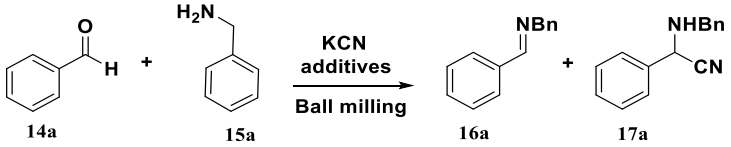

14a 15a 16a 17a

Entry	Additive [mg]	Milling time [h]	Conv. [%][b]	Yield [%][b]	
				16a	**17a**
1	-	2	98	85	15
2[c]	-	-	99	97	Traces
3	peanut shell powder [200]	2	98	41	59
4	cellulose [200]	2	98	53	47
5	beechwood lignin 1 [200]	2	98	10	90
6	beechwood lignin 2 [200]	2	98	12	88
7	oak lignin [200]	2	98	11	89
8	cherry lignin [200]	2	98	25	75
9	kraft lignin [200]	2	99	8	92
10	kraft lignin [250]	3	99	5	95
11	kraft lignin [350]	3	99	4	96
12[c]	kraft lignin [250]	-	60	55	5
13[c]	kraft lignin [250]	-	75	69	6
14	recycled-kraft lignin [250]	3	99	38	62
15	methylated-kraft lignin [200]	2	95	22	78

[a] Reaction conditions: **14a** (53.1 mg, 0.5 mmol), **15a** (53.6 mg, 0.5 mmol), KCN (35.8 mg, 0.55 mmol), and additive (200 mg) were milled in a mixer mill (**MM**) for 2 h at 30 Hz. [b] Determined by ^{1}H NMR spectroscopy. [c] Reactions conducted in solution.

Although cellulose itself promoted the formation of **17a** (higher reactivity compared to the reaction without additives), the imine **16a** was still seen to be formed as the major product (entry 4). Delightfully, reactions conducted in the presence of the lignin samples proved to be highly active in promoting the Strecker reaction by favoring the formation of the desired Strecker product **17a** over the imine **16a** (entries 5–9). Amongst these tested lignin samples, commercially available Aldrich-kraft lignin showed the highest catalytic activity (**17a**/**16a**; 92/8; entry 8) after 2 h at 30 Hz. Further increase in the lignin loading from 200 mg to 250 mg and milling time to 3 h resulted in a higher **17a**:**16a** ratio of 95:5 (entry 10). However, a higher additive loading or longer milling times had a negligible impact on the output of the mechanochemical reaction (entry 11). Subsequent experiments conducted in solution by conventional stirring of reactants for 3 h in organic solvents such as CD_3CN and $CDCl_3$ in the presence of kraft lignin (250 mg) led to an incomplete conversion of the starting materials **14a** and **15a** (entries 12 and 13). Furthermore, the selectivity in solution was again found to mainly favor the formation of the imine **16a**. Additional efforts were made to recover the kraft lignin (**RKL**) after the reaction and reuse the promoter for a second reaction run (entry 14). Although the reactants were fully consumed, the **RKL** resulted in an overall decrease in the selectivity towards the α-aminonitrile (**KL**:**17a**/**16a**; 92/8, **RKL**:**17a/16a**; 62/38).

Having screened a variety of lignin samples and hence obtained the best results with kraft lignin, following experiments were conducted, as a proof of principle study, to insure the role of the Brønsted acidic sites of lignin on the activation of the multicomponent reaction. For this purpose, a sample of kraft lignin was subjected to hydroxy-methylation reaction following the procedure reported by Argyropoulos and co-workers using dimethyl carbonate (DMC) in the presence of NaOH in DMSO.[67] Under the specified conditions, the hydroxyl groups present in lignin are reported to undergo methylation, which could have a direct effect on the overall lignin functionality and hence influence its role as an activator.

4.2. Strecker reaction with methylated kraft lignin as an additive

The functional group changes in the methylated kraft lignin (**MKL**) were determined by comparing the Infrared (IR) spectra and by ^{31}P NMR studies of the lignin samples both before and after the functionalization. Post methylation reaction, the IR of the methylated kraft lignin (**MKL**) showed a considerable reduction in the signals for the hydroxy stretching vibrations at 3400 cm^{-1}, compared to the raw Aldrich-kraft lignin (Figure III.32). Moreover, the ^{31}P NMR studies also highlighted a stark decrease in the amounts of aliphatic and penolic -OH groups for the corresponding kraft and methylated kraft lignins (Figure III.33 and Table III.28).

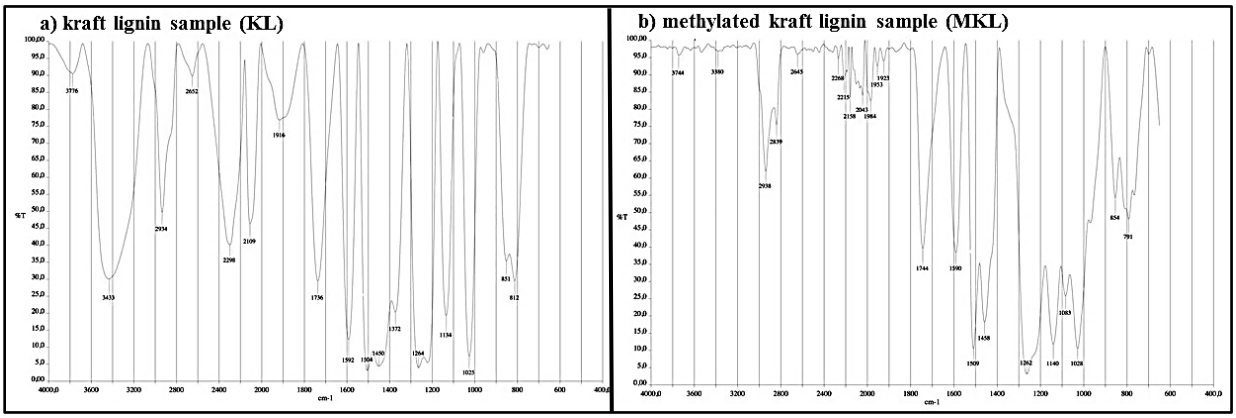

Figure III.32. Representative IR spectra for: a) kraft lignin (KL); b) methylated kraft lignin (MKL).

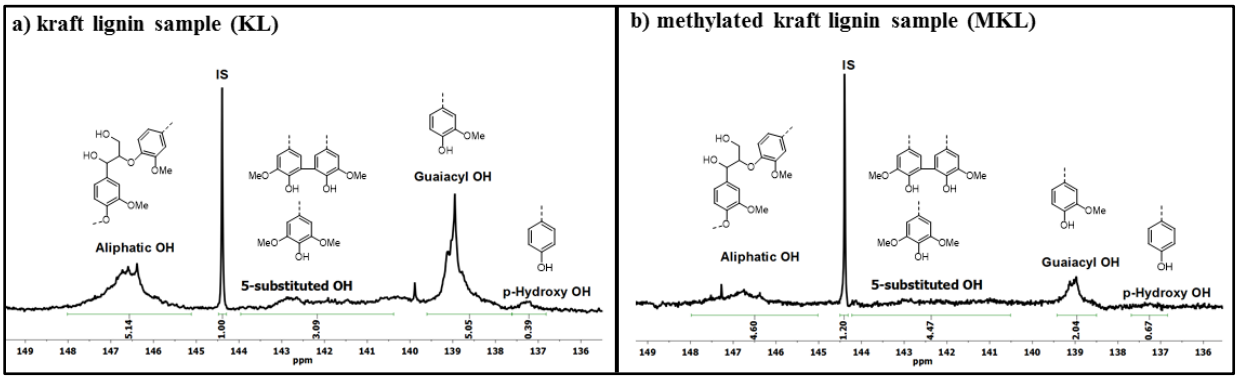

Figure III.33. Representative ^{31}P NMR spectra for: a) kraft lignin (KL); b) methylated kraft lignin (MKL).

Table III.28: Aliphatic hydroxyl / phenolic groups of kraft lignin and methylated kraft lignin samples quantified by ^{31}P NMR using cyclohexanol as internal standard.

Lignins	OH (mmol·g^{-1})[a]				
	Aliphatic OH	5-Substituted+ Syringyl OH	Guaiacyl OH (G)	*p*-Hydroxyphenyl OH (H)	COOH
KL	1.79	0.90	1.77	0.17	0.20
MKL	0.7	0.3	0.5	0.04	0.84

[a] Amounts displayed with respect to a known amount of cyclohexanol.

Indeed performing, the mechanochemical Strecker reaction between **14a**, **15a**, and KCN in the presence of the methylated kraft lignin (**MKL**) resulted in a slight decrease in the conversion of the reactants from 99 to 95%, and in the yield of the desired *α*-aminonitrile product **17a** from 95 to 78% (Table III.27, entry 15).

4.3. Studying the scope of the mechanochemical Strecker reaction

Table III.29: Scope of the Strecker reaction using aldehydes, ketones and amines.[a]

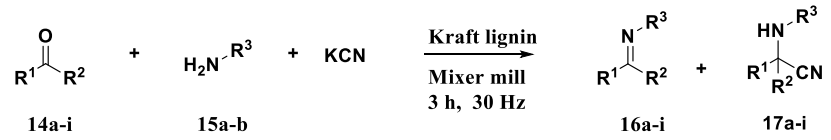

14a-i + 15a-b → 16a-i + 17a-i

Entry	Carbonyl compound 14	Amine 15	Imine 16a-i	α-aminonitrile 17a-i	Yield 16:17 [%][b]
1	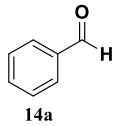 14a	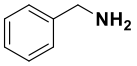 15a	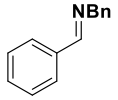 16a	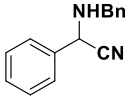 17a	7:92
2	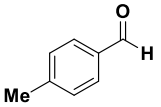 14b	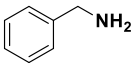 15a	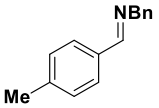 16b	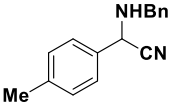 17b	19:78
3	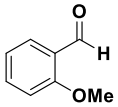 14c	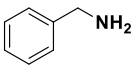 15a	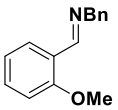 16c	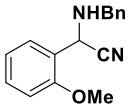 17c	5:91
4	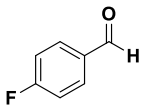 14d	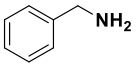 15a	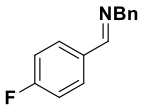 16d	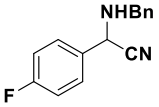 17d	14:84
5	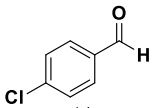 14e	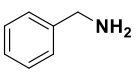 15a	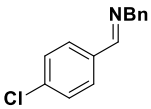 16e	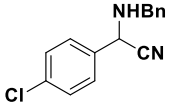 17e	10:88
6	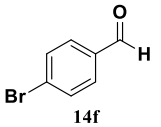 14f	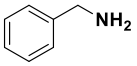 15a	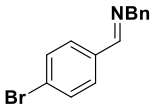 16f	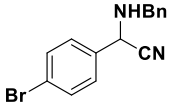 17f	18:79
7	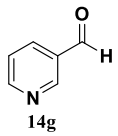 14g	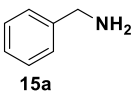 15a	 16g	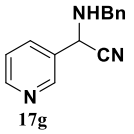 17g	6:76
8	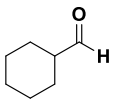 14h	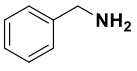 15a	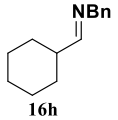 16h	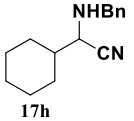 17h	1:95
9	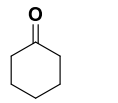 14i	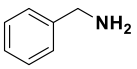 15a	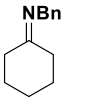 16i	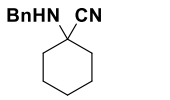 17i	1:92
10	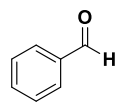 14a	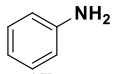 15b	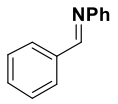 16j	17j	1:70

[a] Reaction conditions: carbonyl compound (0.5 mmol), amine (0.5 mmol), KCN (35.8 mg, 0.55 mmol) and Kraft lignin (250 mg) were milled in a mixer mill (**MM**) at 30 Hz for 3 h using a 10 mL stainless steel milling jar with 1 ball of 10 mm in diameter of the same material. [b] Yields determined by ^{1}H NMR spectroscopy with 1,3,5-trimethoxy-benzene as an internal standard.

Next, the optimized conditions were tested for a variety of aromatic carbonyls substituted with either electron-donating or -withdrawing functionalities (Table III.29 entries 1–6). With benzylamine (**15a**) as an amine partner, both *p*-tolualdehyde (**14b**) and *o*-anisaldehyde (**14c**) afforded the corresponding *α*-aminonitriles **17b** and **17c** in 78% and 91% yields respectively (entries 2 and 3). Furthermore, *p*-fluoro benzaldehyde (**14d**) gave 84% of *α*-aminonitrile **17d** (entry 4). Similar reactivities were observed for both *p*-chloro and *p*-bromo benzaldehydes (**14e** and **14f**) as they individually afforded products **17e** in 88% and **17f** in 79% yield respectively (entries 5 and 6). Moreover, with a hetereocyclic carbonyl Isonicotin aldehyde (**14g**), the amine (**15a**) also resulted in the formation of *α*-aminonitrile (**17g**) in 76% yield (entry 7). The high product selectivities were also maintained for the non-aromatic cyclohexancarbaldehyde (**14h**) and cyclohexanone (**14i**) forming **17h** in 98% and **17i** in a yield of 92% respectively (entries 8 and 9). Lastly, an experiment using aniline (**15b**) as amino component with **14a** (entry 10) was also successful, thus further extending the application range of the developed mechanochemical method.

4.4. Applying the mechanochemical Strecker reaction for the synthesis of heterocyclic scaffolds

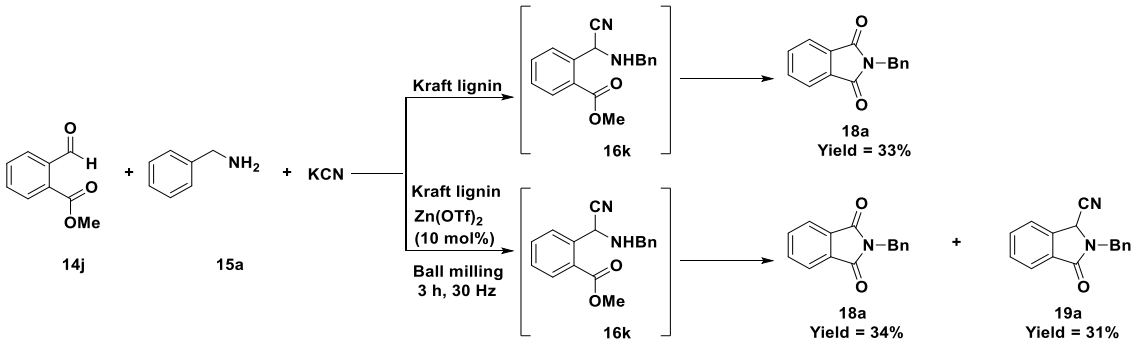

Scheme III.19. Mechanosynthesis of *N*-benzylphthalimide (**18a**) and isoindolinone (**19a**).

To further exhibit the applicability of the mechanochemical Strecker reaction, the protocol was extended to a reaction between 2-(methoxycarbonyl)benzaldehyde (**14j**), **15a**, and KCN. The expected *α*-aminonitrile **16k** was envisioned to undergo a further lactamization process under the milling conditions, leading to the formation of the isoindolinone derivative **19a** (Scheme III.19)[97]. However, the milling process, promoted by kraft lignin, instead resulted in the formation of *N*-benzylphthalimide (**18a**) in 33% yield. This alternate process could be proposed to take place as a result of cyanide-catalyzed oxidative amidation of the isoindolinone **19a** promoted by oxygen atmosphere present in the milling jar (Scheme III.20) [98–100].

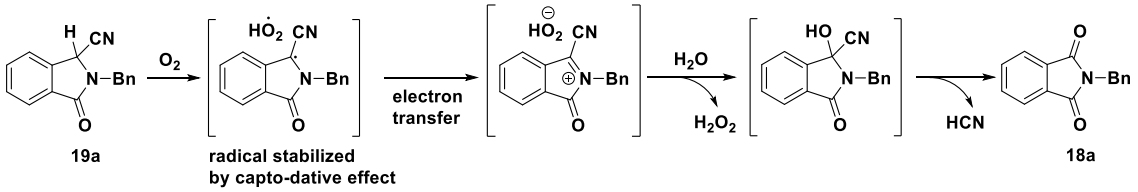

Scheme III.20. Probable reaction mechanism for the formation of **18a** in the ball mill.

A similar process when done in the presence of lewis acid $Zn(OTf)_2$ (10 mol%) in addition to Kraft lignin however, led to the formation of the desired product **19a** in 31% yield along with the presence of 34% **18a** (Scheme III.19). To ascertain the role of kraft lignin for the above transformation, a control reaction was performed only in the presence of $Zn(OTf)_2$ (10 mol %) as a catalyst. Indeed only trace quantities of **18a** and **19a** were obtained towards the end of the milling reaction.

1V. Summary and Outlook

1. Base-catalyzed cleavage of lignin β-O-4 model compounds and lignin initiated by alkali metal bases in dimethyl carbonate

This section of the dissertation first demonstrated the development of a base-catalyzed depolymerization strategy for the cleavage of lignin model compounds containing β-O-4 linkages by employing alkali-metal bases in dimethyl carbonate (DMC). In the presence of Cs_2CO_3, as a catalyst, capped methoxy benzene derivatives (**3a**–**c**) were obtained as the main cleavage products in good yields, for a variety of lignin model compounds (**D1**–**D4**, **D7**, **D8**). However, increased steric hindrance at the aryl ring adjacent to the benzylic hydroxyl group (**D5**, **D6**) was seen to result in a selectivity change, affording the corresponding 2-aryloxyvinyl benzene derivative (**1d**) in very good yields (80–82%). Concurrent research initiatives resulted in the establishment of a base-catalyzed transformation with LiO*t*-Bu for non-phenolic model compounds to 2-aryloxyvinyl benzene derivatives (**1a**–**d**), also in high yields.

Furthermore, a variety of substituted mono- (**M2**) and dilignol β-O-4 model compounds (**D9**–**D13)** were synthesized and studied under the optimized BCD conditions. These reactions demonstrated the involvement of the free aliphatic hydroxy groups and the protons at the α-carbon of the lignin β-O-4 linkage in the base-catalyzed depolymerisation reactions. Based on the cumulative results obtained from the model compound studies, different reaction pathways were proposed for the degradation reactions using LiO*t*-Bu and Cs_2CO_3 in DMC. Additionally, monitoring the reaction of model **D1** for both these bases (LiO*t*-Bu and Cs_2CO_3) also assisted in the elucidation of a reaction pathway and the point of difference for the bases which led to two different product selectivities. The quantum chemical calculations performed in collaboration with Dr. Julien Engel further supported the experimental observations successfully performed for the Cs_2CO_3-catalyzed cleavage reaction on lignin model compound **D1**.

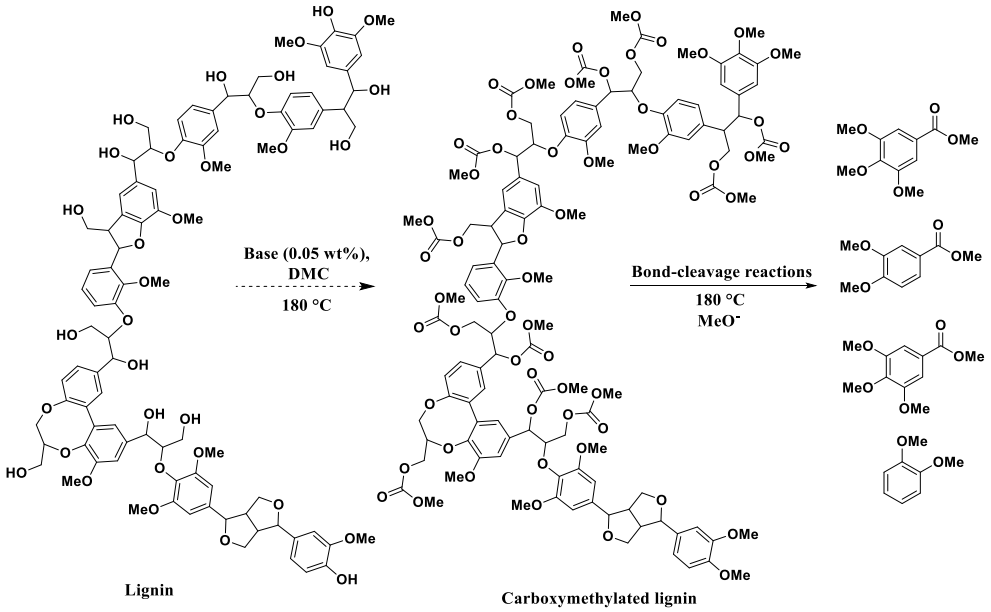

Scheme IV.1. Proposed reaction sequence for the BCD of lignin in DMC.

Next, the scope of the BCD reaction in DMC was directly extended to organosolv lignins extracted from beechwood, oak, cherry and the commercially available Aldrich-kraft lignin. Herein, for the first time a truly catalytic base-catalyzed depolymerization process (catalyst loadings of around 5 mol% with respect

to the starting lignin sample) was demonstrated, producing low-molecular weight oils (Scheme IV.1). For all the lignin samples, the respective low-molecular weight oil and the EtOAc insoluble fractions (solid residue) were quantified and characterized using 2D-NMR (HSQC), ^{31}P NMR, GPC and GC-MS measurements. The oil (extracted with EtOAc after the BCD reaction) fractions for the Cs_2CO_3-catalyzed lignin degradation were found to be within the range of 52–67 wt% of the starting lignin material and contained a range of methoxy capped aromatic monomers. Furthermore, this procedure with the cesium salts was effectively extended towards the direct degradation of milled beechwood chips, a more robust lignocellulosic starting material. Overall, these results were well in agreement with the model compound studies and could hence be directly correlated to the reaction pathways proposed for the BCD of lignin model compounds (Scheme IV.1).

Finally, foreseeing the possibility to scale-up the BCD process (biorefinery applications), readily available NaOH and KOH bases were once again employed as alternatives in catalytic amounts towards the depolymerization of Aldrich kraft lignin. Out of the two, an overnight reaction with KOH (0.05 wt%) afforded similar monomer yields compared to (0.05 wt%) -Cs_2CO_3 catalyzed reaction.

Taking into consideration the diverse applicability of the system, future studies could be directed towards conducting such lignin depolymerization studies in dimethyl carbonate using a continuous flow system where the reaction with DMC could take place in a plug-flow reactor having a bed of heterogeneous base catalysts.

2. Chemoselective oxidation of primary alcohol followed by retro-aldol promoted cleavage of C–C bond in lignin β-O-4 model compounds and lignin

The second project aimed towards the developement of an alternate organocatalytic one-pot two-step degradation strategy for lignin β-O-4 model compounds (**D1**–**D3**, **D8**, **D14**, **D15**) as well as lignin samples from beechwood and oak at room temperature. In contrast to the prevalent methodology resulting in the oxidation of benzylic (secondary) hydroxyl group in the lignin β-O-4 model compounds, this oxidative reaction sequence, initiated by a TEMPO/DAIB catalytic system, specifically addressed the chemoselective oxidation of the primary hydroxyl units. Furthermore, a recyclable polymer-bound hypervalent iodine reagent, poly[4-(diacetoxyiodo)-styrene], was also shown to be an effective and an recyclable oxidant, while maintaining the selectivity of the oxidation reaction.

This step was followed by a DL-proline-catalyzed retro-aldol reaction of the γ-OH oxidized product, resulting in the formation of mono-aromatic C–C bond cleavage products **8**, **9** and **11**. The two-step reaction sequences were then tested on the lignin samples and based on the observations made by 2 D-NMR (HSQC), GPC and GC–MS analysis of the reaction mixtures, a similar degradation pathway, as followed by the model compounds, was confirmed (Scheme IV.2).

Although this study, for the first time, elaborates on an alternative pathway for the one-pot two-step depolymerization of lignin through γ-OH oxidation route under mild reaction conditions, one possible hurdle for extending this approach on an industrially relevant scale would be the use of stoichiometric oxidants and the relatively low mono-aromatic product yields. Consequently, future efforts could be directed towards the screening and optimization of standard lignin samples obtained from different upstream processes along with increasing the overall efficiency of the process in terms of both oxidation as well as the subsequent base (DL-proline) cleavage reaction. In this context, based on our preliminary results with immobilized DAIB variant, one major improvement could be to develop a chemoselective catalytic γ-OH oxidation route using supported oxidants in a continuous flow reactor system.

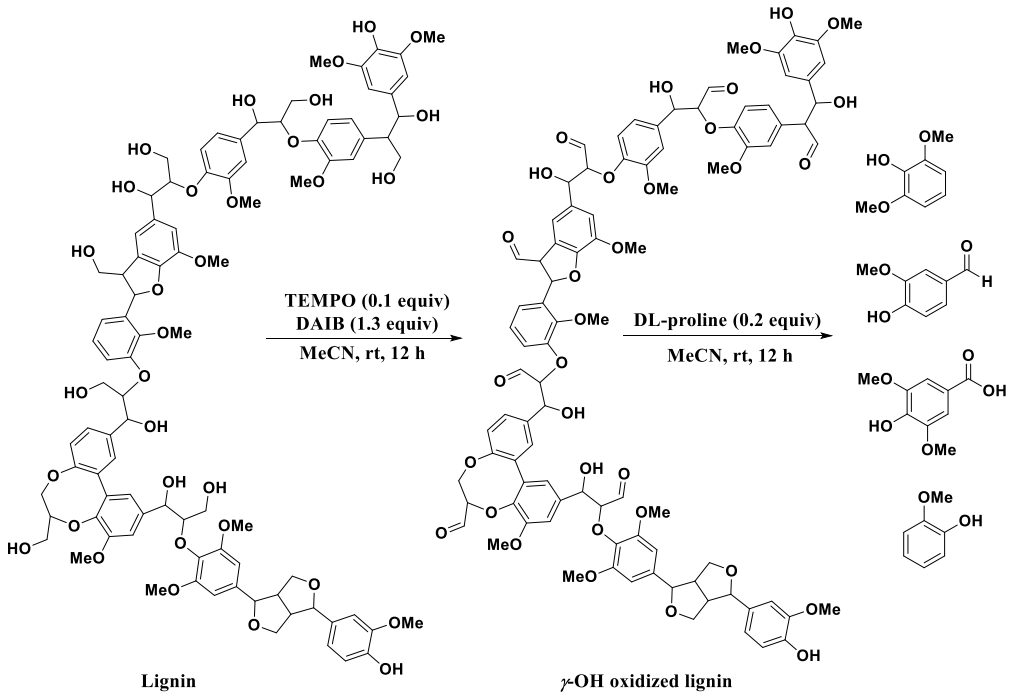

Scheme IV.2. Proposed reaction sequence for the one-pot two-step γ-OH oxidation followed by DL-proline catalyzed depolymerization of lignin.

3. Mechanochemically induced oxidative depolymerization of lignin β-O-4 model-compounds and lignin

The third project described in this thesis was initially envisoned as the extension of the previously optimized chemoselective γ-OH oxidation of lignin β-O-4 model compounds in MeCN, but under mechanochemical conditions. However, after preliminary screening reactions, it was observed that the oxidation reaction of model compound **D1** with TEMPO (0.1 equiv) / DAIB (1.3 equiv) in the mixer mill (**MM**) favoured the secondary (**BO**) alcohol oxidation of the β-O-4 bonds over the primary (**PO**) alcohol oxidation. Nevertheless, realizing that this results under solvent-free conditions was yet another unexplored pathway in the field of oxidative transformations on lignin samples, further screening reactions were conducted aiming to achieve a selective benzylic alcohol oxidation using the ball mill.

At first, TEMPO in combination with several stoichiometric oxidants were screened to catalyze the oxidation on a monolignol model compound **MI** in a mixer mill using a ZrO_2 miling media at 25 Hz for a 3 h reaction time. Having identified the combination of OH-TEMPO (0.2 equiv) / KBr (0.2 equiv) / Oxone (1.5 equiv) to be the most favourable combination for the oxidation of **D1** to **12a** in 45% yield, the screening was continued by further optimizing the milling conditions. After employing a variety of milling medias (ZrO_2, stainless steel (**SS**) and tungsten carbide (**WC**) along with varying the reaction time and milling frequency (25 Hz or 30 Hz), the best results for a OH-TEMPO (0.2 equiv) / KBr (0.2 equiv) / Oxone (1.5 equiv) catalyzed oxidation of **M1** to **2a** was obtained for a 90 min reaction in a mixer mill using **WC** jars at 30 Hz. The reaction conditions were even effective for the oxidation of other substituted monolignol model compounds **M2** and **M3** as well as for the chemoselective oxidation in *erythro* and *threo* dilignols **D1** and **D2**. However, the oxidation of the phenolic dilignols **D7** and **D16** under the ball milling conditions resulted in the formation of cleavage products guaiacol (**9)** and quinones (**13)** in good yields. The formation of these products could be attributed to the reactivity of the phenolic groups under the described oxidation environment.

The optimized reaction conditions for the model compound studies were further extended on real beechwood lignin sample and the oxidation reaction was first attempted in a mixer mill at 30 Hz for a 90 min and a 180 min reaction time in **WC** jars. It was observed in 2D-HSQC NMR that the degree of benzylic oxidation from a 90 min to a 180 min reaction increased considerably from 40 to 80% (Table III.20). This effect was also confirmed by the corresponding IR stectra of the oxidized lignin samples (Figure III.23). Furthermore the GPC analysis of these oxidized samples also pointed towards a decrease in the average molar mass (Mw) compared to the unreacted lignin samples. This led to the analysis of the ether-extract of the ball-mill oxidized lignin sample by GC-MS which confirmed the presence of quinones (**13**) as the major products present in the extract. The observation could be corelated to the model compound studies on **D7** and **D16**, and hence exlplain the formation of quinones as a result of the oxidative cleavage of the aryl-α-carbon bonds of terminal phenolic-β-O-4 substructures present in the lignin fragments along with the benzylic oxidation of the bio-polymer.

The reactions with lignin were also attempted at a much bigger batch (10 g) using a disc mill (DM) and a mortar and pestle mill (PMP). Delightfully, the greater shearing effect and the high energy impact generated while grinding the lignin and the catalysts in a disc mill resulted in the oxidation as well as the further C–C bond cleavage reactions in the lignin polymer. This result was confirmed by the shifts in the mass average values (Mw) of the lignin sample in the GPC measurements, compared to the untreated lignin sample. Furthermore, the detection of a number of mono-aromatics during the GC-MS measurements also confirmed the same. To rule out the role of disc mill in the cleavage of lignin, the reaction was repeated for the lignin sample without any catalyst system. Delightfully no cleavage products were observed. Both these findings can be supported by previoulsy known DFT calculations which mention the increased succeptible of oxidized lignin samples to undergo C–O bond cleavage reactions in comparison to unoxidized lignin samples due to the decrease in the C–O bond dissociation energies (Scheme IV.3).[34] Further attempts in this direction could be made to screen a variety of other lignin sources as well as to carry out the reactions in special milling apparatus having the possibility to purge a constant flow of O_2 and evaluate the oxidation reactions.

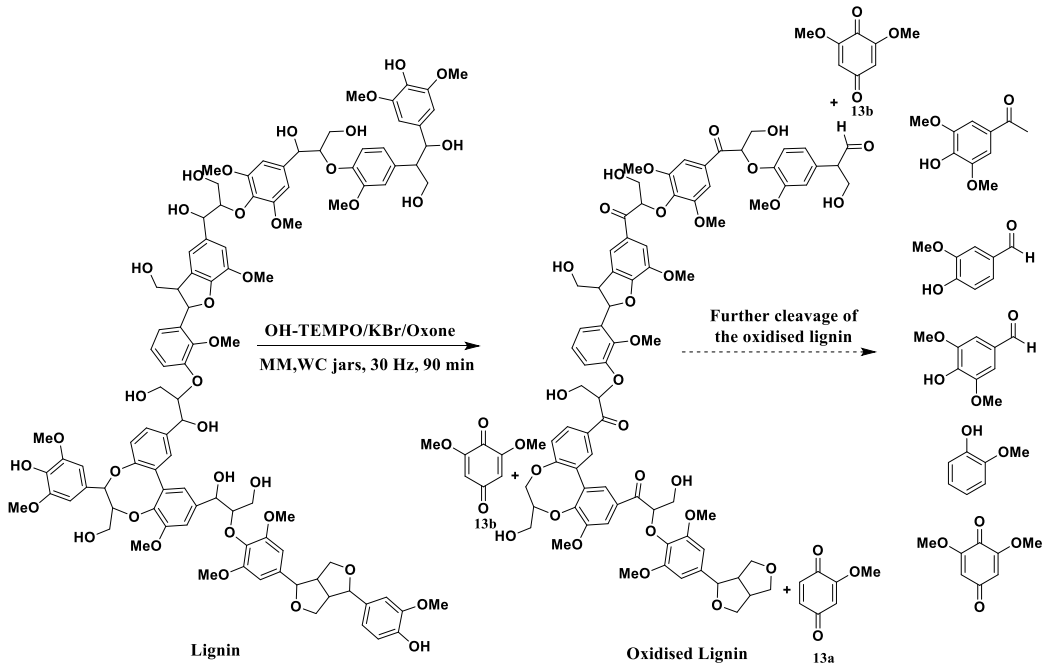

Scheme IV.3. Proposed reaction sequence for the mechanochemically induced oxidative transformations in lignin.

4. Application of lignin as a Strecker reaction promoter under milling conditions

Lastly, besides exploring various pathways to degrade lignin biopolymer into valuable mono-aromatic products, an alternate pathway was investigated for lignin valorization, by directly utilizing it as an activator to carry out organic Strecker reactions. The preliminary investigations were directly attempted with the peanut shell powder (lignocellulosic biomass), followed by the individual screening of cellulose and lignin components of the lignocellulosic biomass, as the solid promoters for the mechanochemical Strecker reaction between **14a**, **15a** and KCN . These results reflected on a higher efficiency of the lignin samples to promote the Strecker reaction in comparison to the other lignocellulosic components. The screening reaction was thus extended to a variety of lignin samples including organosolv beechwood, cherry, oak and commercially available kraft lignin. Out of the tested lignin samples, the kraft lignin was found to be the best activator for the cyanation step of imines in the ball mill. To confirm the role of the hydroxyl groups present in the lignin structure as Bronsted acid donors for the reaction, a sample of kraft lignin was subjected to methylation reaction which resulted in the capping of almost all the aliphatic hydroxyl and phenolic group. This transformation in the lignin structure was confirmed by comparing the quantitative ^{31}P NMR and IR analysis of the raw kraft lignin and methylated (capped) lignin.

As a proof of principle, the reaction attempted with the capped-lignin sample resulted in the loweing of product yield and thus confirmed the role of the hydroxyl group content in lignin and its ability to facilitate the formation of the α-aminonitriles. Furthemore, the kraft lignin also proved to be very effective for promoting the multicomponent Strecker reaction between several aldehydes **14** (aromatic, heteroaromatic, and aliphatic), amines (**15**), and KCN. Besides this, the recycled lignin sample was shown to have high converisons towards the desired product for upto three reaction runs. Finally, an attempt was also made to apply the developed Strecker reaction methodology for the solvent-free synthesis of *N*-benzylphthalimide (**18a**) and the isoindolinone (**19a**) through a one-pot three-component Strecker-lactamization catalyzed by the system $Zn(OTf)_2$-Kraft lignin in the ball mill.

This application of lignin as a promoter indeed opens several research pathways to be investigated. One such interesting followup could be to incorporate chirality onto the lignin structre (surface) and attempt an enantioselective Strecker reaction.

V. Experimental Section

1. General Information

1.1. General

Starting materials were purchased from commercial suppliers and used without further purification. THF and toluene used for the synthesis of lignin model compounds were dried by distillation over Solvona® (sodium on molecular sieves) in the presence of benzophenone and then stored under a nitrogen or argon atmosphere. Acetonitrile, pyridine, DMSO and DMF were purchased as dry solvents from Acros Organics (AcroSeal™). Flash chromatography was performed with Merck silica gel 60 (35–75 mesh). Analytical TLC was performed with aluminum sheets silica gel 60 F254 (Merck), and the products were visualized by UV detection or a cerium ammonium molybdate stain.

1.2. Nuclear Magnetic Resonance (NMR)

The 2D-HSQC NMR spectra for lignin samples were recorded on a Bruker Avance III 500 MHz or a Bruker Ascend 700 MHz spectrometer using previously described methods in DMSO-d_6 solvent.[28e] The ^{31}P NMR analysis for the lignin samples were recorded on a Varian Mercury 300 MHz spectrometer. The ^{1}H and ^{13}C spectra for the analysis of reactions with model compounds and Strecker products were recorded on a Varian Inova 400 (^{1}H NMR: 400 MHz, ^{13}C NMR: 101 MHz) or Agilent VNMRS 600 (^{1}H NMR: 600 MHz, ^{13}C NMR: 151 MHz) spectrometer. Chemical shifts (δ) are given in ppm relative to the residual solvent peak ($CDCl_3$: δ = 7.26 ppm, DMSO-d_6: δ = 2.50 ppm). Spin-spin coupling constants (*J*) are given in Hz. Abbreviations are as follows: s (singlet), d (doublet), t (triplet), m (multiplet), dd (doublet of doublets), dt (doublet of triplet) br.s (broad singlet), br.d (broad doublet), br.t (broad triplet).

1.3. Mass spectrometry

Mass spectra were recorded on a Finnigan SSQ 7000 spectrometer (EI) and HRMS on a Finnigan MAT 95 spectrometer (ESI).

1.4. High performance liquid chromatography (HPLC)

a) The HPLC measurements for the optimization of BCD approach on lignin *β*-O-4 model compounds, were conducted on an Agilent Infinity 1260 HPLC apparatus using an Agilent Eclipse XDB-C18 (4.6 mm ID x 150 mm, 5 µm) column with H_2O:MeOH (60:40) eluent system having a flow rate of 1.0 mL·min^{-1}. As an internal standard 3,4-dimethoxybenzyl alcohol in methanol, c = 0.2 mol·L^{-1}, was used.

b) The HPLC measurements for the BCD approach on advanced lignin *β*-O-4 model compounds (**D9**-**D13**) and reaction time course studies for the BCD of model **D1**, were conducted on a Shimadzu UFLC system equipped with a photodiode detector (Shimadzu SPD-M20A Prominence) and an Agilent Eclipse XDB-C18 Column (5 µm, 4.6 x 150 mm). Analysis was performed using Shimadzu Lab solutions Version 5.51 software. MeCN (0.1% formic acid) (A):H_2O (0.1% formic acid) (B) were used as eluents with a flow rate of 1.0 mL·min^{-1}.

HPLC Method: 5% A:95% B for 10 minutes followed by a gradient to 95% A:5% B over 30 minutes followed by 10 minutes at 95% A:5% B followed by a gradient to 5% A:95% B over 5 minutes followed by 5 minutes at 5% A:95% B at a flow rate of 1.0 mL·min^{-1}.

1.5. Gel Permeation Chromatography (GPC)

a) The GPC analysis for the lignin samples obtained before and after the BCD studies were performed on an Agilent technologies 1200 series system equipped with an Isocratic pump G1310 A. Three PL-gel 3 mL MIXED-E columns were operated in series at 42 °C. A mixture of DMF with 0.2 M LiCl was used as solvent with a flow-rate of 1.0 $mL \cdot min^{-1}$ and an injection volume of 100 µL. The signals were detected with an ECO Sec RI detector. The molecular weights were determined using polystyrene standards of known molecular weight distribution.

b) The GPC analysis for the lignin samples obtained before and after the chemoselective primary alcohol oxidation studies were performed on an Agilent technologies 1200 series instrument equipped with a refractive index (RI) detector and three 100 Å Suprema columns with a particle size of 5 µm (PSS Polymer Service GmbH). The eluent solution consisted of 0.1 M hydrogen phosphate dibasic (Na_2HPO_4) and 0.5 g polyethylene glycol 6000 (PEG) at a pH of 12 in HPLC grade water. The molecular weights were determined using polystyrene standards of known molecular weight distribution.

c) GPC analysis for the lignin samples obtained before and after their oxidative depolymerization initiated in the ball mills, were performed on an Agilent 1200 series instrument equipped with a RI detector. The eluent solution consisted of 0.1M sodium hydroxide (NaOH, 99%, Sigma Aldrich) and 0.01 wt% sodium azide (NaN_3, extra pure, Merck KGaA), prepared using HPLC grade water. The internal standard was a 12.5 $mg \cdot mL^{-1}$ glucose monohydrate solution (biochemistry, Merck KGaA). One pre-column (8 × 50 mm) and three MC X gel columns (8 × 300 mm) were used at a flow rate of 1.0 $mL \cdot min^{-1}$ at 40. The diameter of the gel particles was 5 m, the nominal pore widths were 1000 Å for the three columns. The molecular weights were determined using polystyrene standards of known molecular weight distribution.

1.6 Mechanochemical reactions

a) The preliminary screening for the mechanochemically induced lignin oxidation reactions and the Strecker reactions were carried out in a RETSCH mixer mill MM 400 using 10 mL milling jars made of either Zirconium oxide (ZrO_2), Stainless steel (SS) or Tungsten Carbide (WC) with a milling ball of 10 mm in diameter made up of the material corresponding to the milling jars used.

b) The beechwood chips were milled in a FRITSCH Planetary micro mill “Pulverisette 7 classic line” using 12 mL milling vessels made of ZrO_2 with 20 milling balls (5 mm in diameter) of the same corresponding material.

c) The scale up reactions for oxidative lignin depolymerization were done on two different mills made of WC: (a) A 250 mL SIEBTECHNIK disk swing mill-TS with a disc weighing 1.2 kg; (b) A 250 mL LAARMANN LMM6-100 mortar mill.

1.7. Melting Point

The melting point for the solids was measured with a Büchi Melting Point B-540 apparatus.

1.8. Infrared Spectroscopy

The IR-spectra were recorded on a Perkin Elmer 100 FT/IR spectrometer (Perkin Elmer Life and Analytical Sciences, Shelton, 710 Bridgeport Avenue, CT, USA).

1.9. Reaction profile

Modelled rate analysis lines were obtained using a DYNAFIT software**.**

2.0. Computational Details

All quantum chemical calculations were performed with a Gaussian 09 Revision D.0[101] on the facilities of the IT Centre of RWTH Aachen University. For geometry optimisations Head-Gordon's long-range corrected density functional ζB97X-D[102] was used with the SDD pseudopotential[103] for cesium and Dunning's double-ζ cc-pVDZ basis set[104] for all other atoms. Single-point calculations were performed with the SDD pseudopotential for cesium Pople's triple-ζ basis set 6-311++G (d.p).[105] Solvation effects were simulated with a polarisable continuum model (PCM) for dimethyl carbonate.[106] The static dielectric constant was defined as 3.13[107] and the dynamic dielectric constant as 1.87 based on the refractive index of dimethyl carbonate.[108] The nature of the obtained structure was evaluated with normal mode analysis. Gibbs free energies were calculated for a temperature of 298.15 K. A standard state correction for a 1 M solution was applied.

2. Synthesis and isolation of lignin model compounds

2.1. Synthesis of 1,3-dilignol β-O-4 model compounds (D1–D16).

The synthesis of 1,3-dilignols (**D1**–**D13, D15**) was carried out by following the synthetic protocols previously published by our group in the articles "Preparation of Diastereomerically Pure Dilignol Model Compounds" in the journal "Chemistry-A European Journal"[66] and "Mechanochemicl Degradation of Lignin and Wood" in the journal "Green Chemistry".[64] The model compounds **D14** and **D16** were synthesized following the article by Stahl and co-workers.[28c]

Spectroscopic data are thus consistent to the ones given in the mentioned reference.

***erythro* 1-(3,4-Dimethoxyphenyl)-2-(2-methoxyphenoxy)-1,3-propanediol (D1)[66]**

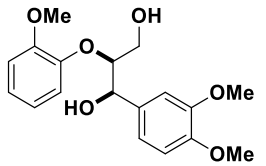

White solid. **mp:** 100–101 °C. **^{1}H NMR (400 MHz, $CDCl_3$):** δ = 7.07 (ddd, *J* = 8.2 Hz, 7.2 Hz and 1.8 Hz, 1H), 6.99–6.89 (m, 5H), 6.84 (d, *J* = 8.2 Hz, 1H), 4.99 (d, *J* = 4.7 Hz, 1H), 4.16 (ddd, *J* = 6.0 Hz, 4.7 Hz and 3.4 Hz, 1H), 3.94–3.90 (m, 1H), 3.89 (s, 3H), 3.88 (s, 3H), 3.87 (s, 3H), 3.66 (ddd, *J* = 12.1 Hz, 7.2 Hz and 3.4 Hz, 1H), 3.55 (br.s, 1H), 2.79 (br.s, 1H).**^{13}C NMR (101 MHz, $CDCl_3$):** δ = 151.6, 149.0, 148.5, 146.9, 132.4, 124.3, 121.7, 121.1, 118.4, 112.2, 111.0, 109.2, 87.5, 72.7, 60.7, 55.9 (3C). **MS (EI, 70 eV):** *m*/*z* (%): 334 [M^+] (31), 167 (16), 166 (12), 151 (17), 150 (100), 139 (20), 124 (11), 121 (12), 109 (10).

***threo* 1-(3,4-Dimethoxyphenyl)-2-(2-methoxyphenoxy)-1,3-propanediol (D2)[66]**

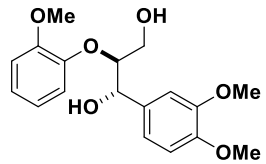

Colorless syrup. **^{1}H NMR (400 MHz, $CDCl_3$):** δ = 7.13 (dd, *J* = 8.0 Hz and 1.6 Hz, 1H), 7.07 (ddd, *J* = 8.0 Hz, 7.2 Hz and 1.6 Hz, 1H), 7.01–6.96 (m, 2H), 6.95 (dd, *J* = 8.0 Hz and 1.6 Hz, 1H), 6.93 (ddd, *J* = 8.0 Hz, 8.0 Hz and 1.6 Hz, 1H), 6.85 (d, *J* = 8.0 Hz, 1H), 4.99 (d, *J* = 4.7 Hz, 1H), 4.03 (dt, *J* = 7.7 Hz and 3.7 Hz, 1H), 3.91 (s, 3H), 3.88 (s, 3H), 3.87 (s, 3H), 3.69 (br.d, *J* = 1.6 Hz, 1H), 3.63 (dt, *J* = 12.0 Hz and 3.7 Hz, 1H), 3.48 (ddd, *J* = 12.0 Hz, 7.7 Hz and 3.7 Hz, 1H), 2.72 (dd, *J* = 7.7 Hz and 4.7 Hz, 1H). **^{13}C NMR (101 MHz, $CDCl_3$):** δ = 151.3, 149.1, 148.9, 147.6, 132.1, 124.3, 121.7, 121.1, 119.6, 112.1, 111.0, 109.9, 89.5, 73.9, 61.0, 55.9 (3C). **MS (EI, 70 eV):** *m*/*z* (%): 334 [M^+] (30), 167 (15), 166 (12), 151 (17), 150 (100), 139 (23), 124 (13), 121 (12), 109 (10).

2-(2,6-Dimethoxyphenoxy)-1-(3,4-dimethoxyphenyl)-1,3-propandiol (D3)[64]

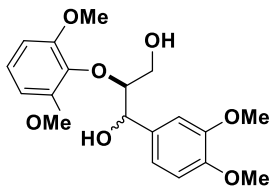

erythro:*threo* = 1.6:1. **Yellow syrup. ^{1}H NMR (400 MHz, $CDCl_3$):** δ = 7.11–6.94 (m, 5H), 6.86–6.82 (m, 3H), 6.65 (d, *J* = 8.4 Hz, 2H), 6.64 (d, *J* = 8.4 Hz, 2H), 5.06 (d, *J* = 8.7 Hz, 1H), 5.02 (d, *J* = 3.2 Hz, 1H), 4.36 (br.s, 1H), 4.18–4.13 (m, 2H), 3.94–3.92 (m, 1H), 3.91 (s, 6H), 3.89 (s, 3H), 3.88 (s, 9H), 3.87 (s, 3H), 3.86 (s, 3H), 3.58 (dd, *J* = 10.8 Hz and 2.7 Hz, 1H), 3.50 (d, *J* = 10.8 Hz, 1H), 3.40–3.26 (m, 2H), 3.16 (br.s, 1H). **^{13}C NMR (101 MHz, $CDCl_3$):** δ = 153.5 (2C), 153.2 (2C), 149.0, 148.9, 148.7, 148.2, 135.3, 135.0, 132.6, 132.0, 124.5, 124.4, 119.8, 118.1, 111.0 (2C), 110.3, 109.0, 105.3 (2C), 105.2 (2C), 89.0, 87.0, 74.0, 72.5, 60.6, 60.5, 56.2 (4C), 55.9 (2C), 55.9 (2C). **MS (EI, 70 eV):** *m*/*z* (%): 364 [M^+] (4), 181 (16), 180 (100), 154 (32), 139 (25).

***erythro* 2-(3,5-Dimethoxyphenoxy)-1-(3,4-dimethoxyphenyl)-1,3-propanediol (D4)[66]**

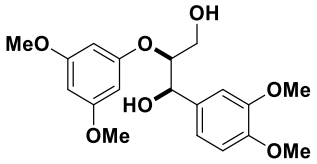

Colorless syrup. **^{1}H NMR (400 MHz, $CDCl_3$):** δ = 6.97–6.91 (m, 2H), 6.83 (d, *J* = 8.2 Hz, 1H), 6.08 (dd, *J* = 2.0 Hz and 2.0 Hz, 1H), 6.06 (d, *J* = 2.0 Hz, 2H), 5.02 (dd, *J* = 4.6 Hz and 3.8 Hz, 1H), 4.35 (dt, *J* = 4.6 Hz, 1H), 3.98–3.87 (m, 2H), 3.86 (br.s, 6H), 3.72 (s, 6H), 2.87 (br.s, 1H), 2.29 (br.s, 1H). **^{13}C NMR (101 MHz, $CDCl_3$):** δ = 161.4 (2C), 159.4, 139.9, 148.6, 132.9, 118.6, 111.0, 109.4, 95.2 (2C), 93.9, 81.7, 73.8, 61.4, 55.8 (2C), 55.3 (2C). **MS (EI, 70 eV):** *m*/*z* (%): 364 [M^+] (1), 210 (21), 181 (14), 180 (100), 167 (33), 155 (24), 151 (19), 139 (33), 138 (12).

***erythro* 2-(2-Methoxyphenoxy)-1-(2,4,6-trimethoxyphenyl)-1,3-propanediol (D5)[66]**

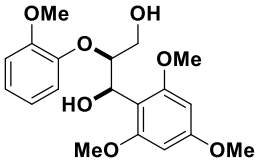

White solid. **mp:** 125–127 °C. **^{1}H NMR (400 MHz, $CDCl_3$):** δ = 6.90 (ddd, *J* = 8.1 Hz, 7.4 Hz and 1.6 Hz, 1H), 6.80 (dd, *J* = 8.1 Hz and 1.6 Hz, 1H), 6.77–6.72 (m, 1H), 6.65 (dd, *J* = 8.0 Hz and 1.6 Hz, 1H), 6.10 (s, 2H), 5.40 (dd, *J* = 11.1 Hz and 7.5 Hz, 1H), 4.45 (ddd, *J* = 7.4 Hz, 6.2 Hz and 3.9 Hz, 1H), 4.04–3.86 (m, 2H), 3.79 (s, 3H), 3.78 (s, 3H), 3.77 (s, 6H), 3.72 (d, *J* = 11.1 Hz, 1H), 3.19 (dd, *J* = 7.3 Hz and 6.1 Hz, 1H). **^{13}C NMR (101 MHz, $CDCl_3$):** δ = 160.9, 159.1 (2C), 150.9, 148.3, 122.8, 121.0, 119.6, 111.9, 109.0, 91.0 (2C), 85.5, 67.3, 63.0, 55.8 (3C), 55.4. **MS (EI, 70 eV):** *m*/*z* (%): 364 [M^+] (2), 198 (11), 197 (100), 150 (22), 109 (10), 77 (15).

***threo* 2-(2-Methoxyphenoxy)-1-(2,4,6-trimethoxyphenyl)-1,3-propanediol (D6)[66]**

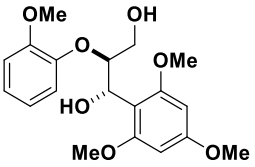

Yellow syrup. **^{1}H NMR (400 MHz, $CDCl_3$):** δ = 7.26–7.20 (m, 1H), 7.00 (ddd, *J* = 8.2 Hz, 7.5 Hz and 1.6 Hz, 1H), 6.94–6.86 (m, 2H), 6.12 (s, 2H), 5.39 (dd, *J* = 9.2 Hz and 8.2 Hz, 1H), 4.58 (ddd, *J* = 8.2 Hz, 7.5 Hz and 3.2 Hz, 1H), 3.89 (s, 3H), 3.81 (s, 3H), 3.80 (s, 6H), 3.71 (d, *J* = 9.2 Hz, 1H), 3.61 (ddd, *J* = 12.1 Hz, 7.2 Hz and 4.2 Hz, 1H), 3.45 (ddd, *J* = 12.1 Hz, 9.2 Hz and 3.2 Hz, 1H), 3.08 (dd, *J* = 9.2 Hz and 4.2 Hz, 1H). **^{13}C NMR (101 MHz, $CDCl_3$):** δ = 161.1, 159.0 (2C), 150.9, 149.1, 123.1, 121.4, 120.6, 112.0, 108.4, 91.1 (2C), 87.8, 67.8, 62.6, 55.9, 55.8 (2C), 55.3. **MS (EI, 70 eV):** *m*/*z* (%): 364 [M^+] (5), 198 (10), 197 (100), 150 (32), 109 (9), 77 (13).

***erythro* 1-(4-Hydroxy-3-methoxyphenyl)-2-(2-methoxyphenoxy)-1,3-propanediol (D7)[66]**

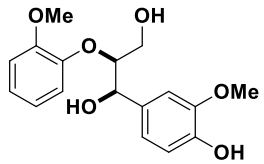

White solid. **mp:** 110–111 °C. **^{1}H NMR (400 MHz, $CDCl_3$):** δ = 7.09–7.05 (m, 1H), 6.99–6.90 (m, 4H), 6.88 (d, *J* = 8.1 Hz, 1H), 6.83 (d, *J* = 8.2 Hz, 1H), 5.60 (br.s, 1H), 4.97 (d, *J* = 4.5 Hz, 1H), 4.18–4.14 (m, 1H), 3.93–3.90 (m, 1H), 3.89 (s, 3H), 3.88 (s, 3H), 3.67–3.64 (m, 1H). **^{13}C NMR (101 MHz, $CDCl_3$):** δ = 151.8, 147.0, 146.7, 145.2, 131.9, 124.5, 121.8, 121.3, 119.1, 114.4, 112.3, 108.7, 87.7, 72.9, 60.9, 56.1, 56.0. **MS (EI, 70 eV):** *m*/*z* (%): 320 [M^+] (1), 153 (16), 151 (15), 150 (100), 124 (15), 121 (15), 109 (17), 93 (19), 77 (15), 65 (15).

***threo* 1-(4-Hydroxy-3-methoxyphenyl)-2-(2-methoxyphenoxy)-1,3-propanediol (D8)[66]**

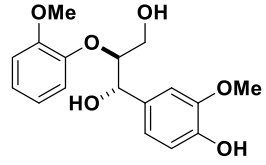

White solid. **mp:** 113–114 °C. **^{1}H NMR (400 MHz, $CDCl_3$):** δ = 7.13 (dd, *J* = 8.0 Hz and 1.6 Hz, 1H), 7.09–7.05 (m, 1H), 6.99–6.88 (m, 5H), 5.65 (s, 1H), 4.97 (d, *J* = 8.1 Hz, 1H), 4.04–3.99 (m, 1H), 3.92 (s, 3H), 3.89 (s, 3H), 3.72–3.59 (m, 1H), 3.48–3.46 (m, 1H), 2.71 (s, 1H), 1.62 (s, 1H). **^{13}C NMR (101 MHz, $CDCl_3$):** δ = 151.5, 147.7, 146.8, 145.7, 131.6, 124.5, 121.9,

121.3, 120.4, 114.4, 112.3, 109.5, 89.8, 74.2, 61.2, 56.1 (2C). **MS (EI, 70 eV):** *m/z* (%): 320 [M^+] (4), 153 (15), 151 (14), 150 (100), 137 (29), 124 (22), 121 (13), 109 (11).

***erythro*-1-(3,4-Dimethoxyphenyl)-3,3-dimethyl-2-(2-methoxyphenoxy)-l,3-propanediol (D9)[64]**

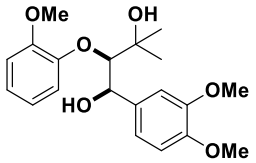

White Solid. mp: 102–103 °C. **^{1}H NMR (400 MHz, $CDCl_3$):**δ = 7.01 (d, *J* = 2.0 Hz, 1H), 6.97 (dd, *J* = 8.0 Hz and 2.0 Hz, 1H), 6.85–6.80 (m, 1H), 6.77 (dd, *J* = 8.0 Hz and 2.0 Hz, 1H), 6.74 (d, *J* = 8.0 Hz, 1H), 6.67 (ddd, *J* = 8.0 Hz, 6.9 Hz and 2.0 Hz, 1H), 6.44 (dd, *J* = 8.0 Hz and 1.6 Hz, 1H), 4.96 (d, *J* = 7.2 Hz, 1H), 4.15 (d, *J* = 7.2 Hz, 1H), 3.81 (s, 3H), 3.79 (s, 3H), 3.75 (s, 3H), 3.55 (br.s, 2H), 1.41 (s, 3H), 1.21 (s, 3H). **^{13}C NMR (101 MHz, $CDCl_3$):** δ =150.0, 148.8, 148.6, 148.5, 134.0, 122.2, 121.0, 119.4, 117.0, 111.9, 110.8, 110.1, 89.1, 74.5, 74.2, 55.9 (2C), 55.8, 27.1, 25.1. **MS (EI, 70 eV):** *m/z* (%): 362 [M^+] (2), 180 (18), 179 (100), 167 (12), 139 (19), 124 (18), 123 (13), 77 (12).

3-(3,4-Dimethoxyphenyl)-2-(2-methoxyphenoxy)-1,3-butanediol (D10)[64]

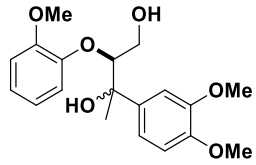

erythro:*threo* = 1.3:0.6. **Colorless syrup. ^{1}H NMR (400 MHz, $CDCl_3$):** δ = 7.14 (d, *J* = 2.1 Hz, 1H), 7.12 (d, *J* = 2.1 Hz, 1H), 7.10 (dd, *J* = 8.3 Hz and 1.5 Hz, 1H), 7.07–6.92 (m, 7H), 6.89–6.84 (m, 3H), 6.83 (d, *J* = 8.3 Hz, 1H), 4.19 (dd, *J* = 5.7 Hz and 3.8 Hz, 1H), 4.15 (t, *J* = 3.9 Hz, 1H), 3.91 (s, 3H), 3.90 (s, 3H), 3.88 (s, 3H), 3.87 (s, 3H), 3.87 (s, 3H), 3.86 (s, 3H), 3.80 (dd, *J* = 12.3 Hz and 5.7 Hz, 1H), 3.68 (dd, *J* = 12.3 Hz and 3.8 Hz, 1H), 3.56 (qd, *J* = 12.6 Hz and 3.9 Hz, 2H), 1.70 (s, 3H), 1.69 (s, 3H). **^{13}C NMR (101 Hz, $CDCl_3$):** δ = 151.1, 150.8, 148.8, 148.6, 148.3, 148.0, 147.9 (2C), 137.6, 137.3, 123.7, 123.6, 121.6, 121.5, 120.0, 119.7, 117.8, 117.1, 112.2, 112.0, 110.9, 110.6, 109.3, 108.6, 89.9, 87.9, 76.6, 75.8, 61.5, 61.0, 55.8, 55.9 (2C), 55.9 (3C), 27.7, 25.1. **MS (EI, 70 eV):** *m/z* (%): 348 [M^+] (3),182 (34), 181 (53), 165 (17), 151 (15), 150 (100), 139 (18), 124 (19), 121 (15), 109 (13), 77 (16).

***erythro*-3-(3,4-Dimethoxyphenyl)-3-methoxy-2-(2-methoxyphenoxy)-1-propanol (D11)[64]**

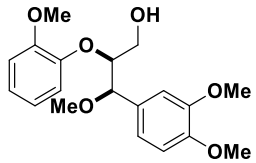

White Solid. mp: 76–77 °C. **^{1}H NMR (400 MHz, $CDCl_3$):** δ = 6.97–6.92 (m, 3H), 6.87–6.82 (m, 2H), 6.76 (td, *J* = 7.8 Hz and 1.5 Hz, 1H), 6.53 (dd, *J* = 8.0 Hz and 1.6 Hz, 1H), 4.43 (d, *J* = 7.2 Hz, 1H), 4.07 (ddd, *J* = 7.2 Hz, 4.6 Hz and 3.8 Hz, 1H), 3.92 (dd, *J* = 12.0 Hz and 4.7 Hz, 1H), 3.88 (s, 3H), 3.87 (s, 3H), 3.84–3.80 (m, 1H), 3.82 (s, 3H), 3.31 (s, 3H), 3.17 (m, 1H). **^{13}C NMR (101 Hz, $CDCl_3$):** δ = 151.2, 149.0, 148.7, 147.5, 131.4, 123.6, 121.3, 120.4, 120.3, 112.0, 110.8, 110.2, 86.7, 82.8, 61.6, 57.1, 55.9, 55.9, 55.8. **MS (EI, 70 eV):** *m/z* (%): 348 [M^+] (3), 182 (17), 181 (100), 151 (11).

***erythro*-1-(3,4-Dimethoxyphenyl)-3-methoxy-2-(2-methoxyphenoxy)-1-propanol (D12)[64]**

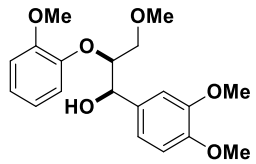

White Solid. mp: 68–69 °C. **^{1}H NMR (400 MHz, $CDCl_3$):** δ = 7.08–7.05 (m, 1H), 7.03–6.99 (m, 2H), 6.92–6.87 (m, 3H), 6.81 (d, *J* = 7.8 Hz, 1H), 4.87 (d, *J* = 3.6 Hz, 1H), 4.34 (m, 1H), 3.86 (s, 3H), 3.85 (s, 3H), 3.85 (s, 3H), 3.63 (dd, *J* = 10.2 Hz and 6.0 Hz, 1H), 3.43 (dd, *J* = 10.2 Hz and 3.6 Hz, 1H), 3.33 (s, 3H). **^{13}C NMR (101 MHz, $CDCl_3$):** δ = 151.4, 148.8, 148.3, 147.3, 132.5, 123.7, 121.4, 120.6, 118.6, 112.1, 110.8, 109.6, 85.1, 72.9, 71.4, 59.3, 55.9, 55.8, 55.8. **MS (EI, 70 eV):** *m/z* (%): 348 [M^+] (2), 181 (11), 167 (12), 166 (12), 165 (10), 151 (20), 150 (100), 139 (24), 124 (15), 121 (18), 109 (15), 95 (14), 77 (18).

***erythro*-1,3-Dimethoxy-1-(3,4-dimethoxyphenyl)-2-(2-methoxyphenoxy) propane (D13)[64]**

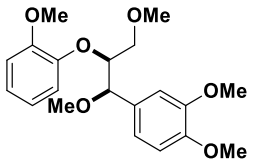

White Solid. mp: 50–51 °C. **^{1}H NMR (400 MHz, $CDCl_3$):** δ = 6.96 (d, *J* = 1.8 Hz, 1H), 6.93–6.87 (m, 2H), 6.85–6.76 (m, 4H), 4.47–4.42 (m, 2H), 3.87 (s, 3H), 3.83 (s, 3H), 3.75 (s, 3H), 3.74–3.70 (m, 1H) 3.64–3.60 (m, 1H), 3.37 (s, 3H), 3.29 (s, 3H).**^{13}C NMR (101 MHz, $CDCl_3$):** δ = 150.8, 148.8, 148.5, 147.9, 130.9, 122.3, 120.8, 120.4, 118.1, 112.2, 110.7, 110.5, 82.6, 82.3, 71.3, 59.3, 57.2, 55.8, 55.8, 55.7. **MS (EI, 70 eV):** *m/z* (%): 362 [M^+] (6), 182 (20), 181 (100), 151 (14), 45 (11).

2-(2-Methoxyphenoxy)-1-(3,4,5-trimethoxyphenyl)-1,3-propanediol (D14)[28c]

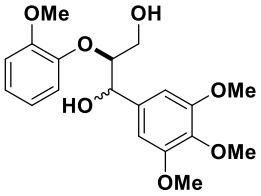

erythro:*threo* = 1.89:1 **Colorless syrup. ^{1}H NMR (400 MHz, $CDCl_3$):** δ = 7.09–6.97 (m, 4H), 6.91–6.82 (m, 4H), 6.66 (s, 2H), 6.59 (s, 2H), 4.96–4.90 (m, 2H), 4.14 (ddd, *J* = 6.1 Hz, 4.6 Hz and 3.2 Hz, 1 H), 4.03 (ddd, *J* = 6.1 Hz, 4.6 Hz and 3.2 Hz, 1 H), 3.87, 3.84, 3.82, 3.81, 3.78 (all singlets for methoxy groups, 12H for both diastereomers), 3.70–3.60 (m, 1H), 3.53–3.46 (m, 1H,), 2.96 (br.s, 2H). **^{13}C NMR (101 MHz, $CDCl_3$):** δ = major diastereomer: 153.4, 151.6, 147.0, 137.5, 135.9, 124.3, 121.7, 120.8, 112.3, 103.3, 89.1, 87.1, 73.1, 61.0, 56.3, 56.0; minor diastereomer: 153.4, 151.3, 147.7, 137.9, 135.5, 124.3, 121.8, 121.0, 112.3, 104.2, 89.1, 87.1, 74.3, 61.2, 61.0, 56.0. **MS (EI, 70 eV):** *m/z* (%): 364 [$M]^+$ (5), 197 (27), 196 (80), 169 (39), 150 (100).

***erythro* 2-(2-Methoxyphenoxy)-1-[3,4-(methylenedioxy)phenyl]-1,3-propanediol (D15)[66]**

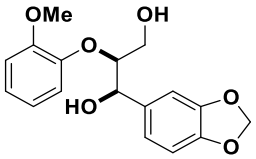

White solid. **mp:** 92–93 °C. **^{1}H NMR (400 MHz, $CDCl_3$):** δ = 6.97 (ddd, *J* = 8.0 Hz, 7.2 Hz and 1.6 Hz, 1H), 6.89 (dd, *J* = 8.0 Hz and 1.6 Hz, 1H), 6.87–6.80 (m, 3H), 6.75 (dd, *J* = 8.0 Hz and 1.6 Hz, 1H), 6.69 (d, *J* = 8.0 Hz, 1H), 5.86 (q, *J* = 1.2 Hz, 2H), 4.87 (d, *J* = 4.7 Hz, 1H), 4.05 (ddd, *J* = 6.0 Hz, 4.7 Hz and 3.7 Hz, 1H), 3.83 (dt, *J* = 12.0 Hz and 6.0 Hz, 1H), 3.79 (s, 3H), 3.57 (dd, *J* = 12.0 Hz and 3.7 Hz, 1H), 2.92 (br.s, 2H). **^{13}C NMR (101 MHz, $CDCl_3$):** δ = 151.5, 147.7, 147.0, 146.8, 133.9, 124.2, 121.6, 120.9, 119.5, 112.2, 108.1, 106.7, 101.0, 87.2, 72.7, 60.6, 55.9. **MS (EI, 70 eV):** *m/z* (%): 318 [$M]^+$ (5), 151 (22), 150 (100), 124 (11), 121 (14), 109 (10), 93 (14), 65 (11).

***erythro* -1-(4-Hydroxy-3,5-dimethoxyphenyl)-2-(2-methoxyphenoxy)propane-1,3-diol (D16)[28c]**

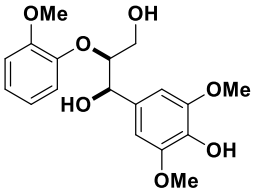

Colorless syrup. ^{1}H NMR (600 MHz, $CDCl_3$): δ = 7.08–7.04 (m, 1H), 6.98–6.89 (m, 3H), 6.62 (s, 2H), 5.55–5.52 (m, 1H), 4.95 (d, *J* = 4.7 Hz, 1H), 4.15 (ddd, *J* = 6.0 Hz, 4.7 Hz and 3.2 Hz, 1H), 3.91 (dd, *J* = 12.0 Hz and 6.0 Hz, 1H), 3.88 (s, 3H), 3.86 (s, 6H), 3.66 (dd, *J* = 12.0 Hz and 3.2 Hz, 1H), 3.57 (br.s, 1H), 2.77 (br.s, 1H). **^{13}C NMR (151 MHz, $CDCl_3$):** δ 151.7, 147.2, 146.9 (2C), 134.2, 131.0, 124.4, 121.8, 121.2, 112.3, 102.9 (2C), 87.6, 73.0, 60.9, 56.5 (2C), 56.0. **MS (EI, 70 eV):** *m/z* (%): 350 [$M]^+$ (14), 182 (22), 181 (9), 151 (13), 150 (100), 123 (17), 77 (10).

2.2. Synthesis of monolignol model compounds (M1–M3)

Monolignols **M1**–**M3** were prepared in a three step procedure. The first two reaction steps were prepared in accordance to the procedure by Picart *et al.*[109] In the final step we used a modified procedure by Bolm and co-workers.[30r]

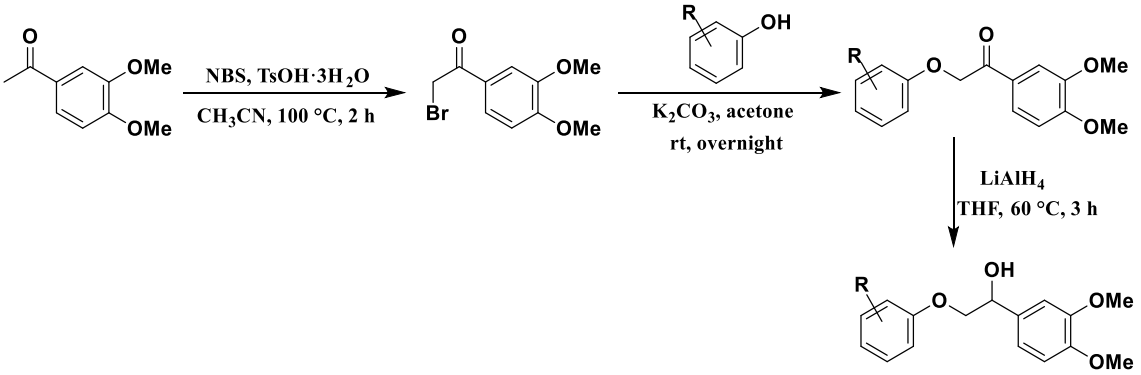

Scheme V.1. Synthesis of monolignol model compounds.

1-(3,4-Dimethoxyphenyl)-2-phenoxyethanol (M1)[28f]

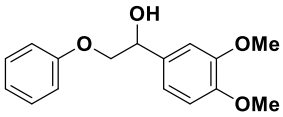

White solid. mp: 96–97 °C. **^{1}H NMR (400 MHz, $CDCl_3$):** δ = 7.32–7.24 (m, 2H), 7.03–6.87 (m, 6H), 5.09–5.06 (m, 1H), 4.11–4.07 (m, 1H), 4.03–3.99 (m, 1H), 3.91 (s, 3H), 3.89 (s, 3H), 2.78 (br.s, 1H). **^{13}C NMR (101 MHz, $CDCl_3$):** δ = 158.5, 149.3, 149.0, 132.4, 129.7 (2C), 121.4, 118.8, 114.8 (2C), 111.2, 109.5, 73.5, 72.5, 56.1 56.0. **MS (EI, 70 eV):** *m*/*z* (%): 274 $[M]^+$ (63), 257 (40), 167 (100), 139 (61), 77 (34).

1-(3,4-Dimethoxyphenyl)-2-(2-methoxyphenoxy)ethanol (M2)[28c]

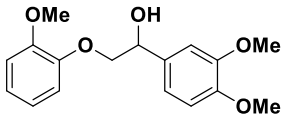

White solid. mp: 133–134 °C. **^{1}H NMR (400 MHz, $CDCl_3$):** δ = 7.03–6.88 (m, 6H), 6.86 (d, *J* = 8.2 Hz, 1H), 5.05 (dd, *J* = 9.8 Hz and 2.9 Hz, 1H), 4.17 (dd, *J* = 10.0 Hz and 3.0 Hz, 1H), 3.97 (t, *J* = 9.4 Hz 1H), 3.90 (s, 3H), 3.89 (s, 3H), 3.88 (s, 3H), 3.44 (br.s, 1H). **^{13}C NMR (101 MHz, $CDCl_3$):** δ = 150.1, 149.0, 148.7, 147.9, 132.2, 122.5, 121.0, 118.6, 116.2, 111.9, 110.9, 109.3, 76.3, 72.0, 55.9, 55.8, 55.7. **MS (EI, 70 eV):** *m*/*z* (%): 305 $[M+1]^+$ (48), 304 $[M]^+$ (90), 288 (14), 287 (55), 181 (10), 180 (56), 168 (18), 167 (100), 164 (10), 151 (73), 149 (28), 139 (90), 138 (80), 137 (10), 124 (43), 122 (16), 121 (15), 109 (19), 108 (11), 95 (11), 77 (30), 65 (10).

2-(2,6-Dimethoxyphenoxy)-1-(3,4-dimethoxyphenyl)ethanol (M3)[28c]

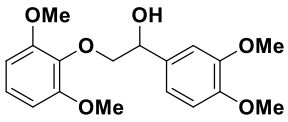

White solid, mp: 126–127 °C. **^{1}H NMR (400 MHz, $CDCl_3$):** δ = 7.03 (t, *J* = 8.4 Hz, 1H), 7.00–6.94 (m, 1H), 6.94–6.87 (m, 1H), 6.82 (d, *J* = 8.2 Hz, 1H), 6.61 (d, *J* = 8.4 Hz, 2H), 4.91 (dd, *J* = 11.0 Hz and 2.5 Hz, 1H), 4.53 (br.s, 1H), 4.39 (dd, *J* = 11.0 Hz and 2.5 Hz, 1H), 3.87 (s, 6H), 3.87 (3H), 3.85 (s, 3H), 3.70 (t, *J* = 10.5 Hz, 1H). **^{13}C NMR (101 MHz, ($CDCl_3$)):** δ= 153.4 (2C), 149.1, 148.7, 136.9, 132.2, 124.2, 118.8, 111.1, 109.5, 105.3 (2C), 80.3, 72.4, 56.2 (2C), 56.1, 56.0. **MS (EI, 70 eV):** *m*/*z* (%): 334 $[M]^+$ (80), 317 (20), 180 (45), 154 (100), 151 (40), 139 (37).

2.3. Isolation of lignin β-β model compound from sesame oil: Sesamin

(1*S*,3a*R*,4*S*,6a*R*)-1,4-Bis(benzo[d][1,3]dioxol-5-yl)tetrahydro-1H,3H-furo[3,4-c]furan (Sesamin)

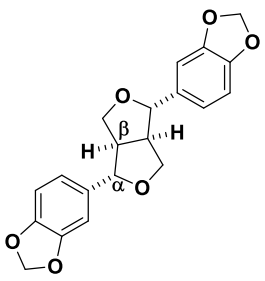

A solution of Kunella Feinkost sesame oil (200 mL) in *n*-pentane (500 mL) was loaded onto a column pre-packed with 50 g of silica in *n*-pentane. Next the column was eluted with *n*-pentane (700 mL) until a colorless eluent was obtained. Elution was then continued using a mixture of *n*-pentane:EtOAc (750 mL of a 9:1 mix followed by 750 mL of a 1:9 mix). The column was then flushed with EtOAc to afford the remaining sesamin. The combined fractions were concentrated *in vacuo* to give a light yellow semi-solid which was triturated with hexanes to afford sesamin **1a** as a white solid in 98% purity. **^{1}H NMR (400 MHz, $CDCl_3$):** δ = 6.85 (s, 2H), 6.83–6.74 (m, 4H), 5.94 (s, 4H), 4.71 (d, *J* = 4.24 Hz, 2H), 4.23 (ddd, *J* = 9.2 Hz, 4.4 Hz and 2.1 Hz, 2H), 3.86 (dd, *J* = 9.2 Hz and 3.6 Hz, 2H), 3.08–2.99 (m, 2H). **^{13}C NMR (101 MHz, $CDCl_3$):** δ 148.1 (2C), 147.2 (2C), 135.2 (2C), 119.5 (2C), 108.3 (2C), 106.6 (2C), 101.2 (2C), 85.9 (2C), 71.8 (2C), 54.5 (2C). **mp:** 121–122 °C (lit. 122–122.5 °C). ^{1}H NMR data are in accordance with those previously reported.[29h]

3. Synthesis of vinyl ketone (I)

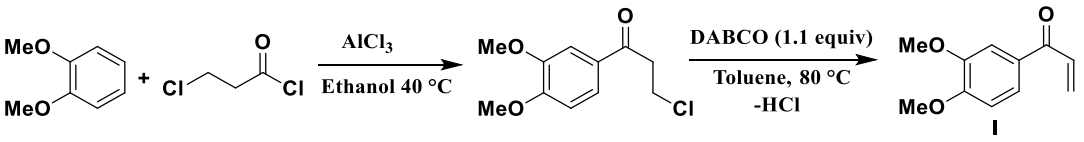

The vinyl ketone (**I**) was synthesized following a two-step procedure. The first step involved a Friedel-Craft acylation reaction between veratrole and 3-chloropropionylchloride, leading to the formation of 3-chloro-1-(3,4-dimethoxy phenyl)propan-1-one in 93% yield. A subsequent elimination of HCl gave **I** in good yield.

Step 1: Preparation of 3-chloro-1-(3,4-dimethoxyphenyl)propan-1-one [110]

A flame-dried and argon flushed 250 mL three-neck round bottom flask equipped with a magnetic stirrer and an argon inlet was charged with $AlCl_3$ (20.0 mmol, 1.0 equiv) and dry DCM (76.0 mL). The solution was cooled to 0 °C followed by the drop-wise addition of 3-chloropropionylchlorid (17.3 mmol, 1.1 equiv). To this, a solution of veratrole (2.0 mL, 16.0 mmol, 1.0 equiv) in dry DCM was added dropwise and the mixture was allowed to warm to room temperature, followed by heating at 40 °C for 3 h. The resulting mixture was then cooled to room temperature followed by the addition of an aq. HCl (6 M, 10.0 mL) solution. The phases were separated and the organic phase was washed with water (100.0 mL), aq. NaOH (10%, 100.0 mL) and brine (100.0 mL), dried over $MgSO_4$, filtered and concentrated under reduced pressure. The title compound was obtained without further purification as a pink solid (4.0 g, 14.6 mmol, 93%) with spectroscopic data in accordance with the literature.[111]

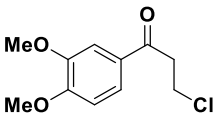

White solid. mp: 110–112 °C. **^{1}H NMR (300 MHz, $CDCl_3$):** δ = 7.57 (dt, *J* = 8.4 Hz and 1.9 Hz, 1H), 7.53 (t, *J* = 1.7, 1H), 6.90 (dd, *J* = 8.4 Hz and 1.4 Hz, 1H), 3.94 (s, 3H), 3.95 (s, 3H), 3.74 (td, *J* = 6.8 Hz and 1.2 Hz, 2H), 3.48–3.60 (td, *J* = 6.8 Hz and 1.2 Hz, 2H).

Step 2: Preparation of 1-(3,4-dimethoxyphenyl)prop-2-en-1-one (I)[110]

A flame-dried and argon flushed 100 mL two-neck round bottom flask equipped with a reflux condenser, a magnetic stirrer and an argon inlet was charged with 3-chloro-1-(3,4-dimethoxyphenyl)propan-1-one (14.7 mmol, 1.0 equiv) and dry toluene (52.0 mL). 1,8-Diazabicyclo[5.4.0]undec-7-ene (16.2 mmol, 1.1 equiv) was added dropwise and the reaction mixture was heated at 80 °C for 3.5 h. The solution was then allowed to cool to room temperature followed by the addition of water (100.0 mL). The phases were separated and the aqueous phase was extracted with DCM (3 × 50 mL). The combined organic phases were washed with water (100.0 mL) and brine (100.0 mL), dried over $MgSO_4$, filtered and concentrated under reduced pressure. The residue was purified by column chromatography over silica gel (*n*-pentane:Et_2O = 1:1) yielding compound **I** (2.0 g, 10.4 mmol, 71%) as a yellow viscous syrup with spectroscopic data in accordance with the literature.[111]

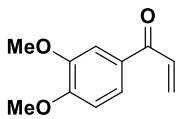

Yellow syrup. ^{1}H NMR (300 MHz, $CDCl_3$): δ = 7.63–7.56 (m, 2H). 7.19 (dd, *J* = 17.0 Hz and 10.5 Hz, 1H), 6.91 (d, *J* = 8.3 Hz, 1H), 6.44 (dd, *J* = 17.0 Hz and 1.8 Hz, 1H), 5.88 (dd, *J* = 10.5 Hz and 1.9 Hz, 1H), 3.95 (s, 3H), 3.96 (s, 3H).

4. Synthesis of 2-aryloxyacetaldehydes 11a and 11b

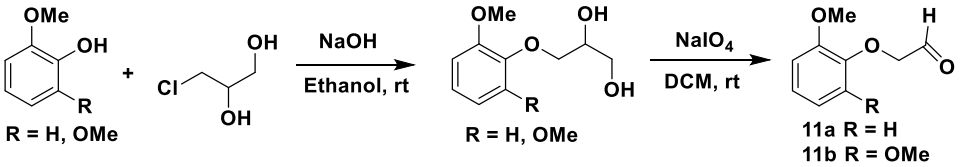

The 2-aryloxyacetaldehydes (**11a** and **11b**) were synthesized following a two-step procedure. Starting from the corresponding phenol derivatives and 3-chloropropane-1,2-diol, a nucleophillic substitution reaction resulted in the formation of 3-substituted propan-1,2-diols. Subsequent oxidation of both the diols followed by decarboxylation resulted in the desired products **11a** and **11b** in good yields.

Step 1: Preparation of 3-aryloxypropane-1,2-diols[112]

A 25 mL two-neck round bottom flask equipped with a reflux condensor and a magnetic stirrer was charged with either of the two corresponding phenol derivatives (25.0 mmol, 1.0 equiv) in ethanol (15.0 mL). To this, was added a solution of NaOH (1.3 equiv) in water (5.0 mL) and the resulting mixture was refluxed for 15 min under vigorous stirring. A solution of racemic 3-chloropropane-1,2-diol (1.2 equiv) in EtOH (2.0 mL) was then added dropwise to the above mixture and the reaction was subsequently refluxed for 3 h. The solution was cooled to room temperature and the volume of the mixture was reduced to half. This was followed by the extraction of the organics with Et_2O. The resulting crude mixture (2.0 g) was used for the subsequent synthesis step.

Step 2: Preparation of 2-aryloxyacetaldehyde 11a and 11b[113]

A 250 mL round bottom flask equipped with a magnetic stirrer was charged with the crude reaction mixture from step 1 and dissolved in DCM (100.0 mL). This was followed by the drop-wise addition of a solution of $NaIO_4$ (1.3 equiv) prepared in water (27.0 mL) to the above mixture. The reaction was continued for 1 h at room temperature after which the solution was filtered and extracted with DCM. The resulting crude mixture was then subjected to flash chromatography (EtOAc:*n*-pentane = 30%). The products obtained contained traces of phenol derivative owing to their instability during column chromatography purification. Pure samples of **11a** and **11b** were obtained as a white solid (70%) and liquid (55%) respectively after washing with minimum amounts of distilled *n*-pentane.

2-(2-methoxyphenoxy)acetaldehyde (11a)[114]

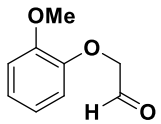

White solid. mp: 66–67 °C**. ^{1}H NMR (400 MHz, CD_3CN):** δ = 9.73 (d, *J* = 1.1 Hz, 1H), 7.01–6.95 (m, 2H), 6.91–6.84 (m, 2H), 4.69 (d, *J* = 1.1 Hz, 2H), 3.82 (s, 3H). **^{13}C NMR (101 MHz, CD_3CN):** δ = 199.9, 150.5, 148.3, 123.2, 121.6, 115.3, 113.5, 74.7, 56.3. **MS (EI, 70 eV):** *m*/*z* (%): 167 [M+1$^+$] (15), 166 [M$^+$] (100), 138 (24), 122 (49), 95 (25), 77 (33).

2-(2,6-dimethoxyphenoxy)acetaldehyde (11b)

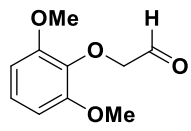

Yellow syrup. ^{1}H NMR (400 MHz, CD_3CN): δ = 9.82 (t, *J* = 1.5 Hz, 1H), 7.03 (t, *J* = 8.4 Hz, 1H), 6.65 (d, *J* = 8.4 Hz, 2H), 4.44 (d, *J* = 1.5 Hz, 2H), 3.83 (s, 6H). **^{13}C NMR (101 MHz, CD_3CN):** δ = 202.0, 153.9 (2C), 137.5, 125.3, 106.3 (2C), 78.4, 56.6 (2C). **MS (EI, 70 eV):** *m*/*z* (%): 197 [M+1$^+$] (14), 196 [M$^+$] (100), 153 (64), 152 (33), 138 (40), 125 (28), 95 (24).

5. Experimental procedures for the catalysis reactions on lignin model compounds

5.1. General procedure for the base-catalyzed degradation of lignin *β*-O-4 and *β*-*β* model compounds in dimethyl carbonate

A 10 mL pressure tube with a teflon screw cap and a magnetic stirrer was charged with model compound (0.25 mmol, 1.0 equiv) and base (0.01 mmol, 0.05 equiv) in dimethyl carbonate (1.3 mL). The mixture was stirred at 180 °C for 8 h or 12 h (depending on the reaction conditions) followed by cooling down to room temperature.

For the estimation of yields under pre-calibrated HPLC conditions, a standard solution (1.0 mL of 3,4-dimethoxybenzyl alcohol in methanol, c = 0.2 mol·L^{-1}, for veratrole (**3a**) and methyl 3,4-dimethoxy benzoate (**4a**) and diphenylether in methanol, c = 0.2 mol·L^{-1}, for alkenes **1a** and **2a**) was added with an Eppendorf pipette to the reaction mixture. The solution was then diluted with water (10.0 mL) and extracted with DCM. The organic phase was successively dried over $MgSO_4$. The solvent was removed under reduced pressure. The resulting residue was dissolved in MeCN (15.0 mL) and three samples were prepared for HPLC measurements by diluting 0.2 mL of the above solution with MeCN (1.0 mL) for each sample, followed by filtration into an HPLC vial.

For the estimation of yields by column chromatography, the cooled reaction mixture was diluted with water (10.0 mL) and extracted with DCM. The organic phase was successively dried over $MgSO_4$ followed by removal of the solvent under reduced pressure. The mixture was then loaded over prepacked silica-gel column and eluted with a known mixture of solvent system (30% EtOAc:*n*-pentane)

In the case of *β*-*β* model (sesamin), the crude reaction mixture was vacuum dried to remove DMC and analyzed by quantitative ^{1}H NMR with respect to 1,4-dinitrobenzene which was added as the internal standard to monitor the progress of the reaction.

5.2. General procedure to monitor the reaction progress for the base-catalyzed degradation of D1 in dimethyl carbonate

Individual reactions were carried out at different time intervals, to monitor the progress of the reaction with dilignol **D1** (chapter III, Figure III.1).

A 20 mL pressure tube with a magnetic stirring bar was charged with dilignol **D1** (0.25 mmol, 1.0 equiv) and a known amount of either Cs_2CO_3 or LiO*t*-Bu (0.05 equiv) in DMC (1.5 mL) and heated at 180 °C. An internal standard (1.0 mL of naphthalene in DMC, c = 0.2 mol·L^{-1}) was added towards the end of the desired reaction time. A requisit amount of sample (50.0 µL) from the mixture was then taken out**,** diluted with MeCN (1.0 mL) and analyzed by HPLC. To measure the changes at the initial start of the reaction (0 h), sample (50.0 µL) was taken out at room temperature .

5.3. Reaction of vinyl ketone with Cs_2CO_3 in dimethyl carbonate

A 20 mL pressure tube with a Teflon screw cap and a magnetic stirrer was charged with vinyl ketone (0.25 mmol, 1.0 equiv) and Cs_2CO_3 (0.05 equiv) in dimethyl carbonate (1.3 mL). The mixture was stirred at 180 °C for 8 h followed by cooling to room temperature. A standard solution (1.0 mL of 3,4-dimethoxy benzylalcohol in methanol, c = 0.2 mol·L^{-1}) was added with an Eppendorf pipette to the reaction mixture. The solution was then diluted with water (10.0 mL) and extracted with DCM. The

solvent was removed under reduced pressure and the resulting residue was re-dissolved in MeCN (15.0 mL). Three samples were prepared for HPLC measurements by diluting 0.2 mL of the above solution with MeCN (1.0 mL) for each sample, followed by filtration into an HPLC vial. The average yield for the 3,4-dimethoxybenzoate (**4a**) was hence calculated to be 40%.

5.4. General procedure for the screening of various nitroxide radical species and oxidants for the γ-alcohol oxidation in D1

A 10 mL glass tube with a teflon screw cap and a magnetic stirrer was charged with model compound **D1** (0.25 mmol, 1.0 equiv) and the requisite amounts of the nitroxide radical species and the terminal oxidant in acetonitrile-d_3 (2.0 mL). The reaction mixture was stirred at room temperature for 7 h. The conversion of **D1** and the yields for **PO** and **8a** were determined by ^{1}H NMR analysis of the crude reaction mixture with respect to 1,4-dinitrobenzene as the internal standard.

5.5. Procedure for the one-pot oxidation and reduction of the γ-OH in D1 to D1-*d*

A 10 mL tube with a teflon screw cap and a magnetic stirrer was charged with model compound **D1** (0.25 mmol, 1.0 equiv), TEMPO (0.1 equiv), DAIB (1.3 equiv) in MeCN (2.0 mL). The mixture was stirred at rt for 7 h. $NaBD_4$ (2.0 equiv) was added to the above reaction mixture along with 1.0 mL MeOH and the resulting mixture was stirred at rt for another 4 h. The reaction was then extracted in EtOAc (10.0 mL), which was evaporated under reduced pressure. The crude reaction mixture was then subjected to 2D-HSQC NMR analysis (chapter III, Figure III.14).

5.6. General procedure for the one-pot chemoselective oxidation / amine catalyzed cleavage of lignin β-O-4 model compounds

A 10 mL glass tube with a teflon screw cap and a magnetic stirrer was charged with lignin β-O-4 model compound (0.25 mmol, 1.0 equiv), TEMPO (0.1 equiv), and DAIB (1.3 equiv) in MeCN (2.0 mL) and stirred for 7 h at room temperature. The requisite amount of the amine (0.2 equiv) was then added to the above mixture and was further stirred for 5 h at room temperature. On completion, the reaction mixture was diluted with water (10.0 mL) and the aqueous phase was extracted with EtOAc (3 x 10 mL). The solvent was removed under reduced pressure, and subsequently, the reaction mixture was subjected to flash chromatography on silica gel using EtOAc:*n*-pentane (1:5) as eluent to give the corresponding products.

5.7. General procedure for monitoring the reactions during the one-pot two-step γ-OH oxidation and cleavage of model compounds D1, D3, and D9

A 10 mL glass tube with a teflon screw cap and a magnetic stirrer was charged with model compound (0.25 mmol, 1.0 equiv), TEMPO (0.1 equiv), DAIB (1.3 equiv) and 1,4-dinitrobenzene (7.0 mg) as an internal standard in CD_3CN (2.0 mL) and stirred at room temperature while monitoring the progress of the reaction by quantitative ^{1}H NMR. To this mixture, a requisite amount of the DL-proline (0.2 equiv) was added and the resulting reaction mixture was further monitored overtime. The data from this study have been plotted in chapter III, Figures III.16–III.18.

5.8. Procedure for the two-step degradation of D1 using the TEMPO / immobilized DAIB catalytic system and DL-proline followed by catalyst regeneration

A 10 mL glass tube with a teflon screw cap and a magnetic stirrer was charged with model compound **D1** (0.25 mmol, 1.0 equiv), TEMPO (0.2 equiv), and poly[4-(diacetoxyiodo)-styrene] (PS-DAIB; 1.3 equiv) in MeCN (2.0 mL) and stirred for 28 h at room temperature. The resulting reaction mixture was centrifuged and filtered to separate the reduced PS-DAIB catalyst. To this filtrate, DL-proline (0.2 equiv) was added and the reaction mixture was further stirred for 5 h at room temperature. Upon completion, propiophenone (0.5 mL, 0.2 M) was added to the reaction mixture as an internal standard. The solution was then diluted with MeCN (15.0 mL) and three samples were prepared for HPLC measurements by diluting 0.2 mL of the above solution with MeCN (1.0 mL) for each sample.

5.8.1. Regeneration of poly[4-(diacetoxyiodo)-styrene][115]

A peracetic acid solution was prepared by the dropwise addition of 30% H_2O_2 (2.0 mL) to Ac_2O (6.0 mL) at 0 °C. The solution was slowly warmed to room temperature and stirred overnight. Then, this solution was added to the recovered poly(4-iodostyrene) (0.22 g, 0.33 mmol). The reaction was stirred at 50 °C overnight. The resulting mixture was precipitated with Et_2O and filtered to give poly[4-(diacetoxyiodo)styrene] (0.30 g) as a light yellow powder.

5.9. General procedure for the oxidative transformations of lignin *β*-O-4 model compounds under milling conditions using MM 400 mixer mill

A 10 mL milling jar made of either ZrO_2, SS or WC, containing one milling ball of 10 mm in diameter was charged with model compound (0.25 mmol, 1.0 equiv) along with the requisite amounts of catalysts (see Tables III.17–III.19). The reaction mixture was then milled at either 25 Hz or 30 Hz for a particular time depending on the conditions employed. After the milling was complete, the reaction mixture was transferred into a beaker using small amounts of DCM. Unless otherwise specified, the conversion and product quantification was done by quantitative ^{1}H NMR spectroscopy with respect to 2,4-dinitrobenzene (7.0 mg) as an internal standard. The conversion and product yields for the phenolic model compounds **D7** and **D16** were quantified after pre-calibrated GC analysis with respect to a standard solution of *n*-octadecane (1.0 mL of *n*-octadecane in MeCN, c = 0.2 mol·L^{-1}), added with an Eppendorf pipette to the reaction mixture.

6. Experimental procedure for the lignin-mediated mechanochemical Strecker reaction

A typical reaction in a RETSCH MM 400 mixer mill: A mixture of the carbonyl compound (**14**; 0.50 mmol), amine (**15**; 0.50 mmol), KCN (35.80 mg, 0.55 mmol), and additive was milled in a 10.0 mL stainless steel milling vessel with one stainless steel milling ball of 10 mm in diameter at 30 Hz for 3 h. After the milling was complete, the content of the milling vessel was transferred into a beaker using small amounts of DCM. Then, a known amount of the internal standard (1,3,5-trimethoxybenzene) was added, and the mixture was filtered to remove the insoluble additive. Next, the filtrate was evaporated under reduced pressure. The residue was dissolved in $CDCl_3$ and analyzed by ^{1}H NMR spectroscopy to determine the corresponding yields for **16** and **17**.

7. Spectroscopic data of the reaction intermediates and cleavage products isolated after performing catalysis on lignin model compounds

***erythro*-3-(3,4-Dimethoxyphenyl)-3-hydroxy-2-(2-methoxyphenoxy)propyl methyl carbonate. (MC)**

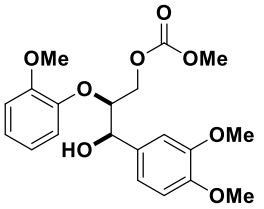

Colorless syrup. ^{1}H NMR (400 MHz, $CDCl_3$): δ = 7.10–7.04 (m, 2H), 6.98 (d, *J* = 1.8 Hz, 1H), 6.96–6.90 (m, 2H), 6.89–6.81 (m, 2H), 4.90 (d, *J* = 3.6 Hz, 1H), 4.51–4.43 (m, 2H), 4.17–4.12 (m, 1H), 3.88 (s, 6H), 3.86 (s, 3H), 3.74 (s, 3H). **^{13}C NMR (101 MHz, $CDCl_3$):** δ = 155.7, 151.6, 148.9, 148.5, 146.8, 131.3, 124.3, 121.6, 121.0, 118.4, 112.2, 110.9, 109.1, 84.6, 71.7, 66.2, 55.9 (2C), 55.8 54.9. **IR (ATR):** ν [cm^{-1}] = 3501, 2951, 2840, 2587, 2284, 2083, 2001, 1919, 1749, 1595, 1504, 1455, 1251, 1171, 1126, 1023, 917, 855, 747. **HRMS (ESI, 70 eV):** *m/z* calcd. for $C_{20}H_{24}O_8$+ Na^+ : 415.13634 [M+Na^+]; found: 415.13535. **HPLC MeCN (0.1% formic acid):** t_R = 26.3 min.

***erythro*-1-(3,4-Dimethoxyphenyl)-2-(2-methoxyphenoxy)-propane-1,3-diyldimethyl biscarbonate (DC)**

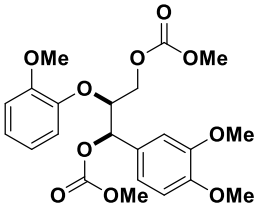

Colorless syrup. ^{1}H NMR (400 MHz, $CDCl_3$): δ = 7.00–6.95 (m, 3H), 6.86–6.79 (m, 4H), 5.87 (d, *J* = 6 Hz, 1H), 4.68 (m, 1H), 4.50 (dd, *J* = 12 Hz and 5.4 Hz, 1H), 4.33 (dd, *J* = 12 Hz and 4.3 Hz, 1H), 3.86 (s, 3H), 3.85 (s, 3H), 3.77 (s, 3H), 3.76 (s, 3H), 3.75 (s, 3H). **^{13}C NMR (101 MHz, $CDCl_3$):** δ = 155.5, 154.7, 151.0, 149.2, 148.8, 146.9, 128.2, 123.6, 120.9, 120.1, 119.4, 112.5, 110.7, 110.5, 79.9, 77.8, 65.9, 55.8 (2C), 55.7, 55.0, 54.9. **IR (ATR):** ν [cm^{-1}] = 2956, 2077, 1747, 1597, 1466, 1242, 952, 759. **HRMS (ESI, 70 eV):** *m/z* calcd. for $C_{22}H_{26}O_{10}$+Na^+: 473.14182 [M+Na^+]; found: 473.14166**. HPLC (MeOH:H_2O, 60:40):** t_R = 8.2 min; **HPLC MeCN (0.1% formic acid):** t_R = 29.6 min.

(*Z*)-1,2-Dimethoxy-4-[2-(2-methoxyphenoxy)vinyl]benzene (1a)

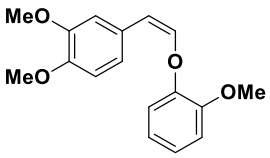

Yellow solid. mp: 77–78 °C. **^{1}H NMR (600 MHz, $CDCl_3$):** δ = 7.60 (d, *J* = 1.8 Hz, 1H), 7.13 (dd, *J* = 8.2Hz and 1.8 Hz, 1H), 7.09 (dd, *J* = 8.1 Hz and 1.6 Hz, 1H), 7.09–7.06 (m, 1H), 6.97 (dd, *J* = 9.9 Hz and 1.5 Hz, 1H), 6.94 (m, 1H), 6.83 (d, *J* = 8.4 Hz, 1H), 6.55 (d, *J* = 6.9 Hz, 1H), 5.56 (d, *J* = 6.9 Hz, 1H), 3.91 (s, 3H), 3.88 (s, 6H). **^{13}C NMR (151 MHz, $CDCl_3$):** δ = 149.9, 148.5, 147.7, 146.5, 140.7, 128.1, 123.7, 121.4, 120.9, 116.6, 112.5, 111.9, 110.8, 109.9, 55.9, 55.8, 55.6. **MS (EI, 70 eV):** *m/z* (%) = 287 [M+1$^+$] (20), 286 [M$^+$] (100), 271 (13), 226 (25), 151 (22), 77 (34). **HRMS (ESI, 70 eV):** *m/z* calcd. for $C_{17}H_{18}O_4$+Na^+: 309.10973 [M+Na^+]; found: 309.11053. **HPLC (MeOH:H_2O, 60:40):** t_R = 21.3 min.

Note: (*E*)-1,2-Dimethoxy-4-[2-(2-methoxyphenoxy)vinyl]benzene (2a): This alkene was obtained as a minor product and the yields were determined by ^{1}H NMR.
HPLC (MeOH:H_2O, 60:40): t_R = 15.3 min.

(*Z*)-2-[(3,4-Dimethoxystyryl)oxy]-1,3-dimethoxybenzene (1b)

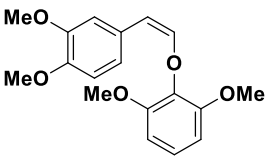

Brown syrup. ^{1}H NMR (600 MHz, $CDCl_3$): δ = 7.62 (d, *J* = 1.8 Hz, 1H), 7.18–7.16 (m, 1H), 7.07 (t, *J* = 8.4 Hz, 1H), 6.83 (d, *J* = 8.4 Hz, 1H), 6.63 (d, *J* = 8.4 Hz, 2H), 6.32 (d, *J* = 6.6 Hz, 1H), 5.36 (d, *J* = 6.6 Hz, 1H), 3.9 (s, 3H), 3.88 (s, 3H), 3.84 (s, 6H). **^{13}C NMR (151 MHz, $CDCl_3$):** δ = 152.8 (2C), 148.4, 147.2, 145.5, 135.9, 128.7, 124.7, 121.3, 112.2, 110.7, 106.5, 105.5 (2C), 56.3 (2C), 55.8, 55.6. **MS (EI, 70 eV)**: *m/z* (%) = 317 [M+1$^+$] (20), 316 [M$^+$] (100), 287 (19), 256(18), 150.9 (12). **HRMS (ESI, 70 eV):** *m/z* calcd. for $C_{18}H_{20}O_5$ +Na$^+$: 339.12029 [M+Na$^+$]; found: 339.12036.

Note: The stereochemistry of the alkene (**1b**) was determined by NOESY experiments.

(*E*)-2-[(3,4-Dimethoxystyryl)oxy]-1,3-dimethoxybenzene (2b)

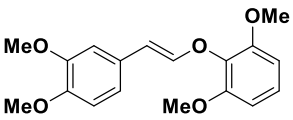

Brown syrup. ^{1}H NMR (600 MHz, $CDCl_3$): δ = 7.11 (t, *J* = 8.4 Hz, 1H), 7.01 (d, *J* = 12.6 Hz, 1H), 6.77–6.75 (m, 3H), 6.65 (d, *J* = 8.4 Hz, 2H), 5.98 (d, *J* = 12.6 Hz, 1H), 3.86 (s, 6H), 3.85 (s, 3H), 3.84 (s, 3H). **^{13}C NMR (151 MHz, $CDCl_3$):** δ = 152.9 (2C), 148.9, 147.4, 146.5, 134, 128.6, 125.1, 118, 111.3, 108.4, 108.2, 105.3 (2C), 56.3 (2C), 55.9, 55.7. **MS (EI, 70 eV)**: *m/z* (%) = 317 [M+1$^+$] (25), 316 [M$^+$] (100), 287 (15), 256 (13), 150.9 (10). **HRMS (ESI, 70 eV):** *m/z* calcd. for $C_{18}H_{20}O_5$+K$^+$: 355.09423 [M+K$^+$]; found: 355.09421.

Note: The stereochemistry of the alkene (**2b**) was determined by NOESY experiments.

(*Z*)-4-[2-(3,5-Dimethoxyphenoxy)vinyl]-1,2-dimethoxybenzene (1c)

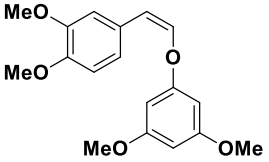

White solid. mp: 61–63 °C. **^{1}H NMR (600 MHz, $CDCl_3$):** δ = 7.33 (d, *J* = 1.8 Hz, 1H), 7.17 (dd, *J* = 8.4 Hz and 2.1 Hz, 1H), 6.83 (d, *J* = 8.3 Hz, 1H), 6.52 (d, *J* = 8.3 Hz, 1H), 6.29 (d, *J* = 2.1 Hz, 2H), 6.22 (t, *J* = 2.1 Hz, 1H), 5.57 (d, *J* = 6.9 Hz, 1H), 3.88 (s, 3H), 3.87 (s, 3H), 3.78 (s, 6H). **^{13}C NMR (151 MHz, $CDCl_3$):** δ= 161.5 (2C), 158.9, 148.5, 147.9, 139.8, 127.8, 121.5, 111.8, 110.9, 110.6, 95.4 (2C), 95.3, 55.8, 55.7, 55.4 (2C). **MS (EI, 70 eV)**: *m/z* (%) = 317 [M+1$^+$] (20), 316 [M$^+$] (100), 162 (30). **HRMS (ESI, 70 eV):** *m/z* calcd. for $C_{18}H_{20}O_5$+Na$^+$: 339.12029 [M+Na$^+$]; found: 339.12030.

Note: The stereochemistry of the alkene (**1c**) was determined by NOESY experiments.

(*Z*)-1,3,5-Trimethoxy-2-[2-(2-methoxyphenoxy)vinyl]benzene (1d)

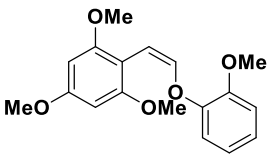

White solid. mp: 90–91 °C. **^{1}H NMR (600 MHz, $CDCl_3$):** δ = 7.51 (d, *J* =12.3 Hz, 1H), 7.09 (dd, *J* = 7.8 Hz and 1.8 Hz, 1H), 7.04–7.01 (m, 1H), 6.95–6.93 (m, 1H), 6.92 (dd, *J* = 7.6 Hz and 1.7 Hz, 1H), 6.70 (d, *J* = 12.3 Hz, 1H), 6.15 (s, 2H), 3.90 (s, 3H), 3.83 (s, 6H), 3.81 (s, 3H). **^{13}C NMR (151 MHz, $CDCl_3$):** δ = 159.3, 158.3(2C), 149.6, 147.1, 145.1, 122.8, 120.8, 116.7, 112.2, 105.5, 105.0, 90.8 (2C), 56.0, 55.7 (2C), 55.3. **MS (EI, 70 eV)**: *m/z* (%) = 317 [M+1$^+$] (10), 316 [M$^+$] (39), 194 (18), 181 (40), 122 (66), 92 (80), 77 (100). **HRMS (ESI, 70 eV):** *m/z* calcd. for $C_{18}H_{20}O_5$+Na$^+$: 339.12029 [M+Na$^+$]; found: 339.12076.

Note: The stereochemistry of the alkene (**1d**) was determined by NOESY experiments.

***Z*)-1,2-Dimethoxy-4-(1-(2-methoxyphenoxy)prop-1-en-2-yl)benzene (1e)**

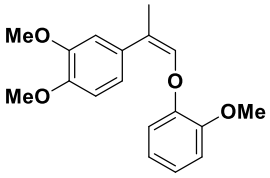

Yellow solid, mp: 82–83 °C. **^{1}H NMR (600 MHz, $CDCl_3$):** δ = 7.06–7.01 (m, 2H), 6.98–6.90 (m, 4H), 6.84 (d, *J* = 8.4 Hz, 1H), 6.68 (q, *J* = 2.4 Hz and 1.2 Hz, 1H), 3.91 (s, 3H), 3.89 (s, 3H), 3.88 (s, 3H), 2.15 (d, *J* = 1.2 Hz, 3H). **^{13}C NMR (151 MHz, $CDCl_3$):** δ = 149.6, 148.8, 148.1, 147.1, 138.9, 132.8, 123,2, 120.9, 120.8, 117.9, 116.8, 112.4, 111.1, 108.9, 56.1, 55.9, 55.8, 13.4. **HRMS (ESI, 70 eV):** *m/z* calcd. for $C_{18}H_{20}O_4$+ Na^+ : 323.12538 [M+Na^+]; found: 323.12497.

Note: (*E*)-1,2-Dimethoxy-4-(1-(2-methoxyphenoxy)prop-1-en-2-yl)benzene (2e): This alkene was obtained as a minor product and the yields were determined by ^{1}H NMR.

1,2-Dimethoxybenzene (3a)[116]

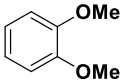

^{1}H NMR (600 MHz, $CDCl_3$): δ = 6.94–6.88 (m, 4H), 3.88 (s, 6H). **^{13}C NMR (151 MHz, $CDCl_3$):** δ = 148.9 (2C), 120.8 (2C), 111.2 (2C), 55.7 (2C). **MS (EI, 70 eV)**: *m/z* (%) = 138 [M^+] (100), 94.9 (14). **HPLC (MeOH:H_2O, 40:60):** t_R = 10.0 min; **HPLC MeCN (0.1% formic acid):** t_R = 22.8 min.

1,2,3-Trimethoxybenzene (3b)[117]

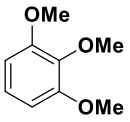

^{1}H NMR (400 MHz, $CDCl_3$): δ = 6.99 (t, *J* = 8.4 Hz, 1H), 6.58 (d, *J* = 8.4 Hz, 2H), 3.85 (s, 6H), 3.84 (s, 3H). **^{13}C NMR (101 MHz, $CDCl_3$):** δ = 153.4 (2C), 138, 123.6, 105.1 (2C), 60.8, 56 (2C). **MS (EI, 70 eV)**: *m/z* (%) = 169 [M+1^+] (10), 168 [M^+] (100), 153 (49), 124.8 (24), 109.8 (23).

1,3,5-Trimethoxybenzene (3c)[118]

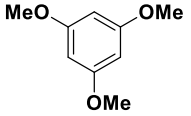

^{1}H NMR (400 MHz, $CDCl_3$): δ = 6.09 (s, 3H), 3.77 (s, 9H). **^{13}C NMR (101 MHz, $CDCl_3$):** δ = 161.4(3C), 92.8 (3C), 55.2 (3C). **MS (EI, 70 eV)**: *m/z* (%) =169 [M+1^+] (14), 168 [M^+] (100), 139 (52), 124.9 (14).

Methyl 3,4-dimethoxybenzoate (4a)[119]

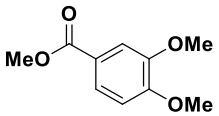

^{1}H NMR (600 MHz, $CDCl_3$): δ = 7.68 (dd, *J* = 8.4 Hz and 1.8 Hz, 1H), 7.54 (d, *J* = 1.8 Hz, 1H), 6.88 (d, *J* = 8.4 Hz, 1H), 3.94 (s, 3H), 3.93 (s, 3H), 3.89 (s, 3H). **^{13}C NMR (151 MHz, $CDCl_3$):** δ = 166.8, 152.9, 148.5, 123.5, 122.6, 111.9, 110.2, 56.0, 55.9, 52.0. **MS (EI, 70 eV)**: *m/z* (%) = 196 [M^+] (100), 165 (83), 124.9 (18), 79(25). **HPLC (MeOH:H_2O, 40:60):** t_R = 14.3 min; **HPLC MeCN (0.1% formic acid):** t_R = 23.6 min.

6-(3,4-Dimethoxyphenyl)-5-(2-methoxyphenoxy)-4,4-dimethyl-1,3-dioxan-2-one (5)

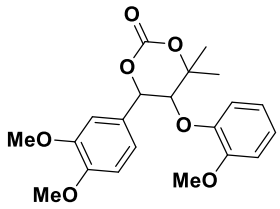

White solid. mp: 133–134 °C. **^{1}H NMR (600 MHz, $CDCl_3$):** δ = 6.96 (dd, *J* = 8.4 Hz and 2.4 Hz, 1H), 6.90 (m, 1H), 6.86 (d, *J* = 2.4 Hz, 1H), 6.81 (d, *J* = 8.4 Hz, 1H), 6.79 (dd, *J* = 8.4 Hz and 1.8 Hz, 1H), 6.64 (m, 1H), 6.24 (dd, *J* = 8.4 Hz and 1.8 Hz, 1H), 5.43 (d, *J* = 9.0 Hz, 1H), 4.38 (d, *J* = 9.0 Hz, 1H), 3.86 (s, 3H), 3.81 (s, 3H), 3.78 (s, 3H), 1.74 (s, 3H), 1.40 (s, 3H). **^{13}C NMR (151 MHz, $CDCl_3$):** δ = 150.3, 149.7, 149.3, 148.5, 147.3, 128.7, 123.9, 121.1, 119.9, 118.3, 112.4, 111.1, 109.7, 82.7, 81.8, 80.0, 56.1, 56.0, 55.8, 26.7, 21.8. **IR (ATR):** ν [cm^{-1}] = 3457, 2954, 2590, 2300, 2085, 1738, 1591, 1497, 1351, 1226, 1121, 645. **MS (EI, 70 eV):** *m/z* (%) = 389 [M+1$^+$] (23), 388 [M$^+$] (94), 189 (32), 178 (100), 165 (32), 124 (42). **HRMS (ESI, 70 eV):** *m/z* calcd. for $C_{21}H_{24}O_7$: 388.15165 [M$^+$]; found: 388.15187.

***erythro*-3-(3,4-Dimethoxyphenyl)-3-methoxy-2-(2-methoxyphenoxy)propyl methyl carbonate (6)**

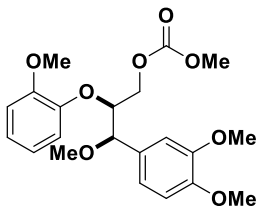

Colorless syrup. ^{1}H NMR (600 MHz, $CDCl_3$): δ = 6.92–6.87 (m, 3H), 6.82–6.80 (m, 2H), 6.78–6.74 (m, 1H), 6.69 (dd, *J* = 1.8 Hz and 7.8 Hz, 1H), 4.54–4.50 (m, 1H), 4.47–4.43 (m, 3H), 3.84 (s, 3H), 3.82 (s, 3H), 3.73 (s, 3H), 3.72 (s, 3H), 3.27 (s, 3H). **^{13}C NMR (151 MHz, $CDCl_3$):** δ = 155.6, 150.9, 148.9, 148.7, 147.5, 130.4, 122.9, 120.8, 120.2, 118.9, 112.3, 110.6, 110.3, 82.1, 81.6, 66.6, 57.1, 55.8 (2C), 55.6, 54.7. **IR (ATR):** ν [cm^{-1}] = 2942, 2316, 2086, 1747, 1596, 1470, 1248, 1119, 1025, 755. **MS (EI, 70 eV):** *m/z* (%) = 407 [M+1$^+$] (8), 406 [M$^+$] (24), 182 (19), 181 (100). **HRMS (ESI, 70 eV):** *m/z* calcd. for $C_{21}H_{26}O_8$+Na^+: 429.15199 [M+Na^+]; found: 429.15155.

***erythro*-1-(3,4-Dimethoxyphenyl)-3-methoxy-2-(2-methoxyphenoxy)propyl methyl carbonate (7)**

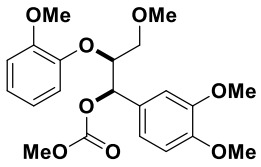

Colorless syrup. ^{1}H NMR (400 MHz, $CDCl_3$): δ = 7.05 (d, *J* = 2 Hz, 1H), 7.00 (dd, *J* = 2 Hz and 8.4 Hz, 1H), 6.97–6.80 (m, 5H), 5.86 (d, *J* = 5.6 Hz, 1H), 4.67–4.63 (m, 1H), 3.86 (s, 3H), 3.85 (s, 3H), 3.76 (s, 3H), 3.74 (s, 3H), 3.69–3.64 (m, 1H), 3.56–3.51 (m, 1H), 3.35 (s, 3H). **^{13}C NMR (101 MHz, $CDCl_3$):** δ = 154.8, 150.8, 149.0, 148.6, 147.5, 128.6, 122.8, 120.8, 120.3, 118.4, 112.4, 110.9, 110.5, 80.7, 78.3, 70.8, 59.2, 55.8, 55.7 (2C), 54.8. **IR (ATR):** ν [cm^{-1}] = 2935, 2087, 1745, 1596, 1475, 1243, 1130, 1024, 757. **MS (EI, 70 eV):** *m/z* (%) = 407 [M+1$^+$] (25),406 [M$^+$] (100), 251 (29), 225 (31), 181 (36). **HRMS (ESI, 70 eV):** *m/z* calcd. for $C_{21}H_{26}O_8$+Na^+ : 429.15199 [M+Na^+]; found: 429.15195

3,4-Dimethoxybenzaldehyde (8a)[26x]

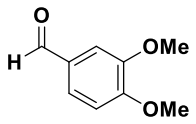

^{1}H NMR (600 MHz, CD_3CN): δ = 9.82 (s, 1H), 7.49 (dd, *J* = 8.4 Hz and 1.8 Hz, 1H), 7.38 (d, *J* = 1.8 Hz, 1H), 7.07 (d, *J* = 8.4 Hz, 1H), 3.89 (s, 3H), 3.85 (s, 3H). **^{13}C NMR (151 MHz, CD_3CN):** δ = 191.9, 155.5, 150.6, 131.1, 127.1, 111.9, 110.1, 56.6, 56.3. **MS (EI, 70 eV):** *m/z* (%): 167 [M+1$^+$] (15), 166 [M$^+$] (100), 165 (48), 151 (11), 95 (17), 77 (11), 51 (14).

4-Hydroxy-3-methoxybenzaldehyde (8b)[120]

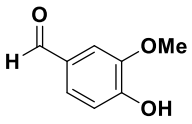

^{1}H NMR (600 MHz, CD_3CN): δ = 9.79 (s, 1H), 7.44–7.41 (m, 2H), 7.36 (br.s, 1H), 7.00–6.96 (m, 1H), 3.91, (s, 3H). **^{13}C NMR (151 MHz, CD_3CN):** δ = 191.8, 153.1, 148.8, 130.9, 127.2, 115.7, 110.9, 56.7. **MS (EI, 70 eV)**: *m/z* (%) = 153 [M+1$^+$] (93), 152 [M$^+$] (100), 109 (18), 81 (35), 53 (22).

3,4,5-Trimethoxybenzaldehyde (8c)[121]

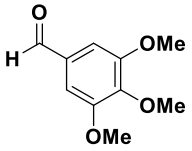

^{1}H NMR (600 MHz, CD_3CN): δ = 9.84 (s, 1H), 7.18 (s, 2H), 3.88 (s, 6H), 3.81 (s, 3H). **^{13}C NMR (151 MHz, CD_3CN):** δ = 192.3, 154.7 (2C), 144.2, 133.1, 107.5 (2C), 61.0, 56.8 (2C). **MS (EI, 70 eV)**: *m/z* (%) = 197 [M+1$^+$] (18), 196 [M$^+$] (100), 181 (35), 125 (90), 110 (53).

Benzo[*d*][1,3]dioxole-5-carbaldehyde (8d)[122]

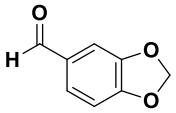

^{1}H NMR (400 MHz, CD_3CN): δ = 9.77 (s, 1H), 7.45 (dd, *J* = 12 Hz and 2.4 Hz, 1H), 7.28 (d, *J* = 2.4 Hz, 1H), 6.99 (d, *J* = 12 Hz, 1H) 6.07 (s, 2H). **^{13}C NMR (101 MHz, CD_3CN):** δ = 191.4, 154.0, 149.7, 132.9, 129.4, 109.2, 107.0, 103.5. **MS (EI, 70 eV)**: *m/z* (%) =151 [M+1$^+$] (15), 150 [M$^+$] (100), 149 (90), 121 (34), 64.4 (37).

2-Methoxyphenol (9a)[26x]

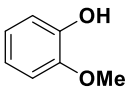

^{1}H NMR (600 MHz, CD_3CN): δ = 6.95–6.91 (m, 1H), 6.85–6.80 (m, 3H), 6.49 (br.s, 1H), 3.84, (s, 3H). **^{13}C NMR (151 MHz, CD_3CN):** δ = 148.2, 147.0, 122.1, 120.9, 115.7, 112.6, 56.5. **MS (EI, 70 eV):** *m/z* (%): 125 [M+1$^+$] (76), 124 [M$^+$] (100), 123 (10), 109 (13), 81 (14).

2,6-dimethoxyphenol (9b)[26x]

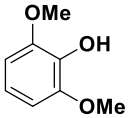

^{1}H NMR (600 MHz, CD_3CN): δ = 6.76 (t, 1H), 6.62 (s, 1H), 6.60 (s, 1H), 6.19 (br.s, 1H), 3.81 (s, 6H). **^{13}C NMR (151 MHz, CD_3CN):** δ = 148.7 (2C), 136.3, 119.8, 106.4 (2C), 56.8 (2C). **MS (EI, 70 eV):** m/z (%) = 155 [M+1$^+$] (20), 154 [M$^+$] (100), 139 (27), 111 (22), 96 (15).

1-(3,4-Dimethoxyphenyl)-2-phenoxyethan-1-one (12a)[123]

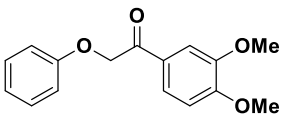

Yellow solid. mp: 91–92 °C. **^{1}H NMR (400 MHz, $CDCl_3$):** δ = 7.65 (dd, *J* = 8.4, 2.0 Hz, 1H), 7.56 (d, *J* = 2.0 Hz, 1H), 7.33–7.23 (m, 2H), 7.00–6.85 (m, 4H), 5.21 (s, 2H), 3.96 (s, 3H), 3.93 (s, 3H). **^{13}C NMR (101 MHz, $CDCl_3$):** δ = 193.2, 158.1, 153.9, 149.3, 129.5, 127.8, 122.9, 121.6, 114.8, 110.4, 110.2, 70.7, 56.1, 56.0. **MS (EI, 70 eV):** m/z (%): 273 [M+1]$^+$ (28), 272 [M]$^+$ (80), 165 (100), 151 (20), 77 (16), 51 (6).

1-(3,4-Dimethoxyphenyl)-2-(2-methoxyphenoxy)ethan-1-one (12b)[109]

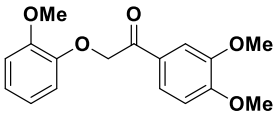

White solid. mp: 94–95 °C. **^{1}H NMR (400 MHz, $CDCl_3$):** δ = 7.67 (dd, *J* = 8.4 Hz and 2.0 Hz, 1H), 7.59 (d, *J* = 2.0 Hz, 1H), 6.96–6.84 (m, 5H), 5.28 (s, 2H), 3.94 (s, 3H), 3.93 (s, 3H), 3.88 (s, 3H). **^{13}C NMR (101 MHz, $CDCl_3$):** δ = 193.4, 153.9, 149.8, 149.3, 147.7, 128.0, 122.9, 122.5, 120.9, 114.8, 112.3, 110.6, 110.3,

72.2, 56.2, 56.1, 56.0. **MS (EI, 70 eV):** m/z (%): 303 $[M+1]^+$ (10), 302 $[M]^+$ (53), 165 (100), 151 (11), 77 (14), 51 (11).

2-(2,6-Dimethoxyphenoxy)-1-(3,4-dimethoxyphenyl)ethan-1-one (12c)[109]

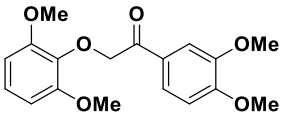

Colorless syrup. ^{1}H NMR (400 MHz, $CDCl_3$): δ = 7.72 (dd, *J* = 8.4 Hz and 1.8 Hz, 1H), 7.64 (d, *J* = 1.8 Hz, 1H), 7.01 (t, *J* = 8.4 Hz, 1H), 6.89 (d, *J* = 8.4 Hz, 1H), 6.58 (d, *J* = 8.4 Hz, 2H), 5.15 (s, 2H), 3.94 (s, 3H), 3.94 (s, 3H), 3.81 (s, 6H). **^{13}C NMR (101 MHz, $CDCl_3$):** δ = 193.7, 153.4 (2C), 153.2, 149.0, 136.6, 128.4, 124.1, 123.0, 110.6, 110.0, 105.3 (2C), 75.3, 56.1 (2C), 56.0 (2C). **MS (EI, 70 eV):** *m*/*z* (%): 332 $[M^+]$ (30), 166 (10), 165 (100), 153 (11), 152 (10), 151 (29), 107 (11).

1-(3,4-Dimethoxyphenyl)-3-hydroxy-2-(2-methoxyphenoxy)propan-1-one (12d)[109]

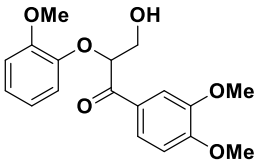

White solid. mp: 116–117 °C. **^{1}H NMR (600 MHz, $CDCl_3$):** δ = 7.75 (dd, *J* = 8.2 Hz and 1.8 Hz, 1H), 7.62 (d, *J* = 1.8 Hz, 1H), 7.00 (td, *J* = 8.1 Hz and 1.2 Hz, 1H), 6.94–6.86 (m, 3H), 6.82 (td, *J* = 8.1 Hz and 1.2 Hz, 1H), 5.40 (t, *J* = 5.1 Hz, 1H), 4.07 (d, *J* = 5.1 Hz, 2H), 3.95 (s, 3H), 3.92 (s, 3H), 3.86 (s, 3H). **^{13}C NMR (151 MHz, $CDCl_3$):** δ = 195.0, 153.9, 150.5, 149.2, 146.9, 128.0, 123.7, 123.6, 121.2, 118.5, 112.2, 110.9, 110.1, 84.6, 63.7, 56.1, 56.0, 55.8. **MS (EI, 70 eV):** *m*/*z* (%): 333 $[M+1^+]$ (7), 332 $[M^+]$ (31), 166 (11), 165 (100), 150 (30), 77 (11).

8. Spectroscopic data of the Strecker products 17a-j, 18a and 19a

2-(Benzylamino)-2-phenylacetonitrile (17a)[124,125]

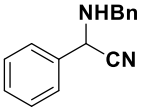

^{1}H NMR (600 MHz, $CDCl_3$): δ = 7.56 (dd, *J* = 7.9 Hz and *J* = 1.4 Hz, 2H), 7.45–7.40 (m, 4H), 7.40–7.36 (m, 3H), 7.33–7.29 (m, 1H), 4.76 (s, 1H), 4.08 (d, *J* = 13.0 Hz, 1H), 3.97 (d, *J* = 13.0 Hz, 1H), 1.89 (br.s, 1H). **^{13}C NMR (150 MHz, $CDCl_3$):** δ = 138.2, 134.8, 129.1, 129.0, 128.7, 128.5, 127.7, 127.4, 118.8, 53.5, 51.3.

2-(Benzylamino)- 2-(*p*-tolyl)acetonitrile (17b)[124,126]

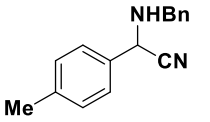

^{1}H NMR (600 MHz, $CDCl_3$): δ = 7.42 (dd, *J* = 7.5 Hz and *J* = 5.7 Hz, 4H), 7.37 (ddd, *J* = 7.6 Hz, *J* = 6.6 Hz and *J* = 1.4 Hz, 2H), 7.31 (ddd, *J* = 6.7 Hz, *J* = 6.3 Hz and *J* = 1.6 Hz, 1H), 7.22 (d, *J* = 7.9 Hz, 2H), 4.72 (s, 1H), 4.06 (d, *J* = 13.0 Hz, 1H), 3.95 (d, *J* = 13.1 Hz, 1H), 2.38 (s, 3H), 1.87 (br. s, 1H). **^{13}C NMR (150 MHz, $CDCl_3$):** δ = 139.1, 138.3, 131.9, 129.7, 128.8, 128.5, 127.7, 127.3, 119.0, 53.3, 51.4, 21.3.

2-(Benzylamino)-2-(2-methoxyphenyl)acetonitrile (17c)[127]

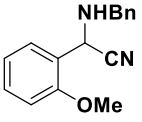

^{1}H NMR (600 MHz, $CDCl_3$): δ = 7.41 (d, *J* = 8.0 Hz, 2H), 7.39–7.35 (m, 4H), 7.33–7.29 (m, 1H), 7.00 (td, *J* = 7.5 Hz and *J* = 1.0 Hz, 1H), 6.95 (dd, *J* = 8.1 Hz and *J* = 1.0 Hz, 1H), 4.83 (s, 1H), 4.09 (d, *J* = 13.0 Hz, 1H), 3.95 (d, *J* = 13.0 Hz, 1H), 3.88 (s, 3H), 2.30 (br s, 1H). **^{13}C NMR (150 MHz, $CDCl_3$):** δ = 156.9, 138.4, 130.6, 128.9, 128.6, 128.5, 127.6, 123.3, 121.0, 119.1, 111.3, 55.7, 51.6, 49.4.

2-(Benzylamino)-2-(4-fluorophenyl)acetonitrile (17d)[128]

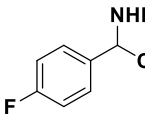

^{1}H NMR (600 MHz, $CDCl_3$): δ= 7.57–7.51 (m, 2H), 7.43–7.39 (m, 2H), 7.39–7.34 (m, 2H), 7.33–7.28 (m, 1H), 7.13–7.07 (m, 2H), 4.74 (s, 1H), 4.06 (d, *J* = 12.9 Hz, 1H), 3.95 (d, *J* = 12.9 Hz, 1H), 1.89 (br. s, 1H). **^{13}C NMR (150 MHz, $CDCl_3$):** δ = 163.1 (d, C_{ipso}–F, $^1J_{CF}$ = 248.2 Hz), 138.0, 130.7 (d, C_{para}–F, $^4J_{CF}$ = 3.1 Hz), 129.3 (d, C_{meta}–F, $^3J_{CF}$ = 8.5 Hz), 128.8, 128.5, 127.8, 118.7, 116.0 (d, C_{ortho}–F, $^2J_{CF}$ = 21.6 Hz), 52.8, 51.3.

2-(Benzylamino)-2-(4-chlorophenyl)acetonitrile (17e)[129]

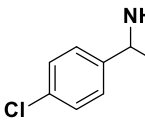

^{1}H NMR (400 MHz, $CDCl_3$): δ = 7.54–7.46 (m, 2H), 7.43–7.39 (m, 2H), 7.39–7.25 (m, 5H), 4.73 (s, 1H), 4.05 (d, *J* = 13.0 Hz, 1H), 3.95 (d, *J* = 13.0 Hz, 1H), 1.89 (br.s, 1H). **^{13}C NMR (100 MHz, $CDCl_3$):** δ = 138.0, 135.2, 133.3, 129.3, 128.8, 128.8, 128.5, 127.9, 118.5, 52.9, 51.3.

2-(Benzylamino)-2-(4-bromophenyl)acetonitrile (17f)[129]

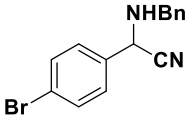

^{1}H NMR (400 MHz, $CDCl_3$): δ = 7.58–7.52 (m, 2H), 7.47–7.33 (m, 6H), 7.33–7.27 (m, 1H), 4.72 (s, 1H), 4.05 (d, *J* = 12.9 Hz, 1H), 3.95 (d, *J* = 13.0 Hz, 1H), 1.89 (br.s, 1H). **^{13}C NMR (100 MHz, $CDCl_3$):** δ = 138.0, 133.9, 132.2, 129.1, 128.8, 128.5, 127.9, 123.3, 118.4, 53.0, 51.3.

2-(Benzylamino)-2-(pyridin-3-yl)acetonitrile (17g)[130,131]

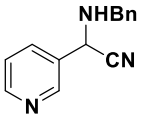

^{1}H NMR (600 MHz, $CDCl_3$): δ = 8.77 (d, *J* = 2.4 Hz, 1H), 8.60 (dd, *J* = 4.8 Hz and 1.7 Hz, 1H), 7.87 (ddd, *J* = 8.0 Hz, *J* = 2.9 Hz and *J* = 1.4 Hz, 1H), 7.41–7.37 (m, 2H), 7.37–7.32 (m, 3H), 7.31–7.27 (m, 1H), 4.78 (s, 1H), 4.05 (d, *J* = 13.0 Hz, 1H), 3.95 (d, *J* = 12.9 Hz, 1H), 2.06 (br.s, 1H). **^{13}C NMR (150 MHz, $CDCl_3$):** δ = 150.4, 148.8, 137.7, 135.0, 130.7, 128.8, 128.5, 127.9, 123.7, 117.8, 51.3, 51.3.

2-(Benzylamino)-2-cyclohexylacetonitrile (17h)[131]

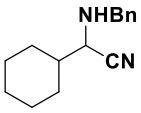

^{1}H NMR (400 MHz, $CDCl_3$): δ = 7.43–7.26 (m, 5H), 4.08 (d, *J* = 13.0 Hz, 1H), 3.82 (d, *J* = 13.0 Hz, 1H), 3.31 (d, *J* = 6.3 Hz, 1H), 1.94–1.62 (m, 6H), 1.34–1.07 (m, 5H). **^{13}C NMR (100 MHz, $CDCl_3$):** δ = 138.6, 128.6, 128.4, 127.6, 119.7, 55.6, 51.9, 40.8, 29.8, 29.0, 26.1, 25.8, 25.7.

1-(Benzylamino)cyclohexane-1-carbonitrile (17i)[132]

^{1}H NMR (400 MHz, $CDCl_3$): δ = 7.42–7.25 (m, 5H), 3.92 (s, 2H), 2.11–2.01 (m, 2H), 1.85–1.76 (m, 2H), 1.73–1.51 (m, 5H), 1.37–1.22 (m, 1H). **^{13}C NMR (100 MHz, $CDCl_3$):** δ = 139.5, 128.7, 128.5, 127.5, 122.3, 57.5, 48.7, 36.2, 25.3, 22.4.

2-Phenyl-2-(phenylamino)acetonitrile (17j)[125,129]

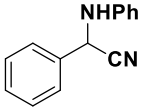

^{1}H NMR (400 MHz, $CDCl_3$): δ = 7.65–7.58 (m, 2H), 7.51–7.41 (m, 3H), 7.32–7.25 (m, 2H), 6.95–6.89 (m, 1H), 6.82–6.76 (m, 2H), 5.44 (s, 1H), 4.05 (br s, 1H). **^{13}C NMR (100 MHz, $CDCl_3$):** δ = 144.8, 134.1, 129.7, 129.7, 129.5, 127.4, 120.4, 118.3, 114.3, 50.4.

***N*-benzylphthalimide (5a)**[133]

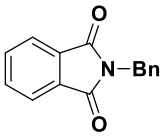

^{1}H NMR (400 MHz, $CDCl_3$): δ = 7.85 (dd, *J* = 5.4 Hz and 3.1 Hz, 2H), 7.70 (dd, *J* = 5.5Hz and 3.1 Hz, 2H), 7.46–7.41 (m, 2H), 7.37–7.27 (m, 3H), 4.85 (s, 2H). **^{13}C NMR (100 MHz, $CDCl_3$):** δ = 168.2, 136.5, 134.1, 132.3, 128.8, 128.7, 127.9 123.4, 41.7. **MS (EI, 70 eV):** *m/z* (%) = 237.9 (10) [M^+], 236.9 (50), 104.0 (100), 91 (27), 77.1 (62).

2-Benzyl-3-oxoisoindoline-1-carbonitrile (6a)[134]

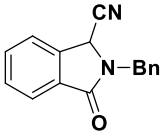

^{1}H NMR (400 MHz, $CDCl_3$): δ = 7.84 (d, *J* = 6.7 Hz, 1H), 7.59–7.46 (m, 3H), 7.31–7.14 (m, 5H), 5.40 (d, *J* = 15.1 Hz, 1H), 4.98 (s, 1H), 4.20 (d, *J* = 15.0 Hz, 1H). **^{13}C NMR (100 MHz, $CDCl_3$):** δ = 167.0, 136.9, 135.3, 133.1, 131.2, 130.5, 129.3, 128.7, 128.5, 124.8, 123.24, 114.6, 48.97, 45.12. **MS (EI, 70 eV):** *m/z* (%) = 248.9 (20) [M^+], 247.9 (100), 144.9 (29), 142.9 (35), 91 (25).

9. Experimental procedures for the extraction of organosolv lignins

9.1. Dioxasolv cherry (OS-CL) and oak (OS-OL) lignin

The lignins were extracted following a previously established literature procedure.[28e] A 2 L flask was charged with either cherry or oak sawdust (200.0 g) and 1,4-dioxane (1.5 L) was added followed by the addition of 2N HCl (0.2 L) solution. The mixture was heated to a gentle reflux under a N_2 atmosphere for 1 h. It was then cooled to room temperature and the lignin containing liquor was collected by filtration. This liquor was concentrated under vacuum, resulting in a gummy residue which was then dissolved in a mixture of acetone and water (9:1, ~250 mL) and precipitated by the addition to rapidly stirring water (2.5 L). The crude lignin was collected by filtration and dried under vacuum. The dried crude lignin was again taken up in mixture of acetone and methanol (9:1) and precipitated by the dropwise addition to rapidly stirring Et_2O (2.0 L). The precipitated lignin was collected by filtration and dried under vacuum to give purified samples of cherry / oak lignin (c.a. 20.0 g). These lignins were used in subsequent experiments without further processing.

9.2. Ethanosolv beechwood Lignin (OS-BWL1 and OS-BWL2)

The beechwood lignins were extracted from the corresponding beechwood chips using the following ethanol-based organosolv process. The lignin was extracted with aqueous ethanol (50% w/w) without the addition of an acid catalyst. Lignin was then precipitated with water and afterwards washed with water to remove the residual carbohydrates. The precipitate was sedimented by centrifugation and the liquor above decanted. Finally, the lignin was dried and pulverized.

10. Characterization of lignin samples

10.1. 2D-HSQC NMR

The organosolv beechwood, oak and cherry lignins along with Aldrich-Kraft lignin were characterized using 2D-HSQC experiments (Figure III.3) following a previously published report.[71] The signals corresponding to the major structural linkages in the 2D-HSQC NMR spectra were identified and their respective areas were used to determine relative quantities of the major linkages. This was done by taking integrals corresponding to the α-proton in various linkages (A: β-O-4, B: β-β, C: β-5) relative to the aromatic signals while maintaining the same contour level (Table III.5).

10.2. Quantitative ^{31}P NMR spectroscopy

The quantitative ^{31}P NMR analysis for the phenolic and the aliphatic hydroxyl groups in the lignins, both before and after the depolymerization reactions (Figure III.4, III.10, III.29, III.33), were conducted on a Brukner 300 MHz spectrometer following previous literature reports.[135] A 30.0 mg vacuum dried lignin sample was dissolved in 700 µL of an anhydrous solvent mixture (pyridine:$CDCl_3$, 1.6:1, v/v). To this, 100 µL of a cyclohexanol solution (10.8 mg·mL^{-1}) was added as an internal standard along with 100 µL of chromium (III) acetylacetonate solution (5.2 mg·mL^{-1}) as the relaxation reagent. Finally, 100 µL of the phosphitylating agent (2-chloro-4,4,5,5-tetramethyl-1,2,3-dioxa phospholane) was added and the mixture was transferred into a 5 mm NMR tube for NMR acquisition using 512 scans, 250 ppm sweep width and a relaxation delay of 10 sec.

11. Experimental procedures for the catalysis reactions on lignin samples

11.1. General procedure for the base-catalyzed depolymerization of lignin in dimethyl carbonate

A 20 mL pressure tube with a Teflon screw cap and a magnetic stirrer was charged with lignin (100.0 mg) and either Cs_2CO_3 (10 wt%, 0.03mmol) or LiO*t*-Bu (10 wt%, 0.125 mmol) in DMC (5.0 mL). The mixture was stirred at 180 °C for 8 h or 12 h (depending on the base) followed by cooling to room temperature.

Workup for 2D-HSQC NMR: The reaction mixture was transferred into a 25 mL round bottom flask, followed by the removal of dimethyl carbonate (DMC) under reduced pressure. Next, the residue was dissolved in deuterated dimethyl sulfoxide (DMSO-d_6) solution and filtered into an NMR tube.

Workup for GPC analysis and ^{31}P NMR: The reaction mixture was transferred into a 25 mL round bottom flask, followed by removal of dimethyl carbonate under reduced pressure. The resulting residue was further analyzed by GPC or dried overnight under reduced pressure and used for ^{31}P NMR analysis.

Workup for GC-MS analysis: After the completion of the reaction, the DMC was removed under reduced pressure. The resulting residue was then transferred into a centrifuge tube with EtOAc as solvent and spun at 5000 rpm for 10 min. The EtOAc soluble products were separated from the insoluble residue by multiple centrifugations using fresh EtOAc for each run (3 × 5 mL). The soluble fractions were combined and the solvents evaporated under reduced pressure resulting in an oil. The insoluble residue was then washed with water (3 × 5 mL) and pentane (3 × 5 mL). The oil and residue fractions were further dried overnight at 40 °C under vacuum and weighed individually. The oil containing the low molecular weight components was re-dissolved in EtOAc and a known amount of external standard *n*-octadecane (200 µl from a 0.062 M solution) was added. This mixture was analyzed by GC-MS for the identification and quantification of methoxy-capped compounds based on individual calibrations.

11.2. General procedure for the base-catalyzed depolymerization of beechwood chips in dimethyl carbonate

11.2.1. Pre-grinding the woodchips in a planetary ball mill

The wood chips were pre-milled in a FRITSCH Planetary micro mill model “Pulverisette 7 premium line” using a ZrO_2 milling jar of 20 mL in volume containing 20 ZrO_2 balls, each of 5 mm diameter. The jars were filled with 2.0 g of beechwood chips and the milling was continued for 1h at 1600 rpm to get a fine brown powder.

11.2.2. Base-catalyzed depolymerization of beechwood powder in dimethyl carbonate

A 20 mL pressure tube with a Teflon screw cap and a magnetic stirrer was charged with beechwood powder (100.0 mg) and Cs_2CO_3 (10.0 mg) in DMC (5.0 mL). The mixture was stirred at 180 °C for 8 h followed by its cooling to room temperature. To the above mixture was added 200 µl of internal standard (*n*-octadecane, 0.062 M solution) and the solvent was evaporated under reduced pressure. The resulting residue was dissolved in EtOAc (5.0 mL) and centrifuged to separate the soluble products from the residual powder which sedimented at the bottom of the tube. This process was repeated 3 times. The combined fractions were then dried under reduced pressure to get an oil residue. A sample of this residue was dissolved in EtOAc and was injected in the GC-MS for further quantitative product analysis. Alternatively, to rule out any cleavage reaction induced during the pre-milling of the wood chips, and

to highlight the role of Cs_2CO_3 in the current system, a control experiment was performed with beechwood powder (100.0 mg) in DMC (5.0 mL) but in the absence of Cs_2CO_3 (10.0 mg). A similar workup procedure and product analysis was performed as above.

11.3. General procedure for the one-pot two-step chemoselective oxidation followed by DL-proline catalyzed degradation of lignin samples

A 20 mL glass tube with a teflon screw cap and a magnetic stirrer was charged with lignin (200.0 mg), TEMPO (0.1 equiv), DAIB (1.3 equiv) in MeCN (4.0 mL) and stirred at rt for 12 h. Then, DL-proline (0.2 equiv) was added and the reaction mixture was further stirred at rt for 12 h. Subsequently, the reaction mixture was transferred into a 25 mL round bottom flask, and MeCN was removed under reduced pressure. Next, the residue was dissolved in deuterated dimethyl sulfoxide (DMSO-d_6) and filtered into an NMR tube or dried overnight under vacuum prior to GPC analysis.

In case of GC-MS analysis the residue after removing MeCN, was extracted with DCM, which was again reduced under pressure. The resulting oil was dissolved in acetone along with the addition of 0.1 mL of 0.05 M *n*-octadecane as an internal standard.

NOTE: The loadings for TEMPO, DAIB and DL-proline were calculated by dividing the mass of the lignin samples by the molar mass of **D1** to estimate the amount of diol fragments.

11.4. Procedure for OH-TEMPO/KBr/Oxone catalyzed oxidative transformation of lignins by mechanochemical activation

11.4.1. Reaction in a RETSCH MM 400 mixer mill (MM)

A 10 mL milling jar made of tungsten carbide (WC) was charged with lignin sample (100.0 mg), OH-TEMPO (0.2 equiv), KBr (0.2 equiv) and Oxone (1.5 equiv). The mixture was then milled at 30 Hz for 90 min followed by filtration over sintered funnel using water (20 × 2 mL) to wash out the inorganic salts. The residue was then washed with Et_2O (20 × 3 mL) in order to separate the low molecular weight organics (oil) or the solid residual lignin.

11.4.2 Reaction in a SIEBTECHNIK disk swing mill-TS

A 250 mL milling vessel was charged with organosolv beechwood lignin sample (**OS-BWL2**, 10.0 kg), OH-TEMPO (0.2 equiv), KBr (0.2 equiv) and Oxone (1.5 equiv). The mixture was then milled at 50 Hz for 10 min followed by a 10 min pause before continuing the cycle for two more times. A 100 mg of the mixture obtained after milling was weighed and filtered over sintered funnel using water (20 × 2 mL) to wash out the inorganic salts. The residue was then washed with distilled Et_2O (10 × 2 mL) in order to separate the low molecular weight organics (oil) or the solid lignin.

11.4.3. Reaction in a LAARMANN LMM6-100 mortar mill (MPM)

A 250 mL milling vessel was charged with lignin sample (10.0 g), OH-TEMPO (0.2 equiv), KBr (0.2 equiv) and Oxone (1.5 equiv). The mixture was then milled at 2 Hz for 10 min followed by a 10 min pause before continuing the cycle for two more times. The solid mixture was collected and filtered over sintered funnel using water (20 × 2 mL) to wash out the inorganic salts. The residue was then washed with distilled Et_2O (10 × 2mL) in order to separate the low molecular weight organics (oil) or the solid lignin. **NOTE:** The loadings for TEMPO, KBr and Oxone were calculated by dividing the mass of the lignin samples by the molar mass of **D1** to roughly estimate the amount of diol fragments.

12. GC-FID spectra for lignin

a) GC-FID spectrum for the EtOAc soluble fraction of beechwood lignin obtained after BCD with Cs_2CO_3

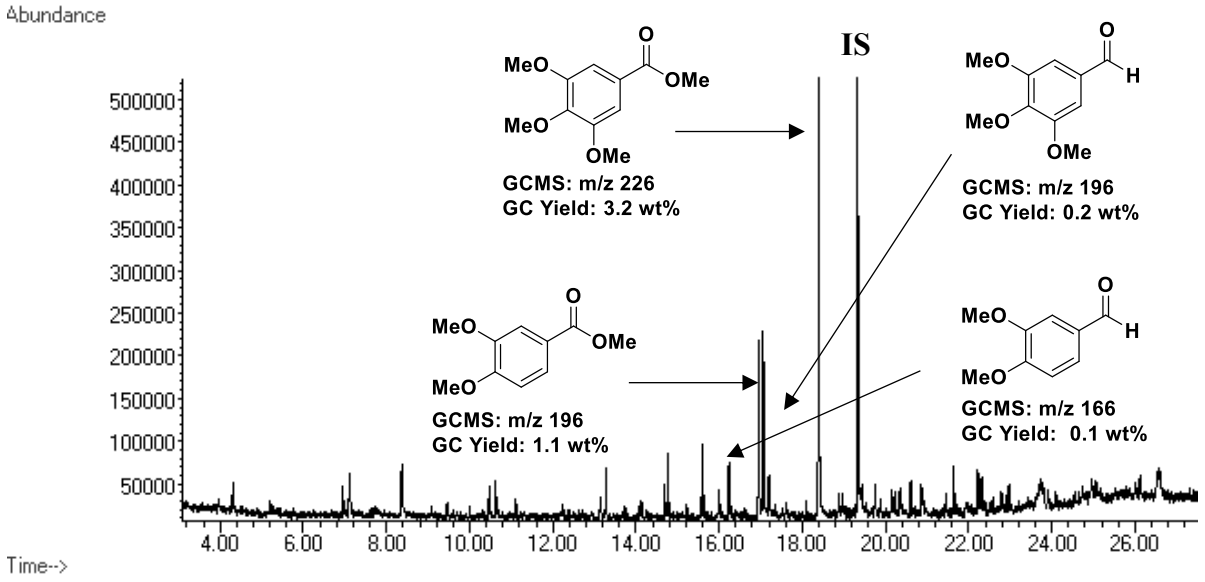

b) GC-FID spectrum for the EtOAc soluble fraction of oak lignin obtained after BCD with Cs_2CO_3

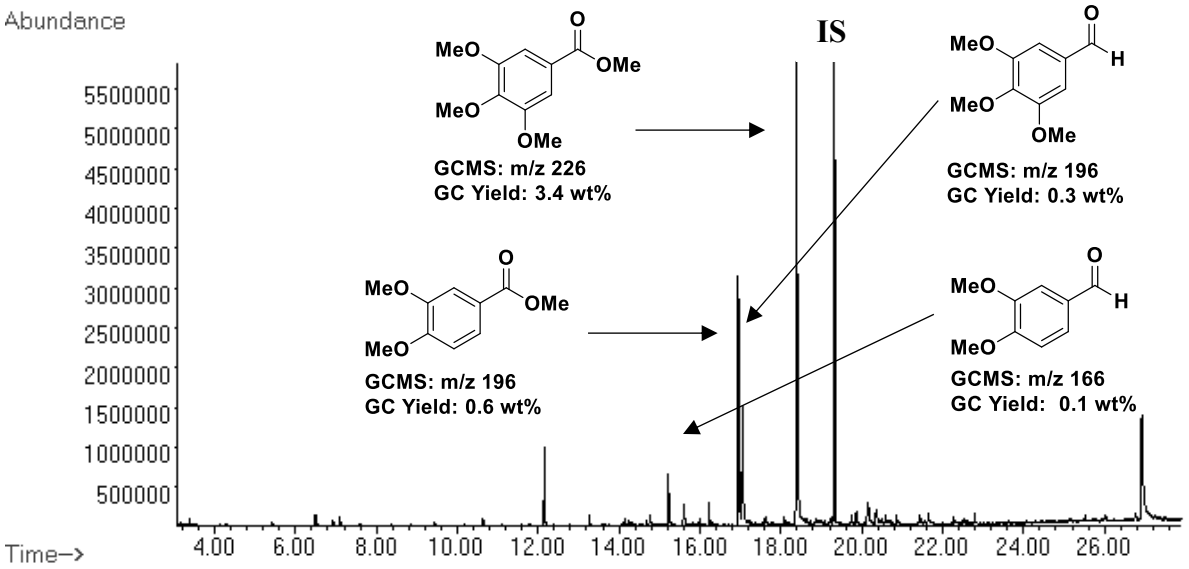

c) GC-FID spectrum for the EtOAc soluble fraction of cherry lignin obtained after BCD with Cs_2CO_3

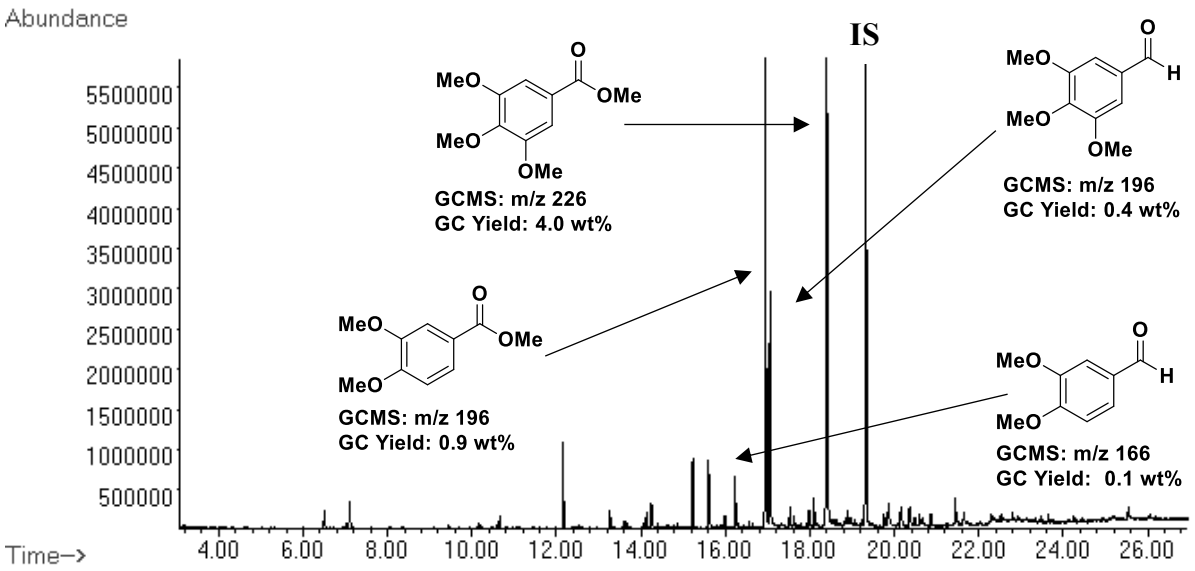

d) GC-FID spectrum for the EtOAc soluble fraction of kraft lignin obtained after BCD with Cs_2CO_3

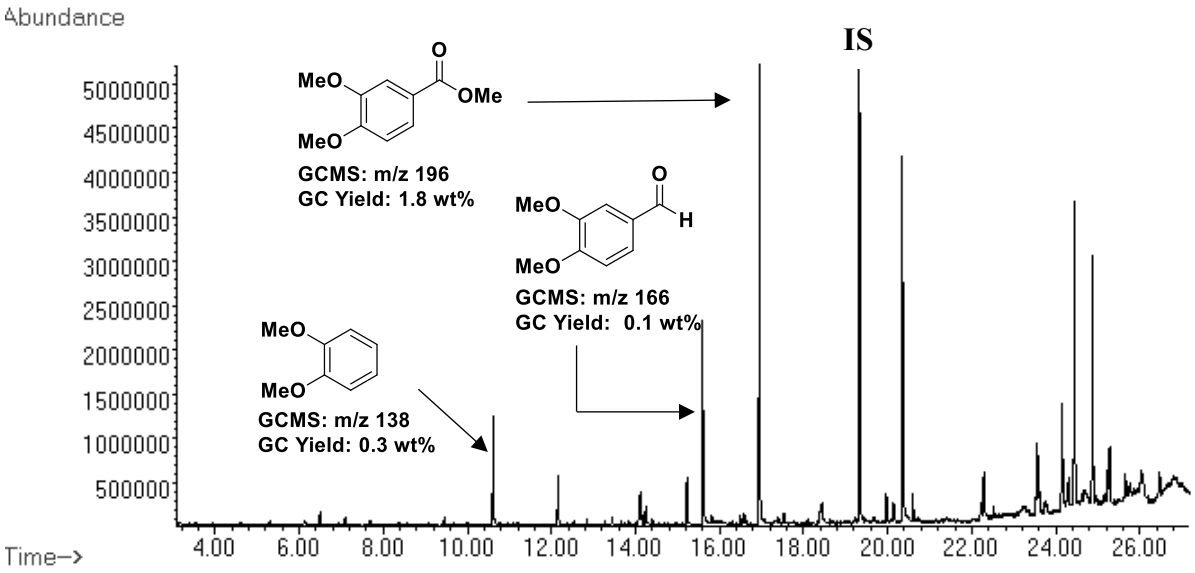

e) GC-FID spectrum for the EtOAc soluble fraction of kraft lignin obtained after BCD with KOH

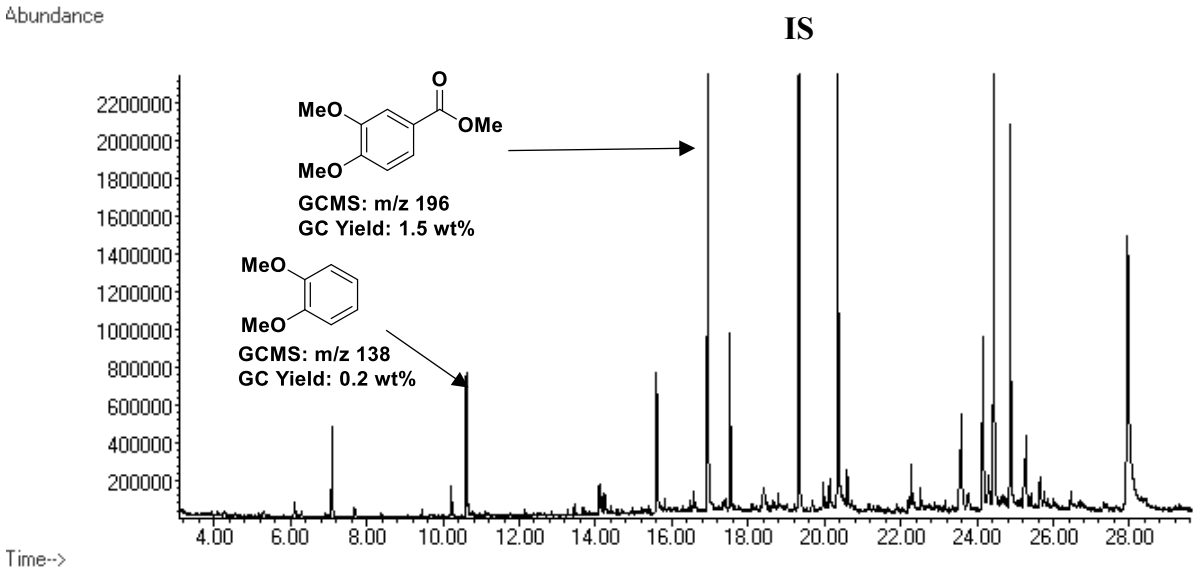

f) GC-FID spectrum of pre-milled beechwood chips after heating it in DMC in the absence of base

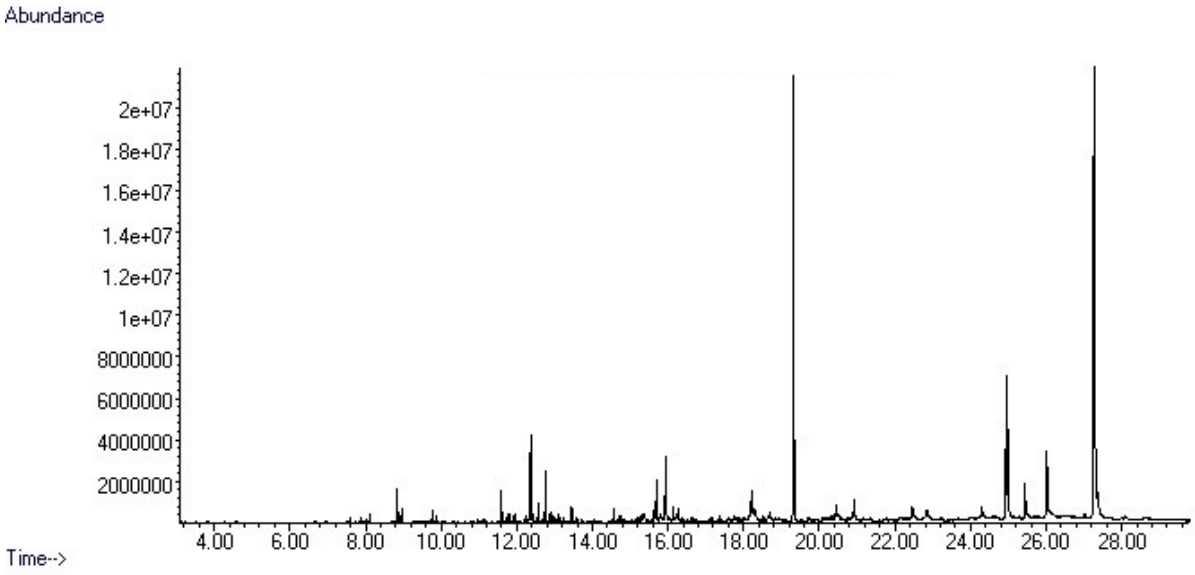

g) GC-FID spectrum for the EtOAc soluble fraction of pre-milled beechwood chips obtained after BCD with KOH

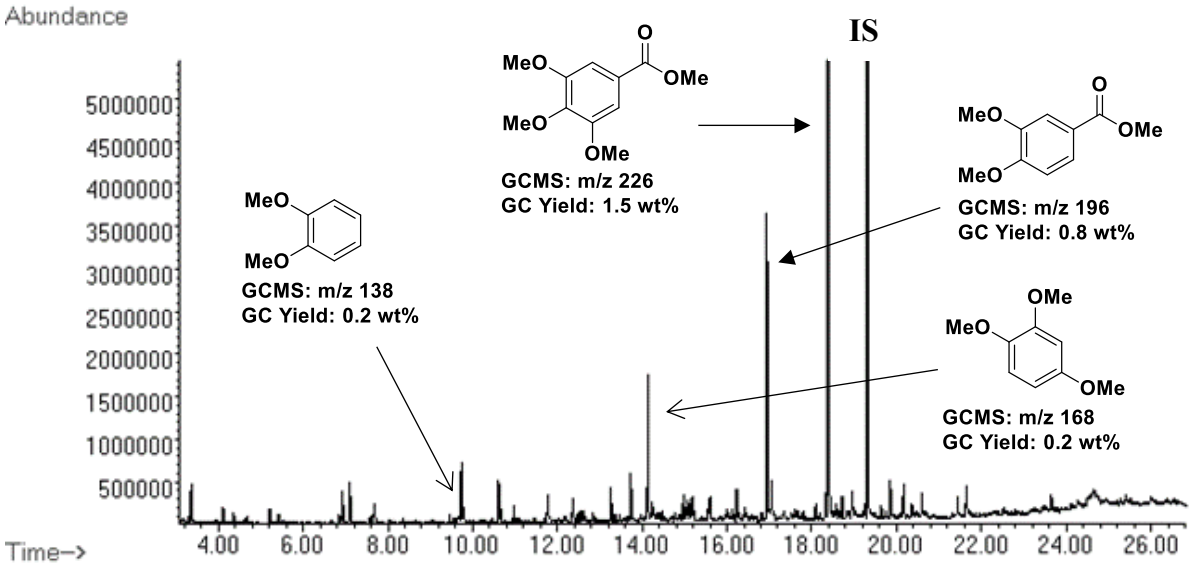

h) GC-FID spectrum for the DCM soluble fraction of the beechwood lignin after one-pot two-step γ-OH oxidation followed by DL-proline catalyzed retor-aldol reaction

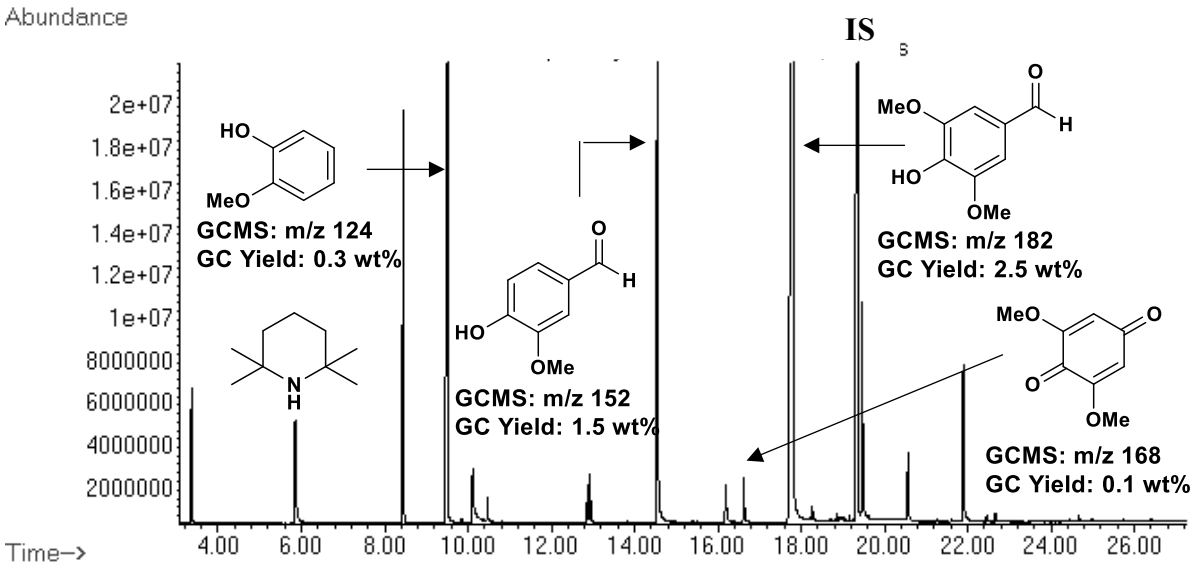

i) GC-FID spectrum for the Et_2O extract of beechwood lignin milled in the absence of catalysts for 180 min in WC jars at 30 Hz in a mixer mill

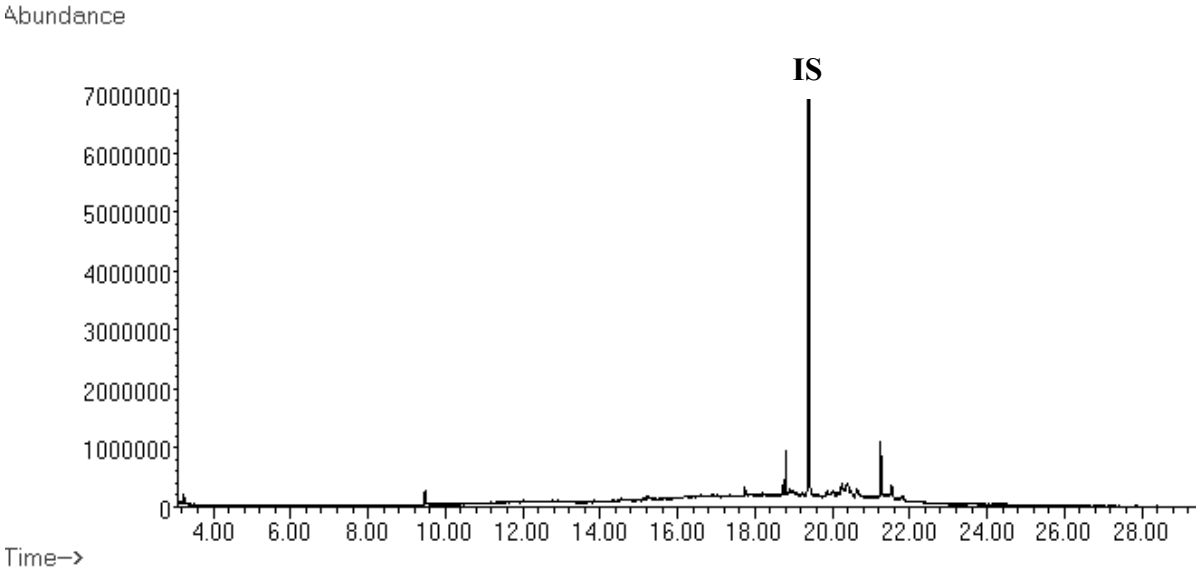

j) GC-FID spectrum for the Et_2O extract of beechwood lignin milled in the presence of OH-TEMPO/KBr/Oxone for 90 min in WC jars at 30 Hz in a mixer mill

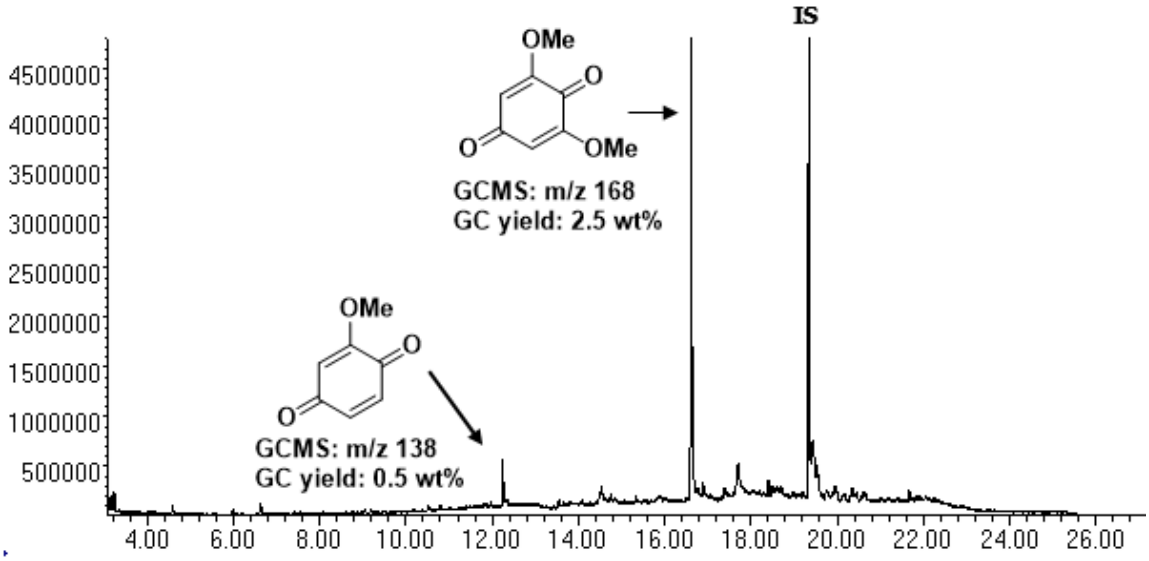

k) GC-FID spectrum for the Et_2O extract of beechwood lignin milled in the presence of OH-TEMPO/KBr/Oxone for 30 min in WC milling media at 50 Hz in a disc mill (DM)

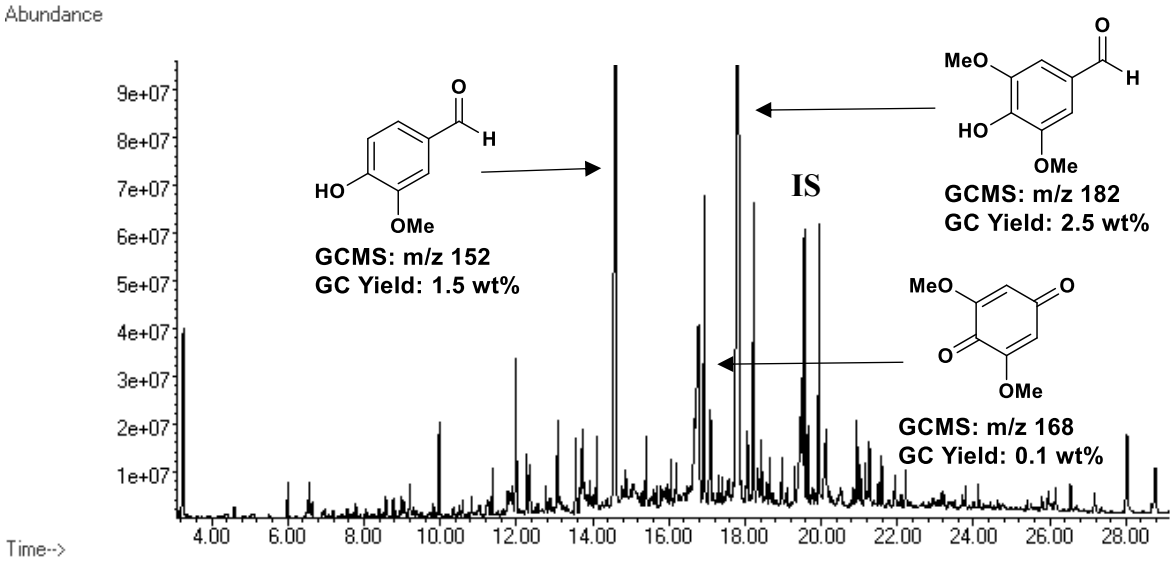

l) GC-FID spectrum for the Et_2O extract of beechwood lignin milled in the presence of OH-TEMPO/KBr/Oxone for 30 min in WC milling media at 20 Hz in a mortar mill (MPM)

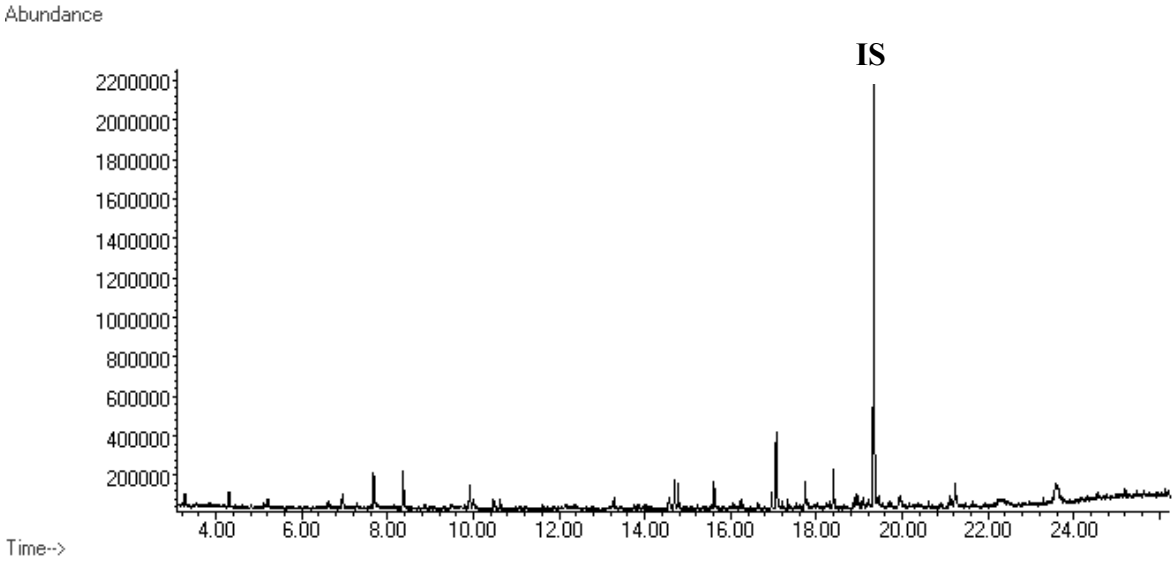

13. Reaction profiles for the cleavage od D1 with Cs_2CO_3 and LiO*t*-Bu in DMC

13.1. Reaction profile for the cleavage of D1 with Cs_2CO_3 in DMC

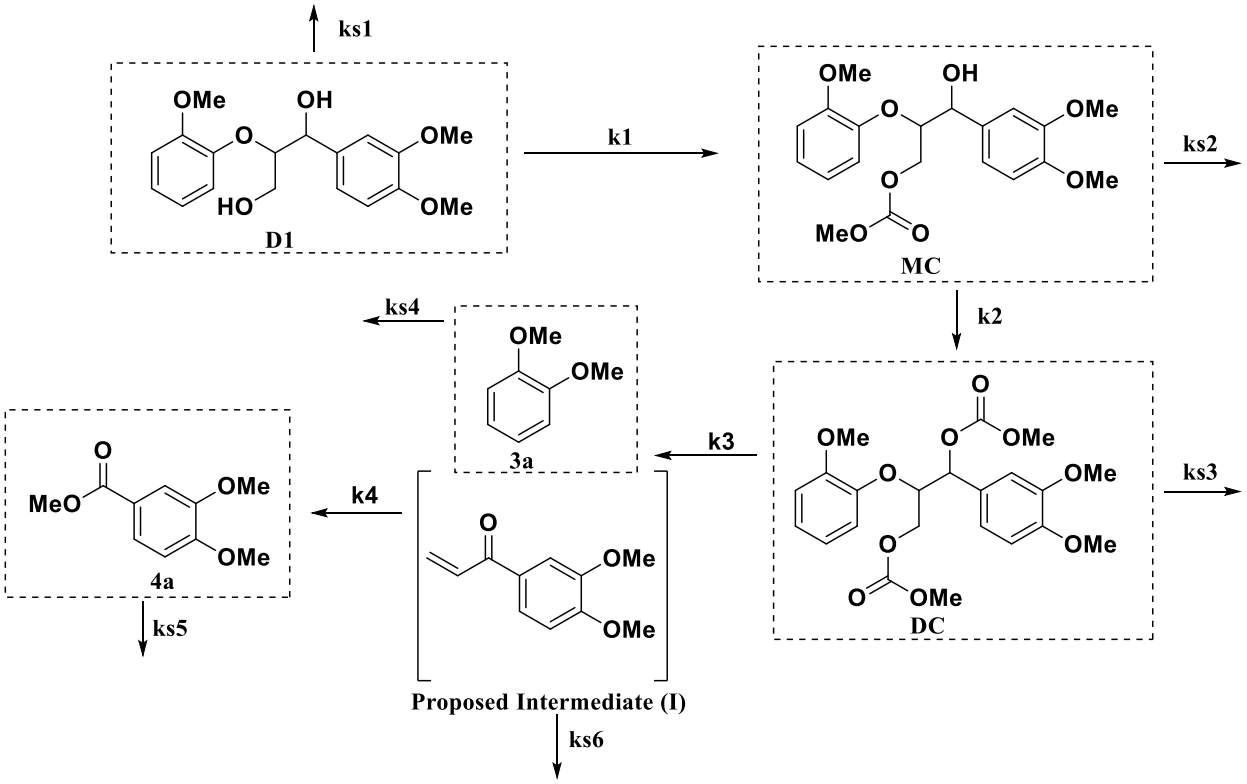

Scheme V.2. Reaction pathways considered in the modelling of reaction parameters for the stepwise catalytic deconstruction of *β*-O-4 model compound **D1** using Cs_2CO_3. End products are veratrole **(3a)** and 3,4-dimethoxy benzoate **(4a)**.

Reaction Pathyways:

Dilignol (**D1**)	-->	monocarboxylated (**MC**) :		k1 (0.69 min^{-1} ±0.07)
monocarboxylated (**MC**)	-->	dicarboxylated (**DC**)	:	k2 (0.15 min^{-1} ±0.01)
dicarboxylated (**DC**)	-->	veratole (**3a**) + **I**	:	k3 (0.0032 min^{-1} ±0.0003)
I	-->	benzoate (**4a**)	:	k4 (0.0014 min^{-1} ±0.002)

Sinks:

dilignol (**D1**)	-->	sink	:	ks1 (0.15 min^{-1} ±0.07)
monocarboxylated (**MC**)	-->	sink	:	ks2 ($1 \cdot 10^{-10}$ min^{-1} ±0.02)
dicarboxylated (**DC**)	-->	sink	:	ks3 (0.00051 min^{-1} ±0.0006)
veratrole (**3a**)	-->	sink	:	ks4 ($9.9 \cdot 10^{-5}$ min^{-1} ±0.0002)
benzoate (**4a**)	-->	sink	:	ks5 (0.00038 min^{-1} ±0.005)
I	-->	sink	:	ks6 (0.002 min^{-1} ±0.01)

13.2. Reaction profile for the cleavage of D1 with LiO*t*-Bu in DMC

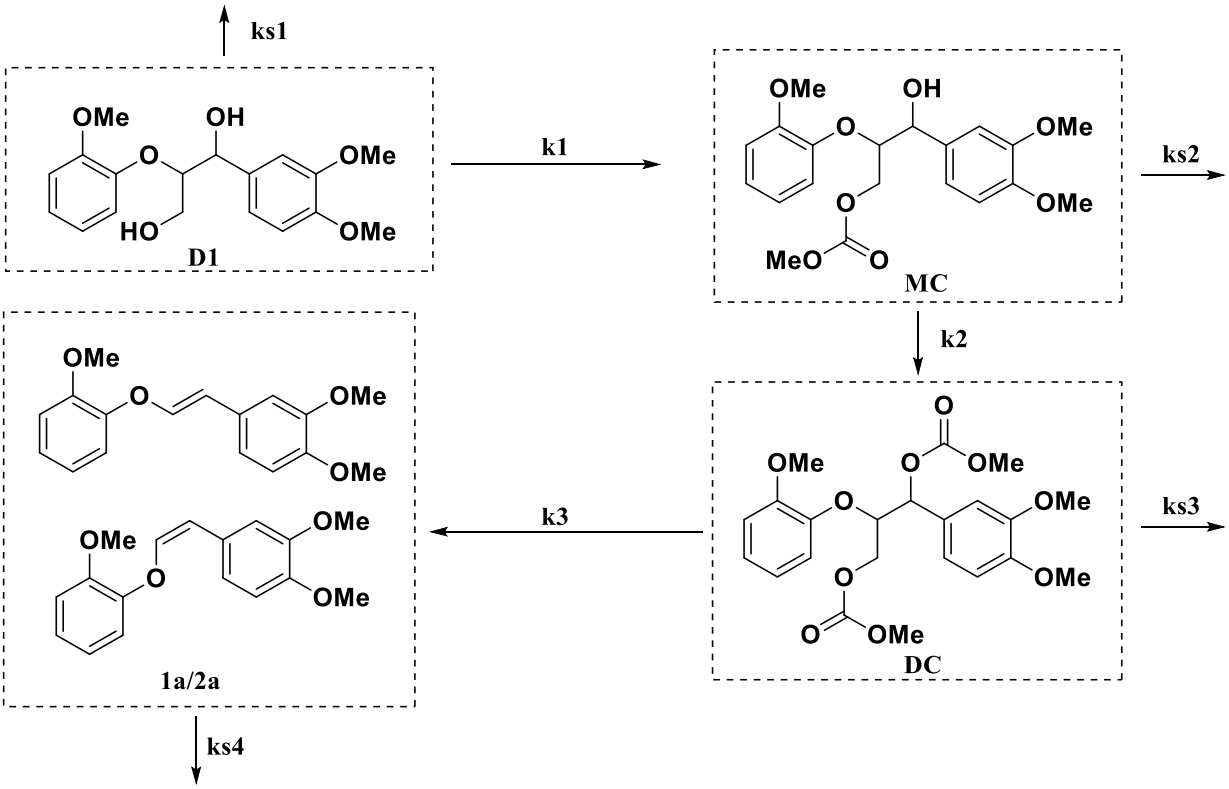

Scheme V.3. Reaction pathways considered in the modelling of reaction parameters for the stepwise catalytic deconstruction of *β*-O-4 model compound **D1** using LiO*t*-Bu. End products are *cis*/*trans* alkenes **(1a/2a)**

Reaction Pathways

dilignol (**D1**)	-->	monocarboxylated (**MC**)	:	k1 (0.2 min^{-1} ±0.04)
monocarboxylated (**MC**)	-->	dicarboxylated (**1h**)	:	k2 (0.025 min^{-1} ±0.003)
dicarboxylated (**DC**)	-->	alkenes (**4a/4b**)	:	k3 (0.005 min^{-1} ±0.0007)

Sinks

dilignol (**D1**)	-->	sink	:	ks1 ($1 \cdot 10^{-11}$ min^{-1} ±0.02)
monocarboxylated (**MC**)	-->	sink	:	ks2 ($1 \cdot 10^{-11}$ min^{-1} ±0.005)
dicarboxylated (**DC**)	-->	sink	:	ks3 (0.0011 min^{-1} ±0.001)
alkenes (**1a/2a**)	-->	sink	:	ks4 ($1 \cdot 10^{-11}$ min^{-1} ±0.0002)

14. Computational Details for the BCD of D1[70]

Table V.1: Calculation of the relative Gibbs energies.

Molecules	GSP+SSC [a.u.]	ΔG [kcal·mol^{-1}]
D1 + 2 DMC − 2 MeOH + CsOMe	−1741.067161	0.0
DC + CsOMe	−1741.06478	1.5
TS-1 + Cs(DMC) – DMC	−1741.00793	37.2
I1 + Cs(DMC) − DMC + MeOH	−1741.0084	36.9
TS-2 + Cs(DMC) − DMC + MeOH	−1741.00788	37.2
I2 + MeOH + G-Cs	−1741.09926	−20.1
TS-3 + MeOH − CsOMe + Cs(DMC) − DMC + G-Cs	−1741.04537	13.7
I3 + MeOH − CsOMe + Cs(DMC) − DMC + G-Cs	−1741.0679	−0.5
TS-4 + MeOH − CsOMe + Cs(DMC) − DMC + G-Cs	−1741.06479	1.5
I4 + MeOH − CsOMe + DMC + G-Cs + CsMMC	−1741.18683	−75.1
TS-5 − 2 CsOMe + Cs(DMC) + MeOH + G-Cs + CsMMC	−1741.186828	−38.3
I5 − 2 CsOMe+ Cs(DMC) + MeOH + G-Cs + CsMMC	−1741.128167	−61.6
TS-6 − 2 CsOMe + Cs(DMC) − DMC + MeOH + G-Cs + CsMMC	−1741.165268	−40.6
I6 − 2 CsOMe + Cs(DMC) − DMC + MeOH + G-Cs + CsMMC	−1741.131792	−48.3
TS-7 − 2 CsOMe + Cs(DMC) − DMC + MeOH + G-Cs + CsMMC	−1741.144158	−41.3
I7 − 2 CsOMe + Cs(DMC) − DMC + MeOH + G-Cs + CsMMC	−1741.133031	−51.0
TS-8 − 2 CsOMe + Cs(DMC) − DMC + MeOH + G-Cs + CsMMC	−1741.148394	−48.0
4a − 2 CsOMe + I8 + MeOH + G-Cs + CsMMC	−1741.167347	−92.8
TS-9a + DMC + Cs(DMC)	−1740.993539	46.2
TS-9b + DMC + Cs(DMC)	−1740.985107	51.5
3a + DMC + CsMMC + FA	−1741.112372	−28.4
4a + DMC + CsMMC + FA	−1741.113758	−29.2

D1

E [a.u.] = −1150.149700
G [a.u.] = −1149.824298
E_{SP} [a.u.] = −1150.392543

Charge = 0; Multiplicity = 1

C	4.6847	0.385571	−1.891936
C	3.336093	0.109354	−1.655256
C	2.805934	0.24542	−0.379097
C	3.625599	0.653207	0.69184
C	4.969832	0.939392	0.447554
C	5.492907	0.803367	−0.84195
H	5.095677	0.275848	−2.896546
H	2.6604 −	0.220018	−2.446381
H	5.624584	1.258987	1.257794
H	6.547456	1.02612	−1.013429
O	1.480631	0.021641	−0.130202
C	1.043642	−1.331837	−0.173837
H	1.864546	−1.979255	−0.525015
C	0.651278	−1.713898	1.247309
H	1.552852	−1.647368	1.881707
H	−0.076165	−0.967584	1.614506
C	−0.105535	−1.481041	−1.176538
H	−0.414625	−2.539698	−1.122402
O	0.107771	−3.021397	1.224661
H	−0.213846	−3.223385	2.108601
O	3.020765	0.724383	1.9052
C	3.797506	1.147162	3.000253
H	3.123584	1.156265	3.86533
H	4.634	0.454782	3.201553
H	4.201439	2.163058	2.847316
O	0.442647	−1.185007	−2.449768
H	−0.282024	−1.196368	−3.084497
C	−1.296678	−0.610097	−0.838003
C	−2.341835	−1.118378	−0.057275
C	−1.362683	0.713921	−1.259607
C	−3.419991	−0.32615	0.308342
H	−2.309044	−2.146513	0.309484
C	−2.447524	1.521699	−0.911385
H	−0.549646	1.12437	−1.858421
C	−3.480141	1.016171	−0.121198
H	−2.467369	2.556332	−1.25273
O	−4.388286	−0.846745	1.123437
O	−4.567034	1.72206	0.286709
C	−4.633816	3.085303	−0.06211
H	−5.554814	3.471147	0.390809
H	−3.771929	3.647882	0.335783
H	−4.682989	3.226902	−1.155874
C	−5.630824	−1.086389	0.483617
H	−6.301485	−1.499796	1.247975
H	−6.065492	−0.157085	0.083421
H	−5.517848	−1.820762	−0.333601

DC

E [a.u.] = −1605.815694
G [a.u.] = −1605.415125
E_{SP} [a.u.] = −1606.149998

Charge = 0; Multiplicity = 1

C	4.4789701344	2.5378402576	1.2940877758
C	3.2193968961	1.9398830653	1.2197928546
C	3.1023447409	0.5643870512	1.0869255394
C	4.2566514654	−0.2397482406	1.0070691798
C	5.513903108	0.3616044115	1.0718461839
C	5.6188308591	1.7476143677	1.2191138489
H	4.5607869263	3.6203804055	1.3987303234
H	2.304823487	2.5316774413	1.2437602565
H	6.4201318594	−0.2403923487	1.0151667729
H	6.609634304	2.2018280954	1.2728948951
O	1.8618811848	−0.0205929704	1.0958792285
C	1.4016483374	−0.5740717686	−0.1335090121
H	2.2317437632	−0.6020336642	−0.8572050461
C	0.9264180745	−1.983194028	0.1996601134
H	1.7929279147	−2.6234570261	0.405740454
H	0.2761304145	−1.9572736443	1.0833772429
C	0.2849405398	0.2886887395	−0.7402010083
H	0.1110966573	−0.0599324691	−1.7666254934
O	0.2029363335	−2.4971492284	−0.9209566699
O	4.0368663458	−1.5734505209	0.8632800612
C	5.1585044561	−2.4204635419	0.7574335261
H	4.7637016806	−3.4372449981	0.645403208
H	5.7734419305	−2.1719800755	−0.1247251493
H	5.7881153199	−2.3759086852	1.6623549878
O	0.8260332121	1.6207995679	−0.7910977755
C	−1.0242196464	0.2585475548	0.0101617245
C	−2.16288397	−0.252604151	−0.6203078655
C	−1.128047038	0.6931519332	1.3294095067
C	−3.3650978194	−0.3759387539	0.0572545626
H	−2.120769174	−0.5945074598	−1.6558079934
C	−2.339583343	0.5994469865	2.0156351517
H	−0.2494492647	1.0886608687	1.8381239953
C	−3.4651788275	0.0550448307	1.3945791867
H	−2.3876410225	0.9373618713	3.0501133047
O	−4.4288432286	−0.9701679862	−0.5691628695
O	−4.6785473438	−0.1014756139	1.9793021337
C	−4.8096200294	0.2671249775	3.3337750561
H	−5.8462627812	0.0419857527	3.6105870379
H	−4.1284886351	−0.3136772356	3.9786661955
H	−4.6202339379	1.3441676248	3.4834835358
C	−5.4700294507	−0.0811516731	−0.9430182756
H	−6.2365957649	−0.6900000155	−1.4389313938
H	−5.9096062461	0.4117742294	−0.0620922385
H	−5.0988833838	0.682826901	−1.6477840679
C	0.2909559576	2.4245887775	−1.7121926629
O	−0.515106046	2.1170965665	−2.5536106141
O	0.8183325636	3.6384676056	−1.5416734968
C	−0.9521356034	−3.1177187367	−0.637990879
O	−1.347001926	−3.4272237407	0.4561188031
O	−1.5817114561	−3.3321984001	−1.7915781434

C	−2.8934555678	−3.8872748917	−1.6558473907
H	−3.2107230576	−4.1350484846	−2.6749048532
H	−2.8712519857	−4.7897435355	−1.0301557122
H	−3.5735598658	−3.1436732786	−1.215294272
C	0.3591145902	4.6172537021	−2.4705504851
H	0.8707550018	5.5457652482	−2.1950487113
H	0.6170967614	4.3307922587	−3.5000121686
H	−0.7303674043	4.7431470749	−2.3977343985

TS-1

E [a.u.] = −1720.915311

G [a.u.] = −1720.483169

E_{SP} [a.u.] = −1721.32861

Charge = −1; Multiplicity = 1

C	4.9976149269	−0.1994748472	1.1316523442
C	3.6151386256	−0.1841798156	0.9253254152
C	3.0821471	−0.4831522635	−0.3268340998
C	3.9572028817	−0.7925496635	−1.394174847
C	5.3343506615	−0.8223581581	−1.1779243051
C	5.8534574025	−0.5222072515	0.0871284541
H	5.3969120865	0.033462604	2.1207002457
H	2.9158869312	0.0434633201	1.7320584546
H	6.0181567243	−1.0655326907	−1.9915995959
H	6.9343796883	−0.5450566287	0.2409568939
O	1.7558506097	−0.5290966314	−0.5691631228
C	0.9638043823	0.6804051586	−0.2961480384
H	1.6562406939	1.4524969513	0.0764361105
C	0.4682892633	1.102413974	−1.6793049457
H	1.3002354592	1.0011637233	−2.3890242604
H	−0.373054645	0.4818555836	−2.013974791
C	−0.1162540149	0.4670271476	0.7289194718
H	−1.0036302163	1.6033623867	0.7709276813
O	0.0927626604	2.4811786314	−1.6669253896
O	3.3545178603	−1.0368019826	−2.5906614195
C	4.1733857169	−1.3759259966	−3.6757398945
H	3.5008732676	−1.5369137383	−4.527758142
H	4.8860216907	−0.569156534	−3.9286319216
H	4.7434316685	−2.3045037396	−3.4883138006
O	0.663757132	0.2605103246	1.97225629
C	−0.9495033205	−0.7567207288	0.4623888266
C	−2.1683917463	−0.585872948	−0.2143345082
C	−0.5804775192	−2.0450941386	0.8401314613
C	−2.9787974218	−1.6667742085	−0.5385429666
H	−2.4651910719	0.4283170103	−0.4772561463
C	−1.4009384003	−3.1393623818	0.5449793562
H	0.3616350662	−2.2038403368	1.3657989254
C	−2.5944467015	−2.9670924447	−0.1496569655
H	−1.0846927241	−4.135920287	0.8559411082
O	−4.1613270646	−1.5674169935	−1.2086398127
O	−3.4597604987	−3.9738385845	−0.4932046913
C	−3.0888401515	−5.2764655358	−0.1463529718
H	−3.8894519085	−5.9353824122	−0.5092810147
H	−2.1353750506	−5.5788567519	−0.619326642
H	−2.988427671	−5.4069893165	0.9478811635
C	−4.5754461925	−0.2647037574	−1.5606335548
H	−5.52076681	−0.3876438944	−2.1061862342
H	−4.7496567491	0.3599717987	−0.6666275587
H	−3.8382087381	0.2516852343	−2.1967252776
C	0.0416842081	0.4137194754	3.1195824792
O	−1.1252862152	0.6158668681	3.3376396847
O	0.9784506948	0.2866909058	4.1006379211
C	−1.1973742646	2.7577826332	−1.8542955602
O	−2.051604225	1.9917613337	−2.2371063326
O	−1.3652631938	4.0723078841	−1.6863564243
C	−2.7261156193	4.4364140055	−1.4828119394
H	−2.7221263866	5.5220873666	−1.3241810249
H	−3.3397388437	4.1806845048	−2.3603289878
H	−3.091513076	3.9062267936	−0.5902588923
C	0.4551821643	0.4226179581	5.4076679533
H	1.3069564163	0.2971300972	6.0888519981
H	−0.0029433022	1.4130149477	5.5550773876
H	−0.3096697687	−0.3418614709	5.6153199407
O	−1.6987770861	2.5549417028	0.7270618688
C	−1.0147709763	3.5122866417	1.4444154018
H	−0.9702821673	4.4896060087	0.9109963539
H	−1.4562826719	3.7105007282	2.4495074923
H	0.0498604301	3.2252814288	1.6294463955

I1

E [a.u.] = −1605.202416

G [a.u.] = −1604.817187

E_{SP} [a.u.] = −1605.587331

Charge = −1; Multiplicity = 1

C	−4.021826342	1.4472463029	0.6490549007
C	−3.1437436525	0.3918968006	0.3792416738
C	−2.6853789273	0.1637423423	−0.9187955713
C	−3.1149332209	1.0335775604	−1.9530941782
C	−3.9979926575	2.0718221538	−1.677514207
C	−4.4538351295	2.2820117828	−0.3689769818
H	−4.3552542744	1.6100354929	1.6760676939
H	−2.7897671893	−0.2371254996	1.1943828707
H	−4.3303855002	2.740893946	−2.4713839169
H	−5.1373424762	3.1084111998	−0.1640442509
O	−1.8686948001	−0.8317741902	−1.284219115
C	−0.9516219945	−1.4637129494	−0.2499796638
H	−1.5741708519	−2.1487153164	0.35031645
C	−0.0887506202	−2.3301602391	−1.1748639258
H	−0.7073479457	−2.8363230937	−1.9279575494
H	0.7015397992	−1.7431772659	−1.6588295115
C	−0.2316560195	−0.5818476888	0.6550387923
O	0.4964819329	−3.366304323	−0.3786863246
O	−2.603936159	0.7622029642	−3.1925712914
C	−2.9679786151	1.6195953494	−4.238647079
H	−2.4494729496	1.2517358836	−5.1341257877
H	−4.0582214317	1.6047061244	−4.4262169327
H	−2.6552523672	2.6626736266	−4.0483267528
O	−0.6981191674	−0.6665976561	2.0217774783
C	0.4176232322	0.6314495145	0.3120273836
C	0.5822943993	1.0154171786	−1.0536731854

C	0.9179300437	1.5447955957	1.2702208102
C	1.2220097197	2.1870641204	−1.4220158697
H	0.1351912871	0.3939306561	−1.8253834535
C	1.5561393855	2.7264730582	0.8895352126
H	0.7980094132	1.3337130436	2.3331818978
C	1.7325561272	3.0681511242	−0.4469143213
H	1.9222975505	3.3900430503	1.6755414434
O	1.3823759245	2.5887480153	−2.7224220526
O	2.3555355548	4.2111137395	−0.9156326783
C	2.829454009	5.0976351444	0.04815424
H	3.2804614201	5.9418033808	−0.4934968788
H	2.0217071873	5.4857594018	0.7003466619
H	3.6009725156	4.6421912952	0.7007835447
C	0.9066490731	1.7204389107	−3.7160054153
H	1.1024289081	2.2176339928	−4.6765839903
H	1.4326199009	0.7476088928	−3.6991231656
H	−0.1751333123	1.5227984297	−3.6166738051
C	0.0465369726	−1.339621164	2.8771993656
O	1.1084590399	−1.8888388363	2.7143161615
O	−0.5999727755	−1.3196821989	4.0704641298
C	1.7639272407	−3.184208482	−0.0067518129
O	2.5578328044	−2.4054388731	−0.4676454262
O	2.038566425	−4.1011240131	0.9334421073
C	3.2912587316	−3.9025690022	1.571292422
H	3.3982593774	−4.7328193159	2.2809530293
H	4.1164797695	−3.9140311513	0.8433001927
H	3.2854692954	−2.9435133512	2.1071670411
C	0.0838505637	−1.9968336618	5.1067266215
H	−0.5538569203	−1.90700247	5.9957438883
H	0.2396079484	−3.0584269018	4.859643466
H	1.0673857471	−1.5423474306	5.3031756158

I1b

E [a.u.] = −1605.175406

G [a.u.] = −1604.792309

E_{SP} [a.u.] = −1605.560929

Charge = −1; Multiplicity = 1

C	4.8535315671	1.5641093724	0.0570525401
C	3.5270952045	1.1472169661	−0.0504682316
C	2.961331351	0.2938535183	0.9037579616
C	3.757175883	−0.1345637859	1.9890394232
C	5.078988018	0.2966167515	2.0882775211
C	5.6357502611	1.1444705163	1.130000578
H	5.2674659165	2.2355763462	−0.6988124684
H	2.8918502948	1.5091812446	−0.8593638081
H	5.659964065	−0.0564058702	2.94292113
H	6.6743323228	1.4696496602	1.2225913299
O	1.6692309718	−0.0889291291	0.8742278035
C	1.1316465334	−0.6412907029	−0.3692822109
H	1.8752040406	−0.5071236306	−1.1725885809
C	0.8893494427	−2.1192506368	−0.2094984802
H	−0.1573204523	−2.3071031736	0.0887735362
C	−0.0695273473	0.24408678	−0.7328728083
H	−0.5054912609	−0.1397937111	−1.6632543721
O	1.0113628166	−2.6948208141	−1.5996682668
O	3.249713708	−0.9202377772	2.980672302
C	2.94387788	−2.2608951198	2.5828960286
H	2.3946508249	−2.7063068568	3.4246769277
H	2.3233202919	−2.3074583023	1.6640305971
H	3.8835870289	−2.8262863427	2.4298845763
O	0.4462021566	1.5885719105	−1.0024553947
C	−1.1407353887	0.325812923	0.3262139025
C	−2.2461012158	−0.5301863968	0.2638087205
C	−1.0431760943	1.2220264048	1.385908312
C	−3.2321235346	−0.4847091821	1.2384355096
H	−2.3251140447	−1.2587007409	−0.5462465249
C	−2.0362362028	1.2840147695	2.3656474816
H	−0.1761365382	1.8784563195	1.4530305114
C	−3.1392611387	0.4332192522	2.2997767163
H	−1.9269912757	1.9953895568	3.1841456929
O	−4.2958853872	−1.355448625	1.1793415894
O	−4.1701533584	0.4157962892	3.198626946
C	−4.0802778557	1.2838675076	4.2967604634
H	−4.9759631914	1.1052308467	4.9060163891
H	−3.1830026846	1.0817932281	4.9087765228
H	−4.061993607	2.3446703508	3.9859425463
C	−5.4705431265	−0.7722984216	0.6583024218
H	−6.233081989	−1.5634377619	0.6300277123
H	−5.8312294703	0.0531569488	1.296538717
H	−5.3074041464	−0.3918234335	−0.366204553
C	−0.2228587363	2.3193684951	−1.8749864271
O	−1.2011244164	2.010770169	−2.5110918539
O	0.3925004603	3.5164315236	−1.9621606999
C	−0.0395490568	−2.8280492357	−2.3489760329
O	−1.1932057479	−2.4833822283	−2.1525093785
O	0.3235165518	−3.476535015	−3.4934655154
C	−0.738749562	−3.6899262005	−4.3995261582
H	−0.2946277045	−4.1862826575	−5.2731048897
H	−1.5203249187	−4.3320040142	−3.9628989431
H	−1.2102841487	−2.7422581071	−4.7040250481
C	−0.203927868	4.4098166015	−2.8872276088
H	0.3801223924	5.3361090576	−2.8247899213
H	−0.1649542405	4.0080012501	−3.911262803
H	−1.2557542733	4.606036313	−2.6312134303

TS-2

E [a.u.] = −1605.201871

G [a.u.] = −1604.816219

E_{SP} [a.u.] = −1605.587231

Charge = −1; Multiplicity = 1

C	−2.0999711254	−2.762471807	2.3273100914
C	−1.1869159807	−2.5974981858	1.280592962
C	−1.6178842349	−2.2631945127	−0.0090572098
C	−3.0143941419	−2.0830184913	−0.2130513078
C	−3.9175177768	−2.2659459018	0.8272530763
C	−3.4595221476	−2.6039539861	2.1090006597
H	−1.7274337608	−3.0143348439	3.3229247081
H	−0.1209365751	−2.7141734243	1.4706280123
H	−4.9869255911	−2.1303172364	0.6624106251

H	−4.1779887149	−2.7319006921	2.9213562918
O	−0.8204035556	−2.1065904234	−1.056369777
C	0.697526675	−1.4926441051	−0.8150315063
H	1.2994250944	−2.393609719	−0.6349395501
C	0.9241576526	−1.0324423334	−2.250476317
H	0.5300183331	−1.7651020472	−2.9641252944
H	0.4974802843	−0.0403812001	−2.4400498212
C	0.883333333	−0.5551118247	0.2336415803
O	2.3439869577	−0.9976150289	−2.4705157379
O	−3.3706844367	−1.7288661824	−1.4890398895
C	−4.7378327286	−1.6099980975	−1.7624641448
H	−4.8202299265	−1.3601120727	−2.8290533245
H	−5.2808770322	−2.5552641005	−1.5732360724
H	−5.2155238015	−0.8057243915	−1.1717663646
O	1.583758166	−1.073682941	1.3839631224
C	0.1663885894	0.660328913	0.4595797578
C	−0.910615346	1.0367686844	−0.3908743137
C	0.4436184006	1.5264260328	1.5352372942
C	−1.6160772387	2.2154145571	−0.207795967
H	−1.2246205628	0.3422858993	−1.1671627434
C	−0.2785469913	2.7066428166	1.7243988666
H	1.2338496728	1.2783550161	2.2438806037
C	−1.3017042231	3.0801324484	0.8608040154
H	−0.0183249706	3.34439684	2.5711192755
O	−2.6604494008	2.6098635812	−0.9983387789
O	−2.0630433613	4.226162362	0.9638254458
C	−1.7677178356	5.0756658681	2.0293999693
H	−2.4680836937	5.9202357924	1.9612931001
H	−1.9017225127	4.5817505594	3.0119073104
H	−0.7323899652	5.466921023	1.9822020298
C	−2.965965893	1.7911708415	−2.0975696488
H	−3.8292898305	2.2560315081	−2.5938296651
H	−2.1244421169	1.7351443578	−2.8127074648
H	−3.2233900945	0.7615677008	−1.7957646152
C	2.8758228012	−0.8154271822	1.4631134831
O	3.5817447733	−0.1809768621	0.7174388815
O	3.3336642198	−1.4046096201	2.5948011458
C	2.9364831971	0.1833042645	−2.29663634
O	2.4147899238	1.2681177028	−2.272998524
O	4.2589120444	−0.0370633745	−2.2310531747
C	5.0073990709	1.1119253297	−1.8643615895
H	4.7188209878	1.4371805775	−0.8553485872
H	6.0588523499	0.7973453583	−1.8757243665
H	4.8482751755	1.9353822468	−2.5769465048
C	4.7118589711	−1.1946250397	2.8362759806
H	4.9403719383	−1.7390806854	3.761519548
H	5.3283387466	−1.5781771843	2.0089294261
H	4.9365922084	−0.1244447848	2.9655963379

I3

E [a.u.] = −1183.903514
G [a.u.] = −1183.632778
E_{SP} [a.u.] = −1184.158208

Charge = 0; Multiplicity = 1

C	1.9246728001	−0.7229104665	−1.6489165134
H	2.4217708641	−1.6938561192	−1.7159783085
C	2.0232833659	0.1494882048	−2.8595044194
H	1.5233749475	−0.3326800302	−3.7111048197
H	1.592225724	1.1452581168	−2.7044868
C	1.2257825588	−0.47501621	−0.5385289196
O	3.3909857822	0.2593852303	−3.2956398117
O	1.0962065502	−1.5476848175	0.3545490605
C	0.4404383774	0.7210332303	−0.1617469771
C	−0.8505898998	0.5330847597	0.370392938
C	0.9486734207	2.0063475082	−0.2868680205
C	−1.6277469438	1.6174314723	0.7474343591
H	−1.2295478082	−0.4822145291	0.4805175507
C	0.1672800216	3.105122891	0.08736816
H	1.9598794903	2.1626486646	−0.6624011522
C	−1.1126024906	2.9303080422	0.6005912879
H	0.5870351497	4.1049445681	−0.0158529389
O	−2.8789133812	1.5398276268	1.2611475164
O	−1.941625655	3.9232338342	0.9949901134
C	−1.4856402396	5.2492749481	0.8619705616
H	−2.2986487844	5.8863759106	1.2294554113
H	−0.5804107354	5.4339910852	1.4660271253
H	−1.2734264531	5.5029432966	−0.1912637057
C	−3.4336046752	0.258002044	1.4361955506
H	−4.4338346405	0.4150419688	1.856701175
H	−3.525676465	−0.2829975191	0.477976849
H	−2.8381428612	−0.3544559968	2.1358964349
C	1.6366096122	−1.3617478788	1.5761493718
O	2.3708735424	−0.4698771752	1.9002535967
O	1.2190977885	−2.3657500027	2.3467882647
C	4.1112415531	1.2349847836	−2.7448486921
O	3.7144053582	2.0916551917	−1.9920163145
O	5.362564075	1.1166392529	−3.1858579733
C	6.2621797993	2.1045025972	−2.6872120727
H	6.320687122	2.0603887651	−1.5904312359
H	7.2347734292	1.866174534	−3.1309311159
H	5.9422127643	3.1123983657	−2.9872531732
C	1.741187181	−2.3401891673	3.6742885492
H	1.3315281158	−3.2277366086	4.1683119753
H	2.8394227325	−2.3812617571	3.6612161595
H	1.4241739071	−1.4278036144	4.1990059534

TS-3

E [a.u.] = −1299.003439
G [a.u.] = −1298.697738
E_{SP} [a.u.] = −1299.343161

Charge = −1; Multiplicity = 1

C	1.808619114	1.0318982114	1.4194194719
H	2.1707676331	2.0370944116	1.6491772841
C	2.708265082	−0.0923594493	1.8045787737
H	2.8935345933	−0.0900553676	2.8891796643
H	2.3261891504	−1.0741508723	1.5037906718
C	0.5597158349	0.9427821472	0.9324018806
O	4.0400751707	0.1067529548	1.2522731195
O	−0.1639202734	2.1151740457	0.9269751289

C	−0.1997891362	−0.2768310665	0.5724770791
C	−1.5450292506	−0.3220931055	0.9603315851
C	0.343072973	−1.3339428915	−0.1503359167
C	−2.3530153139	−1.3957578836	0.6202525819
H	−1.9711889173	0.5502791218	1.4428379626
C	−0.4508921574	−2.4434929285	−0.4565608793
H	1.3716841298	−1.2964086354	−0.507600077
C	−1.7915497998	−2.4855392481	−0.0791006554
H	−0.0114094785	−3.2606750647	−1.0281394096
O	−3.6789165652	−1.4616695037	0.8911982986
O	−2.647143514	−3.5128643514	−0.3582855112
C	−2.1545735626	−4.560327661	−1.1452624008
H	−2.9876402769	−5.2624803643	−1.2835644028
H	−1.8119037631	−4.2085501623	−2.1357244165
H	−1.3174292046	−5.0928877739	−0.6554537132
C	−4.293823392	−0.2424341178	1.3015200754
H	−5.3722183614	−0.3922135722	1.1532702878
H	−4.1088539315	−0.0635784438	2.3784490888
H	−3.9183508023	0.6247144978	0.7141240292
C	−0.5540483716	2.6055849619	−0.3066679607
O	−0.1183516008	2.1897287402	−1.3516575152
O	−1.0367460017	3.835464279	−0.0555819738
C	4.3228012405	−0.5160734461	0.119887185
O	3.6661116555	−1.3538252802	−0.4503103758
O	5.5193979642	−0.0763170997	−0.302248572
C	5.9552002345	−0.6605243177	−1.52239395
H	5.232515377	−0.4716607333	−2.3291772524
H	6.9153698389	−0.1833606468	−1.7512983141
H	6.0870327369	−1.7476675999	−1.4153703783
C	−1.7998463512	4.3709669108	−1.1256666502
H	−1.9776747581	5.4264406226	−0.8753761438
H	−1.2483606601	4.2942033303	−2.076015137
H	−2.7302363794	3.7847913512	−1.175625256
O	−2.7033460992	1.8065962536	−0.3999476305
C	−2.8667410012	1.1247733738	−1.5657510514
H	−3.5253952614	0.2138035266	−1.4739182603
H	−3.3400986787	1.7276087541	−2.3982123183
H	−1.9073918649	0.7449600927	−2.004517046

I3

E [a.u.] = −1299.022607
G [a.u.] = −1298.715763
E_{SP} [a.u.] = −1299.366834

Charge = −1; Multiplicity = 1

C	−1.6635489544	1.062150764	−1.379616871
H	−2.1769941138	1.9836223004	−1.6664018381
C	−2.271039545	−0.2107880893	−1.8472666168
H	−2.3493437707	−0.2536725134	−2.944973978
H	−1.7402825623	−1.1005543976	−1.4868571909
C	−0.4743344	1.2155534552	−0.7532025579
O	−3.6785014559	−0.2965795729	−1.4452331035
O	0.0407676179	2.4404690447	−0.6421991927
C	0.3987102258	0.0800202098	−0.3246292684
C	1.7352048951	0.1096389731	−0.749886975
C	−0.0242631351	−0.9531332587	0.4980465123
C	2.6371075458	−0.8649607342	−0.357459173
H	2.0553445864	0.9704743115	−1.3318424878
C	0.870700653	−1.9625596748	0.8743691575
H	−1.0498224565	−0.9756082665	0.8625424398
C	2.1969647299	−1.9314399693	0.4560705629
H	0.5141128885	−2.7624833154	1.5232692713
O	3.9648495126	−0.8603885721	−0.6775984533
O	3.1484363418	−2.8559710425	0.787073408
C	2.7620211287	−3.8860302325	1.6539306971
H	3.6527084727	−4.5093059518	1.8101789369
H	2.4180075758	−3.4982775469	2.6303393035
H	1.9585162917	−4.5129839371	1.2245678603
C	4.4486308952	0.3059614839	−1.3009594264
H	5.5402329937	0.1971339965	−1.3505269991
H	4.05302466	0.4174344864	−2.3272202888
H	4.1891691146	1.2136757455	−0.7291692914
C	0.5120222065	2.8524495172	0.7750939815
O	−0.1350078048	2.3480600169	1.7070401951
O	0.4231919436	4.2665085325	0.543882529
C	−3.9534893866	−0.9514031238	−0.3350933278
O	−3.2165128815	−1.6408685403	0.3303221615
O	−5.2564891622	−0.7575892507	−0.053717246
C	−5.6949295238	−1.4016082174	1.1323923699
H	−5.1129150528	−1.0651856882	2.0026818178
H	−6.7488041891	−1.1209972845	1.249443593
H	−5.6009665343	−2.4953061292	1.0499697502
C	0.7298913745	4.9805435955	1.7021685772
H	0.4717955059	6.0370945746	1.5223155001
H	0.1547675563	4.6060114216	2.5686450691
H	1.8096746678	4.9220475283	1.9532912049
O	1.9506548076	2.5798209706	0.7437583638
C	2.3999033997	1.8242903451	1.835301661
H	3.4153642167	1.4688089084	1.5867743346
H	2.4560964916	2.422894386	2.7669159773
H	1.7521655595	0.9566182114	2.0399683705

TS-4

E [a.u.] = −1299.021223
G [a.u.] = −1298.715297
E_{SP} [a.u.] = −1299.36281

Charge = −1; Multiplicity = 1

C	1.736252	0.995813	1.515065
H	2.093992	1.99478	1.779751
C	2.6143	−0.132876	1.898597
H	2.863031	−0.123484	2.972233
H	2.211987	−1.118184	1.633703
C	0.453274	0.952407	1.045913
O	3.963637	0.003847	1.305561
O	−0.28073	2.033726	1.018775
C	−0.256741	−0.317079	0.657794
C	−1.614815	−0.395298	1.006077
C	0.297645	−1.347514	−0.092168
C	−2.407381	−1.457577	0.607119
H	−2.033408	0.462418	1.52766
C	−0.485277	−2.447531	−0.469678

H	1.337283	−1.301094	−0.41493
C	−1.832183	−2.515656	−0.130188
H	−0.022855	−3.237932	−1.061287
O	−3.749968	−1.54796	0.841512
O	−2.682294	−3.529717	−0.477182
C	−2.153944	−4.562349	−1.261577
H	−2.977208	−5.266039	−1.443955
H	−1.774003	−4.193072	−2.232237
H	−1.333005	−5.097273	−0.748417
C	−4.372643	−0.37997	1.32618
H	−5.453729	−0.567948	1.27804
H	−4.092734	−0.169302	2.374392
H	−4.116614	0.502557	0.714763
C	−0.901586	2.665407	−0.547502
O	−0.034966	2.607664	−1.407564
O	−1.264851	3.876784	0.062959
C	4.204837	−0.617619	0.174841
O	3.526539	−1.445293	−0.392068
O	5.407058	−0.206845	−0.279973
C	5.795075	−0.797862	−1.50915
H	5.058695	−0.589579	−2.29916
H	6.761489	−0.345433	−1.763647
H	5.902533	−1.889208	−1.411163
C	−1.568423	4.845657	−0.90165
H	−1.753496	5.790028	−0.367047
H	−0.736842	4.984675	−1.614618
H	−2.479562	4.584048	−1.477839
O	−2.100879	1.945958	−0.70956
C	−2.081742	1.053009	−1.79989
H	−3.048103	0.525463	−1.781509
H	−1.967243	1.58904	−2.758264
H	−1.268463	0.314444	−1.724858

I4

E [a.u.] = −651.8439394

G [a.u.] = −651.675224

E_{SP} [a.u.] = −651.9780577

Charge = 0; Multiplicity = 1

C	3.2538628417	−1.9050174816	−0.5061586971
H	2.4431905159	−2.559379548	−0.8286629661
C	4.5009259355	−2.3720992589	−0.4228800003
H	4.7436797052	−3.4058573656	−0.6747982076
H	5.3057988936	−1.7097323463	−0.094814169
C	2.9576763358	−0.4823717248	−0.1461832699
O	3.8451563901	0.241399359	0.2749434991
C	1.5666747228	0.0395915466	−0.3019432352
C	1.3321052172	1.3607720416	0.1283454945
C	0.5153701366	−0.6891569239	−0.8476585088
C	0.0800600325	1.9371730943	0.0223338684
H	2.1792267836	1.9030334974	0.5452262877
C	−0.7557592265	−0.1173628919	−0.9661648923
H	0.6541793661	−1.7099341053	−1.2012289666
C	−0.9883122103	1.1849062175	−0.5369325055
H	−1.5642498698	−0.7043080002	−1.3996919384
O	−0.2416344918	3.1915493744	0.4108055647
O	−2.1716694263	1.8265075275	−0.6028726544
C	−3.2698999521	1.1325182364	−1.1506599951
H	−4.1169300475	1.8268447288	−1.1087885025
H	−3.0869146491	0.8465014974	−2.2007751637
H	−3.5124384762	0.2287806075	−0.5653717471
C	0.7835878231	3.9790870576	0.9742345055
H	0.3233150761	4.943351492	1.2196365048
H	1.1872406421	3.5230431118	1.8945967905
H	1.6105924614	4.1408554366	0.2616080744

TS-5

E [a.u.] = −766.9163463

G [a.u.] = −766.716208

E_{SP} [a.u.] = −767.154704

Charge = 0 Multiplicity = 1

C	2.71482	−0.36656	−1.38371
H	2.18394	−1.13351	−1.96477
C	3.39988	0.59923	−2.00469
H	3.53649	0.63416	−3.08982
H	3.82399	1.42004	−1.41371
C	2.0255	0.25221	0.30047
O	2.49802	1.30864	0.62829
C	0.58181	−0.10865	0.22782
C	−0.31088	0.94959	−0.01418
C	0.10727	−1.4018	0.37618
C	−1.67244	0.71133	−0.11135
H	0.09823	1.95363	−0.1134
C	−1.26692	−1.64871	0.28733
H	0.80254	−2.21372	0.57992
C	−2.16161	−0.61251	0.04137
H	−1.63031	−2.66732	0.4164
O	−2.61589	1.65328	−0.34145
O	−3.50108	−0.74767	−0.0682
C	−4.04559	−2.03874	0.07898
H	−5.12844	−1.92687	−0.0496
H	−3.65963	−2.73359	−0.68711
H	−3.84017	−2.45616	1.07994
C	−2.18191	2.98491	−0.4971
H	−3.08595	3.57828	−0.6772
H	−1.67745	3.35804	0.41094
H	−1.49912	3.09331	−1.35764
O	2.83566	−1.11271	0.98481
H	3.08337	−0.89342	−0.22187
C	3.78872	−0.77188	1.9699
H	3.96543	0.31684	1.9699
H	3.41976	−1.0804	2.96039
H	4.73505	−1.29308	1.75929

I5

E [a.u.] = −766.9666954

G [a.u.] = −766.762786

E_{SP} [a.u.] = −767.1955756

Charge = −1 Multiplicity = 1

C	3.41784	−0.86374	0.06313
H	3.10289	−1.90737	0.00676
C	4.86566	−0.58	0.08809
H	5.42292	−1.10232	−0.72656
H	5.01073	0.51008	−0.03956
C	2.49309	0.17148	0.09359
O	2.7405	1.41279	0.12073
C	1.00563	−0.2006	0.06115
C	0.11042	0.87771	−0.01437
C	0.46974	−1.48488	0.1128
C	−1.26388	0.693	−0.04723
H	0.59383	1.85676	−0.0371
C	−0.91538	−1.69022	0.08039
H	1.12607	−2.3522	0.18903
C	−1.79335	−0.6132	−0.00143
H	−1.29908	−2.71068	0.1242
O	−2.18676	1.7029	−0.12037
O	−3.16235	−0.70894	−0.0379
C	−3.71111	−1.99324	0.0198
H	−4.80207	−1.86651	−0.01427
H	−3.3976	−2.62194	−0.83523
H	−3.44237	−2.52175	0.95404
C	−1.68027	3.01122	−0.15766
H	−2.55369	3.6759	−0.2106
H	−1.09133	3.2545	0.74472
H	−1.03873	3.18263	−1.04053
O	5.49966	−0.98935	1.32675
C	6.85817	−0.71872	1.31517
H	7.2874	−1.04185	2.27818
H	7.39709	−1.25555	0.49932
H	7.07983	0.36395	1.18172

TS-6

E [a.u.] = −1110.490152

G [a.u.] = −1110.195236

E_{SP} [a.u.] = −1110.790278

Charge = −1 Multiplicity = 1

C	−1.82876	0.31227	−0.29935
C	−3.06303	1.1475	−0.21111
H	−3.9653	0.51014	−0.28589
H	−3.08784	1.66576	0.76687
C	−0.68835	0.78269	0.44492
O	−0.74391	1.56148	1.41257
C	0.68922	0.27771	0.05654
C	1.79106	0.99573	0.54698
C	0.91792	−0.84576	−0.72824
C	3.09118	0.62866	0.23501
H	1.56162	1.84258	1.19351
C	2.22644	−1.23451	−1.03918
H	0.07871	−1.45815	−1.05827
C	3.31689	−0.50439	−0.57678
H	2.3791	−2.12817	−1.64482
O	4.21446	1.28406	0.66012
O	4.62774	−0.7965	−0.8364
C	4.88514	−1.92727	−1.62184
H	5.97684	−1.99224	−1.72321
H	4.5131	−2.85487	−1.14893
H	4.43603	−1.84548	−2.62906
C	4.01603	2.39105	1.49949
H	5.01511	2.78219	1.73473
H	3.42358	3.18359	1.00786
H	3.50556	2.11138	2.4386
O	−3.09826	2.12629	−1.26252
C	−4.2681	2.87314	−1.22447
H	−4.24577	3.59303	−2.05867
H	−5.17883	2.24255	−1.32993
H	−4.37796	3.4427	−0.27558
H	−1.5933	0.02454	−1.33015
C	−2.40762	−1.59599	0.41207
O	−3.6183	−1.51665	0.62584
O	−1.49371	−1.8186	1.42493
O	−1.91725	−2.37238	−0.64947
C	−2.81602	−2.45946	−1.72365
H	−2.93569	−1.48616	−2.23578
H	−2.38915	−3.18574	−2.43093
H	−3.81007	−2.79299	−1.38674
C	−1.90487	−1.26935	2.65741
H	−1.10522	−1.50154	3.37498
H	−2.01861	−0.17584	2.58887
H	−2.85666	−1.71226	2.99456

I6

E [a.u.] = −1110.503019

G [a.u.] = −1110.206575

E_{SP} [a.u.] = −1110.804172

Charge = −1 Multiplicity = 1

C	3.43705	−1.29618	−0.34375
C	4.83331	−0.85284	0.03422
H	5.52486	−1.69882	−0.11653
H	5.15612	−0.02426	−0.6216
C	2.50657	−0.10375	−0.44836
O	2.92467	1.03221	−0.60467
C	1.02368	−0.30942	−0.26462
C	0.24412	0.83301	−0.0228
C	0.41038	−1.55443	−0.32198
C	−1.12314	0.73824	0.18142
H	0.76653	1.78912	−0.01031
C	−0.97141	−1.65791	−0.12726
H	1.00274	−2.44126	−0.5647
C	−1.74466	−0.52991	0.13039
H	−1.43624	−2.64203	−0.18808
O	−1.95454	1.79338	0.435
O	−3.09272	−0.53351	0.34279
C	−3.74932	−1.77046	0.27088
H	−4.811	−1.56774	0.46433
H	−3.64787	−2.2353	−0.72662
H	−3.37652	−2.48383	1.02847
C	−1.3632	3.0658	0.47225
H	−2.17263	3.77527	0.68992

H	−0.59403	3.14134	1.26191
H	−0.89681	3.33296	−0.49306
O	4.83538	−0.42638	1.39226
C	6.06847	0.09602	1.76435
H	6.01135	0.38794	2.82461
H	6.89077	−0.64247	1.6458
H	6.34127	0.9911	1.16666
H	3.0652	−1.94794	0.4619
C	3.50459	−2.18042	−1.68469
O	4.65864	−2.47108	−2.10004
O	2.63191	−1.46588	−2.59349
O	2.63239	−3.40568	−1.39537
C	3.35662	−4.44838	−0.82788
H	3.60024	−4.26902	0.24594
H	2.74593	−5.36714	−0.8816
H	4.30984	−4.60172	−1.36306
C	2.67052	−1.97908	−3.89393
H	2.11075	−1.28249	−4.53852
H	3.71058	−2.06889	−4.25123
H	2.20061	−2.97998	−3.94948

TS-7

E [a.u.] = −1110.498703

G [a.u.] = −1110.200417

E_{SP} [a.u.] = −1110.794888

Charge = −1 Multiplicity = 1

C	−2.19689	0.21314	−0.69374
C	−3.22389	1.31006	−0.96222
H	−4.18021	0.84668	−1.23331
H	−3.36627	1.89921	−0.03893
C	−1.10335	0.64774	0.31044
O	−1.27775	1.63753	1.03241
C	0.32119	0.21026	0.02505
C	1.34515	1.06461	0.45293
C	0.65403	−0.95711	−0.6504
C	2.67954	0.77186	0.20494
H	1.03191	1.95907	0.9912
C	1.99472	−1.26416	−0.90334
H	−0.13614	−1.64683	−0.95006
C	3.01376	−0.41098	−0.487
H	2.23296	−2.19094	−1.42607
O	3.73524	1.55622	0.58017
O	4.35014	−0.62129	−0.69272
C	4.71374	−1.78154	−1.38734
H	5.80951	−1.76828	−1.4608
H	4.40198	−2.70042	−0.85726
H	4.2865	−1.8065	−2.40702
C	3.42817	2.73664	1.27464
H	4.38743	3.23053	1.47975
H	2.79326	3.41526	0.67701
H	2.91325	2.53324	2.23055
O	−2.88691	2.16117	−2.0497
C	−1.74894	2.94705	−1.82372
H	−1.68082	3.66683	−2.65493
H	−1.80604	3.49453	−0.86449
H	−0.81591	2.34992	−1.80233
H	−1.74333	−0.07405	−1.65454
C	−2.86143	−1.02769	−0.07879
O	−4.00224	−1.02986	0.37905
O	−1.61696	−1.01039	1.32081
O	−2.35847	−2.1705	−0.7237
C	−2.73493	−3.36676	−0.08758
H	−3.82789	−3.42201	0.04171
H	−2.38738	−4.1936	−0.72506
H	−2.25575	−3.43163	0.90472
C	−2.17189	−0.67236	2.53685
H	−1.95906	0.39172	2.78801
H	−3.27657	−0.78926	2.50973
H	−1.77052	−1.30973	3.3536

11

E [a.u.] = −1110.509036

G [a.u.] = −1110.21304

E_{SP} [a.u.] = −1110.807961

Charge = −1 Multiplicity = 1

C	2.25914	−0.2369	−0.85813
H	2.08255	−0.94846	−1.67684
C	3.74463	0.19077	−0.92864
H	4.30935	−0.57827	−1.47894
H	3.79148	1.1366	−1.49547
C	1.2822	0.99019	−1.06794
O	1.54553	2.05964	−0.39442
C	−0.18049	0.48346	−0.90136
C	−0.89028	0.95447	0.20759
C	−0.80192	−0.41029	−1.76233
C	−2.18246	0.52505	0.4745
H	−0.35003	1.67909	0.8191
C	−2.11007	−0.84755	−1.51363
H	−0.26756	−0.75863	−2.64751
C	−2.80553	−0.39425	−0.39675
H	−2.57826	−1.54851	−2.20606
O	−2.93324	0.92878	1.54623
O	−4.0811	−0.7669	−0.0569
C	−4.711	−1.70357	−0.88266
H	−5.69631	−1.89662	−0.43674
H	−4.85361	−1.32518	−1.91267
H	−4.14957	−2.6551	−0.93821
C	−2.31571	1.82146	2.43624
H	−3.04511	2.01191	3.23555
H	−1.39531	1.39613	2.87521
H	−2.05175	2.77681	1.94851
O	4.40004	0.30024	0.31901
C	4.20939	1.5546	0.94438
H	3.16136	1.88963	0.85313
H	4.50802	1.43631	1.99846
H	4.86267	2.32306	0.47888
C	1.99676	−1.0345	0.39435
O	1.98733	−2.24533	0.4632
O	1.75951	−0.26512	1.47545
C	1.46242	−0.97286	2.66138

H	1.31774	−0.20966	3.43686
H	0.54514	−1.57089	2.54459
H	2.28583	−1.64867	2.93999
O	1.46889	1.14308	−2.57141
C	0.95548	2.35473	−3.03073
H	1.41129	2.57585	−4.01195
H	−0.14943	2.32349	−3.1636
H	1.18855	3.16447	−2.31648

TS-8

E [a.u.] = −1110.49772
G [a.u.] = −1110.202863
E_{SP} [a.u.] = −1110.802058

Charge = −1 Multiplicity = 1

C	2.18193	0.22725	−0.48183
H	3.10278	0.81544	−0.41412
C	2.34355	−1.21214	−0.16024
H	2.70284	−1.30814	0.88422
H	1.36835	−1.73344	−0.23281
C	1.2774	0.9823	1.35876
O	1.7878	0.30304	2.26134
C	−0.15479	0.78438	0.93985
C	−0.75808	−0.42995	1.2883
C	−0.88445	1.7286	0.231
C	−2.05489	−0.7228	0.89572
H	−0.15091	−1.12508	1.86684
C	−2.20139	1.45016	−0.15159
H	−0.41284	2.6665	−0.05465
C	−2.79254	0.23096	0.16159
H	−2.75435	2.19908	−0.71936
O	−2.70598	−1.8934	1.16794
O	−4.06401	−0.1406	−0.18728
C	−4.77465	0.73285	−1.01862
H	−5.73766	0.24727	−1.22675
H	−4.96596	1.70925	−0.53489
H	−4.24825	0.91542	−1.97388
C	−1.95118	−2.90292	1.78623
H	−2.61264	−3.77645	1.86299
H	−1.05878	−3.1713	1.19294
H	−1.6194	−2.61238	2.79956
O	3.27774	−1.88014	−1.02975
C	3.42444	−3.21643	−0.68467
H	2.46761	−3.78043	−0.75526
H	4.14776	−3.67618	−1.37763
H	3.80133	−3.35049	0.35388
C	1.37497	0.63609	−1.59619
O	1.38428	1.71711	−2.17471
O	0.43283	−0.31533	−1.95181
C	−0.46782	0.08768	−2.95292
H	−1.21118	−0.71836	−3.03917
H	−0.97273	1.03054	−2.69085
H	0.03685	0.2339	−3.92421
O	1.61416	2.3267	1.21187
C	2.87768	2.65669	1.7215
H	2.99023	3.74356	1.59928
H	2.97372	2.37916	2.78377
H	3.68405	2.14683	1.16377

TS-9a

E [a.u.] = −1377.341918
G [a.u.] = −1376.999245
E_{SP} [a.u.] = −1377.687576

Charge = −1; Multiplicity = 1

C	−3.9295406587	1.3544225159	−1.5187164451
C	−2.8735482522	1.3018003623	−0.6006811654
C	−2.7869694701	0.2533413938	0.3109122191
C	−3.7793946148	−0.7593623452	0.2975140743
C	−4.8231829199	−0.6965889379	−0.6202583141
C	−4.9017321332	0.3666196077	−1.5313465623
H	−3.9698157148	2.1803958379	−2.2318203674
H	−2.0812011355	2.0524203044	−0.6199270794
H	−5.5900737096	−1.4716382208	−0.6352657122
H	−5.7258429466	0.4008847023	−2.2469483171
O	−1.8059391609	0.0998956819	1.2238093317
C	−0.9446854071	1.1785323335	1.5236779652
H	−1.4679901594	2.0610500306	1.906911262
C	−0.0261208994	0.4336200105	3.3132082928
H	−0.9784067007	0.6509447751	3.8612310589
H	−0.0429344761	−0.5824685106	2.8485511817
C	0.2435158745	1.3640423795	0.8007814694
H	0.9343252658	2.0241774754	1.3337292777
O	1.0352470379	0.998501014	3.6253980676
O	−3.6156162736	−1.7463725146	1.22271551
C	−4.532128151	−2.8033214897	1.2122562577
H	−4.2136476008	−3.4936912934	2.0039200108
H	−5.5639861706	−2.4660663079	1.4262890697
H	−4.533324981	−3.3422659583	0.2462974045
O	0.0143553098	2.4604689934	−0.6367837935
C	0.9041162874	0.1665086435	0.1986927421
C	1.9677633539	−0.4317368755	0.886234011
C	0.4764017192	−0.3927915792	−0.9998721959
C	2.5922071686	−1.5597252216	0.3762906474
H	2.2756439607	−0.0282774257	1.8562003592
C	1.1051359002	−1.523453999	−1.5258972265
H	−0.3477810514	0.0717994468	−1.5413664739
C	2.1712425242	−2.1118954338	−0.8470313316
H	0.751186662	−1.9338781954	−2.471696271
O	3.6154530097	−2.1571445876	1.0780050765
O	2.8676286651	−3.2084750485	−1.2794161431
C	2.4624104232	−3.7900115294	−2.4891756875
H	3.1339186199	−4.6412737156	−2.6624765624
H	1.4212756375	−4.1575156818	−2.4428744814
H	2.5485329443	−3.0862207714	−3.337319418
C	4.8963171132	−1.8237635552	0.588976735
H	5.6262866977	−2.3409083309	1.2277904786
H	5.0303787841	−2.1563334186	−0.4552064137
H	5.0754226868	−0.734610922	0.64545963
C	1.0112322548	3.0872238725	−1.1589507843
O	0.9813752424	3.8544507024	−2.1057432798
O	2.197352904	2.8095128972	−0.5174161628
C	3.3296765516	3.4445543459	−1.065075993
H	3.4783388298	3.164724993	−2.1201916145
H	3.2439017719	4.5420578216	−1.0154832135
H	4.186135387	3.1087307284	−0.4643411232

TS-9b

E [a.u.] = −1377.331905
G [a.u.] = −1376.989989
E_{SP} [a.u.] = −1377.678388

Charge = −1; Multiplicity = 1

C	3.0317328161	2.4880831307	1.9092187312
C	2.3592617447	1.7762330158	0.9076882606
C	3.0330825178	0.8485131007	0.1152486439

C	4.4201347223	0.6406484075	0.3426361395
C	5.0787911857	1.352896211	1.3380391337
C	4.3839513097	2.2823619207	2.1270606843
H	2.4768256195	3.2065012961	2.5164510329
H	1.2943084312	1.9329151305	0.7368181319
H	6.1430427938	1.1936114113	1.5134533476
H	4.9167152556	2.8327997863	2.9048741795
O	2.4848428739	0.1166998376	−0.8693948767
C	1.1097365169	0.3025738976	−1.1921243292
H	0.8680430749	1.3200859814	−1.5071076231
C	1.0197746903	−0.3340823907	−3.2988200546
H	2.0896871885	−0.0121107828	−3.340946164
H	0.8863948797	−1.3877042156	−2.9801752026
C	0.1991487831	−0.3660026209	−0.3299588738
H	0.5788332096	−0.6810890319	0.6473089983
O	0.1465088949	0.2770316398	−3.9338341756
O	5.0063275907	−0.2803588919	−0.4707061318
C	6.3683559674	−0.5388558586	−0.2792957269
H	6.6422164134	−1.3065139951	−1.0143641703
H	6.9906245708	0.3598544814	−0.4505614908
H	6.579402258	−0.9225480094	0.7364608657
O	−0.045376605	−2.0075487608	−0.9286608159
C	−1.1928664421	0.1581911933	−0.2961859876
C	−1.8775006237	0.2698947664	0.9198947103
C	−1.8476349108	0.5396247745	−1.47047427
C	−3.1694163885	0.7731352417	0.9757456155
H	−1.4080231501	−0.0443669843	1.8528870324
C	−3.1503471787	1.0369114737	−1.4223474415
H	−1.3409353812	0.4385281334	−2.4376401741
C	−3.8229203548	1.1624147941	−0.2053194341
H	−3.633424993	1.3220401817	−2.3570763073
O	−3.8015732407	0.8964307959	2.193973485
O	−5.098842993	1.6356887117	−0.0571847995
C	−5.7800549404	2.0188220508	−1.2231803163
H	−6.7683459574	2.3720009951	−0.9007444797
H	−5.261322225	2.8375200886	−1.7531377145
H	−5.9096390072	1.1735027807	−1.9228093306
C	−4.7487500193	−0.1239390958	2.4344739068
H	−5.1721708214	0.0618031263	3.4318659291
H	−5.5609685343	−0.1050799508	1.6881704957
H	−4.2723353771	−1.1212510272	2.4228293552
C	−0.4163597609	−2.9568319827	−0.1427125359
O	−0.6316193309	−4.115329876	−0.447677254
O	−0.5581408055	−2.545545772	1.1701752717
C	−0.9782306532	−3.55614772	2.0587059985
H	−1.9491410142	−3.9808531868	1.7587030228
H	−0.2494085002	−4.380845279	2.1082157517
H	−1.0675701001	−3.078226924	3.0445899565

4a

E [a.u.] = −688.991895

G [a.u.] = −688.823222

E_{SP} [a.u.] = −689.1384311

Charge = 0; Multiplicity = 1

C	0.7144255579	2.2912523201	−0.0009690461
C	1.4126417875	1.0702196577	−0.0007234795
C	0.7229020236	−0.1317143271	−0.0002765126
C	−0.6968317092	−0.1238343175	−0.0000716669
C	−1.3779783468	1.0902582491	−0.0002808124
C	−0.6731846346	2.2959647777	−0.0007422152
H	2.5001269361	1.0914875938	−0.0009201921
H	−2.4669235919	1.1101575644	−0.0000529367
H	−1.2002041913	3.2497388949	−0.0009074633
O	1.2919772033	−1.360220256	−0.000013287
O	−1.2778480293	−1.3413307761	0.0004099713
C	−2.6866081128	−1.3985554921	−0.0008241304
H	−2.9455887511	−2.4636670936	−0.0013720515
H	−3.113118719	−0.9217625163	0.8984024625
H	−3.1115188104	−0.9211870668	−0.9004991979
C	2.6990018243	−1.4250192997	−0.0003704077
H	2.9531542822	−2.4912721731	−0.0001293052
H	3.1288928073	−0.9498852753	−0.899361363
H	3.1293860798	−0.9493653399	0.8981081287
C	1.4219631381	3.5974013739	−0.0014305836
O	0.8773166157	4.6774890849	−0.0017720216
O	2.7619448424	3.4554878413	−0.0011729572
C	3.5022784845	4.6720412928	−0.001245359
H	4.5578817097	4.3782172467	0.0001240488
H	3.2724602331	5.2698329806	−0.8947575253
H	3.270445351	5.2711651957	0.8908417829

MMC

E [a.u.] = −303.65836996

G [a.u.] = −303.633228

E_{SP} [a.u.] = −303.81911238

Charge = −1; Multiplicity = 1

C	0.0003165909	0.0986938132	0.0354847962
O	−0.0008579944	−0.0820267186	1.2646073542
O	0.0002664247	1.1094370659	−0.6707195809
O	0.0000080758	−1.120199363	−0.7640480139
C	−0.0007734554	−2.2999226757	−0.0233283766
H	−0.885871603	−2.3965711604	0.6361792809
H	−0.0008990276	−3.140621755	−0.743480886
H	0.883789989	−2.3973322062	0.6367794261

DMC

E [a.u.] = −343.521334

G [a.u.] = −343.455881

E_{SP} [a.u.] = −343.6056438

Charge = 0; Multiplicity = 1

C	−0.0466694862	1.7610133752	0.2249446763
O	1.1431915721	1.6363233391	0.0730722627
O	−0.6966460067	2.9102774696	0.4117353513
C	0.1404317403	4.0644532801	0.4232753851
H	−0.5320299726	4.9138193357	0.584287979
H	0.8796904711	4.0028379465	1.2345076405
H	0.6704610473	4.1719551055	−0.5337039202
O	−0.9430271465	0.7737954823	0.2355262093
C	−0.3887433513	−0.5261863614	0.046394486
H	0.3290187458	−0.7644489628	0.844107219
H	−1.2388002719	−1.2160019367	0.0797143127
H	0.1222414128	−0.5955887676	−0.9244173236

Formaldehyde (FA)

E [a.u.] = −114.4687442

G [a.u.] = −114.463678

E_{SP} [a.u.] = −114.5018821

Charge = 0; Multiplicity = 1

O	0.0994633333	1.0827003942	−0.6494304743
C	1.0995797342	1.4650995789	−1.1918942641
H	1.7971926997	0.7676545438	−1.7167906177
H	1.3955861752	2.5424986467	−1.2060732734

Methanol (MeOH)

E [a.u.] = −115.6872615

G [a.u.] = −115.658462

E_{SP} [a.u.] = −115.7266544

Charge = 0; Multiplicity = 1

O	−0.0013579627	1.1494312637	−0.6170425745
C	1.330145292	1.451316151	−0.9596080745
H	2.0200003071	1.4036186882	−0.0953329807
H	1.729982506	0.7951481068	−1.7561928906
H	1.3425203644	2.4825847617	−1.3397438706
H	−0.0196175467	0.2460795787	−0.2854507291

Methanolate

E [a.u.] = −115.0400258

G [a.u.] = −115.027059

E_{SP} [a.u.] = −115.1724325

Charge = −1; Multiplicity = 1

O	−0.0119416269	1.0755238896	−0.7120948882
C	1.2126659765	1.4258391436	−0.9665300804
H	1.9995857154	1.3550897726	−0.1018606678
H	1.7918707418	0.8456227037	−1.8030538786
H	1.4119538291	2.5246119303	−1.3199194652

G

E [a.u.] = −421.29245611

G [a.u.] = −421.200784

E_{SP} [a.u.] = −421.45239422

Charge = −1; Multiplicity = 1

C	−3.971061819	−3.522317575	−1.0818866767
C	−2.935857669	−2.9070182505	−0.3787440579
C	−2.9984696916	−1.5553437681	0.1112188571
C	−4.265875991	−0.8955455654	−0.2074637265
C	−5.2867227639	−1.5170293081	−0.9065394734
C	−5.1579360708	−2.8488363835	−1.3591158917
H	−3.8434971558	−4.5578163802	−1.4213949312
H	−2.0076538401	−3.4482926929	−0.1674515275
H	−6.2156417158	−0.9802820482	−1.1198932163
H	−5.9734559129	−3.32436514	−1.9096730033
O	−2.0804198335	−0.9812396712	0.745411042
O	−4.3362198425	0.4059683945	0.2601308966
C	−5.5038310086	1.108977692	0.0026165696
H	−5.3793946957	2.1104155561	0.4429521028
H	−5.7055178173	1.2250582574	−1.083219395
H	−6.4002221724	0.6349598831	0.4553374314

3a

E [a.u.] = −461.16415614

G [a.u.] = −461.031057

E_{SP} [a.u.] = −461.2606828

Charge = 0; Multiplicity = 1

C	−4.0102853057	−3.5297434208	−1.1613541191
C	−2.9064248088	−2.8490227592	−0.6287842431
C	−3.0262912696	−1.528543408	−0.2116019133
C	−4.2763993145	−0.87051498	−0.3283009605
C	−5.3636723232	−1.5557006682	−0.8577936169
C	−5.2304800474	−2.8875481374	−1.2749311444
H	−3.8962963671	−4.5657856554	−1.4832877137
H	−1.9505845644	−3.3653012492	−0.5444840275
H	−6.32968517	−1.0605960878	−0.9525465079
H	−6.0954037548	−3.4083670884	−1.6880665284
O	−2.0270187893	−0.779740504	0.3154100314
O	−4.2948032419	0.41392727	0.1037377146
C	−5.5111207482	1.1155384065	0.0159599791
H	−5.3122430897	2.1179873484	0.4135454079
H	−5.8591020286	1.2041205517	−1.0283754795
H	−6.3040955554	0.638990671	0.6189427895
C	−0.7631149337	−1.3817771642	0.4547981048
H	−0.1100212654	−0.6176346609	0.8929506268
H	−0.7971678819	−2.2562826036	1.1281095694
H	−0.3484341505	−1.6953383606	−0.5194614193

G−Cs

E [a.u.] = −441.4865854

G [a.u.] = −441.396953

E_{SP} [a.u.] = −441.6126241

Charge = 0; Multiplicity = 1

C	−1.73999	−0.74641	−0.00002
C	−1.38807	0.60054	−0.00009
C	−0.03784	1.05075	−0.00007
C	0.93565	−0.01664	0.00007
C	0.58345	−1.35802	0.00016
C	−0.76593	−1.74102	0.0001
H	−2.79827	−1.02367	−0.00005
H	−2.15574	1.3789	−0.00019
H	1.34874	−2.13683	0.00026
H	−1.03326	−2.79862	0.00016
O	0.29541	2.28741	−0.00007
O	2.26866	0.41836	0.00012
C	3.26062	−0.56821	0.
H	4.23226	−0.0476	−0.00008
H	3.21097	−1.21377	0.8961
H	3.21077	−1.21373	−0.89611
Cs	2.80989	3.33337	0.00042

Cs(DMC)

E [a.u.] = −363.5757014
G [a.u.] = −363.51729
E_{SP} [a.u.] = −363.7130839

Charge = 1; Multiplicity = 1

O	−0.59122	−1.33189	0.04279
C	−0.44704	−0.02768	−0.07324
O	0.49461	0.54376	−0.584
O	−1.46106	0.66881	0.43999
Cs	0.45199	3.52415	−0.48462
C	−2.56256	−0.03454	1.04494
H	−3.26382	0.74437	1.36085
H	−3.03893	−0.70345	0.3172
H	−2.21821	−0.6115	1.9128
C	0.47743	−2.13387	−0.49123
H	0.56342	−1.97385	−1.57348
H	1.42352	−1.87581	0.00105
H	0.19604	−3.16815	−0.27358

I8−Cs

E [a.u.] = −441.6927223
G [a.u.] = −441.594039
E_{SP} [a.u.] = −441.8250543

Charge = 0 Multiplicity = 1

C	0.28593	−0.86071	0.66621
H	0.60031	−1.80704	1.1099
C	1.22358	0.27976	0.61471
H	0.697	1.24207	0.63313
H	1.95571	0.2607	1.44477
O	2.04489	0.38455	−0.61981
C	3.03706	−0.60011	−0.65698
H	2.6102	−1.62551	−0.62507
H	3.61248	−0.47966	−1.58968
H	3.74185	−0.51205	0.19414
C	−1.0845	−0.75709	0.40697
O	−1.98278	−1.59919	0.47131
O	−1.44319	0.53308	−0.1217
C	−2.83111	0.73556	−0.24838
H	−2.97223	1.80047	−0.48547
H	−3.2741	0.11944	−1.05504
H	−3.37209	0.48305	0.6758
Cs	−0.07524	−0.56093	−2.59088

CsOMe

E [a.u.] = −135.2455828
G [a.u.] = −135.238188
E_{SP} [a.u.] = −135.3287795

Charge = 0 Multiplicity = 1

O	1.17909	−0.71294	0.00013
Cs	2.49739	1.58673	0.00549
C	2.03154	−1.74523	−0.0002
H	1.5715	−2.77481	−0.00241
H	2.75637	−1.80258	−0.89161
H	2.75379	−1.80526	0.89312

CsMMC

E [a.u.] = −323.85830037
G [a.u.] = −323.836347
E_{SP} [a.u.] = −323.9718611

Charge = 0 Multiplicity = 1

C	−0.85521	−0.14508	−0.18332
O	−0.01017	−0.51729	0.66955
O	−2.08356	0.02096	−0.02812
O	−0.40198	0.12172	−1.46053
C	0.98061	−0.05815	−1.66241
H	1.29362	−1.09753	−1.46864
H	1.1739	0.19422	−2.7153
H	1.58107	0.59683	−1.00955
Cs	−2.0166	−0.73036	2.73038

.....

VI. Abbreviations

Å	Ångstrom
A	Ampere
Ac	acetyl
AcOH	acetic acid
BM	ball mill
Bn	benzyl
br.s	broad (NMR signal)
Bu	butyl
*t*Bu	*tert*-butyl
BWL	beechwood lignin
°C	degree celsius
CL	cherry lignin
δ	chemical shift
d	doublet (NMR signal)
dd	doublet of doublets (NMR signal)
ddd	doublet of doublet of doublets (NMR signal)
Da	dalton
DAIB	(diacetoxyiodo)benzene
DCM	dichloromethane
DM	disc mill
DMC	dimethyl carbonate
DMF	*N*,*N*-Dimethylformamide
DMP	Dess-Martin periodinane
DMSO	dimethylsulfoxide
DCM	dichloromethane
equiv	equivalent
ESI	electronspray ionization

Et	ethyl
Et_3N	triethylamine
EtOAc	ethyl acetate
eV	electron volt
G	gauss
GC	gas chromatography
GC-MS	gas chromatography-mass spectrometry
GPC	gel permeation chromatography
h	hour
HPLC	high-performance liquid chromatography
HRMS	high resolution mass spectrometry
HSQC	heteronuclear single quantum coherence
Hz	Hertz
IBX	*o*-iodoxybenzoic acid
IR	infrared
J	Joule
J	coupling constant (in NMR spectroscopy)
L	liter
LDA	lithium diisopropylamide
m	multiplet (NMR signal)
M	molar
Me	methyl
min	minutes
MM	mixer mill
mol	mole (s)
mp.	melting point
MPI	Max-Planck-Institute
MPM	mortar and pestle mill
MS	mass spectrometry

NBS	*N*-bromosuccinimide
NCS	*N*-chlorosuccinimide
NMR	nuclear magnetic resonance
OAc	acetate
OL	oak lignin
OMe	methoxy
OH-TEMPO	4-hyroxy(2,2,6,6-tetramethylpiperidin-1-yl)-oxyl
Pa	Pascal
ppm	parts per million
*i*Pr	*iso*-propyl
q	quartet (NMR signal)
RI	refractive index
rt	room temperature
s	singlet (NMR signal)
SS	stainless steel
t	triplet (NMR signal)
TCCA	trichloroisocyanuric acid
td	triplet of doublets (NMR signal)
TEMPO	(2,2,6,6-tetramethylpiperidin-1-yl)-oxyl
TGA	thermogravimetric analysis
THF	tetrahydrofuran
TLC	thin layer chromatography
V	Volt
W	Watt
WC	tungsten carbide

VII. Acknowledgements

First and foremost, I would like to express my sincere gratitude to Professor Dr. Carsten Bolm for extending me an opportunity to join his group as a Marie Curie Early Stage Researcher. This journey has been an absolute life time opportunity for me to not only grow as a researcher but also have an all-round development. Thank you Prof. Bolm for being a truely inspiring mentor during my doctoral studies at RWTH Aachen University and for your constant support along with the amount of freedom and trust you bestowed upon me during my research here as well as during my SuBiCat secondments. I also want to thank you for fostering my scientific ideas and for encouraging and supporting me to present my work at various national and internaltional conferences.

Furthermore, I would like to thank Prof. Paul C. J. Kamer for letting me conduct my interdoc under his supervision at the University of St Andrews in United Kingdom. I thank you for supporting my ideas and trusting my findings along with your valuable suggestions throughout my stay there. It has been an absolute privilege to have both you and Prof. Bolm as my scientific mentors.

I would also like to thank all the fellow SuBiCat members for their research collaborations, help with the analytics, discussions and for all the beautiful memories during our yearly meetings. Never have I seen so much love and support for each other in any other consortium. Thank you all for making my journey at SuBiCat an enjoyable experience.: Dr. Fanny Tran, Dr. Irshad Baig, Dr. Elisa Lanfranchi, Stephanie Spoehrle, Selin Ece, Ciaran Lahive, Monica Raquel Caseiro Fernandes, Andrey Charkovskiy, Davide di Marino, April Liwanag, Khaled Khalili, Mila Marinovic, Antonio Martinez Pascual, Paola Forero Cortes.

I thank Dr. Nico Anders for helping me with the GPC measurements and Dr. Christoph Räuber for the NMR and lignin HSQC measurements and the fruitful discussions.

I extend my greetings to Dr. Ingo Schiffers, Frau Voss and Daniela for helping me adjust so well in the group and at Vossen during my stay at Aachen. Thank you so mush Susi Grünebaum and Pierre Winandy for helping me synthesize my starting materials.

I would like to thank all the former and current co-workers in the Bolm group for their support, pep-up-talks, guidance, and the nice working atmosphere. Special thanks to Dr. Christa Lehmann, Dr. Carl Albrecht Dannenberg, Dr. Jakob Mottweiler, Dr. Peter Becker, Dr. Laura Buglioni, Dr. José Hernández, Dr. Deo Prakash, Dr. Laure Konnert, Plamena Staleva, Torsten Rinesch, Karen J. Ardila Fierro for supporting me and my research throughout my doctoral research.

To my lab mates at St Andrews Sherry, Ciarian, Paola, Stephanie, Amanda, Frank; it was awesome having you as my lab mates and welcoming me to your group.

I thank my former research students for their synthetic contributions and their fruitful discussions.

I am grateful to Dr. Carl Albrecht Dannenberg, Dr. Suruchi Chauhan, Dr. Pankaj Chauhan, Torsten Rinesch, Dr. José Hernández and Dr. Jakob Mottweiler for proofreading parts of this dissertation.

Last, but not the least, my grandparents Dadda, Nani, Nana (Dadda, even though you did not see me finish up I know your love and blessings shall always stay with me), parents (Anjali and Sameer Dabral), brother (Suyash Dabral) and my best friend Mujahid (Mujji) for always supporting me emotionally and holding me at my low. Thank you Mujji for listening to me patiently when my Chemistry did not work and always trying to help me out. Special thanks to my grandaunt (Dr. Vibhuti Klingler Dabral) and granduncle (Dr. Franz Klingler) for being my guardian angels in Germany and for being so protective

and making Germany a home away from home. Thank you Nittu mausi, mummy, papa, nani, nana, dadda and mujji for supporting my decision to come to Germany and trusting me that I could make it happen.

This journey took a lot from me but also gave me eternal memories to cherish.

In the end thank you Almighty for everything.

VIII. References

[1] N. Y. Chen, *Chem. Innovations* **2001**, *31*, 14–20.

[2] Euratom Scientific and Technical Committee. *THE ENERGY CHALLENGE OF THE 21ST CENTURY: the role of nuclear energy*: Brussel, EUR 20634 EN, **2003**.

[3] International Energy Agency. 2016 World Energy Outlook; IEA Publications: Paris, **2016**.

[4] International Energy Agency. 2014 World Energy Outlook; IEA Publications: Paris, **2014**.

[5] Intergovernmental Panel on Climate Change. Climate Change 2014: Mitigation of Climate Change; Cambridge University Press, Cambridge, United Kingdom and New York, NY, USA, **2014**.

[6] United Nations Framework Convention on Climate Change (UNFCC). *The Paris Agreement* (FCCC/CP/2015/L.9/Rev.1), **2015**.

[7] a) M. Parikka, *Biomass Bioenerg*. **2004**, *27*, 613–620; b) A. J. Ragauskas, C. K. Williams, B. H. Davison, G. Britovsek, J. Cairney, C. A. Eckert, W. J. Frederick Jr., J. P. Hallett, D. J. Leak, C. L. Liotta, J. R. Mielenz, R. Murphy, R. Templer, T. Tschaplinski, *Science* **2006**, *311*, 484–489.

[8] Biofuel Research Advisory Council. *Biofuels in the European Union- A vision for 2030 and beyond*: Luxemburg, EUR 22066, **2006**.

[9] a) Á. T. Martínez, J. Rencoret, G. Marques, A. Gutiérrez, D. Ibarra, J. Jiménez-Barbero, J. C. del Río, *Phytochemistry* **2008**, *69*, 2831–2843; b) R. Vanholme, B. Demedts, K. Morreel, J. Ralph, W. Boerjan, *Plant Physiol.* **2010**, *153*, 895–905; c) K. Sanderson, *Nature* **2011**, *474*, 12–14; d) A. J. Ragauskas, G. T. Beckham, M. J. Biddy, R. Chandra, F. Chen, M. F. Davis, B. H. Davison, R. A. Dixon, P. Gilna, M. Keller, P. Langan, A. N. Naskar, J. N. Saddler, T. J. Tschaplinski, G. A. Tuskan, C. E. Wyman, *Science* **2014**, *344*, 1–10.

[10] A. Carroll, C. Somerville, *Annu. Rev. Plant Biol.* **2009**, *60*, 165–182.

[11] L. A. Lucia, *BioResources* **2008**, *3*, 981–982.

[12] a) J. Zakzeski, P. C. A. Bruijnincx, A. L. Jongerius, B. M. Weckhuysen, *Chem. Rev.* **2010**, *110*, 3552–3599; b) M. P. Pandey, C. S. Kim, *Chem. Eng. Technol.* **2011**, *34*, 29–41; c) C. Xu, R. A. D. Arancon, J. Labidi, R. Luque, *Chem. Soc. Rev.* **2014**, *43*, 7485–7500; d) R. Ma, Y. Xu, X. Zhang, *ChemSusChem* **2015**, *8*, 24–51.

[13] a) R. Parthasarathi, R. A. Romero, A. Redondo, S. Gnanakaran, *J. Phys. Chem. Lett.* **2011**, *2*, 2660–2666; b) S. Kim, S. C. Chmely, M. R. Nimlos, Y. J. Bomble, T. D. Foust, R. S. Paton, G. T. Beckham *J. Phys. Chem. Lett.* **2011**, *2*, 2846–2852.

[14] M. Li, Y. Pu, A. J. Ragauskas, *Front. Chem.* **2016**, *4*, 45.

[15] a) A. Johansson, O. Aaltonen, P. Ylinen, *Biomass* **1987**, *13,* 45–65; b) V. Chaturvedi, P. Verma, *Biotech.* **2013**, *5*, 415-431.

[16] A. Ferrer, A. Vega, A. Rodríguez, L. Jiménez, *Bioresour. Technol.* **2013**, *132*, 115–120.

[17] N. Shukry, S. M. Fadel, F. A. Agblevor, S. F. El-Kalyoubi, *J. Appl. Polym. Sci.* **2008**, *109*, 434–444.

[18] S. Laurichesse, L. Avérous, *Prog. Polym. Sci.* **2014**, *39*, 1266–1290.

[19] C. Zhao, J. A. Lercher, *Catalytic depolymerization and deoxygenation of lignin, in: The role of catalysis for the sustainable production of bio-fuels and bio-chemicals*; 1st edition, (Eds.: K. Triantafyllidis, A. Lappas, M. Stocker), Elsevier, **2013**, 289–320.

[20] a) F. S. Chakar, A. J. Ragauskas, *Ind. Crops Prod*. **2004**, *20*, 131–141; b) P. Ferrini, R. Rinaldi, *Angew. Chem. Int. Ed*. **2014**, *53*, 8634–8639.

[21] J. J. Bozell, J. E. Holladay, D. Johnson, J. F. White, *Top Value Added Candidates from Biomass, Volume II: Results of Screening for Potential Candidates from Biorefinery Lignin*; Pacific Northwest National Laboratory: Richland, WA, **2007**.

[22] K. P. Kringstad, R. Mörck, *Holzforschung* **1983,** *37*, 237–244.

[23] a) F. Cotana, G. Cavalaglio, A. Nicolini, M. Gelosia, V. Coccia, A. Pertozzi, L. Brinchi, *Energy Procedia.* **2014**, *45*, 52–60; b) C. Vanderghem, N. Jacquest, A. Richel, *Aust. J. Chem*. **2014**, *67*, 1693–1699.

[24] **Selected reductive lignin depolymerization approaches:** a) N. Yan, C. Zhao, P. J. Dyson, C. Wang, L. Liu, Y. Kou, *ChemSusChem* **2008**, *1*, 626–629; b) A. G. Sergeev, J. F. Hartwig, *Science* **2011**, *332*, 439–443; c) A. L. Jongerius, R. Jastrzebski, P. C. A. Bruijnincx, B. M. Weckhuysen, *J. Catal*. **2012**, *285*, 315–323; d) J. Zakzeski, A. L. Jongerius, P. C. A. Bruijnincx, B. M. Weckhuysen, *ChemSusChem* **2012**, *5*, 1602–1609; e) A. G. Sergeev, J. D. Webb, J. F. Hartwig, *J. Am. Chem. Soc*. **2012**, *134*, 20226–20229; f) J. He, C. Zhao, J. A. Lercher, *J. Am. Chem. Soc.* **2012**, *134*, 20768–20775; g) Z. Strassberger, A. H. Alberts, M. J. Louwerse, S. Tanase, G. Rothenberg, *Green Chem*. **2013**, *15*, 768–774; h) T. H. Parsell, B. C. Owen, I. Klein, T. M. Jarrell, C. L. Marcum, L. J. Haupert, L. M. Amundson, H. I. Kenttämaa, F. Ribeiro, J. T. Miller, M. M. Abu Omar, *Chem. Sci*. **2013**, *4*, 806–813; i) J. A. Barrett, Y. Gao, C. M. Bernt, M. Chui, A. T. Tran, M. B. Foston, P. C. Ford, *ACS Sustain. Chem. Eng.* **2016**, *4*, 6877−6886.

[25] **Selected redox-neutral lignin depolymerization approaches:** a) M. Nagy, K. David, G. J. P. Britovsek, A. J. Ragauskas, *Holzforschung* **2009**, *63*, 513–520; b) J. M. Nichols, L. M. Bishop, R. J. Bergman, J. A. Ellman, *J. Am. Chem. Soc*. **2010**, *132*, 12554–12555; c) T. vom. Stein, T. Weigand, C. Merkens, J. Klankermayer, W. Leitner, *ChemCatChem* **2013**, *5*, 439–441; d) D. Weickmann, B. Plietker, *ChemCatChem* **2013**, *5*, 2170–2173; e) R. G. Harms, I. I. E. Markovits, M. Drees, W. A. Herrmann, M. Cokoja, F. E. Kìhn, *ChemSusChem* **2014**, *7*, 429–434; f) J. D. Nguyen, B. S. Matsuura, C. R. J. Stephenson, *J. Am. Chem. Soc.* **2014**, *136*, 1218–1221; g) T. vom. Stein, T. den. Hartog, J. Buendia, S. Stoychev, J. Mottweiler, C. Bolm, J. Klankermayer, W. Leitner, *Angew. Chem. Int. Ed.* **2015**, *54*, 5859–5863.

[26] **Selected homogeneously catalyzed oxidative lignin depolymerization approaches**: a) R. Di. Cosimo, H. C. Szabo, *J. Org. Chem.* **1988**, *53*, 1673–1679; b) P. A. Watson, L. J. Wright, T. J. Fullerton, *J. Wood Chem. Tech.* **1993**, *13*, 371–389; c) G. Wu, M. Heitz, *J. Wood Chem. Tech.* **1995***, 15,* 189–202; d) I. A. Weinstock, E. M. G. Barbuzzi, M. W. Wemple, J. J. Cowan, R. S. Reiner, D. M. Sonnen, R. A. Heintz, J. S. Bond, C. L. Hill, *Nature* **2001**, *414*, 191–195; e) C. Canevali, M. Orlandi, L. Pardi, B. Rindone, R. Scotti, J. Sipila, F. Morazzoni, *J. Chem. Soc., Dalton Trans.* **2002**, *15*, 3007–3014; f) C. L. Chen, E. A. Capanema, H. S. Gracz, *J. Agric. Food Chem.* **2003**, *51,* 1932–1941; g) C. Crestini, P. Pro, V. Nerib, R. Saladino, *Bioorg. Med. Chem.* **2005**, *13*, 2569–2578; h) W. Partenheimer, *Adv. Synth. Catal.* **2009**, *351*, 456–466; i) S. K. Hanson, R. T. Baker, J. C. Gordon, B. L. Scott, D. L. Thorn, *Inorg. Chem.* **2010**, *49*, 5611–5618; j) S. Son, F. D. Toste, *Angew. Chem. Int. Ed.* **2010**, *49*, 3791–3794; k) J. Zakzeski, P. C. A. Bruijnincx, B. M. Weckhuysen, *Green Chem.* **2011**, *13*, 671–680; l) B. Biannic, J. J. Bozell, *Org. Lett.* **2013**, *15*, 2730–2733; m) J. M. W. Chan, S. Bauer, H. Sorek, S. Sreekumar, K. Wang, F. D. Toste, *ACS Catal.* **2013**, *3*, 1369–1377; n) B. Sedai, C. Díaz-Urrutia, R. T. Baker, R. Wu, L. A. "Pete" Silks, S. K. Hanson, *ACS Catal.* **2013**, *3*, 3111−3122; o) S. Nanayakkara, A. F. Patti, K. Saito, *Green Chem.* **2014**, *16*, 1897–1903; p) B. Sedai, T. Baker, *Adv. Synth. Cat.* **2014**, *356*, 3563–3574; q) S. Liu, C. Zhang, L. Li, S. Yu, C. Xie, F. Liu, Z. Song, *Ind. Eng. Chem. Res.* **2014**, *53*, 19370−19374; r) F. Napoly, L. Jean-Gérard, C. Goux-Henry, M. Draye, B. Andrioletti, *Eur. J. Org. Chem.* **2014**, 781–787; s) C. Zhu, W. Ding, T. Shen, C. Tang, C. Sun, S. Xu, Y. Chen, J. Wu, H. Ying, *ChemSusChem* **2015**, *8*, 1768–1778; t) J. Zeng, C. G.

Yoo, F. Wang, X. Pan, W. Vermerris, Z. Tong, *ChemSusChem* **2015**, *8*, 861–871; u) C. Zhu, W. Ding, T. Shen, C. Tang, C. Sun, S. Xu, Y. Chen, J. Wu, H. Ying, *ChemSusChem* **2015**, *8*, 1768–1778; v) J. Zeng, C. G. Yoo, F. Wang, X. Pan, W. Vermerris, Z. Tong, *ChemSusChem* **2015**, *8*, 861–871; w) J. Mottweiler, M. Puche, C. Räuber, T. Schmidt, P. Concepción, A. Corma, C. Bolm, *ChemSusChem* **2015**, *8,* 2106–2113; x) J. Mottweiler, T. Rinesch, C. Besson, J. Buendia, C. Bolm, *Green Chem*. **2015**, *17*, 5001–5008.

[27] **Selected heterogeneously catalyzed oxidative lignin depolymerization approaches:** a) D. B. Akolekar, S. K. Bhargava, I. Shirgoankar, J. Prasad, *Appl. Catal. A: Gen.* **2002**, *236*, 255–262; b) C. Crestini, M. C. Caponi, D. S. Argyropoulos, R. Saladino, *Bioorg. Med. Chem.* **2006**, *14*, 5292–5302; c) F. G. Sales, L. C. A. Maranhão, N. M. Lima-Filho, C. A. M. Abreu, *Chem. Eng. Sci.* **2007**, *62*, 5386–5391; d) H. Deng, L. Lin, Y. Sun, C. Pang, J. Zhuang, P. Ouyang, Z. Li, S. Liu, *Catal. Lett.* **2008**, *126*, 106–111; e) O. A. Makhotkina, S. V. Preis, E. V. Parkhomchuk, *Appl. Catal. B: Environ.* **2008**, *84*, 821–826; f) Y. S. Ma, C. N. Chang, Y.-P. Chiang, H. F. Sung, A. C. Chao, *Chemosphere* **2008**, *71*, 998–1004; g) J. Zhang, H. Deng, L. Lin, *Molecules* **2009**, *14*, 2747–2757; h) H. Deng, L. Lin, Y. Sun, C. Pang, J. Zhuang, P. Ouyang, J. Li, S. Liu, *Energy Fuel* **2009**, *23*, 19–24; i) H. Deng, L. Lin, S. Liu, *Energy Fuel* **2010,** *24*, 4797–4802; j) L. Das, P. Kolar, R. Sharma-Shivappa, *Biofuels* **2012**, *3*, 155–166; k) Y. Zhao, Q. Xu, T. Pan, Y. Zuo, Y. Fu, Q. X. Guo, *Appl. Catal. A: Gen.* **2013**, *467*, 504–508.

[28] **Selected oxidative lignin degradation approach by benzylic alcohol oxidation:** a) A. Wu, B. O. Patrick, E. Chung, B. R. James, *Dalton Trans*. **2012**, *41*, 11093–11106; b) A. Rahimi, A. Azarpira, H. Kim, J. Ralph, S. S. Stahl, *J. Am. Chem. Soc.* **2013**, *135*, 6415–6418; c) A. Rahimi, A. Ulbrich, J. J. Coon, S. S. Stahl, *Nature* **2014**, *515*, 249–252; d) K. Walsh, H. F. Sneddon, C. J. Moody, *Org. Lett*. **2014**, *16*, 5224−5227; e) C. S. Lancefield, O. S. Ojo, F. Tran, N. J. Westwood, *Angew Chem. Int. Ed.* **2015**, *54*, 258–262; f) M. Dawange, M. V. Galkin, J. S. M. Samec, *ChemCatChem* **2015**, *7*, 401–404; g) R. Zhu, B. Wang, M. Cui, J. Deng, X. Li, Y. Ma, Y. Fu, *Green Chem.* **2016**, *18*, 2029–2036; h) M. Wang, J. Lu, X. Zhang, L. Li, H. Li, N. Luo, F. Wang, *ACS Catal.* **2016**, *6*, 6086−6090; i) C. Zhang, H. Li, J. Lu, X. Zhang, K. E. MacArthur, M. Heggen, F. Wang, *ACS Catal.* **2017**, *7*, 3419−3429.

[29] **Selected acid-catalyzed lignin depolymerization pathways:** a) S. Jia, B. J. Cox, X. Guo, Z. C. Zhang, J. G. Ekerdt, *ChemSusChem* **2010**, *3*, 1078−1084; b) M. R. Sturgeon, S. Kim, K. Lawrence, R. S. Paton, S. C. Chmely, M. Nimlos, T. D. Foust, G. T. Beckham, *ACS Sustain. Chem. Eng.* **2014**, *2*, 472−485; c) T. J. Yokoyama, *J. Wood Chem. Technol.* **2014**, *35*, 27−42; d) R. G. Harms, I. I. E. Markovits, M. Drees, W. A. Herrmann, M. Cokoja, F. E. Kühn, *ChemSusChem* **2014**, *7*, 429−434; e) A. Kaiho, M. Kogo, R. Sakai, K. Saito, T. Watanabe, *Green Chem.* **2015**, *17*, 2780−2783; f) P. J. Deuss, M. Scott, F. Tran, N. J. Westwood, J. G. de Vries, K. Barta, *J. Am. Chem. Soc.* **2015**, *137*, 7456−7467; g) M. Scott, P. J. Deuss, J. G. de Vries, M. H. G. Prechtl, K. Barta, *Catal. Sci. Technol.* **2016**, *6*, 1882−1891; h) C. W. Lahive, P. J. Deuss, C. S. Lancefield, Z. Sun, D. B. Cordes, C. M. Young, F. Tran, A. M. Z. Slawin, P. C. J. Kamer, J. G. de Vries, N. J. Westwood, K. Barta, *J. Am. Chem. Soc.* **2016**, *138*, 8900−8911.

[30] **Selected homogeneous base-catalyzed degradation of lignin model compounds and lignin:** a) R. W. Thring, *Biomass Bioenergy* **1994**, *7*, 125–130; b) J. E. Miller, I. Evans, A. Littlewolf, D. E. Trudell, *Fuel* **1999**, *78*, 1363–1366; c) E. Chornet, J. S. Shabtai, W. W. Zmierczak, *Process for conversion of lignin to reformulated hydrocarbon gasoline*. U.S. Patent 5,959,167 A, September 28, **1999**; d) J. S. Shabtal, W. W. Zmierczak, E. Chornet, *Process for conversion of lignin to reformulated, partially oxygenated gasoline*. U. S. Patent US 6,172,272 B1, January 9, **2001**; e) J. S. Shabtal, W. W. Zmierczak, E. Chornet, D. Johnson, *Process for converting lignins into a high octane blending component*. U. S. Patent US 2003/0115792 A1, June 26, **2003**; f) J. S. Shabtal, W. W. Zmierczak, E. Chornet, D. Johnson, *Process for converting lignins into a high-octane additive.* U. S. Patent US 20,030,100.807 A1, May 29, **2003**; g) S. Karagöz, T. Bhaskar, A. Muto, Y. Sakata, *Fuel* **2004**, *83*, 2293–2299; h) A. Vigneault, D. K. Johnson, E. Chornet, *Can. J. Chem. Eng*. **2007**, *85*, 906–916; i) J. E. Miller, L. R. Evans, A. E. Littlewolf, D. E. Trudell, *Batch microreactor studies of lignin depolymerization by bases. 1. Alcohol solvents*. Sandia National Laboratories Report SAND2002-1317, USA, **2002**; j) J. E. Miller, L. R. Evans, J. E. Mudd, K. A. Brown, *Batch microreactor studies of lignin depolymerization by bases. 2. Aqueous solvents*. Sandia National Laboratories Report SAND2002-1318, USA, **2002**; k) S. Nenkova, T. Vasileva, K. Stanulov,

Chem. Nat. Compd. **2008**, *44*, 182–185; l) J. -M. Lavoie, W. Baré, M. Bilodeau, *Bioresour. Technol*. **2011**, *102*, 4917–4920; m) V. M. Roberts, V. Stein, T. Reiner, A. Lemonidou, X. Li, J. A. Lercher, *Chem. Eur. J*. **2011**, *17*, 5939–5948; n) R. Beauchet, F. Monteil-Rivera, J. M. Lavoie, *Bioresour. Technol*. **2012**, *121*, 328–334; o) A. Toledano, L. Serrano, J. Labidi, *J. Chem. Technol. Biotechnol*. **2012**, *87*, 1593–1599; p) A. Toledano, L. Serrano, J. Labidi, *Fuel* **2014**, *116*, 617–624; q) E. M. Karp, B. S. Donohoe, M. H. O'Brien, P. N. Ciesielski, A. Mittal, M. J. Biddy, G. T. Beckham, *ACS Sustain. Chem. Eng.* **2014**, *2*, 1481–1491; r) S. Dabral, J. Mottweiler, T. Rinesch, C. Bolm, *Green Chem*. **2015**, *17*, 4908−4917; s) R. Katahira, A. Mittal, K. Mc Kinney, X. Chen, M. P. Tucker, D. K. Johnson, G. T. Beckham, *ACS Sustain. Chem. Eng.* **2016**, *4*, 1474−1486.

[31] a) J. Gierer, *Svensk Papperstidning-Nordisk Cellulosa* **1970**, *73*, 571−596; b) T. J. Mcdonough, *Tappi journal* **1993**, *76*, 186−193.

[32] T. Lankau, C. -H. Yu, *Gren Chem.* **2016**, *18*, 1590–1596.

[33] **Selected heterogeneous base-catalyzed degradation of lignin model compounds and lignin:** a) G. S. Macala, T. D. Matson, C. L. Johnson, R. S. Lewis, A. V. Iretskii, P. C. Ford, *ChemSusChem* **2009**, *2*, 215–217; b) Z. Yuan, S. Cheng, M. Leitch, C. C. Xu, *Bioresour. Technol*. **2010**, *101*, 9308–9313; c) K. Barta, T. D. Matson, M. L. Fettig, S. L. Scott, A. V. Iretskii, P. C. Ford, *Green Chem*. **2010**, *12*, 1640–1647; d) T. D. Matson, K. Barta, A. V. Iretskii, P. C. Ford, *J. Am. Chem. Soc.* **2011**, *133*, 14090–14097; e) M. R. Sturgeon, M. H. O'Brien, P. N. Ciesielski, R. Katahira, J. S. Kruger, S. C. Chmely, J. Hamlin, K. Lawrence, G. B. Hunsinger, T. D. Foust, R. M. Baldwin, M. J. Biddy, G. T. Beckham, *Green Chem*. **2014**, *16*, 824–835; f) K. Barta, G. R. Warner, E. S. Beach, P. T. Anastas, *Green Chem*. **2014**, *16*, 191–196; g) J. Long, Q. Zhang, T. Wang, X. Zhang, Y. Xu, L. Ma, *Bioresour. Technol.* **2014**, *154*, 10–17; h) J. S. Kruger, N. S. Cleveland, S. Zhang, R. Katahira, B. A. Black, G. M. Chupka, T. Lammens, P. G. Hamilton, M. J. Biddy, G. T. Beckham, *ACS Catal.* **2016**, *6*, 1316–1328; i) R. Chaudhary, D. L. Dhepe, *Green Chem.* **2017**, *19*, 778– 788.

[34] a) S. Kim, S. C. Chmely, M. R. Nimlos, Y. J. Bomble T. D. Foust, R. S. Paton, G. T. Beckham, *J. Phys. Chem. Lett.* **2011**, *2*, 2846–2852; b) R. Parthasarathi, R. A. Romero, A. Redondo, S. Gnanakaran, *J. Phys. Chem. Lett.* **2011**, *2*, 2660–2666.

[35] F. Guo, Z. Fang, T. J. Zhou, *Bioresour. Technol.* **2012**, *112*, 313–318.

[36] F. Guo, Z. L. Xiu, Z. X. Liang, *Applied Energy* **2012**, *98*, 47–52.

[37] L. Hu, X. Tang, Z. Wu, L. Lin, J. Xu, N. Xu, B. Dai, *Chem. Eng. J.* **2015**, *263*, 299–308.

[38] H. Xie, Z. K. Zhao, Q. Wang, *ChemSusChem* **2012**, *5*, 901– 905.

[39] W. Chen, X. wen Peng, L. -xin Zhong, Y. Li, R. cang Sun, *ACS Sustain. Chem. Eng.* **2015**, *3*, 1366−1373.

[40] Z. Wu, H. Xie, X. Yu, E. Liu, *ChemCatChem* **2013**, *5*, 1328–1333.

[41] a) A. J. Lynch, C. A. Rowland, *The History of Grinding*. Society for Mining, Metellurgy, and Exploration, Littleton, Colorado, **2005**; b) L. Takacs, *Chem. Soc. Rev*. **2013**, *42*, 7649–7659.

[42] A. Stolle, Technical Implications of Organic Synthesis in BallMills. In: *Ball Milling Towards Green Synthesis: Applications, Projects, Challenges*, (A. Stolle, B. Ranu.), The Royal Society of Chemistry, **2015**, 241–276.

[43] a) B. Rodríguez, A. Bruckmann, T. Rantanen, C. Bolm, *Adv. Synth. Catal.* **2007**, *349*, 2213–2233; b) A. Stolle, T. Szuppa, S. E. S. Leonhardt, B. Ondruschka, *Chem. Soc. Rev.* **2011**, *40*, 2317–2329; c) G. W. Wang, *Chem. Soc. Rev*. **2013**, *42*, 7668–7700; d) J. G. Hernández, T. Friščić, *Tetrahedron Lett.* **2015**, *56*, 4253–4276.

[44] P. Baláž, M. Achimovičová, M. Baláž, P. Billik, A. Cherkezova-Zheleva, J. M. Criado, F. Delogu, E. Dutková, E. Gaffet, F. J. Gotor, R. Kumar, I. Mitov, T. Rojac, M. Senna, A. Streletskii, K. Wieczorek-Ciurowa, *Chem Soc Rev.* **2013**, *42*, 7571–7637; b) E. Boldyreva, *Chem. Soc. Rev*. **2013**, *42*, 7719–7738.

[45] N. R. Rightmire, T. P. Hanusa, *Dalton Trans*. **2016**, *45*, 2352–2362.

[46] a) J. B. Ravnsbæk, T. M. Swager, *ACS Macro Lett*. **2014**, *3*, 305–309; b) S. Grätz, L. Borchardt, *RSC Adv.* **2016**, *6*, 64799–64802.

[47] a) J. G. Hernández, M. Frings, C. Bolm. *ChemCatChem*, **2016**, *8*, 1769–1772; b) J. G. Hernández, K. J. Ardila-Fierro, D. Crawford, S. L. James, C. Bolm, *Green Chem.* **2017**, *19*, 2620–2625.

[48] T. Friščić, *Chem. Soc. Rev.* **2012**, *41*, 3493–3510.

[49] a) C. Mottillo, T. Friščić, *Molecules* **2017**, *22*, 144; b) A. L. Garay, A. Pichon, S. L. James, *Chem. Soc. Rev.* **2007**, *36*, 846–855; c) D. Braga, S. L. Giaffreda, F. Grepioni, A. Pettersen, L. Maini, M. Curzi, M. Polito, *Dalton Trans.* **2006**, 1249–1263.

[50] a) D. Tan, L. Loots, T. Friščić, *Chem. Commun*. **2016**, *52*, 7760–7781; b) S. Quaresma, V. André, A. Fernandes, T. Duarte*, Inorg. Chim. Acta*. **2016**, *455*, 309–318.

[51] S. L. James, C. J. Adams, C. Bolm, D. Braga, P. Collier, T. Friščić, F. Grepioni, K. D. M. Harris, G. Hyett, W. Jones, A. Krebs, J. Mack, L. Maini, A. G. Orpen, I. P. Parkin, W. C. Shearouse, J. W. Steed, D. C. Waddell *Chem. Soc. Rev.* **2012**, *41*, 413–447.

[52] K. Komatsu, G.-W. Wang, Y. Murata, M. Shiro, *Nature* **1997**, *387*, 583–586.

[53] J. G. Hernández, C. Bolm, *J. Org. Chem*. **2017**, *82*, 4007–4019.

[54] K. Horie, M. Barón, R. B. Fox, J. He, M. Hess, J. Kahovec, T. Kitayama, P. Kubisa, E. Maréchal, W. Mormann, R. F. T. Stepto, D. Tabak, J. Vohlidal, E. S. Wilks, W. J. Work, *Pure Appl. Chem*. **2004**, *76*, 889–906.

[55] S. M. Kim, B. S. Dien, V. Singh, *Biotechnol. Biofuels* **2016**, *9,* 263.

[56] a) Y. Yu, H. Wu, *AIChE J.* **2011**, *57*, 793–800; b) A. Barakat, X. Rouau, *Biotechnol. Biofuels* **2014**, *7*, 138.

[57] M. Laka, S. Chernyavskaya, *Proc. Estonian Acad. Sci. Chem*. **2006**, *55*, 78–84; b) W. Zhang, J. Zhang, W. Xia, *Int. J. Food Prop.* **2014**, *17*, 26–37.

[58] C. Miao, W. Y. Hamad, *J. Appl. Polym. Sci.* **2017**, *134*, 44669.

[59] S. M. Hick, C. Griebel, D. T. Restrepo, J. H. Truitt, E. J. Buker, C. Bylda, R. G. Blair, *Green Chem*. **2010**, *12*, 468–474.

[60] J. Hilgert, N. Meine, R. Rinaldi, F. Schuth, *Energy Environ. Sci.* **2013**, *6*, 92–96.

[61] a) M. Käldström, N. Meine, C. Farès, F. Schüth, Roberto Rinaldi *Green Chem.* **2014**, *16*, 3528–3538; b) G. Calvaruso, M. T. Clougha, R. Rinaldi, *Green Chem.* **2017**, *19*, 2803−2811.

[62] M. D. K. Rechulski, M. Kaldstro, U. Richter, F. Schüth, R. Rinaldi, *Ind. Eng. Chem. Res.* **2015**, *54*, 4581−4592.

[63] a) R. Carrasquillo-Flores, M. Käldström, F. Schüth, J. A. Dumesic, R. Rinaldi, *ACS Catal.* **2013**, 3, 993–997; b) F. Schüth, R. Rinaldi, N. Meine, M. Käldström, J. Hilgert, M. D. Kaufman Rechulski, *Catal. Today* **2014**, *234*, 24–30.

[64] T. Kleine, J. Buendia, C. Bolm, *Green Chem*. **2013**, *15*, 160–166.

[65] X. Chen, H. Yang, Z. Zhong, Ning Yan, *Green Chem*. **2017**, *19*, 2783–2792.

[66] J. Buendia, J. Mottweiler, C. Bolm, *Chem. Eur. J.* **2011**, *17*, 13877–13882.

[67] S. Sen, S. Patil, D. S. Argyropoulos, *Green Chem.* **2015**, *17*, 1077–1087.

[68] a) W. C. Shieh, S. Dell, O. Repic, *Org. Lett*. **2001**, *3*, 4279–4281; b) P. Tundo, M. Selva, *Acc. Chem. Res.* **2002**, *35*, 706–716; c) Y. Ji, J. Sweeney, J. Zoglio, D. J. Gorin, *J. Org. Chem*. **2013**, *78*, 11606–11611; d) J. N. G. Stanley, M. Selva, A. F. Masters, T. Maschmeyer, A. Perosa, *Green Chem*. **2013**, *15,* 3195–3204.

[69] a) H. Kawamoto, S. Horigoshi, S. Saka, *J. Wood Sci.* **2006**, *53*, 168–174; b) J. Gierer, *Wood Sci. Technol*. **1980**, *14*, 241–266.

[70] J. Engel, PhD. Dissertation, RWTH Aachen University, **2017**.

[71] J. L. Wen, S. L. Sun, B. L. Xue, R. C. Sun, *Materials* **2013**, *6*, 359−391.

[72] a) D. S. Argyropoulos, *Res. Chem. Intermed*. **1995**, *21*, 373–395; b) M. Balakshin, E. Capanema, *J. Wood Chem. Technol*. **2015**, *35*, 220–237; c) Y. Pu, S. Cao, A. Ragauskas, *J. Energy Environ. Sci.* **2011**, *4*, 3154–3166; d) S. Constant, H. L. J. Wienk, A. E. Frissen, P.de. Peinder, R. Boelens, D. S. van Es, R. J. H. Grisel, B. M. Weckhuysen, W. J. J. Huijgen, R. J. A. Gosselink, P. C. A. Bruijnincx, *Green Chem*. **2016**, *18*, 2651–2665.

[73] a) N. Ambreen, R. Kumar, T. Wirth, *Beilstein J. Org. Chem*. **2013**, *9*, 1437–1442; b) Z. Q. Liu, X. Shang, L. Chai, Q. Sheng, *Catal. Lett.* **2008**, *123*, 317–320.

[74] a) V. V. Zhdankin, *Hypervalent Iodine Chemistry: Preparation, Structure and Synthetic Application of Polyvalent Iodine Compounds,* Wiley, New York, **2013**; b) *Hypervalent Iodine Chemistry, Top. Curr. Chem.*, vol. 373 (Ed. T. Wirth), Springer, Switzerland, **2015**; c) M. Ochiai, *Chem. Rec.* **2007**, *7*, 12–23; d) V. V. Zhdankin, P. J. Stang, *Chem. Rev.* **2008**, *108*, 5299–5358; e) M. Uyanik, K. Ishihara, *Chem. Commun*. **2009**, 2086–2099; f) V. V. Zhdankin, *ARKIVOC* **2009**, *1*, 1–62; g) M. Uyanik, K. Ishihara, *ChemCatChem* **2012**, *4*, 177–185; h) F. V. Singh, T. Wirth, *Chem. Asian J.* **2014**, *9*, 950–971; i) M. S. Yusubov, V. V. Zhdankin, *Resource-Efficient Technol*. **2015**, *1*, 49-67; j) A. Yoshimura, V. V. Zhdankin, *Chem. Rev.* **2016**, *116*, 3328–3435.

[75] **Selective oxidation of primary hydroxyl groups in the presence of secondary ones using TEMPO and DAIB:** a) A. De Mico, R. Margarita, L. Parlanti, A. Vescovi, G. Piancatelli, *J. Org. Chem.* **1997**, *62*, 6974–6977; b) T. M. Hansen, G. J. Florence, P. L. Mas, J. Chen, J. N. Abrams, C. J. Forsyth, *Tetrahedron Lett.* **2003**, *44*, 57–59; c) C. I. Herrerías, T. Y. Zhang, C. J. Li, *Tetrahedron Lett.* **2006**, *47*, 13–17; d) J. M. Vatèle, *Tetrahedron Lett*. **2006**, *47*, 715–718; **for immobilized DAIB/TEMPO catalytic systems:**e) K. Sakuratani, H. Togo *Synthesis* **2003**, 21–23; f) T. Dohi, K. I. Fukushima, T. Kamitanaka, K. Morimoto, N. Takenagab, Y. Kita, *Green Chem*. **2012**, *14*, 1493–150.

[76] a) A. H. Despointes, V. A. Yaylayan, *J. Agri. Food. Chem*. **1996**, *44*, 672–681; b) S. Chandrasekhar, Ch. Narsihmulu, N. R. Reddy, S. S. Sultana*, Chem. Commun.* **2004**, 2450–2451; c) M. F. Angelika, M. M. R. Christine, C. Bolm, *Chem. Eur. J*. **2010**, *16*, 3918–3921.

[77] **DAIB-assisted oxidation of guaiacol to benzoquinone derivatives:** a) S. Quideau, L. Pouységu, D. Deffieux, A. Ozanne, J. Gagnepain, I. Fabre, M. Oxoby, *ARKIVOC* **2003**, *6*, 106–119; b) T. C. Kao, G. J. Chuang, C. C. Liao, *Angew. Chem. Int. Ed.* **2008**, *47*, 7325–7327; c) S. Y. Gao, S. K. Chittimalla, G. J. Chuang, C. C Liao, *J. Org. Chem.* **2009**, *74*, 1632–1639; d) T. Dohi, T. Nakae, N. Takenaga, T. Uchiyama, K. I. Fukushima, H. Fujioka, Y. Kita, *Synthesis* **2012**, *44*, 1183–1189; e) S. K. Chittimalla, R. Kuppusamy, N. Akavaram, *Synlett* **2015**, *26*, 613–618; f) S. K. Chittimalla, C. Bandi, *Tetrahedron Lett.* **2016**, *57*, 15–19.

[78] S. Shimizu, T. Yokoyama, T. Akiyama and Y. Matsumoto, *J. Agric. Food Chem.* **2012**, *60*, 6471–6476.

[79] T. Q. Yuan, S. N. Sun, F. Xu, R. C. Sun, *J. Agric. Food Chem.* **2011**, *59*, 10604–10614.

[80] a) S. Seth, S, Jhulki, J. N. Moorthy, *Eur. J. Org. Chem*. **2013**, *12*, 2445–2452; b) T. K. Achar, S. Maiti, P. Mal, *RSC Adv.* **2014**, *4*, 12834–12839; c) P. K. Sahoo, A. Bose, P. Mal, *Eur. J. Org. Chem*. **2015**, *32*, 6994–6998; d) A. K. Mishra, J. N. Moorthy, *Org. Chem. Front.* **2017**, *4*, 343–349.

[81] a) C. Bolm, A. S. Magnus, J. P. Hildebrand, *Org. Lett.* **2000**, *2*, 1173–1175; b) K. Moriyama, M. Takemura, H. Togo, *J. Org. Chem*. **2014**, *79*, 6094−6104.

[82] S. L. Collom, P. T. Anastas, E. S. Beach, R. H. Crabtree, N. Hazari, T. J. Sommer, *Tetrahedron Lett.* **2013,** *54*, 2344−2347.

[83] D. Bandyopadhyay, J. M. Velazquez, B. K. Banik, *Org Med Chem Lett.* **2011**, *1*, 11.

[84] A. Strecker, *Ann. Chem. Pharm*. **1850**, *75*, 27–45.

[85] a) F. A. Davis, P. S. Portonovo, R. E. Reddy, Y.-h. Chiu, *J. Org. Chem*. **1996**, *61*, 440–441; b) H. Kunz, W. Sager, *Angew. Chem. Int. Ed*. **1987**, *26*, 557–559; C) K. Harada, Nature **1963**, *200*, 1201; d) J. Wang, X. Liu, X. Feng, *Chem. Rev.* **2011**, *111*, 6947–6983.

[86] a) E. J. Corey, M. J. Grogan, *Org. Lett.* **1999**, *1*, 157–160; b) T. Ooi, Y. Uematsu, K. Maruoka, *J. Am. Chem. Soc.* **2006**, *128*, 2548–2549; c) M. Rueping, E. Sugiono, C. Azap, *Angew. Chem. Int. Ed.* **2006**, *45*, 2617–2619; d) S. C. Pan, B. List, *Org. Lett.* **2007**, *9*, 1149–1151; e) S. J. Zuend, M. P. Coughlin, M. P. Lalonde, E. N. Jacobsen, Nature **2009**, *461*, 968–970; f) S. Mahajan, P. Chauhan, U. Kaya, K. Deckers, K Rissanen, D. Enders, *Chem. Commun*. **2017**, *53*, 6633–6636.

[87] H. Ishitani, S. Komiyama, Y. Hasegawa, S. Kobayashi, *J. Am. Chem. Soc*. **2000**, *122*, 762–766.

[88] a) L. M. Weinstock, P. Davis, B. Handelsman, R. Tull, *J. Org. Chem*. **1967**, *32*, 2823–2829; b) W. L. Mantier, D. A. Owens, W. T. Comer, D. Deitchman, H. C. Ferguson, R. J. Seidehamel, J. R. Young, *J. Med. Chem*. **1973**, *16*, 901–908; c) R. O. Duthaler, *Tetrahedron*. **1994**, *50*, 1539–1650; d) N. Otto, T. Opatz, *Chem. Eur. J.* **2014**, *20*, 13064–13077.

[89] L. Kürti, B. Czakó, *Strategic Applications of Named Reactions in Organic Synthesis, Elsevier Academic: San Diego*, **2005**.

[90] M. Ayaz, F. De Moliner, G. A. Morales, C. Hulme (Ed.) in Third Component Cyanide (Strecker and Strecker-Type Reactions), Vol. 1 (Ed.: T. J. J. Müller), Science of synthesis: multicomponent reactions, Thieme, Stuttgart, **2014**, 99–122.

[91] a) K. Surendra, N. S. Krishnaveni, A. Mahesh, K. R. Rao, *J. Org. Chem*. **2006**, *71*, 2532–2534; b) A. Heydari, A. Arefi, S. Khaksar, R. K. Shiroodi, *J. Mol. Catal. A: Chem*. **2007**, 271, 142–144.

[92] M. M. Mojtahedi, M. S. Abaee, H. Abbasi, *Can. J. Chem*. **2006**, *84*, 429–432.

[93] W. Shearouse, M. Shumba, J. Mack, *Appl. Sci*. **2014**, *4*, 171–179.

[94] P. K. Sahoo, A. Bose, P. Mal, *Eur. J. Org. Chem*. **2015**, 6994–6998.

[95] L. A. Polindara-García, E. Juaristi, *Eur. J. Org. Chem*. **2016**, 1095–1102.

[96] J. G. Hernández, M. Turberg, I. Schiffers, C. Bolm, *Chem. Eur. J.* **2016**, *22*, 14513 –14517.

[97] S. Dhanasekaran, A. Suneja, V. Bisai, V. K. Singh, *Org. Lett*. **2016**, *18*, 634–637.

[98] H. A. Seo, Y. H. Cho, Y. S. Lee, C. H. Cheon, *J. Org. Chem*. **2015**, *80*, 11993–11998.

[99] W. Chen, W. An, Y. Wang, A. Yu, A, *J. Org. Chem.* **2016**, *81*, 10857–10862.

[100] A. Beillard, T. X. Métro, X. Bantreil, J. Martinez, F. Lamaty, F. *Chem. Sci.* **2017**, *8*, 1086–1089.

[101] Gaussian 09, Revision D.01, M. J. Frisch, G. W. Trucks, H. B. Schlegel, G. E. Scuseria, M. A. Robb, J. R. Cheeseman, G. Scalmani, V. Barone, G. A. Petersson, H. Nakatsuji, X. Li, M. Caricato, A. Marenich, J. Bloino, B. G. Janesko, R. Gomperts, B. Mennucci, H. P. Hratchian, J. V. Ortiz, A. F. Izmaylov, J. L. Sonnenberg, D. Williams-Young, F. Ding, F. Lipparini, F. Egidi, J. Goings, B. Peng, A. Petrone, T. Henderson, D. Ranasinghe, V. G. Zakrzewski, J. Gao, N. Rega, G. Zheng, W. Liang, M. Hada, M. Ehara, K. Toyota, R. Fukuda, J. Hasegawa, M. Ishida, T. Nakajima, Y. Honda, O. Kitao, H. Nakai, T. Vreven, K. Throssell, Jr. J. A. Montgomery, J. E. Peralta, F. Ogliaro, M. Bearpark, J. J. Heyd, E. Brothers, K. N. Kudin, V. N.; Staroverov, T. Keith, R. Kobayashi, J. Normand, K. Raghavachari, A. Rendell, J. C. Burant, S. S. Iyengar, J. Tomasi, M. Cossi, J. M. Millam, M. Klene, C. Adamo, R. Cammi, J. W. Ochterski, R. L. Martin, K. Morokuma, O. Farkas, J. B. Foresman, D. J. Fox, Gaussian, Inc., Wallingford CT, **2016**.

[102] a) J. D. Chai, M. Head-Gordon, *Phys. Chem. Chem. Phys.* **2008**, *10*, 6615–6620; b) J. D. Chai, M. Head-Gordon, *J. Chem. Phys.* **2008**, *128,* 084106; c) A. D. Becke, *J. Chem. Phys.* **1997**, *107*, 8554–8560.

[103] P. Fuentealba, H. Preuss, H. Stoll, L. Von Szentpály, *Chem. Phys. Lett.* **1982**, *89*, 418–422.

[104] a) T. H. Dunning, *J. Chem. Phys.* **1989**, *90*, 1007–1023; b) D. E. Woon, T. H. Dunning, *J. Chem. Phys.* **1993**, *98*, 1358–1371.

[105] a) R. Krishnan, J. S. Binkley, R. Seeger, J. A. Pople, *J. Chem. Phys.* **1980**, *72*, 650–654; b) A. D. McLean, G. S. Chandler, *J. Chem. Phys.* **1980**, *72*, 5639–5648; c) T. Clark, J. Chandrasekhar, G. W. Spitznagel, P. V. R. Schleyer, *J. Comput. Chem.* **1983**, *4*, 294–301.

[106] a) S. Miertuš, E. Scrocco, J. Tomasi, *Chem. Phys.* **1981**, *55*, 117–129; b) S. Miertuš, J. Tomasi, *Chem. Phys*. **1982**, *65*, 239–245; c) J. L. Pascual-ahuir, E. Silla, I. Tuñon, *J. Comput. Chem*. **1994**, *15*, 1127–1138; d) M. Cossi, V. Barone, R. Cammi, J. Tomasi, *Chem. Phys. Lett*. **1996**, *255*, 327–335; e) V. Barone, M. Cossi, J. Tomasi, *J. Chem. Phys*. **1997**, *107*, 3210–3221; f) E. Cancès, B. Mennucci, J. Tomasi, *J. Chem. Phys.* **1997**, *107*, 3032–3041; g) B. Mennucci, E. Cancès, J. Tomasi, *J. Phys. Chem. B* **1997**, *101*, 10506–10517; h) B. Mennucci, J. Tomasi, *J. Chem. Phys*. **1997**, *106*, 5151–5158; i) V. Barone, M. Cossi, J. Tomasi, *J. Comput. Chem*. **1998**, *19*, 404–417; j) M. Cossi, V. Barone, B. Mennucci, J. Tomasi, *Chem. Phys. Lett*. **1998**, *286*, 253–260; k) R. Cammi, B. Mennucci, J. Tomasi, *J. Phys. Chem. A* **1999**, *103*, 9100–9108; l) J. Tomasi, B. Mennucci, Cancès, E. *THEOCHEM* **1999**, *464*, 211–226; m) R. Cammi, B. Mennucci, J. Tomasi, *J. Phys. Chem. A* **2000**, *104*, 5631–5637; n) M. Cossi, V. Barone, *J. Chem. Phys.* **2000**, *112*, 2427–2435; o) M. Cossi, V. Barone, *J. Chem. Phys*. **2001**, *115*, 4708–4717; p) M. Cossi, G. Scalmani, N. Rega, V. Barone, *J. Chem. Phys*. **2002**, *117*, 43–54; q) M. Cossi, N. Rega, G. Scalmani, V. Barone, *J. Comput. Chem*. **2003**, *24*, 669–681.

[107] M. A. Rivas, S. M. Pereira, N. Banerji, T. P. Iglesias, *J. Chem. Thermodyn.* **2004**, *36*, 183−191.

[108] A. Rodríguez, J. Canosa, J. Tojo, *J. Chem. Eng. Data* **2001**, *46*, 1476−1486.

[109] P. Picart, C. Müller, J. Mottweiler, L. Wiermans, C. Bolm, P. Domínguez de María, A. Schallmey, *ChemSusChem* **2014**, *7*, 3164–3171.

[110] A. Bianco, C. Cavarischia, M. Guiso, *Eur. J. Org. Chem.* **2004**, 2894–2898.

[111] H. Stetter, J. Nienhaus, *Chem. Ber.* **1978**, *111*, 2825–2832.

[112] G. Egri, A. Kolbert, J. Bálint, E. Fogassy, L. Novák, L. Poppe, *Tetrahedron: Asymmetry* **1998**, *9*, 217−283.

[113] C. A. Gandolfi, R. Di Domenico, S. Spinelli, L. Gallico, L. Fiocchi, A. Lotto, E. Menta, A. Borghi, C. D. Rosa, S. Tognella, *J. Med. Chem.* **1995**, *38*, 466−472.

[114] J. M. Gaudin, J. Y. de Saint Laumer, *Eur. J. Org. Chem*. **2015**, 1437–1447.

[115] K. Sakuratani, H. Togo, *Synthesis* **2003**, 21–23.

[116] R. G. Harms, I. I. E. Markovits, M. Drees, W. A. Herrmann, M. Cokoja, F. E. Kühn, *ChemSusChem* **2014**, *7*, 429–434.

[117] W. H. Chen, R. Wang, Y. P. Shi, *J. Nat. Prod.* **2010**, *73*, 1398–1403.

[118] R. Mudududdla, R. Sharma, S. Abbat, P. V. Bharatam, R. A. Vishwakarma, S. B. Bharate, *Chem. Comm*. **2014**, *50*, 12076–12079.

[119] Y. Yamamoto, *Adv. Synth. Catal*. **2010**, *352*, 478–492.

[120] J. A. Jiang, C. Chen, Y. Guo, D. H. Liao, X. D. Pan, Y. F. Ji, *Green Chem*. **2014**, *16*, 2807–2814.

[121] L. Li, R. Matsuda, I. Tanaka, H. Sato, P. Kanoo, H. J. Jeon, M. L. Foo, A. Wakamiya, Y. Murata, S. Kitagawa, *J. Am. Chem. Soc.* **2014**, *136***,** 7543−7546.

[122] R. A. Fernandes, V. Bethi, *RSC Adv.* **2014**, *4*, 40561–40568.

[123] M. Wang, J. Lu, L. Li, H. Li, H. Liu, F. Wang, *J. Catal.* **2017**, *348*, 160–167.

[124] G. Broggini, L. Garanti, G. Molteni, G. Zecchi, *Tetrahedron* **1998**, *54*, 14859–14868.

[125] A. Majhi, S. S. Kim, S. T. Kadam, *Tetrahedron* **2008**, *64*, 5509–5514.

[126] J. Wang, Y. Masui, M. Onaka, *Eur. J. Org. Chem*. **2010**, 1763–1771.

[127] N. H. Khan, S. Saravanan, R. I. Kureshy, S. H. Abdi, A. Sadhukhan, H. C. Bajaj, *J. Organomet. Chem.* **2010**, *695*, 1133–1137.

[128] B. Ramalingam, A. M. Seayad, L. Chuanzhao, M. Garland, K. Yoshinaga, M. Wadamoto, T. Nagata, C. L. L. Chia, *Adv. Synth. Catal.* **2010**, *352*, 2153–2158.

[129] C. Wiles, P. Watts, *Eur. J. Org. Chem.* **2008**, 5597–5613.

[130] P. Galletti, M. Pori, D. Giacomini, *Eur. J. Org. Chem.* **2011**, *2001*, 3896–3903.

[131] J. Jarusiewicz, Y. Choe, K. S. Yoo, C. P. Park, K. W. Jung, *J. Org. Chem.* **2009**, *74*, 2873–2876.

[132] B. C. Ranu, S. S. Dey, A. Hajra, *Tetrahedron* **2002**, *58*, 2529–2532.

[133] B. Nammalwar, N. P. Muddala, F. M. Watts, R. A. Bunce, *Tetrahedron* **2015**, *71*, 9101−9111.

[134] S. Dhanasekaran, A. Suneja, V. Bisai, V. K. Singh, *Org. Lett.* **2016**, *18*, 634−637.

[135] a) D. S. Argyropoulos, *Res. Chem. Intermed*. **1995**, *21*, 373–395; b) S. Constant, H. L. J. Wienk, A. E. Frissen, P. de. Peinder, R. Boelens, D. S. van Es, R. J. H. Grisel, B. M. Weckhuysen, W. J. J. Huijgen, R. J. A. Gosselink, P. C. A. Bruijnincx, *Green Chem*. **2016**, *18*, 2651–2665.

IX. Curriculum Vitae

Personal Information

Name:	Saumya Dabral
Nationality:	Indian
Date of Birth:	August 2nd, 1989
Place of Birth:	New Delhi, India

Education

Since 04/2014	Doctoral studies in the group of Professor Dr. Carsten Bolm, Institute of Organic Chemistry, RWTH Aachen University, Germany
01/2012 – 06/2013	M. S. Materials Science (Dual degree), Japan Advanced Institute of Science and Technology (JAIST), Ishikawa, Japan
07/2010 – 05/2013	M. Tech. Chemical Synthesis and Process Technologies, Department of Chemistry, University of Delhi, Delhi, India
07/2007 – 05/2010	B. Sc. (Hons.) Chemistry, Hindu College, University of Delhi, Delhi, India
04/2001 – 04/2007	Springdales School, Dhaula Kuan, New Delhi, India

.

Research Experience

09/2016 – 11/2016	Interdoc research studies at Sasol Technology, Fifie, United Kingdom
05/2015 – 08/2015	Interdoc research studies at the University of St Andrews, Fife, United Kingdom under the supervision of Professor Dr. Paul C. J. Kamer
01/2012 – 12/2012	Master's thesis under the supervision of Professor Dr. Kohki Ebitani at the Japan Advanced Institute of Science and Technology (JAIST), Japan: "Synthesis and utilization of heterogeneous catalysts for the conversion of Raffinose to value-added platform chemicals"
05/2011 – 07/2012	Research assistant, Dr. Reddy's Institute of Life Sciences, Hyderabad, India

Scholarships

04/2014 – 04/2017	Marie Curie Early Stage Researcher
04/2014 –	DAAD doctoral research scholarship (declined)
01/2012 – 12/2012	Japan Government Scholarship for Masters studies